Alma Mater Studiorum – Università di Bologna

FACOLTÀ DI INGEGNERIA

CORSO DI LAUREA IN CIVIL ENGINEERING

Tesi di laurea in
ADVANCED DESIGN OF STRUCTURES

Interaction between Axial Force, Shear and Bending Moment in Reinforced Concrete Elements

Candidato:
GIULIA CASTORI

Relatore:
Prof. Ing. STEFANO SILVESTRI

Correlatore:
Prof. Ing. TOMASO TROMBETTI
Dott. Ing. MICHELE PALERMO

Sessione III

Anno accademico 2013/1014

Abstract

Il collasso di diverse colonne, caratterizzate da danneggiamenti simili, quali ampie fessure fortemente inclinate ad entrambe le estremità dell'elemento, lo schiacciamento del calcestruzzo e l'instabilità dei ferri longitudinali, ha portato ad interrogarsi riguardo gli effetti dell'interazione tra lo sforzo normale, il taglio ed il momento flettente.

Lo studio è iniziato con una ricerca bibliografica che ha evidenziato una sostanziale carenza nella trattazione dell'argomento.

Il problema è stato approcciato attraverso una ricerca di formule della scienza delle costruzioni, allo scopo di mettere in relazione lo sforzo assiale, il taglio ed il momento; la ricerca si è principalmente concentrata sulla teoria di Mohr.

In un primo momento è stata considerata l'interazione tra solo due componenti di sollecitazione: sforzo assiale e taglio. L'analisi ha condotto alla costruzione di un dominio elastico di taglio e sforzo assiale che, confrontato con il dominio della *Modified Compression Field Theory*, trovata tramite ricerca bibliografica, ha permesso di concludere che i risultati sono assolutamente paragonabili.

L'analisi si è poi orientata verso l'interazione tra sforzo assiale, taglio e momento flettente. Imponendo due criteri di rottura, il raggiungimento della resistenza a trazione ed a compressione del calcestruzzo, inserendo le componenti di sollecitazione tramite le formule di Navier e Jourawsky, sono state definite due formule che mettono in relazione le tre azioni e che, implementate nel software Matlab, hanno permesso la costruzione di un dominio tridimensionale. In questo caso non è stato possibile confrontare i risultati, non avendo la ricerca bibliografica mostrato niente di paragonabile.

Lo studio si è poi concentrato sullo sviluppo di una procedura che tenta di analizzare il comportamento di una sezione sottoposta a sforzo normale, taglio e momento: è stato sviluppato un modello a fibre della sezione nel tentativo di condurre un calcolo non lineare, corrispondente ad una sequenza di analisi lineari.
La procedura è stata applicata a casi reali di crollo, confermando l'avvenimento dei collassi.

Table of Contents

1. Literature Review

The study begun with a literature review in order to analyse how other researchers approached the problem. Many articles examined, only most important have reported. They divide into analytical, numerical and experimental articles.

1.1. Analytical Articles

1.1.1. Article 1

Authors: Frank J. Vecchio and Michael P. Collins

Journal: ACI Structural Journal, 1986

Title: The Modified Compression-Field Theory for Reinforced Concrete Elements Subjected to Shear

Focus of Research

The article presents an analytical model capable of predicting the load-deformation response of reinforced concrete elements subjected to in-plane shear and normal stresses. In the model, cracked concrete is treated as a new material with its own stress-strain characteristics. Equilibrium, compatibility, and stress-strain relationships are formulated in terms of average stresses and average strains. Consideration is also given to local stress conditions at crack locations. The stress-strain relationships for the cracked concrete were determined testing 30 RC panels.

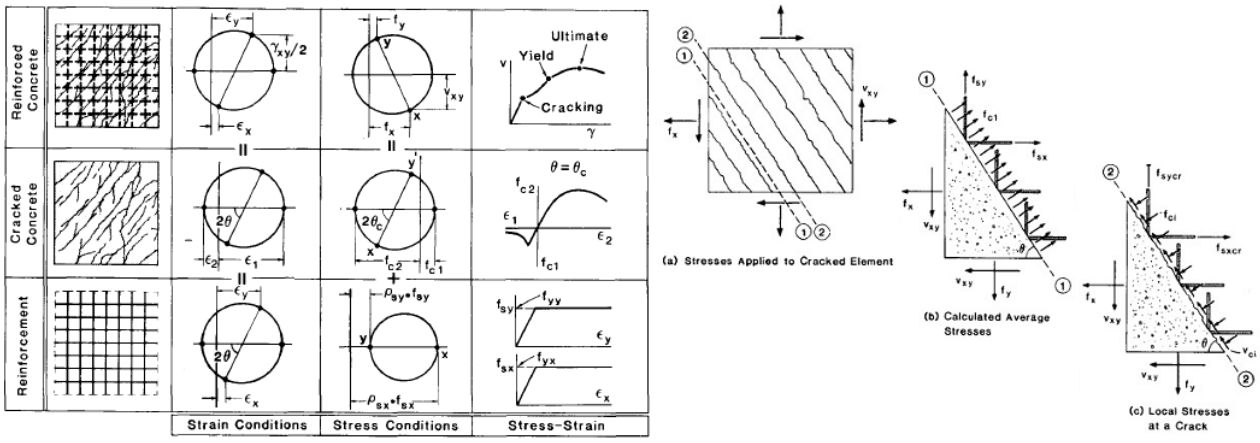

Figure 1.1.1.1 – Approach of the modified compression field theory

The membrane element considered is a portion of a reinforced concrete structure, containing an orthogonal grid of reinforcement with the longitudinal, x, and transverse, y, axes coincident with the reinforcement directions. Loads applied consist of uniform axial stresses f_x and f_y, and uniform shear stress v_{xy}. The problem is to determine how the three in-plane stresses f_x, f_y, and v_{xy} are related to the three in-plane strains $\varepsilon_x, \varepsilon_y$ and γ_{xy}. Assuming that concrete and steel bars are perfectly bonded together corresponds to: $\varepsilon_{sx} = \varepsilon_{cx} = \varepsilon_x$ and $\varepsilon_{sy} = \varepsilon_{cy} = \varepsilon_y$. If $\varepsilon_x, \varepsilon_y$ and γ_{xy} are known, then the strain in any other direction can be obtained from the Mohr's circle of strain: $\gamma_{xy} = \frac{2(\varepsilon_1 - \varepsilon_2)}{\tan\theta}$ where $\varepsilon_x + \varepsilon_y = \varepsilon_1 + \varepsilon_2$ and $tan^2\theta = \frac{\varepsilon_x - \varepsilon_2}{\varepsilon_y - \varepsilon_2} = \frac{\varepsilon_1 - \varepsilon_y}{\varepsilon_1 - \varepsilon_x} = \frac{\varepsilon_1 - \varepsilon_y}{\varepsilon_y - \varepsilon_2} = \frac{\varepsilon_x - \varepsilon_2}{\varepsilon_1 - \varepsilon_x}$.

The forces applied to the reinforced concrete element are carried by stresses in the concrete and in the reinforcement. The requirement that forces sum to zero in the x-direction corresponds to: $\int_A f_x dA = \int_{A_c} f_{cx} dA_c + \int_{A_s} f_{sx} dA_s$, which is $f_x = f_{cx} + \rho_{sx} * f_{sx}$. The following equilibrium conditions: $f_y = f_{cy} + \rho_{sy} * f_{sy}, v_{xy} = v_{cx} + \rho_{sx} * v_{sx}, \quad v_{xy} = v_{cy} + \rho_{sy} * v_{sy}$. Assuming $v_{cx} = v_{cy} = v_{yx}$, stresses in concrete are defined: $f_{cx} = f_{c1} - v_{cx} / \tan\theta_c$, $f_{cy} = f_{c1} - v_{cx} * \tan\theta_c$.

Constitutive relationships to link average stresses to average strains for reinforcement and concrete: $f_{sx} = E_s * \varepsilon_x \le f_{xy}$, $f_{sy} = E_s * \varepsilon_y \le f_{xy}$ and $v_{sx} = v_{sy} = 0$. Concerning the concrete, principal stress axes and principal strain axes assume coincident: $\theta_c = \theta$.

Thanks to experimental tests was found that principal compressive stress in the concrete, f_{c2}, was a function, not only of the principal compressive strain, ε_2, but also of the co-existing principal tensile strain, ε_1. The relationship suggested is: $f_{c2} = f_{c2,max} * \left[2\left(\frac{\varepsilon_2}{\varepsilon_{c'}}\right) - \left(\frac{\varepsilon_2}{\varepsilon_{c'}}\right)^2\right]$ where $\frac{f_{c2,max}}{f'_c} = \frac{1}{0.8 - 0.34\frac{\varepsilon_1}{\varepsilon_{c'}}} \le 1$.

Concerning the average principal tensile stress in the concrete, prior cracking $f_{c1} = E_c * \varepsilon_1$, after $f_{c1} = \frac{f_{cr}}{1 + \sqrt{200\varepsilon_1}}$. The stresses and strains formulations described deal with average values and do not give information about local variation. At a crack, there are no average conditions.

As the applied external stresses f_x, f_y, and v_{xy} are fixed, the internal stresses must be statically equivalent: $\rho_{sx} f_{sx} \sin\theta + f_{c1} \sin\theta = \rho_{sx} f_{sxcr} \sin\theta - f_{ci} \sin\theta - v_{ci} \cos\theta$; the same in y direction: $\rho_{sy} f_{sy} \cos\theta + f_{c1} \cos\theta = \rho_{sy} f_{sycr} \cos\theta - f_{ci} \cos\theta - v_{ci} \sin\theta$. The two equilibrium equations can be satisfied with no shear and compression stresses on the crack, which means: $\rho_{sy}(f_{sycr} - f_{sy}) = \rho_{sx}(f_{sxcr} - f_{sx}) = f_{c1}$. However, the stress in the reinforcement at a crack cannot exceed the yield strength, that is: $f_{sxcr} \le f_{sx}, f_{sycr} \le f_{sy}$. If the calculated average stress in reinforcement is high, it may not be possible to satisfy the equilibrium. In this case, equilibrium will require shear stresses on the crack. The relationship between the shear on the crack v_{ci}, the crack width w and the compressive stress on the crack f_{ci} has experimentally studied, Walraven formula is: $v_{ci} = 0.18\, v_{ci,max} + 1.64\, f_{ci} - 0.82 \frac{f_{ci}^2}{v_{ci,max}}$, $v_{ci,max} = \frac{\sqrt{-f_{c'}}}{0.31 + 24\, w/(a+16)}$.

Obtained Results

The MCFT is a powerful analytical tool, but is simple enough to be programmed with a handheld calculator. Not only is it capable of predicting the test results reported in this paper, but it has used by other researchers to successfully predict their test results.

1.1.2. Article 2

Authors: Michael P. Collins, Denis Mitchell, Perry Adebar, and Frank J. Vecchio

Journal: ACI Structural Journal, 1996

Title: A General Shear Design Method

Focus of Research

The objective of this paper is to briefly present a simple, general shear design method based on the Modified Compression Field Theory, *MCFT*.

The principal compressive stress in the concrete, f_2, relates to both principal compressive and tensile strain, ε_1 and ε_2: $f_2 = f_{2,max}\left[\frac{2\varepsilon_2}{\varepsilon'_c} - \left(\frac{\varepsilon_2}{\varepsilon'_c}\right)^2\right]$, where $f_{2,max} = \frac{f'_c}{0.8+170\,\varepsilon_1} \le f'_c$. From the first equation derives $\varepsilon_2 = -0.002\left(1 - \sqrt{1 - \frac{f_2}{f_{2,max}}}\right)$. After cracking: $f_1 = \frac{f_{cr}}{1+\sqrt{500\,\varepsilon_1}}$, with $f_{cr} = 4\sqrt{f'_c}$. For large values of ε_1, cracks become wide, the magnitude of f_1 is governed by the yielding of reinforcement at crack and by the ability to transmit shear stresses, v_{ci}, across the interface, which is a function of the crack width, w, and the aggregate size, a: $v_{ci} = \frac{0.18\sqrt{f'_c}}{0.3+\frac{24\,w}{a+16}}$. Is stirrups have reached their yielding stress and crack begins to slip, the average tensile stress in the concrete, $f_1 = v_{ci}\,tan\theta$.

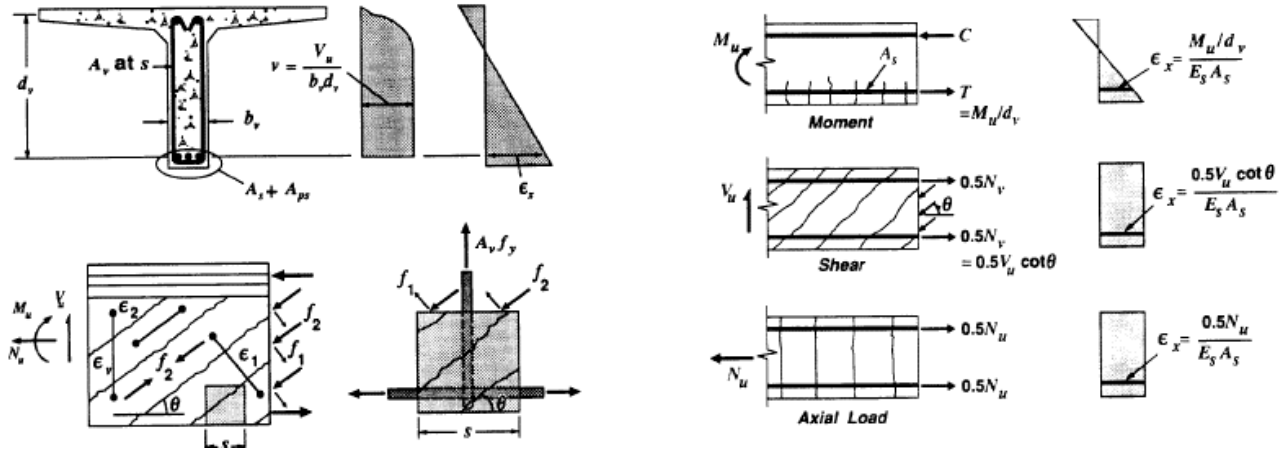

Figure 1.1.2.1 – Approach of GSM

For the design, ε_x, the highest longitudinal strain occurring within the web, can be approximated as the strain in the flexural tension reinforcement: $0 \le \varepsilon_x = \frac{\left(\frac{M_u}{d_v}\right)+0.5\,N_u+0.5\,V_u\,cot\theta-A_{ps}\,f_{po}}{E_s\,A_s+E_p\,A_p} \le 0.002$. From strain compatibility: $\varepsilon_1 = \varepsilon_x + (\varepsilon_x - \varepsilon_2)\,cot^2\theta$; hence, as longitudinal strain, ε_x, increases and the inclination of principal compressive stress, θ, reduces, the "damage indicator", ε_1, increases. The nominal strength of a member $V_n = V_c + V_s + V_p = f_1\,b_v\,d_v\cot\theta + \frac{A_v\,f_y}{s}d_v\cot\theta + V_p = \beta\sqrt{f'_c}\,b_v\,d_v + \frac{A_v\,f_y}{s}d_v\cot\theta + V_p$, where tensile stress factor $\beta = \frac{0.33\cot\theta}{1+\sqrt{500\,\varepsilon_1}} \le \frac{0.18}{0.3+\frac{24\,w}{a+16}}$, $w = s\,\varepsilon_1$. The value of principal tensile strain, ε_1, depends on the magnitudes of longitudinal strain, ε_x, the principal compressive

strain, ε_2, which can be computed through equation, defined above, imposing $f_2 = \left(\frac{V_n - V_p}{b_v\, d_v}\right)(\tan\theta + \cot\theta)$.

Using the relationship above: $\varepsilon_1 = \varepsilon_x + \left[\varepsilon_x + 0.002\left(1 - \sqrt{1 - \frac{v}{f'_c}(\tan\theta + \cot\theta)\,(0.8 + 170\varepsilon_1)}\right)\right] cot^2\theta$.

The amount of shear reinforcement must satisfy $V_s \geq \frac{V_u}{\varphi} - V_c - V_p$, where $V_u \leq \varphi\, V_n$.

The shear influences the tensile forces in longitudinal reinforcement. At the inner edge of the bearing area, the tensile force has to be: $T = \left(\frac{V_u}{\varphi} - 0.5\, V_s\right)\cot\theta$. This equation gives additional tension due to shear, and therefore, at a section subjected to shear, V_u, a moment, M_u, and an axial force, N_u, longitudinal bars on the flexural tension side of the element must satisfy: $A_s\, f_y + A_{ps}\, f_{ps} \geq \frac{M_u}{\varphi\, d_v} + 0.5\, \frac{N_u}{\varphi} + \left(\frac{V_u}{\varphi} - 0.5\, V_s - V_p\right)\cot\theta$.

The general equation of the *MCFT*, intended to account for the complex behaviour of diagonally cracked concrete, are more suited for computer solution, like RESPONSE-2000, than for hand calculation. With tables of θ and β, the method becomes simple enough to solve by hand. For the design. Using formulae mentioned above, the steps are the following:

1. At the design section, calculate the shear stress v;
2. Calculate the longitudinal strain ε_x;
3. Choose the values of θ and β
4. Determine the nominal strength;
5. Check the capacity of longitudinal reinforcement.

Obtained Results

This approach has verified through experimental tests. 528 specimens were tested and as many shear failures resulted. Those failures were compared to the failure shear predicted by the method presented in this paper. The proposed General Method predicts the failure shears more accurately than those given by the ACI code do. A key feature of this procedure is the explicit consideration of the influence of shear upon longitudinal reinforcement, aspect that could avoid serious errors.

1.1.3. Article 3

Authors: M.J. Nigel Priestley, Ravindra Verma, and Yan Xiao

Journal: Journal of Engineering Mechanics, 1999

Title: Seismic Shear Strength of Reinforced Concrete Columns

Focus of Research

This paper examines a number of methods to predict shear strength of columns and compares the results with existing database. A refinement and simplification of the method developed by Ang et al. (1989) and Wong et al. (1993) is proposed, which results in close agreement between predicted and measured shear strength over the full range of experimental database.

The ASCE/ACI 426 approach does not consider the influence of ductility; the Ang-Wong model work well in low ductility, but scatter increases at moderate to high ductility levels, apparently as a consequence of the residual shear strength, being assumed independent of the axial load level and the aspect ratio. The Watanabe-Ichinose approach provides good prediction for rectangular columns at low axial load levels, the lack of specific consideration about axial loads leads to increased conservatism as the axial load level increases. In this model, for ductile shear strength, the strength of both arch and truss mechanisms are reduced. Experimental data indicate a reduction in the inclination of diagonal cracking to the column axis as the ductility increases, implying an increase in the truss mechanism.

The proposed equation bases on the formulation given by Ang and Wong. The shear strength of a column is supposed to consist of three independent components: a concrete component, V_c, whose magnitude depends on the level of ductility, an axial load component, V_p, depending on the column aspect ratio, and a truss component, V_s, function of transverse reinforcement: $V_n = V_c + V_p + V_s$. The concrete term reduces with increasing ductility: $V_c = k\sqrt{f'_c}\,A_c$, where k depends on the member displacement ductility level, on the system of unit used and whether the column is subjected to uniaxial or biaxial ductility demand; the effective shear area, $A_c = 0.8\,A_{gross}$.

It is considered that the column axial force enhance the shear strength by arch action and inclined strut. In this approach, the arch action only depends on the axial load level. The enhancement of the shear strength relates to the horizontal component of the diagonal compression strut, since this component directly resists the applied force. Thus: $V_p = P\,\tan\alpha = \frac{D-c}{2a}P$, where D is the overall section depth or diameter, c the depth of the compression zone, $a = L$ for cantilever columns and $a = \frac{L}{2}$ for column in reversed bending.

The contribution of transverse reinforcement to shear strength bases on truss mechanism using 30° angle between the compression diagonals, the crack pattern, and the column axis. For rectangular column: $V_s = \frac{\pi}{2}\frac{A_{sh}\,f_{yh}\,D'}{S}\cot 30°$, where D' is the distance between centres of the peripheral hoops or spirals.

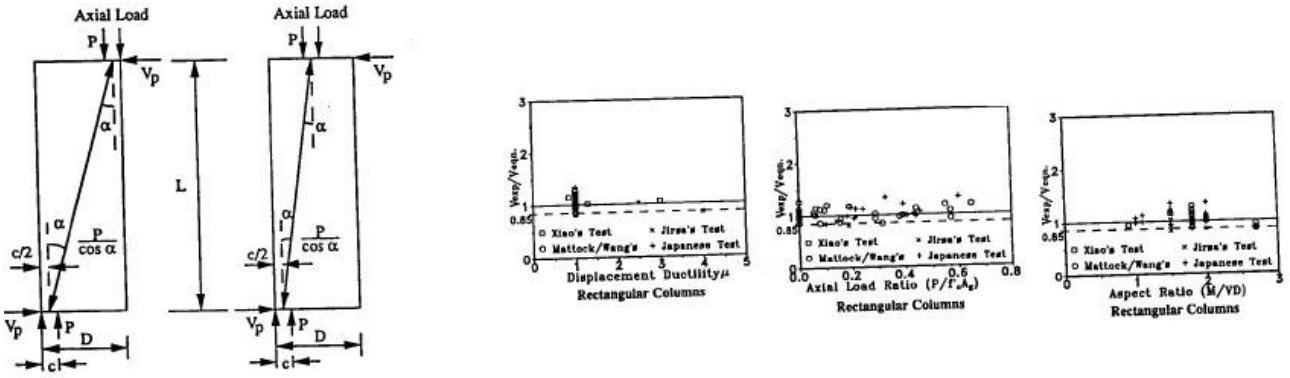

Figure 1.1.3.1 – Equations compared to experimental results

Obtained Results

Results reported in the figure indicates a greatly improvement prediction. The influence of ductility, axial load and aspect ratio appear to be well represented by the proposed method. With respect to the methods discussed at the beginning, the model proposed in this paper provides the closest agreement with the data, with a mean strength ratio of 1.021 and a standard deviation of 0.124. This standard deviation is less than 40% of that resulting from the ASCE/ACI 426 and Watanabe-Ichinose, and 61% than Ang-Wong model.

It could be argued that the proposed method is a predictive equation, whereas the alternative ones are design equations. Consequently, higher values of the strength ratio are desirable. This is true, but the final determination of the appropriateness of the design approach depends only on the lower limit to the data/prediction comparison. As can be observed from the figure, a strength reduction factor $\varphi_s = 0.85$, represents a reasonable lower bound to all methods.

Also, in the comparison provided in this paper, shear strength was predicted using measured concrete compression strength and transverse reinforcement yield strength; in design situation, nominal material strength would be used, which in vast majority of cases will result in additional conservatism. Preliminary comparison of the proposed shear model with results from reinforced concrete structural walls indicates that the method may also apply, without modification, to structural walls.

1.1.4. Article 4

Authors: Evan C. Bentz, Frank J. Vecchio, and Michael P. Collins

Journal: ACI Structural Journal, 2006

Title: Simplified Modified Compression Field Theory for Calculating Shear Strength of Reinforced Concrete Elements

Focus of Research

The research reported in this paper has resulted in a significant simplification of the MCFT. It is shown that this simplified MCFT is capable of predicting the shear strength of a wide range of reinforced concrete elements with almost the same accuracy as the full theory. The expressions developed in the paper can form the basis of a simple, general, and accurate shear design method for reinforced concrete members.

Since the used element models a section of the flexural region of a beam, it is assumed that the clamping stresses, f_z, will be negligible. For the transverse reinforcement to yield at failure, ε_z, will need to be greater than approximately 0.002, while to crush the concrete, ε_2 will need to be approximately 0.002. If ε_x is also equal to 0.002 at failure, the maximum shear stress will be approximately $0.28\,f'_c$, whereas for very low values of ε_x the shear stress at failure is predicted to reach approximately $0.32\,f'_c$. It assumes that, if failure occurs before yielding of the transverse reinforcement, the failure shear stress will be $0.25\,f'_c$. For failures occurring below this shear stress level, it assumes that at failure both f_{zs} and f_{zscr} are equal to the yield stress of the transverse reinforcement, called f_y. Considering the sum of the forces in the z-direction for the free body diagram. For $f_z = 0$ and $f_{szcr} = f_y$, the equation can be rearranged to give $v = v_c + v_s = v_{ci} + \rho_z f_y \cot\theta = f_1 \cot\theta + \rho_z f_y \cot\theta = \beta\sqrt{f'_c} + \rho_z f_y \cot\theta$, where $\beta = \frac{0.33\ \cot\theta}{1+\sqrt{500\,\varepsilon_1}}$. The crack width w corresponds to the product of the crack spacing s_θ and the principal tensile strain ε_1, a_g represents the maximum coarse aggregate size in mm. To relate the longitudinal strain ε_x to ε_1: $\varepsilon_1 = \varepsilon_x(1 + cot^2\,\theta) + \varepsilon_2\,cot^2\,\theta$. The principal compressive strain ε_2 depends on the principal compressive stress f_2. When ρ_z and f_z are zero: $f_2 = f_1\,cot^2\,\theta$.

Because the compressive stresses for these elements will be small, it is sufficiently accurate to assume that ε_2 equals f_2/E_c, and that E_c can be taken as $4950\sqrt{f'_c}$ in MPa units. The equation then becomes: $\varepsilon_1 = \varepsilon_x(1 + cot^2\,\theta) + \frac{cot^4\,\theta}{15000(1+\sqrt{500\,\varepsilon_1})}$.

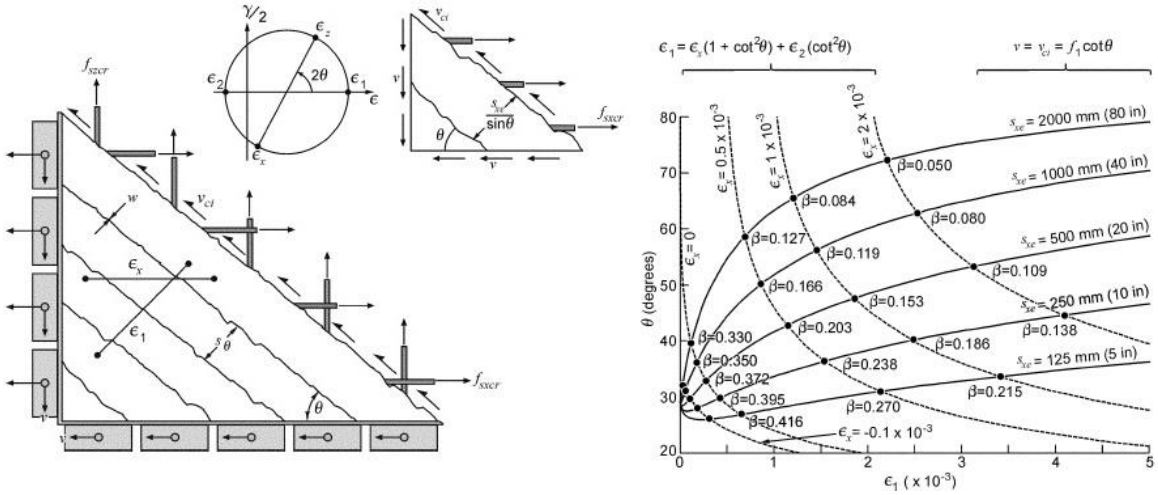

Figure 1.1.4.1 – Simplified Modified Compression Field Theory charts

It can be seen that as the crack spacing increases, s_{xe}, the values of β and, hence, the shear strengths, decrease. The observed fact is that large reinforced beams that do not contain transverse reinforcement fail at lower shear stresses than geometrically similar smaller beams; this corresponds to the size effect in shear. It is of interest that the predictions of the MCFT agree well with the results of the extensive experimental studies on size effect done in the years since the theory has first formulated. The MCFT β values for elements without transverse reinforcement depend on both the longitudinal strain ε_x and the crack spacing parameter s_{xe}. Authors refer to these two effects as the "strain effect factor" and the "size effect factor." The two factors are not completely independent, but in the simplified version of the MCFT, this interdependence of the two factors is ignored and it assumes that β can be taken as simply the product of a *strain factor* and a *size factor*: $\beta = \frac{0.4}{1+1500\,\varepsilon_x} * \frac{1300}{1000+\,s_{xe}}$. The simplified MCFT uses the following expression for the angle of inclination $\theta = (29\,deg + 7000\varepsilon_x)\left(0.88 + \frac{s_{xe}}{2500}\right) \leq 75deg$.

Obtained Results

This paper summarizes the relationships of the MCFT. This theory can model the full load-deformation response of reinforced concrete panels subjected to arbitrary biaxial and shear loading. Solving the equations, however, requires special-purpose computer programs and the method is, thus, not practical. On many occasions, a full load-deformation analysis is not needed; rather, a quick calculation of shear strength is required. This paper presents a simplified version of the MCFT. At the heart of the method is a simple equation for β and a simple equation for θ. While simple, the method provides excellent predictions of shear strength. The average ratio of experimental-to-predicted shear strength of the simplified MCFT is 1.11 with a COV of 13.0%.

1.1.5. Article 5

Authors: Hossein Mostafei and Toshimi Kabeyasawa

Journal: ACI Structural Journal, 2007

Title: Axial-Flexure-Shear Interaction Approach for Reinforced Concrete Columns

Focus of Research

The article presents an approach for displacement-based analysis of reinforced concrete columns considering principles of axial-shear-flexure interaction.

The main objective of the study is to modify the conventional section analysis approach in case of shear behaviour, in order to be applicable for a displacement-based evaluation of reinforced concrete columns and beams subjected to shear, flexural, and axial loads.

This approach uses the traditional section analysis, also called fiber model, to assess axial-flexural behaviour, while the MCFT, *Modified Compression Field Theory*, is employed to determine axial-shear behaviour of the reinforced concrete element. The mechanisms of shear and flexure are coupled considering axial deformations interaction and concrete strength degradation, and satisfying compatibility and equilibrium relationships.

Thus, the ASFI method consists of two models, an axial-flexural one, which is a conventional fiber model, and an axial-shear one, which is a biaxial shear model.

Axial deformation plays a very important role by interconnecting the two models of axial-shear and axial-flexure. The axial deformation due to flexure mechanism increases shear crack width as well as principle tensile strain in the web of the column, which results into a lower shear capacity for the element. Concrete strength degradation or concrete compression softening is another interaction term in the ASFI method.

The proposed approach is simplified in order to model a reinforced concrete column using a single section analysis with a single shear model for the entire element.

Analytical results, such as ultimate lateral loads, drifts and post-peak responses, have compared with the experimental data; consistent agreements were achieved.

In the ASFI method, only axial-flexure model relates to the structural input data, such as material properties and geometry of a column. Later, input data for the axial-shear model are determined basing on the converted stresses and strains, derived from the axial-flexure model components. Thus, the ASFI method can be extended to three-dimensional analysis and for all types of section.

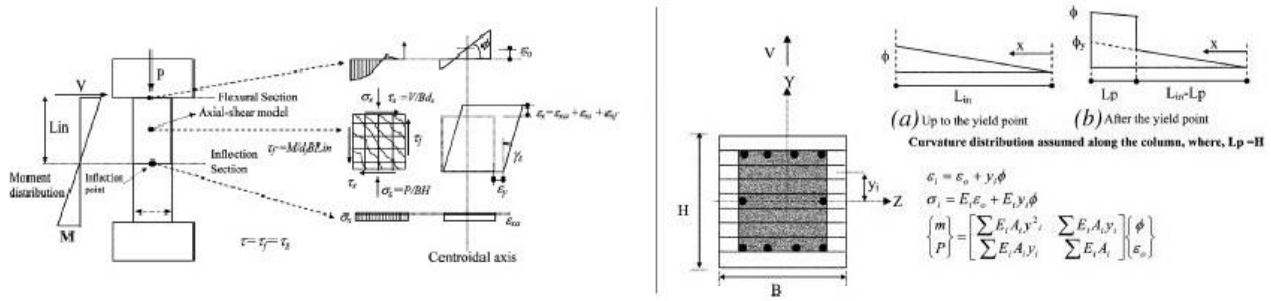

Figure 1.1.5.1 – Axial-flexure and shear-flexure models of the ASFI method

Obtained Results

To assess the efficacy of axial-shear-flexure interaction approach, the response of a reinforced concrete column specimen is evaluated following four different analyses.

First, by applying only the axial-flexure model, which corresponds to the fiber model, the displacement-based analysis was implemented for the specimen.

Then, only the axial-shear model of the ASFI method was used to obtain the shear response of the specimen considering the same displacement history.

After that, the analysis was carried out for the column by the simplified ASFI method, based on the process described in the paper.

Finally, similar to the ASFI method, the axial-shear model and the axial-flexure model were coupled as springs in series, without any axial deformation interaction and concrete strength degradation. Then the displacement-based response of the specimen was obtained by the method. Results obtained from the aforementioned four methods are derived and compared: the axial-shear-flexure interaction has a significant effect on the structural response and is an essential consideration in the analysis.

To assess the applicability of the simplified ASFI method, three full-scale columns, a reinforced – concrete column of a bridge and a beam subjected to zero axial force, were tested.

For all specimens, reasonable correlations were attained between the analytical results and the test data. Hence, it might be concluded that the simplified ASFI method is a proper analytical tool for displacement-based evaluation of reinforced concrete columns.

1.1.6. Article 6

Authors: H. Mostafaei and F. J. Vecchio

Journal: Journal of Structural Engineering, 2008

Title: Uniaxial Shear-Flexure Model for Reinforced Concrete Elements

Focus of Research

This paper presents a performance-based analysis of RC columns subjected to shear, flexure and axial loads; the Uniaxial Shear-Flexure Model, *USFM*, bases on a relatively more complex approach, known as the Axial-Shear-Flexure Interaction, *ASFI*, method that is able to predict the full load-deformation relationships of reinforced concrete columns subjected to axial, flexure and shear force. The USFM can also predict comparable full load-deformation responses, but the formulation has simplified by eliminating the iteration process for the shear modelling.

In the ASFI method, the flexure mechanism has modelled by applying traditional sectional analysis, and shear behaviour has modelled based on the modified compression field theory. However, the application of the MCFT requires a relatively intensive computation and iteration process.

This study tries to simplify the shear modelling of the *ASFI* approach introducing the *USFM*, where axial and principal tensile strain of a RC column or beam, between two consecutive flexural sections, is determined based on the average axial strains and average resultant concrete compression strains of the two sections. This simplifies the approach significantly by eliminating the iteration process for the shear model.

The steps in an analysis performed according to the USFM method, for a given curvature, φ, and axial strain, ε_{xi}, are as follows:

1. Apply the section analysis procedure for two adjacent sections, at least one of them in correspondence of the section with maximum moment and the other one at the inflection point, where moment is zero; then determine the average centroidal strain and concrete principal compression strain between the two sections;
2. Compute average concrete principal tensile strain, ε_1, assuming an initial value of $0.56f_t'$ for f_{c1};
3. If the transverse reinforcement has yielded, determine the average concrete principal tensile strain, ε_1;

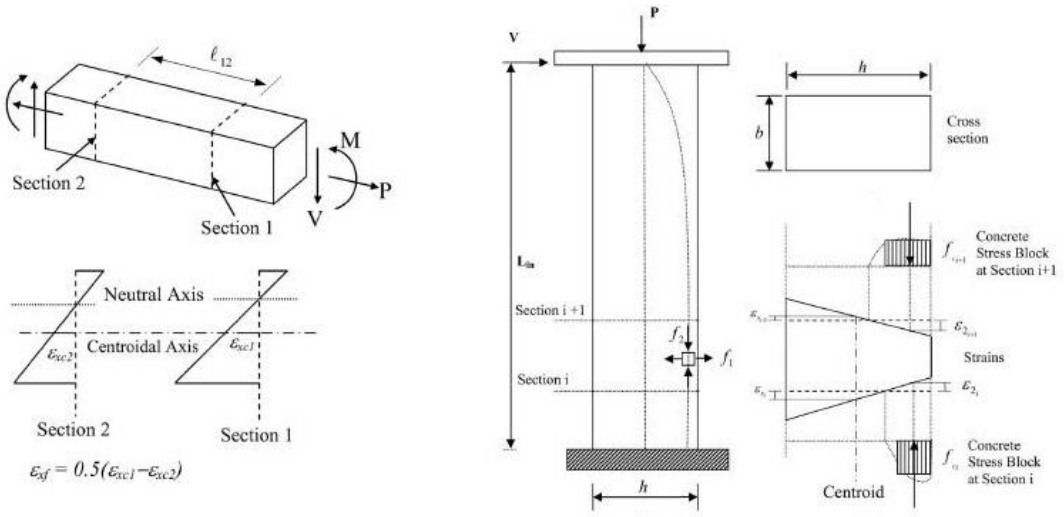

Figure 1.1.6.1 – Approach of uniaxial Shear-Flexure Model for Reinforced Concrete Elements

4. Calculate the compression-softening factor, which represents the degradation of the concrete strength due to shear deformation, then compute the concrete compression stress of the stress block, multiplied by the compression-softening factor;
5. Obtain moment, shear force and the centroidal strain at the sections using section analysis;
6. Check for maximum shear stress on crack;
7. Obtain the total lateral drift ratio and the axial strain.

Obtained Results

To verify the applicability and accuracy of the USFM approach for reinforced concrete columns and beams, specimens with various performance characteristics have selected and evaluated using the developed method. The column specimens scaled to 1/3 of actual columns. Comparing experimental results from the first four columns to the test outcomes of the columns with different hysteretic loading patterns indicated no significant effects on column response due to the different lateral loading patterns. Therefore, for the analysis by the USFM method, which bases on a monotonic loading pattern, the effects of hysteretic loading pattern were neglected for these specimens. Considering the symmetric conditions of the specimens, the two sections required for USFM analysis were chosen as one at the inflection point and one at an end section. As a result, the drift ratio-lateral load responses for the columns have estimated and compared to the test data; consistent correlations resulted. Furthermore, to assess the efficiency of the USFM, its outcomes have compared to those of the traditional ASFI method: results clearly indicate the benefit of using the USFM without sacrificing the accuracy of the ASFI approach. To conclude, consistently strong correlations were attained between analytical results and experimental outcomes.

1.2. Numerical Researches

1.2.1. Article 7

Authors: Marco Petrangeli, Paolo Emilio Pinto, and Vincenzo Ciampi

Journal: Journal of Engineering Mechanics, 1999

Title: Fiber Element for Cyclic Bending and Shear of RC Structure, I: Theory

Focus of Research

This paper presents a new finite-beam element for modelling the shear behaviour and its interaction with the axial force and the bending moment in RC beams and columns. This new element, based on the fiber section discretization, shares many features with the traditional fiber beam element to which it reduces, as a limit case, when the shear forces are negligible. The element basic concept is to model the shear mechanism at each concrete fiber of the cross sections, assuming the strain field of the section as given by the superposition of the classical plane section hypothesis for the longitudinal strain field with an assigned distribution over the cross section for the shear strain field. Transverse strains are instead determined by imposing the equilibrium between the concrete and the transverse steel reinforcement. The nonlinear solution algorithm for the element uses an innovative equilibrium-based iterative procedure. The resulting model, although computationally more demanding than the traditional fiber element, has proved to be very efficient in the analysis of shear sensitive RC structures under cyclic loads where the full 2D and 3D models are often too onerous.
The principal ingredients of this classical fiber element that have retained in the new model are as follows:

- Equilibrium-based integrals for the element solution;
- Fixed monitoring sections located at Gauss's points along the element;
- Fiber discretization for force and stiffness integration over the sections;
- Explicit algebraic constitutive relations for concrete and steel.

The new element, while incorporating the above features, differentiates from the previous element by having two additional strain fields to be monitored at each cross section, namely, the shear strain field and the lateral field. The shear strain field comes explicitly in the element formulation the lateral field has condensed statically at each section by imposing the equilibrium between transverse steel and concrete. For a 2D beam, the section strain and stress field vectors therefore read: $q(\xi) = (\varepsilon_0, \varphi, \gamma)$ and $p(\xi) = (N, M, T)$. Given the section strain vector $q(\xi)$, the fiber longitudinal and shear strains have found using suitable section shape functions.

Constant and parabolic shape functions have tested, with equally acceptable results in both cases. The strain of the i-th fiber found from the section kinematic variables $q(\xi)$ and the above-mentioned

hypotheses can therefore be written: $\varepsilon'_x(\xi) = \varepsilon_0(\xi) - \varphi(\xi)Y^i$ and $\varepsilon'_{xy}(\xi) = \frac{3}{2}\gamma(\xi)\left[1 - \left(\frac{Y^i}{H/2}\right)^2\right]$, where Y^i is the distance of the i-th fiber from the section centroid.

Since ε_x^i and ε_{xy}^i are found from the equations above, the strain in the transverse direction ε_y^i remains the only unknown. By imposing the equilibrium in the lateral direction, the 2D strain tensor at each concrete fiber $\varepsilon^i = (\varepsilon_x, \varepsilon_y, \varepsilon_{xy})$ therefore has found. When imposing the equilibrium between concrete and steel in the transverse direction, we can choose any solution within two extreme options, which are: (1) Impose equilibrium at each fiber separately; and (2) impose equilibrium over the whole section. The difference between the two approaches is that, in the second, there exists only one transverse steel fiber, compared with the first, where the transverse steel fibers are as numerous as the longitudinal concrete fibers subjected to its confinement action.

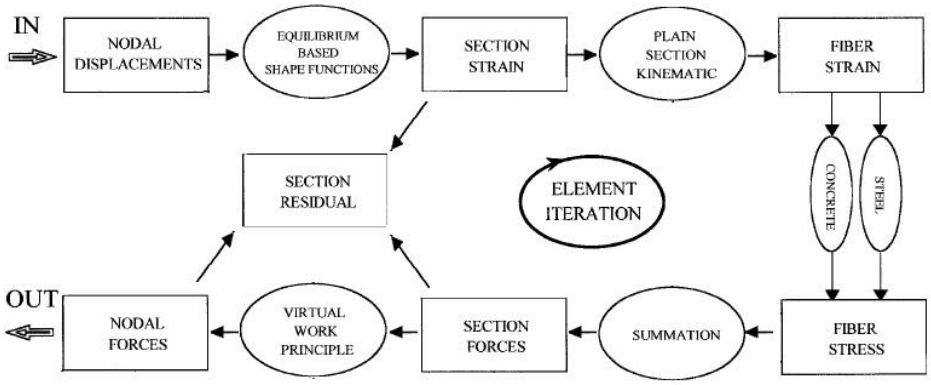

Figure 1.2.1.1 – Flow chart representing the approach

Obtained Results

Although much more complicated than the classical fiber model without shear flexibility and still retaining the basic limitations that are intrinsic to the beam theory, the proposed model appears to be capable of modelling the principal mechanisms of shear deformation and failure. It is also believed to represent a substantial step forward with respect to the current models based on truss, strut and tie analogies, which, apart from their grossly idealized mechanics, cannot account, on physical bases, for the interaction between axial, flexural, and shear responses. The model is capable of a good description of a broad range of existing test data, still keeping the input data and computational demand within acceptable limits.

1.2.2. Article 8

Authors: Marco Petrangeli

Journal: Journal of Engineering Mechanics, 1999

Title: Fiber Element for Cyclic Bending and Shear of RC Structure, II: Verification

Focus of Research

Following the general theoretical formulation discussed in the companion paper, *Petrangeli et al. 1999*, in this paper is performed a calibration and verification of the new fiber beam model with shear modelling using test data available from literature. A qualitative description of the section behaviour has also presented.

The stress-strain law used for the micro-plane normal "weak" component bases on the work of Mander et al. (1988). The skeleton curve in compression has the following expression: $s_k^w = \frac{f_{cc}\, x\, r}{r-1.0+x^r}$, where $x = \frac{e_k^w}{\varepsilon_{cc}}$, $r = \frac{E_c}{E_c - E_{sec}}$, $E_{sec} = \frac{f_{cc}}{\varepsilon_{cc}}$, f_{cc} is the peak strength, ε_{cc} the corresponding deformation and E_c is the initial elastic modulus. For the unloading branch, defining $(\varepsilon_{un}, \sigma_{un})$ the coordinates of the reversal point, the unloading branch is given by the expression: $s_k^w = \sigma_{un} - \frac{\sigma_{un}\, x\, r}{r-1.0+x^r}$, where $x = \frac{e_k^N - \varepsilon_{un}}{\varepsilon_{pl} - \varepsilon_{un}}$, $r = \frac{E_u}{E_u - E_{sec}}$, $E_{sec} = \frac{\sigma_{un}}{\varepsilon_{pl} - \varepsilon_{un}}$, E_u is the unloading tangent modulus at reversal, $\varepsilon_{pl} = \varepsilon_{un} - \frac{(\varepsilon_{un} + \varepsilon_a)\sigma_{un}}{\sigma_{un} + E_c \varepsilon_a}$ is the inelastic strain, ε_a is function of the maximum strain during the analysis. The reloading branch is linear elastic with a polynomial transition curve joining to the skeleton curve. For tensile branch of concrete: $s_k^w = E_c\, e_k^w \left(1 - e^{\left[-\left(e_k^w / e_1\right)^{P_1}\right]}\right)$, e_1 and p_1 are two parameters depending on the strength and fracture energy required.

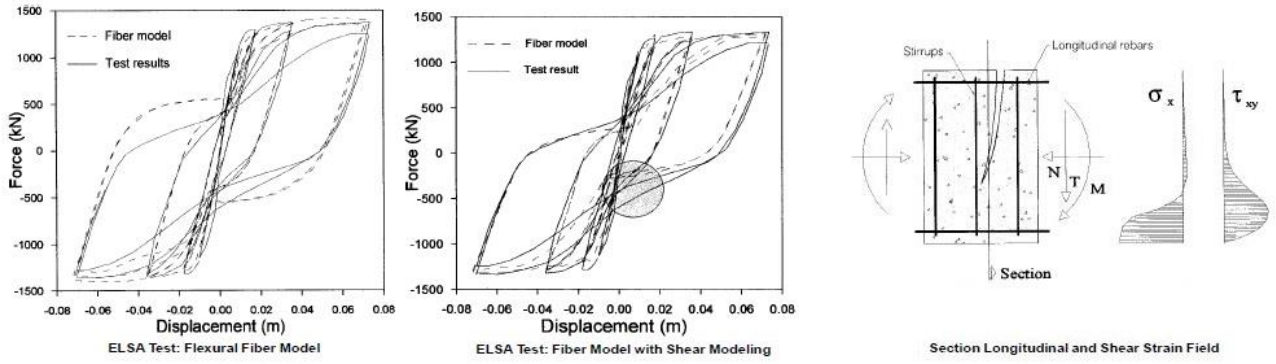

Figure 1.2.2.1 – Fiber model results compared with experimental results

The first proposed simulation refers to the uniaxial compression test by van Mier (1986). The prediction of the model's lateral response is fairly good, taking into account that in the post-peak regime these types of results are influenced by the structural response of the specimen and cannot be taken as representative of the materials' behaviour, even on a macro-scale. The second test refers to the combined compression-shear stress state; the failure envelope of the model compared with

the test results by Goode and Helmy (1967). Application of the shear strain causes, in the nonlinear regime, an increase of the axial force due to the dilatancy of the material, followed by a sudden drop in both shear and axial components when failure occurs. Finally, the model's biaxial failure envelope has compared with results by Kupfer and Gerstle (1973). In the tension-tension and compression-tension quadrants, the model response is very accurate. In the biaxial compression zone, the model failure envelope deviates from the experimental one. The stress-strain law for the longitudinal steel fibers bases on work of Menegotto and Pinto (1977).

The skeleton branch for the steel has divided in three parts: a linear elastic branch, a perfectly plastic one and a hardening branch. The hardening branch defines as: $\sigma_s = \sigma_{su} + (\sigma_y - \sigma_{su}) \left| \frac{\varepsilon_{su} - \varepsilon_s}{\varepsilon_{su} - \varepsilon_{sh}} \right|^p$, $P = E_{sh} \left(\frac{\varepsilon_{su} - \varepsilon_{sh}}{\sigma_{su} - \sigma_y} \right)$, ε_s and σ_s are current stress and strain in steel. Unloading and reloading branches defines instead by the following expression $\sigma_s = \sigma_0 + (\varepsilon_s - \varepsilon_0) E_m \left[Q + \frac{1-Q}{\left(1 + \left| E_m \frac{\varepsilon_s - \varepsilon_0}{\sigma_{ch} - \sigma_0} \right|^R \right)^{1/R}} \right]$, where ε_0 and σ_0 are the coordinates of the last reversal from the skeleton branch, E_m, is the initial modulus of elasticity at reversal, σ_{ch}, is a characteristic stress, Q is the ratio of the final tangent modulus to the initial one at reversal, and, R is a curvature parameter.

The analysis refers to columns that initially develop bending hinging, then significant shear deformations, and eventually fail. In these elements the interaction between axial, bending, and shear force is fundamental, as the bending both provides the initial cracking and activates the confining effect of the hoops caused by the lateral dilatancy of concrete. Examples presented are a single pier tested in the European Laboratory for Structural Assessment (ELSA) and those tested at the University of Rome "La Sapienza" (De Sortis and Nuti 1996). The numerical results found with the model reproduce the experimental findings. Piers showed a degraded strength and stiffness that had to be accounted in the numerical model, imposing two cycles at the same maximum amplitude, 20 mm, reached by the two specimens during the previous tests. Yield penetration and bond slip should be included in the model as they account for a large percentage in the flexural degradation of the specimens. Satisfactory prediction resulted also for RC beams.

1.2.3. Article 9

Authors: Pier Paolo Diotallevi, Luca Landi, Filippo Cardinetti

Journal: The 14th World Conference on Earthquake Engineering, 2008, Beijing, China

Title: A Fibre Beam Column Element for Modelling the Flexure-Shear Interaction in the Non-Linear Analysis of RC Structures

Focus of Research

The principal purpose of this research is to develop a fibre beam-column element able of describing the flexure-shear interaction and the shear response in the non-linear range.

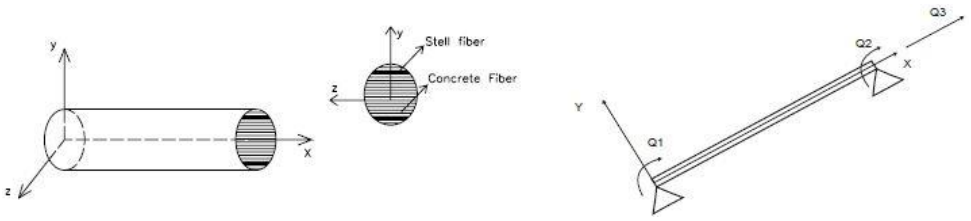

Figure 1.2.3.1 – Fiber model representation

The algorithm organizes in the following step:

1. Creation of initial stiffness structural matrix;
2. Use of load increment and Newton-Rapson iteration: each NR iteration indicated by i subscript;
3. Calculation of nodal element displacements trough a condensation and a rotation matrix;
4. Beginning of element state determination procedure: calculation of nodal forces. Each iteration of element state determination is indicated by a superscript j;
5. Calculation of section forces in control sections;
6. Calculation of section deformations;
7. Calculation of fibre deformations;
8. Beginning DSFM at fibre level. Each fibre characterized by a deformation $\varepsilon = [\varepsilon_x;\ \varepsilon_y = 0;\ \gamma_{xy}]$ Initially it assumed $\varepsilon = \varepsilon_c$. With application of Mohr circle, principal strains ε_1 and ε_2 for concrete are obtained. The average strains ε_{sx} and ε_{sy} for steel assumes equal to those of concrete along x and y axis. After calculating average stresses in concrete and steel through constitutive relations, local deformations in reinforcements ε_{sxcr} and ε_{sycr} on crack location calculated through an iterative procedure: $(\varepsilon_{sxcr} = \varepsilon_{sx} + \Delta\varepsilon_{1cr}\, cos^2\theta_\sigma)$ and $(\varepsilon_{sycr} = \varepsilon_{sy} + \Delta\varepsilon_{1cr}\, cos^2(\theta_\sigma - \frac{\pi}{2})$. At beginning $\Delta\varepsilon_{1cr} = 0$, then it increases at each iteration until subsequent equilibrium equation satisfies: $\rho_x(f_{sxcr} - f_{sx})cos^2\theta_\sigma + \rho_y(f_{sycr} - f_{sy})cos^2\left(\theta_\sigma - \frac{\pi}{2}\right) = f_{c1}$.

   Where stresses f_{sxcr} and f_{sycr} are functions of ε_{sxcr} and ε_{sycr} through constitutive relationship of steel. Then shear stress along crack surfaces are calculated: $v_{ci} = \rho_x(f_{sxcr} - f_{sx})\cos\theta_\sigma \sin\theta_\sigma + \rho_y(f_{sycr} - f_{sy})\cos\left(\theta_\sigma - \frac{\pi}{2}\right)\sin\left(\theta_\sigma - \frac{\pi}{2}\right)$, θ_σ is the angle of principal stresses. Being s_x and s_y crack spacing in x and y directions it is possible to determine the crack spacing s and the crack

width w: $s = \frac{1}{\frac{\sin\theta_\sigma}{s_x}+\frac{\cos\theta_\sigma}{s_x}}$, $w = \varepsilon_{c1}\, s$. Once calculated the shear slip, it is possible to evaluate γ_s and strain components due to shear slip ε_s; then strain components, $\varepsilon_c = \varepsilon - \varepsilon_s$, are obtained. Concerning ε_c, an iterative procedure begins, it stops when the difference between subsequent values are small enough. Reached the convergence, values of tangent modulus for the two principal directions are calculated form equations of constitutive laws; they are then introduced in diagonal matrices referred to principal directions. Rotation matrix allows passing from principal axes system to original one. The stiffness matrices of each fibre are assembled in order to obtain the modulus matrices E_s and E_c of all fibres. From these matrices, is possible to obtain the stiffness matrix of section;

9. Calculation of section resisting forces $\boldsymbol{D}_R^j(x)$;
10. Calculation of unbalanced section forces $\boldsymbol{D}_u^j(x) = \boldsymbol{D}^j(x) - \boldsymbol{D}_R^j(x)$;
11. Determination of section residual deformations;
12. Determination of residual nodal displacements, check of the convergence by energy criterion;
13. Calculation of resisting nodal forces $\boldsymbol{F}_R^i$ and of stiffness matrix of structure;
14. Calculation of unbalanced nodal forces $\boldsymbol{F}_u^i = \boldsymbol{P} - \boldsymbol{F}_R^i$ then check of the convergence at structural level.

Obtained Results

The proposed model has calibrated and validated through a comparison with experimental results, various numerical analyses have performed in order to study the influence of non-linear flexural-shear interaction. Analyses underlined that the model was able to reproduce flexure and shear non-linear response and above all, the coupling between flexure and shear in the non-linear range. This aspect did affect significantly the response of examined squat reinforced concrete structural elements, especially in terms of deformation.

1.2.4. Article 10

Authors: Luca Martinelli

Journal: ACI Structural Journal, 2008

Title: Modelling Shear-Flexure Interaction in Reinforced Concrete Elements Subjected to Cyclic Lateral Loading

Focus of Research

This paper presents a beam-column fiber element able to describe the interaction between the bending moment, the axial and shear forces. In RC elements, shear forces are due to many complex interacting mechanisms, involving a significant part of the volume of the element; in this work, however, these are considered in an independent way and are modelled mainly at a cross section level. Each structural member is discretized in fiber elements and the stress-strain history for both steel and concrete is evaluated throughout the analysis by means of uniaxial constitutive laws at different positions within selected cross sections.

This approach bases on the consideration that, even if shear effects actually spread throughout the element, the shear-flexure interaction is more pronounced in limited zones, for example, the fixed-end region in a cantilever. Only regions where the shear-flexure coupling takes place, both for strength and stiffness, are modelled with the proposed fiber model. This strategy aims to reduce the computational effort in view of the application to seismic problems, recalling that the purpose of the element is rather to capture the behaviour of a relevant portion of the structural element than to model its complex local mechanics. The limited length of the fiber element facilitates the choice of the shape functions and allows the adoption of a stiffness-based approach that, in turn, eliminates the need for the iteration at the element level in the state determination phase, and is therefore convenient from the computational point.

The shear force is computed in the cross section by superposition of several contributions. The most important are due to the truss and the arch mechanisms and are reproduced with mechanical models coupled with the behaviour in bending of the element and depending only on the mechanical properties of the materials and geometric parameters. The truss is oriented as in the classical truss analogy, and comprises the transverse reinforcement and two concrete diagonals, reproducing the tensile strength of the concrete. This avoids the need to identify which diagonal is in compression and allows for the presence of only one truss for cyclic loading also. The model for the arch effect, coupling the axial force with bending, can be, in principle, also adopted for an element kinematics different from the one chosen herein.

The other main characteristic of this approach is the uniaxial constitutive relation for concrete, which involves that the principal direction of the compressive stress rotates during the analysis to account for the arch action, and thus it may be non-normal to the cross section.

In this stiffness-based element, which adopts the Timoshenko beam theory, shear and flexural behaviour are linked by means of kinematical assumptions. In bending, differently from standard fiber elements, the cross-sectional fibers have the direction of the compressive principal stress, not aligned with the element longitudinal axis. This accounts for the contributions to shear strength due to both the arch action and the inclined thrust-line developing in squat elements.
The nonlinear behaviour of materials described by means of appropriate constitutive relations.

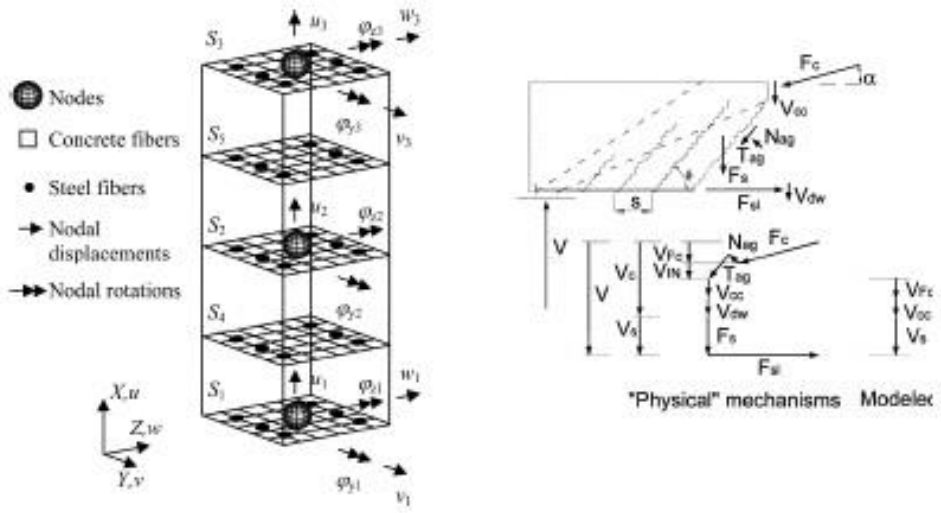

Figure 1.2.4.1 – Model approaching

Obtained Results

Despite the limitations, the overall performance shows that the proposed element is able to represent the experimental response in selected test cases, strongly influenced by shear. A limited number of elements is required and the computational efficiency allows for the study of the dynamic behaviour of complete three-dimensional structures with very short computer times. This aspect is of interest in view of the diffusion that nonlinear analysis has gained in seismic design regulations.

1.3. Experimental Studies

1.3.1. Article 11

Authors: Pawan R. Gupta and Michael P. Collins

Journal: ACI Structural Journal, 2001

Title: Evaluation of Shear Design Procedures for RC Members under Axial Compression

Focus of Research

To understand better the response of reinforced concrete members subjected to combined axial compression, shear, and moment, 24 reinforced concrete elements were tested. The parameters that changed from specimen to specimen were the ratio of compression-to-shear N/V, the concrete strength f_c', the specimen width b, and the amount of shear reinforcement ρ_z.
During loading, equal and opposite moments have applied at each end of the specimen. In each experiment, the axial load, the moment, and shear force have increased proportionally up to failure.

Obtained Results

Failures were classified as either shear failures, expected to occur on diagonal planes sloping from the ends of the specimens towards the middle of the specimen, or flexural failures, expected near the ends of the specimens where the moment was highest. Eighteen of the specimens had classified as having failed in shear, while six of them in flexure.
For these six specimens, the longitudinal reinforcement yielded and the moment at the ends of the specimens, M_E, approximately equalled or exceeded the predicted failure moment M_o. Priestley and Park have reported that for members under high compression, confinement can increase flexural capacity by more than 30%; for one specimen the ratio M_E/M_o reached 1.19. Even for the flexural failures, the final failure involved opening of significant diagonal cracks as is typical of shear failures.

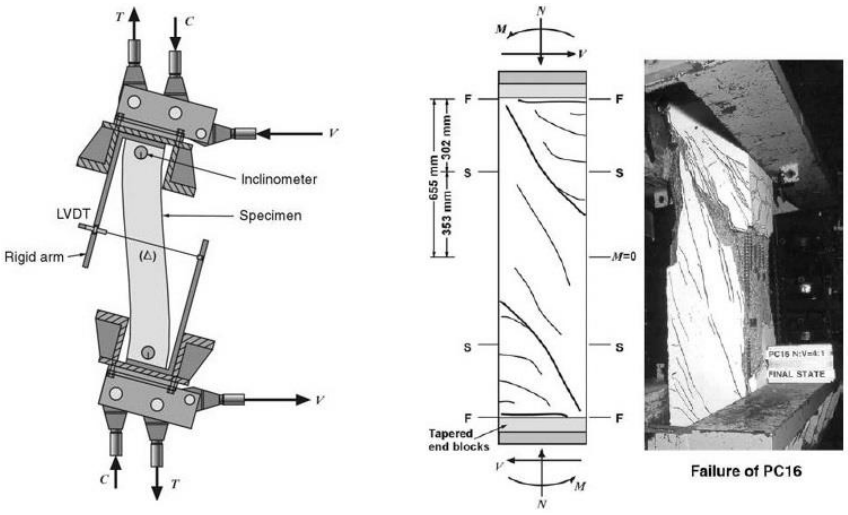

Figure 1.3.1.1 – Testing machine and main results

The shear stresses at failure for the 24 specimens had compared. Based on concrete strengths and amount of shear reinforcement, the specimens can be divided into six groups. Within each group, the shear stress at failure increases as the compression-shear loading ratio N/V is increased from 0 to 4, then stays approximately constant or decreases from 4 to 8.

Three of the groups have the same amount of shear reinforcement but have different concrete strengths. For each loading ratio, as the concrete strength increases from 43 to 60 MPa, the shear stress at failure increases, from 60 to 86 MPa stays constant or decreases.

Wider specimens, more representative of concrete walls, typically failed at a lower shear stress than the comparable narrower specimens. For what concerns the influence of the ratio of N/V on the load-deformation response and crack development for very similar specimens, when there was no axial compression, the response was very ductile. Flexural cracks initiated at the ends of the member at approximately 20% of the maximum load. Some of the flexural cracks developed into flexural-shear cracks when the load reached 40% of the maximum. At 2/3 of the maximum, new diagonal cracks inclined at approximately 25 degrees to the vertical formed. As the load was further increased, new diagonal cracks formed and existing cracks widened. The loading stopped when the shear reached 490 kN because the 50 mm displacement was near the limit of the equipment; at this stage, the largest diagonal crack was more than 3 mm wide. The application of compression increased the stiffness of the members by suppressing the formation of cracks until higher levels of load. Thus, when the axial compression was four times the shear, flexural cracks at the ends of the member did not form until 35% of the failure load, while small flexural-shear cracks developed at approximately 60% of failure load. Even at 90% of the failure load, there were relatively few cracks. The specimen failed at 680 with the opening of a diagonal crack inclined at approximately 12 degrees to the vertical. For the specimens loaded with very high ratios of compression-to-shear, no significant cracking appeared until just prior to failure, at which vertical splitting cracks appeared in the flexural compression zones near the ends of the members. Specimens failed in a very violent way with the formation of a new nearly vertical diagonal crack, which perhaps started from the existing vertical splitting cracks.

The specimen loaded at a compression-to-shear ratio of 20, failed at only 52% of the failure shear of Specimen with N/V equal to 8. A large amount of shear reinforcement caused the members loaded at low compression-to-shear ratios to display a very ductile response, and the specimens at intermediate levels of compression-to-shear to show some ductility. This amount of shear reinforcement, however, was not sufficient to prevent the very brittle response of elements loaded at high levels of compression-to-shear. Increasing the amount of shear reinforcement can significantly increase both the strength and ductility of the specimen. Under higher levels of compression, however, the beneficial effects of shear reinforcement reduced considerably.

For the 10 specimens that failed in shear and were loaded with compression-shear ratios of between 3 and 6, the failure shear was, on average, only 68% of the detailed ACI value. The simple ACI expression for V_c was found to give more consistent predictions for shear strength and mode of failure. Experimental tests demonstrated that the AASHTO-LRFD method gave the most accurate estimates of the failure shear.

1.3.2. Article 12

Authors: Liping Xie, Evan C. Bentz, and Michael P. Collins

Journal: ACI Structural Journal, 2011

Title: Influence of Axial Stress on Shear Response of Reinforced Concrete Elements

Focus of Research

Many structures contain members subjected to significant axial and shear forces. There is strong disagreement between different code provisions concerning the influence of axial stress on shear strength. This research clarifies the effect of both axial compression and axial tension on shear response. To examine this influence, six nominally identical reinforced concrete panels, representing web regions of girders or walls, were loaded under different combinations of shear stress and uniaxial compression or tension. This enabled, for the first time, to experimentally determine the interaction between the shear strength and longitudinal axial stress of such elements. In the paper, the experimentally determined influence of axial stress on shear response was compared with the predictions of shear strength expressions given by the ACI, the Canadian and the European Code, along with the shear strength and response predictions made by the MCFT.
The tested specimens were made of reinforced concrete with strengths of approximately 40 MPa, with dimensions of 890 x 890 mm square and 73 mm thick, specific amount of reinforcements both in longitudinal and transversal direction. The loads were applied to the specimens in a monotonic and proportional manner, meaning that the axial stress, f_x, and shear stress, v, both simultaneously increased at a fixed ratio, f_x/v. The specimens were loaded until they failed by concrete crushing, reinforcement rupturing, or sliding on an existing crack.

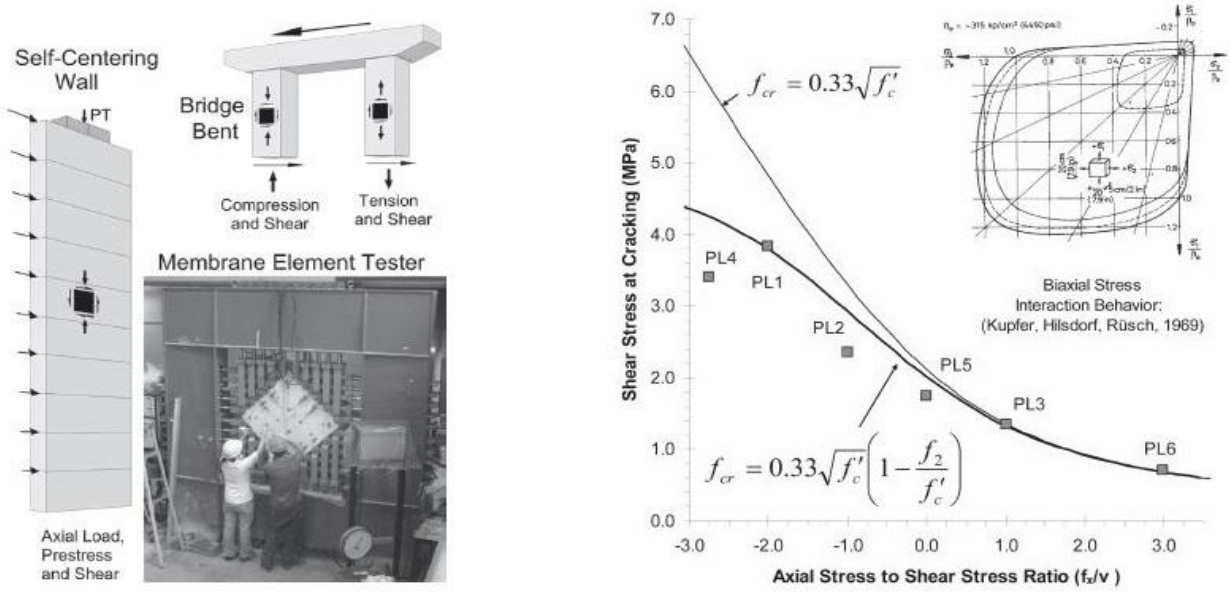

Figure 1.3.2.1 – Testing machine and comparison of results

Obtained Results

The experimental tests showed that specimens with f_x/v ratios of +1.0, 0.0, and -1.0 all failed at approximately the same shear stress v_u, indicating only a small effect of axial stress, f_{xu}, on shear strength. The element with the highest tension, failed by rupture of both the transverse and longitudinal reinforcement. The two specimens with higher compression-to-shear ratios, failed by sudden crushing of the concrete.

For the members subjected to pure shear or shear and tension, the peak shear stress occurred at a shear strain of approximately 1%, whereas for the compression and shear specimens, the shear strains at peak shear stress were smaller. In terms of post-peak response, the most gradual loss of resistance was for specimens with f_x/v ratios of +1.0, 0.0, and -1.0.

The longitudinal strain at peak shear stress is only compressive for the most highly compressed specimen. For all the others, the strain is tensile with strains increasing as the loading ratio becomes more tensile. Only for element with the highest tension, the longitudinal strain in the longitudinal reinforcement exceed the yield strain.

The transverse strain at peak stress considerably exceeded the longitudinal strain and was in excess of the yield strain for all specimens, except the highly compressed one, which reached 98% of the yield strain. The calculated principal compressive strain ε_2, compression positive, was highest for the members resisting the highest shear stress and considerably smaller than the strain at peak stress for the cylinders even for the specimens that failed by diagonal crushing.

For the two highest compression-to-shear ratios, these load-deformation predictions were reasonable, whereas for the other axial load levels, they were excellent.

The results demonstrated that the application of the basic ACI shear approach could significantly overestimate both the beneficial effect of compression, both the disadvantageous effect of tension on shear strength. The ACI simple expression for the benefits of compression gave excellent predictions, whereas the simple expression for tension was very conservative. The CSA shear provisions, based on the modified compression field theory, provided the best code-based estimates of the shear strength. The full MCFT provided not only the best estimates of conditions at failure, including failure shear stresses and failure crack angles for the full range of axial stresses, but also provided predictions of the complete load-deformation response of the elements, although the prediction is not as good for higher axial compression levels.

1.3.3. Article 13

Authors: Matthew T. Smith, Daniel A. Howell, Mary Ann T. Triska, and Christopher Higgins

Journal: ACI Structural Journal, 2014

Title: Effects of Axial Tension on Shear-Moment Capacity of Full-Scale Reinforced Concrete Girders

Focus of Research

Many cast-in-place reinforced concrete deck-girder bridges remain in the national inventory, and routine bridge evaluations have conducted to ensure operational performance. Many of these bridges exhibit varying degrees of diagonal-tension cracking in the girders and bent caps. Diagonal-tension cracks have attributed to the design practice at the time, which overestimated the concrete contribution to shear resistance and resulted in poorly detailed flexural reinforcement as well as increasing service load magnitudes and volume. Current codes for rating and evaluation of bridges permit analysts to neglect axial force effects due to temperature and shrinkage effects when calculating load ratings for bridge components with well-distributed reinforcement. The proportions and details of many older bridges, however, are unlikely considered well detailed; moreover, this definition is not clearly established. To develop new data on the influence of axial load on the shear-moment behaviour of reinforced concrete girders, experimental tests have performed using seven full-scale realistically proportioned girders with straight-bar cut-offs and light shear reinforcement to study the role of externally applied axial tension on shear-moment capacity. Specimens were loaded to failure, with varying amounts of axial tension applied in combination with vertical load. Results showed that axial tension and the presence of flexural cut-offs reduced member stiffness and strength. Using these results, different analytical and design methods have compared.

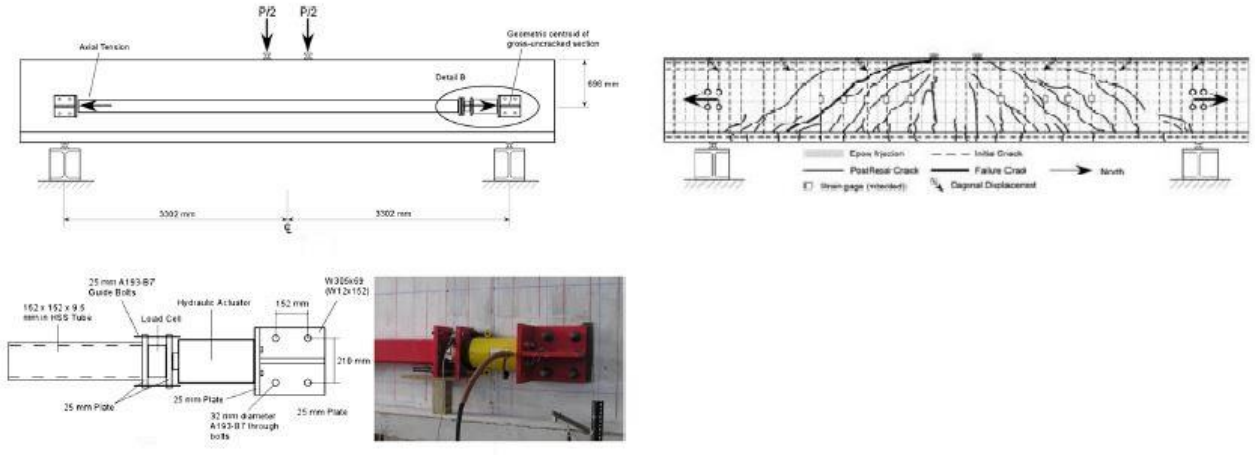

Figure 1.3.3.1 – Tested elements

Obtained Results

Based on the experimental observations and analysis results, the following conclusions presented:

1. Presence of axial tension reduced global member stiffness and its shear-moment capacity;

2. Flexural reinforcement cut-offs in the flexural tension region combined with axial tension, reduced global member stiffness, but not significantly the shear-moment capacity of the specimens beyond that resulting from axial tension alone;
3. Applied axial tension reduced the magnitude of vertical load required to initiate diagonal cracking and more vertically oriented diagonal expected to occur in the field of tension stresses combined with live and dead load ones than those produced by live and dead loads alone;
4. Axial load applied in proportion to and simultaneously with transverse load, further reduced the magnitude of the transverse load required to initiate diagonal cracking;
5. Presence of axial tension tended to reduce specimen capacity below that considering shear and flexure alone. This may indicate lower reserve strength for in-place bridge members that have shrinkage- and temperature-induced axial tensions than previously considered;
6. R2K slightly overestimated shear capacity of specimens for axial tension forces of 890 kN, and underestimated capacity for the higher tension force level;
7. AASHTO LRFD (2013) and ACI 318-11 methods underestimated shear capacity for axial tension forces at or below 1334 kN;
8. Nonlinear finite element analyses captured the general behaviour from axial tension loading, but given the modelling assumptions considered, it underestimated shear capacity and mid-span displacement;
9. Present ACI 318 methods for discounting the concrete contribution to shear strength in the presence of axial tension stresses were quite conservative over the range of parameters considered;
10. The inclination of diagonal cracks in the field may be an indicator of the presence of shrinkage- or temperature-induced axial stress, or both, in the members with steeper crack angles, indicating higher axial tension stress;
11. For the poorly detailed flexural anchorage in the present study, there was not a significant change in the member strength compared with an otherwise similar specimen.

2. The Modified Compression Field Theory

2.1. Theoretical Approach

2.1.1. Introduction

The theoretical approach of the Modified Compression Filed Theory focuses on the response of rectangular reinforced concrete elements subjected to in-plane shear and axial stresses, which corresponds to membrane state of stress.

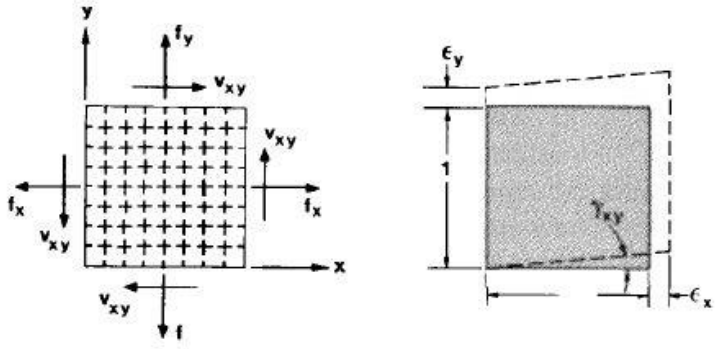

Figure 2.1.1.1 – Membrane element considered in the Modified Compression Field Theory

It has assumed of uniform thickness, relatively small size, containing an orthogonal grid of steel reinforcement with the longitudinal and transverse axes coincident with the directions of the reference axes.

Considered loads consist of uniform axial stresses, f_x and f_y, and uniform shear stresses, v_{xy}. They are assumed acting on the edges of the element, which remain straight and parallel also after deformation. The two normal strains, ε_x and ε_y, and the shear strain, γ_{xy}, describe the deformed shape of the membrane element.

This approach aims to determine how the three in-plane stresses relate to the corresponding in-plane strain. To solve the problem, the following additional assumptions have made:

1. For each strain state there exists only one corresponding stress state; the loading history cannot influence the problem, situations not respecting this assumption will not be considered;

2. Stresses and strain appear as average values when taken over areas or distances large enough to include several cracks;
3. The concrete and steel bars are perfectly bounded together at boundaries of the element;
4. Longitudinal and transversal rebar are distributed uniformly over the element.

Tensile stresses and strain appears as positive quantities while compressive ones as negative.

The model bases on equilibrium, compatibility and stress-strain relationship, formulated in terms of average stresses and average strain. The cracked concrete is treated as a new material, having its own stress-strain relationship, determined by testing thirty reinforced concrete panels under a variety of uniform biaxial stresses, including pure shear.

2.1.2. Compatibility Conditions

Assuming that steel reinforcements are perfectly anchored to the concrete, requires that any deformation experienced by the concrete element must be matched by an identical deformation of the reinforcements:

$$\varepsilon_{sx} = \varepsilon_{cx} = \varepsilon_x$$

$$\varepsilon_{sy} = \varepsilon_{cy} = \varepsilon_y$$

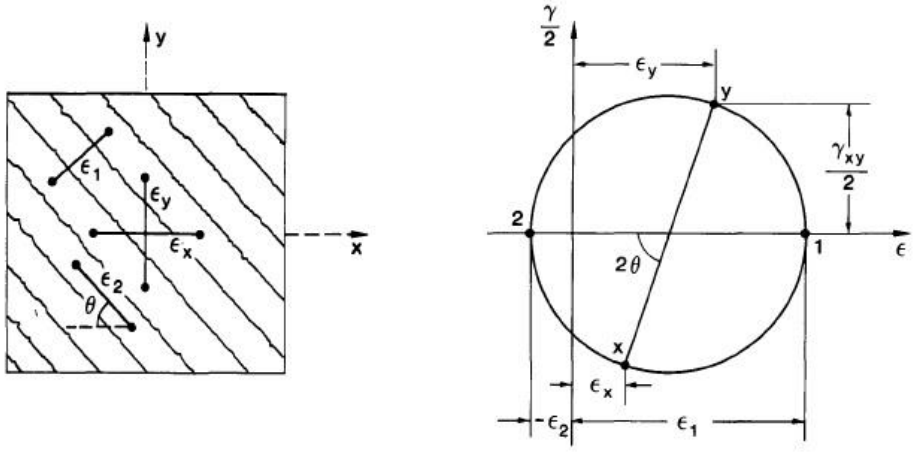

Figure 2.1.2.1 – Average strains in the concrete and corresponding Mohr's circle

Knowing the three strain components, ε_x, ε_y, and γ_{xy}, the strain in any other direction derives from the geometry of Mohr's circle, which gives the following relationships:

$$\gamma_{xy} = \frac{2(\varepsilon_1 - \varepsilon_2)}{\tan\theta}$$

$$\varepsilon_x + \varepsilon_y = \varepsilon_1 + \varepsilon_2$$

$$tan^2\theta = \frac{\varepsilon_x - \varepsilon_2}{\varepsilon_y - \varepsilon_2} = \frac{\varepsilon_1 - \varepsilon_y}{\varepsilon_1 - \varepsilon_x} = \frac{\varepsilon_1 - \varepsilon_y}{\varepsilon_y - \varepsilon_2} = \frac{\varepsilon_x - \varepsilon_2}{\varepsilon_1 - \varepsilon_x}$$

Where ε_1 and ε_2 are respectively principal tensile and compressive strain.

2.1.3. Equilibrium Conditions

The forces applied to the reinforced concrete element are resisted by stresses in the concrete and stresses in the steel reinforcement. To respect equilibrium conditions, the sum of acting forces has to be equal to zero both in x and y directions.

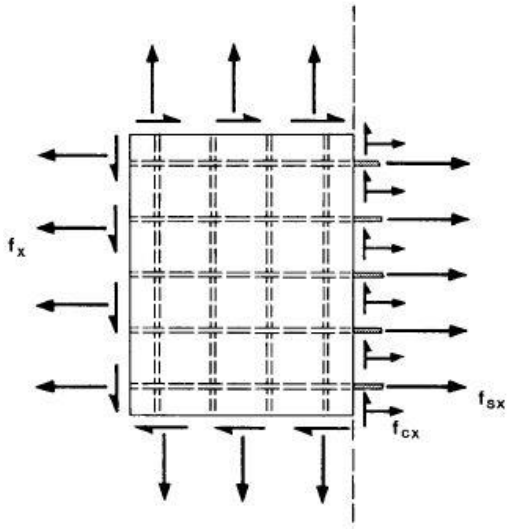

Figure 2.1.3.1 – Free-body diagram of part of the element

$$\int_A f_x \, dA = \int_{A_c} f_{cx} \, dA_c + \int_{A_s} f_{sx} \, dA_s$$

Assuming that the small reduction in the concrete cross-section area, due to the presence of steel reinforcements, is negligible, the equation turns into the following one.

$$f_x = f_{cx} + \rho_{sx} \, f_{sx}$$

Similar relationships can derive for the equilibrium of normal stresses in y direction and for shear stresses.

$$f_y = f_{cy} + \rho_{sy} \, f_{sy}$$

$$\nu_{xy} = \nu_{cx} + \rho_{sx} \, \nu_{sx}$$

$$\nu_{xy} = \nu_{cy} + \rho_{sy} \, \nu_{sy}$$

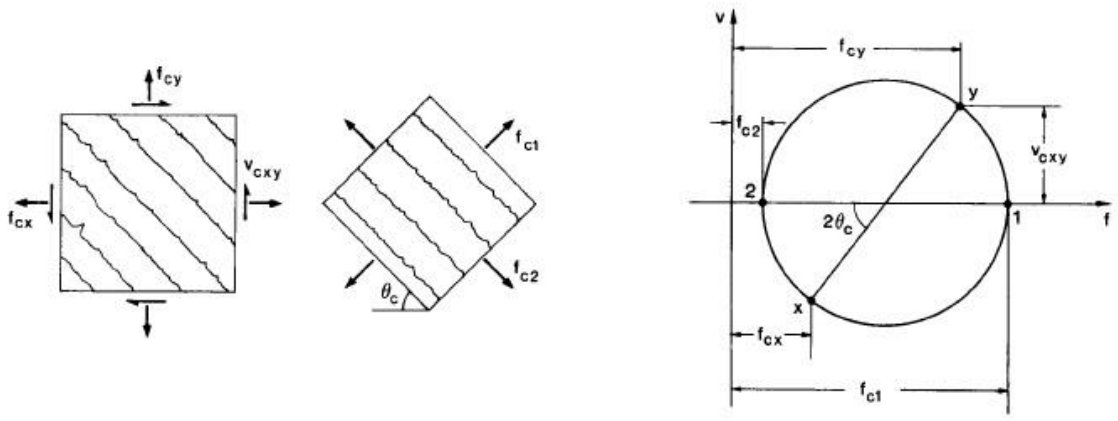

Figure 2.1.3.2 – Average and principal stresses and corresponding Mohr's circle

Assuming that shear stresses in the concrete in x direction, v_{cx}, and those in y direction, v_{cy}, are equal, the stress condition in the concrete is fully defined if f_{cx}, f_{cy} and v_{cxy} are known. From the geometry of Mohr's circle, the following useful relationship derive.

$$f_{cx} = f_{c1} - \frac{v_{cxy}}{\tan\theta_c}$$

$$f_{cy} = f_{c1} - v_{cxy} * \tan\theta_c$$

$$f_{c2} = f_{c1} - v_{cxy}\left(\tan\theta_c + \frac{1}{\tan\theta_c}\right)$$

2.1.4. Constitutive Laws

Constitutive relationships link average stresses to average strains, both for reinforcements and for concrete.

The axial stress in the steel bars is assumed to depend only on the axial strain in the reinforcement. It is further assumed that average shear stress resisted by the steel rebar, on the plane normal to reinforcement, is null. The bilinear uniaxial stress-strain relationship is adopted.

$$f_{sx} = E_s * \varepsilon_x \leq f_{yx}$$

$$f_{sy} = E_s * \varepsilon_y \leq f_{yy}$$

$$v_{sx} = v_{sy} = 0$$

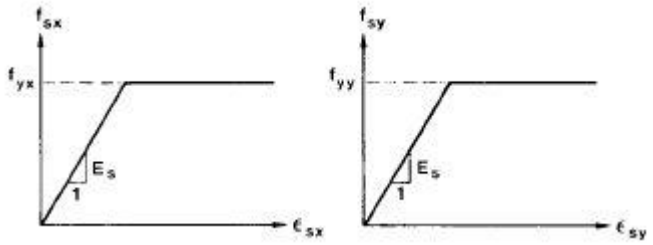

Figure 2.1.4.1 – Stress-strain relationships for reinforcement

Concerning the concrete, the principal stresses axes and principal strain one, assume coincident.

$$\theta_c = \theta$$

2.1.5. Average Stress-Average Strain Response of Concrete

To obtain average stress-average strain relationship of concrete, an experimental program conducted on thirty reinforced concrete elements. In the test, known values of stress applied to the reinforced concrete, resulting specimen strains measured.

From experimental program resulted the directions of principal strain deviates somewhat from the directions of principal stresses; however, it is a reasonable simplification to assume they are coincident.

The principal compressive stress in the concrete, f_{c2}, resulted function of both the principal compressive strain, ε_2, both the corresponding principal tensile strain, ε_1. The relationship suggested is the following.

$$f_{c2} = f_{c2,max}\left[2\left(\frac{\varepsilon_2}{\varepsilon_c'}\right) - \left(\frac{\varepsilon_2}{\varepsilon_c'}\right)^2\right]$$

Where:

$$\frac{f_{c2,max}}{f_c'} = \frac{1}{0.8 - 0.34\,\frac{\varepsilon_1}{\varepsilon_c'}} \leq 1.0$$

The term ε_c' is negative quantity usually set equal to -0.002; thus, increasing ε_1, reduces $f_{c2,max}/f_c'$. The relation between the average principal tensile stresses in the concrete and average principal strain is nearly linear prior cracking, then shows decreasing values of f_{c1} for increasing values of ε_1. The relationship suggested before cracking is:

$$f_{c1} = E_c\,\varepsilon_1$$

After cracking:

$$f_{c1} = \frac{f_{cr}}{1 + \sqrt{200\,\varepsilon_1}}$$

2.1.6. Transmitting Loads across Cracks

Formulations mentioned in previous paragraphs, deal with average values of stresses and strain, they do not give information about local variations. At crack, tensile stresses in reinforcement are higher than average, while midway between cracks, they are lower. On the other hand, concrete tensile stresses are null in correspondence of the crack and higher than the average midway between cracks. These local variations have to be accounted because ultimate capacity may closely depend on the reinforcement ability to transmit tension across cracks.

Since external applied stresses f_x, f_y and v_{xy} are fixed, the two sets of stresses shown in the figure has to be statically equivalent.

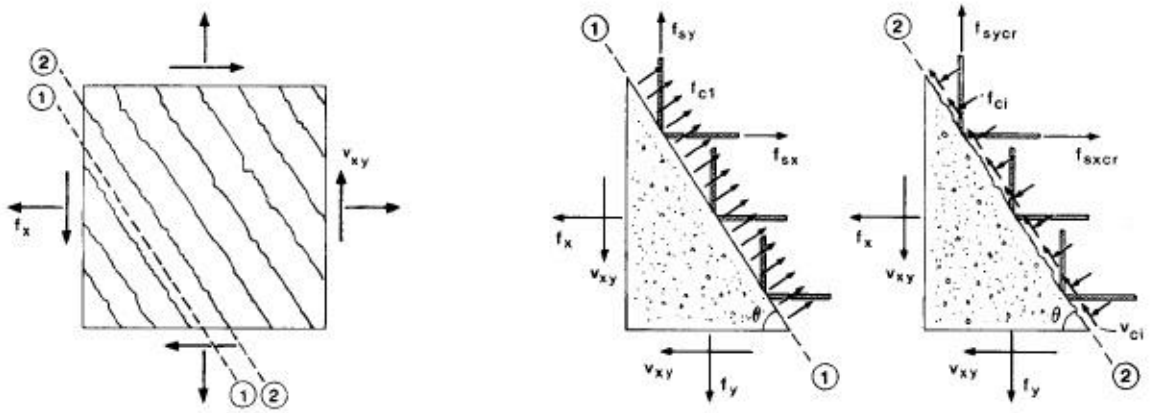

Figure 2.1.6.1 – Comparison between local stresses at crack and average calculated stresses

Considering unit areas, the requirement that the two sets of stresses produce the same force in x and y directions correspond to the following conditions:

$$\rho_{sx}\, f_{sx}\, \sin\theta + f_{c1}\, \sin\theta = \rho_{sx}\, f_{sx,cr}\, \sin\theta - f_{ci}\, \sin\theta - v_{ci}\, \cos\theta$$

$$\rho_{sy}\, f_{sy}\, \cos\theta + f_{c1}\, \cos\theta = \rho_{sy}\, f_{sy,cr}\, \cos\theta - f_{ci}\, \cos\theta + v_{ci}\, \sin\theta$$

Simplifying:

$$\rho_{sx}\left(f_{sx,cr} - f_{sx}\right) = f_{c1} + f_{ci} + \frac{v_{ci}}{\tan\theta}$$

$$\rho_{sy}\left(f_{sy,cr} - f_{sy}\right) = f_{c1} + f_{ci} - v_{ci}\, \tan\theta$$

These two equilibrium equations can be satisfied without shear and compressive stresses at crack, only if:

$$\rho_{sx}\left(f_{sx,cr} - f_{sx}\right) = \rho_{sy}\left(f_{sy,cr} - f_{sy}\right) = f_{c1}$$

Where:

$$f_{sx,cr} \le f_{yx}$$

$$f_{sy,cr} \le f_{yy}$$

Therefore, if calculated average stresses in reinforcement is higher than the yielding strength, it is not possible to satisfy the equation.

In such cases, to satisfy equilibrium, shear stresses are required. The relationship between the shear across the crack, v_{ci}, the crack width, w, and the required compressive stress on the crack, f_{ci}, was experimentally determined through several investigation. Based on Walraven's work, the following relationship derived:

$$v_{ci} = 0.18\, v_{ci,max} + 1.64\, f_{ci} - 0.82\, \frac{{f_{ci}}^2}{v_{ci,max}}$$

Where:

$$v_{ci,max} = \frac{\sqrt{-f_c'}}{0.31 + 24\frac{w}{a+16}}$$

$$w = \varepsilon_1 \, s_\theta$$

$$s_\theta = \frac{1}{\frac{\sin\theta}{s_{mx}} + \frac{\cos\theta}{s_{my}}}$$

The term, a, corresponds to the maximum aggregate size expressed in millimetres, s_{mx} and s_{my} are the indicators of crack control characteristics of the reinforcement in x and y directions, stresses are expressed in MPa.

2.2. Implementation of the MCFT

The Modified Compression Field Theory was implemented on Excel in order to create the interaction domain of axial and shear force.

2.2.1. Problem Definition

First, the considered problem has to be defined in terms of geometrical and material properties. Information required are the following.

Geometrical properties:

1. The dimension of the cross section of the element as b, the base, multiplied by h, the height;
2. The reinforcement ratios in x and y direction, ρ_{sx} and ρ_{sy}, corresponding to:

$$\rho_{sx} = \frac{A_{stirr}}{A_{conc}} = \frac{A_{stirr}}{b\ h} = \frac{n°_{transv,bars} * A_{bar}}{b\ h}$$

$$\rho_{sx} = \frac{A_{long}}{A_{conc}} = \frac{A_{long}}{b\ h} = \frac{n°_{long,bars} * A_{bar}}{b\ h}$$

Material properties:

3. Characteristic and design compressive concrete strength, f_{ck} and f_{cd};
4. Design tensile concrete strength, f_{ctd};
5. Characteristic and design tensile steel strength, f_{yk} and f_{yd};
6. Concrete Young's modulus, E_c;
7. Steel Young's modulus, E_s;
8. Maximum dimension of the aggregate size expressed in millimetres, a.

Set those quantities, it is possible to evaluate the average spacing of cracks perpendicular to the x reinforcement, s_{mx}, and the average spacing of cracks perpendicular to the y reinforcement, s_{my}, as follows:

$$s_{mx} = 1.5 * maximum\ distance\ from\ x - bar$$

$$s_{my} = 1.5 * maximum\ distance\ from\ y - bar$$

The crack spacing depends on these two terms:

$$s_\theta = \frac{1}{\frac{\sin\theta}{s_{mx}} + \frac{\cos\theta}{s_{my}}}$$

The crack width is a function of both the crack spacing and the principal tensile strain:

$$w = \varepsilon_1\, s_\theta$$

It is moreover possible to compute the concrete strain at crack:

$$\varepsilon_{cr} = \frac{f_{ctd}}{E_c}$$

2.2.2. Input Data

Input data required to solve the problem, correspond to the desired stress state on the reinforced concrete element, which are σ_x, σ_y and τ_{xy}.
For a fixed state of stress acting on the whole reinforced concrete element, the approach calculates strains and stresses both in the concrete and in the steel.

2.2.3. Iterative Procedure

2.2.3.1. First Iteration

The first iterations begins defining standard, fixed values of the strain components ε_x, ε_y and γ_{xy}. They should be all set equal to zero, but the iteration could not start assuming a null strain state. This is the reason why, as first guess values, only two of three components are set equal to zero, ε_x and ε_y; the remaining one, γ_{xy}, defines as a very small value, close to zero, which could be *0.00001*.

The procedure also requires the first guess value of principal tensile and compressive stresses, f_1 and f_2; they are both fixed equal to *0.0001*.

Once established these quantities, is then possible to evaluate the corresponding Mohr's circle by computing the following parameters:

1. The radius of the circle:

$$R = \frac{\sqrt{(\gamma_{xy})^2 + (\varepsilon_y - \varepsilon_x)^2}}{2}$$

2. The centre of the Mohr's circle:

$$C = \frac{\varepsilon_y + \varepsilon_x}{2}$$

3. Principal tensile strain:

$$\varepsilon_1 = C + R$$

4. Principal compressive strain:

$$\varepsilon_2 = C - R$$

5. Angle between the compressive strut and the horizontal direction, expressed in radians:

$$\theta = \frac{\tan^{-1}\left(\frac{\gamma_{xy}}{\varepsilon_y - \varepsilon_x}\right)}{2}$$

6. The complementary angle:

$$\theta_{comp} = \pi - \theta$$

7. The concrete Young's modulus resulting from the principal tensile state of stress:

$$E_{c1} = E_c \qquad if \quad |f_2| \leq 0.001$$

$$E_{c1} = \frac{f_1}{\varepsilon_1} \qquad if \quad |f_2| > 0.001$$

8. The concrete Young's modulus resulting from the principal compressive state of stress:

$$E_{c2} = E_c \qquad if \quad |f_2| \leq 0.001$$

$$E_{c1} = \frac{f_2}{\varepsilon_1} \qquad if \quad |f_2| > 0.001$$

9. The shear concrete modulus:

$$G_c = \frac{E_{c1}\, E_{c2}}{E_{c1} + E_{c2}}$$

10. The elasticity modulus of the steel in x direction:

$$E_{sx} = 200 \qquad if \quad \varepsilon_x = 0.000$$

$$E_{sx} = \frac{1}{\varepsilon_x}\left(min\left[200\, \varepsilon_x; f_{yd}\right]\right) \qquad if \quad \varepsilon_x \neq 0.000$$

11. The elasticity modulus of the steel in y direction:

$$E_{sy} = 200 \qquad if \quad \varepsilon_y = 0.000$$

$$E_{sy} = \frac{1}{\varepsilon_y}\left(min\left[200\, \varepsilon_y; f_{yd}\right]\right) \qquad if \quad \varepsilon_y \neq 0.000$$

12. The concrete matrix in principal direction:

$$D_c = \begin{bmatrix} E_{c2} & 0 & 0 \\ 0 & E_{c1} & 0 \\ 0 & 0 & G_c \end{bmatrix}$$

13. The steel matrix:

$$D_s = \begin{bmatrix} E_{sx}\,\rho_{sx} & 0 & 0 \\ 0 & E_{sy}\,\rho_{sy} & 0 \\ 0 & 0 & 0 \end{bmatrix}$$

14. The transformation matrix:

$$T = \begin{bmatrix} \cos\theta^2 & \sin\theta^2 & (\cos\theta * \sin\theta) \\ \sin\theta^2 & \cos\theta^2 & (-\cos\theta * \sin\theta) \\ (-2\cos\theta\sin\theta) & (2\cos\theta\sin\theta) & (\cos\theta^2 - \sin\theta^2) \end{bmatrix}$$

15. The load vector:

$$l = \begin{bmatrix} \sigma_x \\ \sigma_y \\ \tau_{xy} \end{bmatrix}$$

16. The full stiffness matrix:

$$K_{tot} = (T^T\, D_c\, T) + D_s$$

17. Since the product of the total stiffness matrix and the strain vector is equal to the load vector, the strain components can be determined as the product of the inverse full stiffness matrix and the load vector, which are known:

$$\begin{bmatrix} \varepsilon_x \\ \varepsilon_y \\ \gamma_{xy} \end{bmatrix} = (K_{tot})^{-1} * l$$

Knowing the new vector of strain components, the new Mohr's circle derives.

18. Evaluate the radius, R^{interm}, and the centre, C^{interm}, of the new Mohr's circle, the principal tensile strain, ${\varepsilon_1}^{interm}$, and compressive strain, ${\varepsilon_2}^{interm}$, and the angle of the compressive strut, θ^{interm}, using same formulae of steps from 1 to 5.

From the new Mohr's circle is possible to derive state of stress of both the steel and the concrete.

19. Estimate the state of stress in reinforcement in x direction, both in the elastic case and beyond the yield limit:

$$\sigma_{sx} = 200\,\varepsilon_x \qquad if\ \sigma_{sx} \le f_{yd}$$

$$\sigma_{sx} = f_{yd} \qquad if\ \sigma_{sx} > f_{yd}$$

20. Calculate the state of stress in reinforcement in y direction, both in the elastic case and beyond the yield limit:

$$\sigma_{sy} = 200\,\varepsilon_y \qquad if\ \sigma_{sy} \le f_{yd}$$

$$\sigma_{sy} = f_{yd} \qquad if\ \sigma_{sy} > f_{yd}$$

21. Evaluate the maximum principal compressive stress:

$$f_{c2,max} = \frac{f_{cd}}{0.8 - 0.34\frac{{\varepsilon_1}^{interm}}{{\varepsilon_c}'}} = \frac{f_{cd}}{0.8 - 0.17\,{\varepsilon_1}^{interm}} \le f_{cd}$$

Hence, if the maximum principal compressive stress, $f_{c2,max}$, is higher than the compressive strength of the concrete, f_{cd}, the maximum principal compressive stress has to be set equal to f_{cd}.

22. Compute the principal compressive stress in the concrete:

$$f_{c2} = f_{c2,max}\left[2\left(\frac{{\varepsilon_2}^{interm}}{{\varepsilon_c}'}\right)+\left(\frac{{\varepsilon_2}^{interm}}{{\varepsilon_c}'}\right)^2\right]$$

23. Calculate the principal tensile stress in the concrete:

$${f_{c1}}^{computed} = {\varepsilon_1}^{interm}\, E_c \qquad if\ \ {\varepsilon_1}^{interm} \le \varepsilon_{cr}$$

$${f_{c1}}^{computed} = \frac{f_{cr}}{1+\sqrt{200\ {\varepsilon_1}^{interm}}} = \frac{f_{ctd}}{1+\sqrt{0.5\ {\varepsilon_1}^{interm}}} \qquad if\ \ {\varepsilon_1}^{interm} > \varepsilon_{cr}$$

24. The value of the principal tensile stress has to be limited by means of several crack checks.

In correspondence of the cracking of concrete, reinforcement in both x and y directions generate additional reserve capacities, which can be determined by means of the following relationship:

$$f_{reserve}^{x-steel} = \rho_{sx}(f_{yd} - \sigma_{sx})$$

$$f_{reserve}^{y-steel} = \rho_{sy}(f_{yd} - \sigma_{sy})$$

The first crack check correspond to the biaxial yielding:

$$f_{check}^{1} = f_{reserve}^{x-steel}\ \sin\theta^{interm\,2} + f_{reserve}^{y-steel}\ \cos\theta^{interm\,2}$$

In order to make the remaining check, the following quantities need to be computed:

$$f_{check}^{2a} = \frac{\left|f_{reserve}^{x-steel} - f_{reserve}^{y-steel}\right|}{\tan\theta^{interm} + \frac{1}{\tan\theta^{interm}}}$$

$$v_{ci,max} = \frac{\sqrt{f_{cd}}}{0.31 + 24\frac{w}{a+16}}$$

$$f_{check}^{2b} = f_{reserve}^{x-steel} + \frac{min\left[v_{ci,max}; f_{check}^{2a}\right]}{\tan\theta^{interm}}$$

$$f_{check}^{2c} = f_{reserve}^{y-steel} + min\left[v_{ci,max}; f_{check}^{2a}\right]\ \tan\theta^{interm}$$

The final value of the principal tensile stress defines as the minimum between the calculated value, ${f_{c1}}^{computed}$, f_{check}^{1}, f_{check}^{2b} and f_{check}^{2c}:

$$f_{c1} = min\left[{f_{c1}}^{computed};\ f_{check}^{1};\ f_{check}^{2b};\ f_{check}^{2c}\right]$$

All parameters necessary to compute the new Mohr's circle and, consequently, the new stress in x and y directions and shear stress, are defined. The following equations conclude the first iteration.

25. The new Mohr's circle defines through its radius and its centre:

$$R = \frac{f_{c1} - f_{c2}}{2}$$

$$C = \frac{f_{c1} + f_{c2}}{2}$$

26. The new state of stress in the concrete follows:

$$\sigma_x{}^{1st\ iter.} = C - R\ \cos(2\theta) + \rho_{sx}\sigma_{sx}$$

$$\sigma_y{}^{1st\ iter.} = C + R\ \cos(2\theta) + \rho_{sy}\sigma_{sy}$$

$$\tau_{xy}{}^{1st\ iter.} = R\ \sin(2\theta)$$

2.2.3.2. Following Iterations

The iterations that follow the first one proceed through the same steps listed in the previous paragraph. What changes are initial strain components and the initial values for principal tensile and compressive stresses: in the first iteration were assumed the strain state approximately null and both the tensile and compressive principal stress equal to *0.0001*. The following iterations begin using the state of strain and principal stresses, equal to the final values of the previous iteration.

The procedure terminates when the state of stress computed by means of the MFCT, in terms of $\sigma_x{}^{n-th\ iter.}$, $\sigma_y{}^{n-th\ iter.}$, $\tau_{xy}{}^{n-th\ iter.}$, converges to the desired state of stress, defined at the beginning of the procedure as input datum.

To conclude, the Modified Compression Field Theory is an iterative procedure, which evaluates the strain state and the state of stress in both the steel reinforcements both in the concrete of a reinforced concrete cross-section, for a desired applied stress, σ_x, σ_y and τ_{xy}.

2.3. N.T Interaction Domain based on MFCT

The Modified Compression Field Theory was used to build up the axial force-shear force interaction domain.

The interaction domain was built defining, by means of a trial and error approach, those state of stress which produce a principal tensile stress, f_1, equal to the tensile strength of concrete, f_{ctd}.

Since this study mainly focuses on reinforced concrete columns, the states of stress considered are characterised by one of the two normal stresses equal to zero; thus, to build the interaction domain of a generic column, the input datum concerning the stress in x direction, σ_x, is always null.

Let us consider a specific value of the desired normal stress in y direction:

$$\sigma_y = 1$$

To construct the N-T interaction domain, the desired tangential stress has to be changed, through a trial and error approach, since the resulting principal tensile stress equals the tensile strength of the concrete, f_{ctd}.

Using the Excel spreadsheet, one of the couple (σ_y, τ_{xy}), which generates the tensile strength of concrete as principal tensile stress is the following:

$$\sigma_y{}^{(i)} = 1 \ MPa$$

$$\tau_{xy}{}^{(i)} = 0.0701 \ MPa$$

Once defined the state of stress corresponding to the development of cracks, is then possible to determine the corresponding axial force, N, and shear stress, T, which correspond to one point of the interaction domain, by integrating over the cross-section area the two stresses.

Considering rectangular cross sections, the corresponding axial force is:

$$N^{(i)} = \sigma_y{}^{(i)} * A_{cls} = \sigma_y{}^{(i)} * (bh)$$

Concerning the shear force, the Jourawsky's relationship is used, hence:

$$T^{(i)} = \frac{\tau_{xy}{}^{(i)} \ I \ b}{S}$$

Where, I is the moment of inertia, b corresponds to the width and S represents the static moment of the cross section.

In case of rectangular cross-section element, the equation simplifies:

$$T^{(i)} = \frac{2}{3} \tau_{xy}{}^{(i)} \ b \ h$$

The point whose coordinates are $N^{(i)}$ and $T^{(i)}$, belongs to the outer limit of the interaction domain for the considered column.

To draw the entire domain this procedure has to be repeated for several values of $\sigma_y{}^{(i)}$.Therefore, for $\sigma_y{}^{(i)}$ varying from $+f_{ctd}$ to $-f_{cd}$, at step interval equal to 1, the corresponding $\tau_{xy}{}^{(i)}$, generating a principal tensile stress equal to the tensile strength of the considered concrete, were evaluated.

For each couple $(\sigma_y{}^{(i)}, \tau_{xy}{}^{(i)})$, the corresponding $(N^{(i)}, T^{(i)})$, was estimated.

Thus, the axial force-shear force domain was defined.

3. Mohr's Theory to Construct the Interaction Domains

3.1. Construction of N-T Domain

Interaction domains have created basing on the Mohr's theory.
The objective was to identification of those states of stress, in terms of normal and tangential stresses, generating a principal tensile stress equal to the design tensile strength of the considered concrete. To this purpose, a relationship has defined: for different values of tangential stresses, the equation gives the corresponding normal one such that the principal tensile stress equals the tensile strength of the concrete.
In order to determine this equation, a generic Mohr's circle was considered. Given that this research focuses on columns, the considered stress states are characterised by one normal stress equal to zero, the one in the direction perpendicular to the axis of the column. This involves that the generic state of stress on the Mohr's plane is always identified by a couple of points, whose, one of them, lays on the vertical axis.

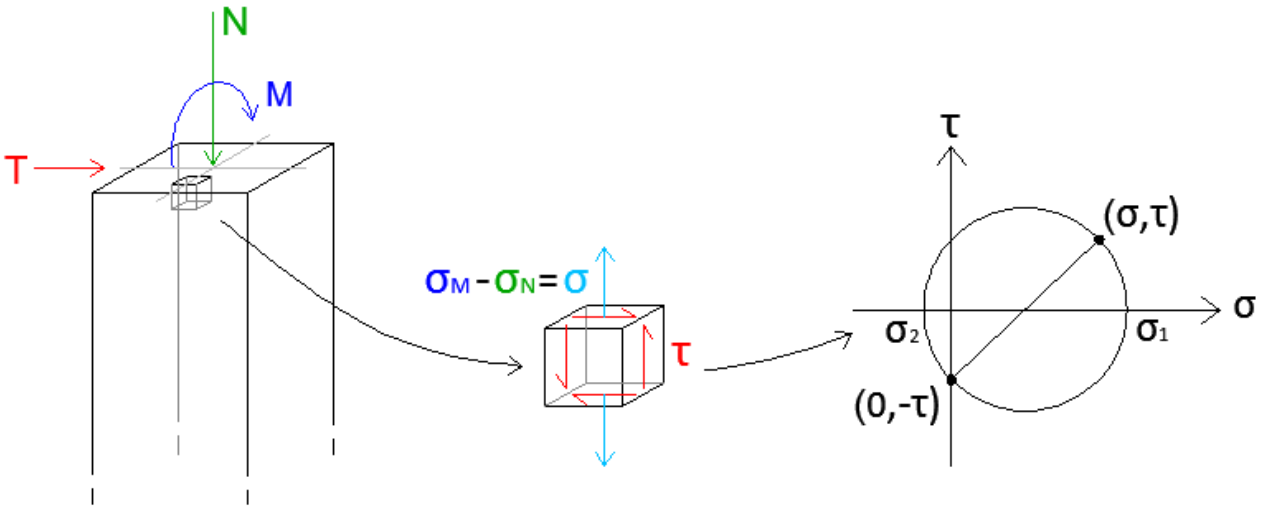

Figure 3.1.1 – Generic state of stress considered

The equation has to impose the principal tensile stress, σ_1, coincident with the tensile strength of concrete, f_{ctd}; it also has to be expressed as a function of the stress state acting on the element, σ_x and τ_{xy}. This concept can be obtained by observing that the radius of the circle can be defined as a function of the acting stress state, σ_x and τ_{xy}, but also depending only on σ_x and σ_1.

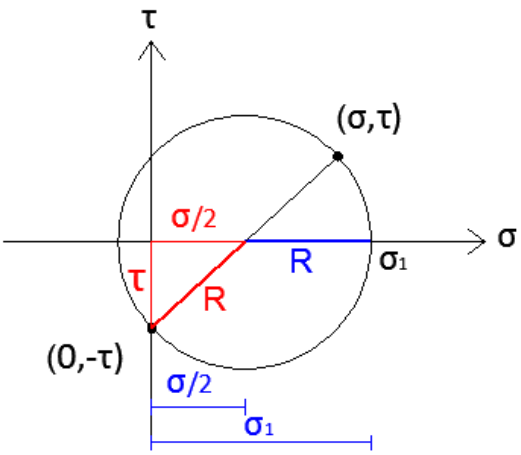

Figure 3.1.2 – Geometrical evidences

The equation at the base of the construction of the interaction diagram using the Mohr's theory was obtained as follows:

$$\begin{cases} R = \sqrt{{\tau_{xy}}^2 + \left(\frac{\sigma_x}{2}\right)^2} \\ R = \sigma_1 - \frac{|\sigma_x|}{2} \end{cases}$$

Equating the two formulation of the radius:

$$\sqrt{{\tau_{xy}}^2 + \left(\frac{\sigma_x}{2}\right)^2} = \sigma_1 - \frac{|\sigma_x|}{2}$$

$${\tau_{xy}}^2 + \frac{{\sigma_x}^2}{4} = \left(\sigma_1 - \frac{|\sigma_x|}{2}\right)^2$$

$${\tau_{xy}}^2 + \frac{{\sigma_x}^2}{4} = {\sigma_1}^2 - 2\,\frac{|\sigma_x|}{2}\,\sigma_1 + \frac{{\sigma_x}^2}{4}$$

$${\tau_{xy}}^2 + \frac{{\sigma_x}^2}{4} - \frac{{\sigma_x}^2}{4} + |\sigma_x|\,\sigma_1 - {\sigma_1}^2 = 0$$

$${\tau_{xy}}^2 + |\sigma_x|\,\sigma_1 - {\sigma_1}^2 = 0$$

$$|\sigma_x|\,\sigma_1 = {\tau_{xy}}^2 + {\sigma_1}^2$$

$$|\sigma_x| = \frac{{\sigma_1}^2 - {\tau_{xy}}^2}{\sigma_1}$$

$$|\sigma_x| = \sigma_1 - \frac{{\tau_{xy}}^2}{\sigma_1}$$

As previously mentioned, the states of stress belonging to the limit surface of the N-T domain are those producing a principal tensile stress, σ_1, equal to the tensile strength of the concrete, f_{ctd}. Hence, in the equation, f_{ctd} has to replace σ_1.

The equation at the base of the construction of the N-T domain is the following:

$$|\sigma_x| = f_{ctd} - \frac{{\tau_{xy}}^2}{f_{ctd}}$$

It can be also:

$$\tau_{xy} = \sqrt{{f_{ctd}}^2 - |\sigma_x| f_{ctd}}$$

Varying τ_{xy}, the relationship returns the corresponding value of σ_x such that, stress states defined by the couple (σ_x, τ_{xy}) generate σ_1 equal to f_{ctd}.

The set of couples $({\sigma_x}^{(i)}, {\tau_{xy}}^{(i)})$ defines the interaction domain in terms of stresses, not forces.
To obtain the N-T diagram, stresses need to be integrated on the cross section area of the element considered. For what concerns the axial force the integration consists in multiplying the normal stress by the cross section area of the column. For rectangular elements:

$$N^{(i)} = {\sigma_x}^{(i)} * A_{cls} = {\sigma_x}^{(i)} * (bh)$$

Concerning the shear force, Jourawsky's formulae was employed to move from stresses to forces. The relationship between tangential stresses and shear force given by Jourawsky is the following:

$$\tau_{xy} = \frac{T\,S}{I\,b}$$

Where:

- T is the shear force related to tangential stress τ_{xy};
- S corresponds to the static moment of the cross section;
- I represents the moment of inertia of the element;
- b is the base of the cross section.

Jourawsky's equation solved for T:

$$T = \frac{\tau_{xy}\,I\,b}{S}$$

Considering a rectangular cross section element the formulae simplifies:

$$T = \frac{\tau_{xy}\,b\,h^3}{6\left(\frac{h^2}{4} - y^2\right)}$$

With:

- h is the height of the cross section;

- y corresponds to the y-coordinate of the fiber considered with respect to the centroid.

Considering the fiber in correspondence of the centroid where tangential stresses reach the maximum value, the equation simplifies further:

$$T = \frac{2}{3}\,\tau_{xy}\,b\,h$$

Thus, to pass from the generic tangential stress, $\tau_{xy}{}^{(i)}$, to the shear force, $T^{(i)}$, the formulation employed is the following one:

$$T^{(i)} = \frac{2}{3}\,\tau_{xy}{}^{(i)}\,b\,h$$

The set of couples $(N^{(i)}, T^{(i)})$ defines the axial force-shear force interaction domain.

3.1.1. Matlab Implementation

The procedure explained in the previous paragraph, aimed at constructing the interaction domain of axial and shear forces, was implemented on the software Matlab.

3.1.1.1. Problem Definition

The first step consists in the definition of the considered problem, which means geometrical properties and material ones. Information required are the ones that follow.
Geometrical properties:

- b, the base of the cross section of the structural element considered;
- h is the height of the cross section;
- c, the clear cover of steel reinforcement;

Properties of the material:

- f_{cd} corresponds to the design compressive strength of the concrete;
- f_{ctd} is the design tensile strength of the concrete.

Once established those parameters, it is possible to compute some relevant quantities depending on them.
The maximum tensile and compressive axial force directly depend on the cross section area and design strength of the concrete:

$$N_{c,max} = f_{cd}\,b\,h$$

$$N_{t,max} = f_{ctd}\,b\,h$$

Those two terms define the boundaries of the interaction domain.

Boundaries has to be imposed also on tangential stresses: the maximum value for τ_{xy} is the one corresponding to the highest compressive normal stress, $\sigma_x = f_{cd}$. It derives from the equation mentioned in the previous paragraph:

$$\tau_{xy,max} = \sqrt{{f_{ctd}}^2 - |f_{ctd}| f_{ctd}}$$

The minimum value of tangential stress correspond to $\tau_{xy,min} = -\tau_{xy,max}$.

3.1.1.2. Formulae Implementation

As previously explained, the equation that correlates normal to tangential stresses, producing principal tensile stress equal to the tensile strength of concrete, is the following:

$$|\sigma_x| = f_{ctd} - \frac{{\tau_{xy}}^2}{f_{ctd}}$$

To construct of the N-T domain, τ_{xy} has to vary from $\tau_{xy,min}$ to $\tau_{xy,max}$; for each value of τ_{xy}, the code has to evaluate the corresponding σ_x, by means of the equation just mentioned.

This can be obtained through a for-cycle with τ_{xy} changing from its minimum value to its maximum one. Since Matlab-for-cycles work only with positive and integer values, in the script, τ_{xy} varies from 0 to $\tau_{xy,max}$, then the domain is reflected with respect to the x-axis.

To translate the interaction domain in terms of stresses to the one in terms of forces, the following formula implemented:

$$N = \sigma_x \, b \, h$$

$$T = \frac{2}{3} \, \tau_{xy} \, b \, h$$

Two additional points added to close the domain corresponding to $(N_{c,max}, 0)$ for the portion of domain resulting from positive values of $T^{(i)}$, $(N_{c,max}, 0)$ for the portion of domain resulting from negative values of $T^{(i)}$.

At the end, the plot of the vector N, for normal forces, as a function of vector T, shear forces.
The script also plots a point whose coordinates corresponds to the axial force and the shear force acting on the considered column: if the point falls inside the domain, the element is verified, otherwise is not.

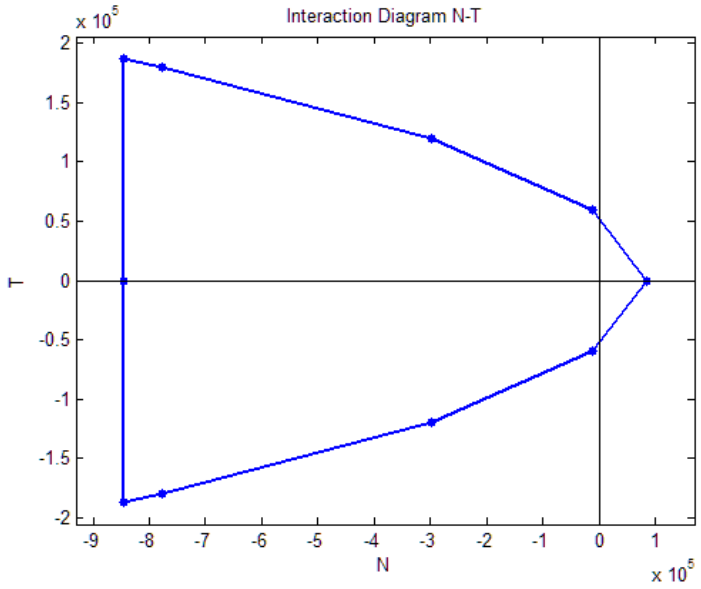

Figure 3.1.1.2.1 – Generic N-T interaction domain using Matlab

3.1.2. Construction of the N-T domain for a Real Column

The construction of N-T domain applied to real cases. One of them, a column in the Policlinic of Modena, which showed a noticeable crack at the top of the element, inclined of 45° to the horizontal, typical of shear failures.

The column was characterised by the following geometrical and material properties.
Geometrical properties:

- b equal to 300 mm;
- h equal to 300 mm;

Material properties:

- f_{cd}, from laboratory tests, 9.4 $\frac{N}{mm^2}$;
- f_{ctd}, assumed $\frac{1}{10}$ the compressive strength of the concrete, therefore 0.94 $\frac{N}{mm^2}$;

For tangential stress, τ_{xy}, varying from the maximum value, $\tau_{min} = 0.00\ \frac{N}{mm^2}$, to the maximum value, corresponding to $\sigma_{c,max} = -9.4\ \frac{N}{mm^2}$, at step interval of 0.2, normal stresses were evaluated through the formula:

$$|\sigma_x| = f_{ctd} - \frac{{\tau_{xy}}^2}{f_{ctd}}$$

Knowing the couples $\left({\sigma_x}^{(i)}, {\tau_{xy}}^{(i)}\right)$, producing principal tensile stresses equal to $0.9437\frac{N}{mm^2}$, to move to shear and axial forces the formulae employed:

$$N^{(i)} = {\sigma_x}^{(i)} * (bh)$$

$$T^{(i)} = \frac{2}{3}\,{\tau_{xy}}^{(i)}\,b\,h$$

Numerical results listed in the following table.

${\tau_{xy}}^{(i)}$ $[N/mm^2]$	${\sigma_x}^{(i)}$ $[N/mm^2]$	$T^{(i)}$ $[N]$	$N^{(i)}$ $[N]$
± 0.0	0.940	± 0	84600
± 0.5	0.674	± 30000	60660
± 1.0	-0.124	± 60000	-11145
± 1.5	-1.454	± 90000	-130860
± 2.0	-3.315	± 120000	-298379
± 2.5	-6.000	± 150000	-540000
± 3.0	-8.634	± 180000	-777102
± 3.2	-9.400	± 181683	-849330

Table 2.2.1 – Axial and shear force values for the construction of the N-T domain

Plotting those values on a diagram having axial force on the x-axis and shear force on the y-axis, the result is the N-T interaction domain for the considered column.

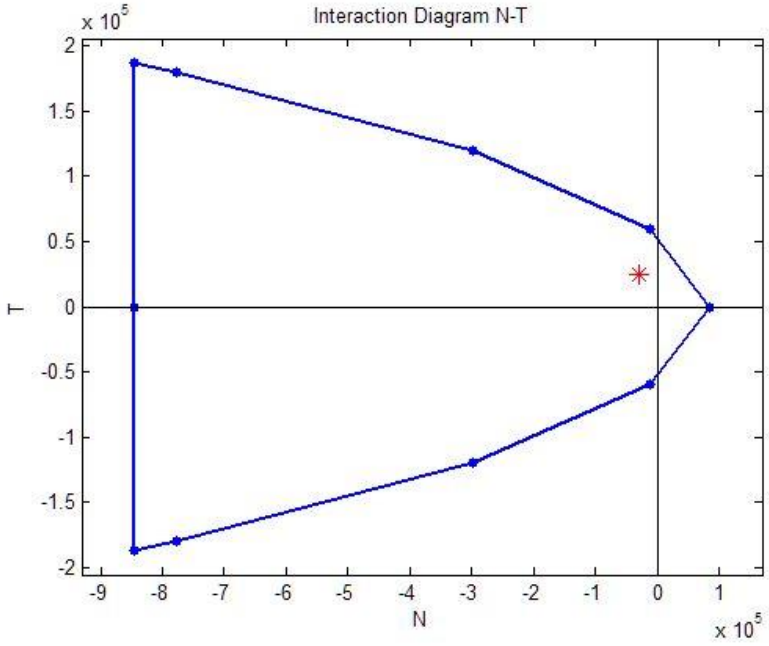

Figure 3.1.2.1 – N-T interaction domain for the column of the Policlinic of Modena

The figure above shows the interaction domain for the column of the Policlinic of Modena. The red asterisk corresponds to the acting forces on the considered column; as it can be observed from the image, it falls inside the domain. This means that, also considering the interaction between the axial force and shear force, the column results verified for the solicitation acting on it.

3.2. Construction of N-T-M Domain

Once considered the interaction between the axial force and the shear, the further step consists in detecting the interaction between axial force, shear and bending moment.

The presence of the bending moment has considered through two simplification.
The first one models the acting bending moment as two concentrated forces, applied on the cross section at a distance equal to a half of the base of the element, one of them producing traction, the other producing compression. This correspond to a constant tensile stress on a half of the cross section, followed by a constant tensile stress on the remaining half cross section, having same magnitude equal to the acting moment divided by the distance between the application points.

The second simplification founds on Navier's formula for state of stresses corresponding to the simultaneous action of axial force and bending moment, and Jourawsky's formulation for shear tangential stresses.

3.2.1. Stress-Block distribution of Normal Stresses due to Bending

The strongest simplification models the bending moment as two concentrated forces: one producing traction and the other one compression. They apply at a half cross-section of the element; the application points lays on the centroid of the two half cross-sections, which means that the distance of the concentrated forces results:

$$d = 2\,\frac{h}{4} = \frac{h}{2}$$

The two concentrated forces, applied at a distance d, one producing traction and the other compression, are characterised by the same magnitude defined as follows:

$$F_T^{M_{act}} = F_C^{M_{act}} = \frac{M}{d} = \frac{M}{\frac{h}{2}} = \frac{2\,M}{h}$$

This first modelling considers the generic column subjected to a certain external axial force, a specific external shear, a half of the cross section subjected to an additional traction force equal to $F_T^{Mact}$and the other half submitted to a compression force, F_C^{Mact}.

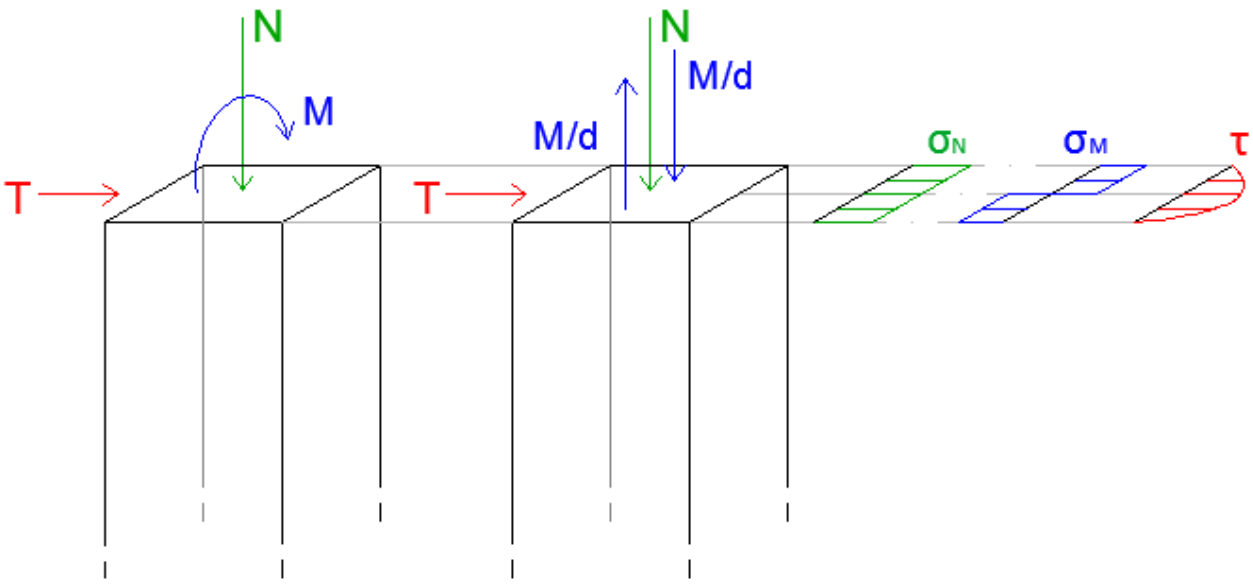

Figure 3.2.1.1 – Stress-block distribution of normal stresses due to bending

The two half cross-sections are separately considered.

3.2.1.1. Half Cross-Section Subjected to Traction Force related to the Moment

The element considered in the paragraph is the one in the figure below.

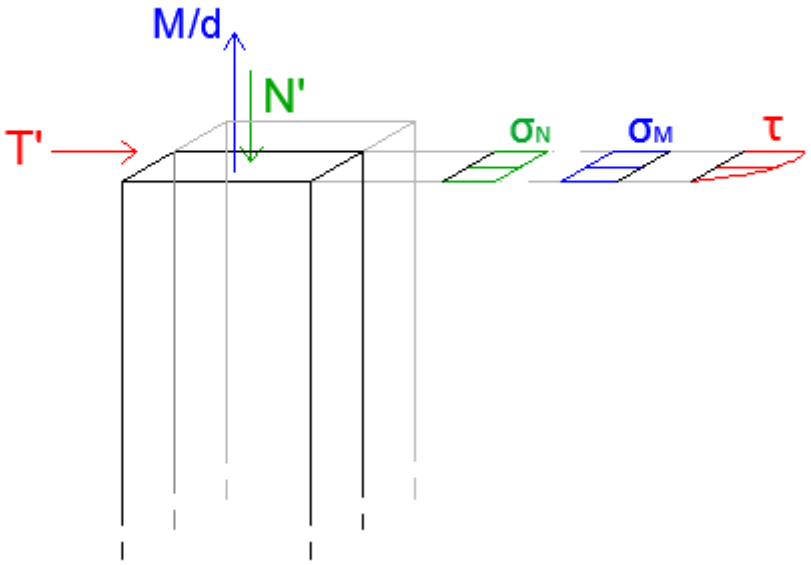

Figure 3.2.1.1.1 – Half cross-section under the traction force related to the bending moment

The half cross section is subjected to an external shear force, T, an applied axial force, N, and the traction force due to the bending moment, $F_T^{M_{act}}$.

Considering an infinitesimal portion of the element at the centroid of the half cross section, it is subjected to tangential stresses, τ_{xy}, produced by T, normal stresses, σ_x, related to the difference between $F_T^{M_{act}}$ and N.

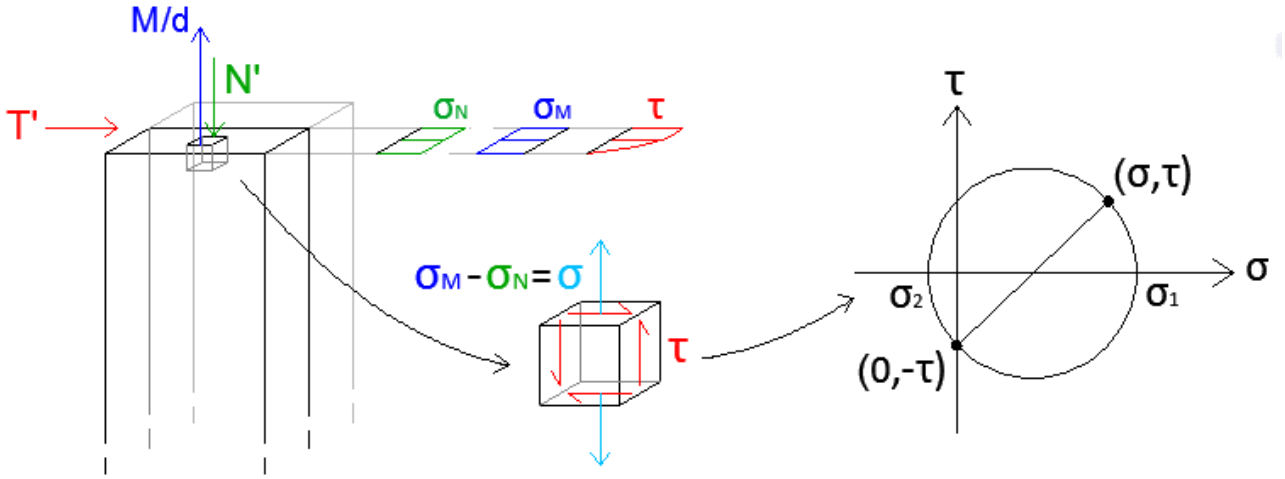

Figure 3.2.1.1.2 – Infinitesimal element subjected to stresses due to N, T and $F_T^{M_{act}}$

Thus, the infinitesimal element results subjected to following solicitations:

- On the horizontal face of the infinitesimal element:
  - Normal stresses defined as:

$$\sigma_y^N = \frac{N}{A}$$

$$\sigma_y^M = \frac{F_T^{M_{act}}}{A}$$

$$\sigma_y = -\sigma_y^N + \sigma_y^M = -\frac{N}{A} + \frac{F_T^{M_{act}}}{A}$$

  - Tangential stresses defined as, τ_{xy}.
- On the vertical surface of the infinitesimal element:
  - Only tangential stress, τ_{xy}.

As already explained in previous paragraphs, since elements considered are columns, subjected to no axial force in the direction perpendicular to the axis of the column, the corresponding stress states are characterised by one normal stress equal to zero. This involves that the generic state of stress on the Mohr's plane is always identified by a couple of points, whose, one of them, lays on the vertical axis.

Therefore, the point representing the vertical surface defines through the coordinates $(0, -\tau_{xy})$, while the point standing for the horizontal edge corresponds to $\left((\sigma_y^N + \sigma_y^M), \tau_{xy}\right)$. Since σ_y^N and σ_y^M have opposite signs, σ_y^N is negative and σ_y^M positive, the presence of the bending moment, compared with the condition of only axial and shear force acting, produces a translation of the point standing for the horizontal surface towards traction normal stresses. This corresponds to a rotation of the Mohr's circle towards positive normal stresses.

To conclude, the presence of the traction force related to the bending moment increases the principal tensile stress. This results in a translation of the N-T interaction domain towards the left portion of the diagram.

As for the construction of the axial force-shear force interaction diagram, to define the basic equation, it has to impose the principal tensile stress, σ_1, equal to the tensile strength of concrete, f_{ctd}; it has to be expressed as a function of the stress state acting on the element, σ_x and τ_{xy}. This concept can be obtained by equating two different expression of the radius of the Mohr's circle.

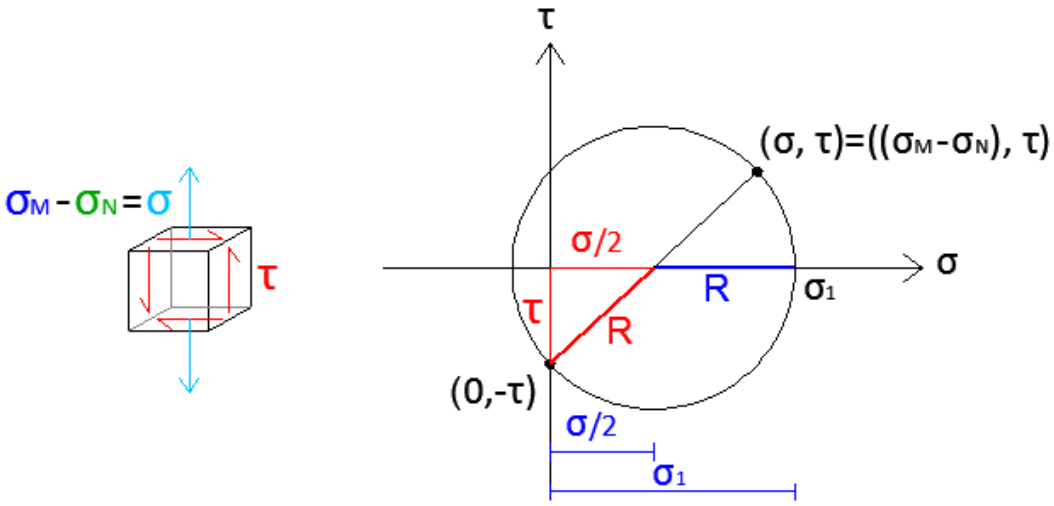

Figure 3.2.1.1.3 – Geometrical evidences to get the equation of the failure criterion

$$\begin{cases} R = \sqrt{{\tau_{xy}}^2 + \left(\dfrac{\sigma_y^M - \sigma_y^N}{2}\right)^2} \\ R = \sigma_1 - \dfrac{\left|\sigma_y^M - \sigma_y^N\right|}{2} \end{cases}$$

Equating the two formulation of the radius:

$$\sqrt{{\tau_{xy}}^2 + \left(\frac{\sigma_y^M - \sigma_y^N}{2}\right)^2} = \sigma_1 - \frac{\left|\sigma_y^M - \sigma_y^N\right|}{2}$$

$${\tau_{xy}}^2 + \frac{\left(\sigma_y^M - \sigma_y^N\right)^2}{4} = \left(\sigma_1 - \frac{\left|\sigma_y^M - \sigma_y^N\right|}{2}\right)^2$$

$${\tau_{xy}}^2 + \frac{\left(\sigma_y^M - \sigma_y^N\right)^2}{4} = \frac{\left(\sigma_y^M - \sigma_y^N\right)^2}{4} - 2\,\frac{\sigma_y^M - \sigma_y^N}{2}\,\sigma_1 + {\sigma_1}^2$$

$${\tau_{xy}}^2 + \frac{\left(\sigma_y^M - \sigma_y^N\right)^2}{4} - \frac{\left(\sigma_y^M - \sigma_y^N\right)^2}{4} + \left(\sigma_y^M - \sigma_y^N\right)\sigma_1 - {\sigma_1}^2 = 0$$

$${\tau_{xy}}^2 + \left(\sigma_y^M - \sigma_y^N\right)\sigma_1 - {\sigma_1}^2 = 0$$

$$\left(\sigma_y^M - \sigma_y^N\right)\sigma_1 = {\sigma_1}^2 - {\tau_{xy}}^2$$

$$\left(\sigma_y^M - \sigma_y^N\right) = \frac{{\sigma_1}^2 - {\tau_{xy}}^2}{\sigma_1}$$

$$\sigma_y^N = \frac{{\tau_{xy}}^2}{\sigma_1} - \sigma_1 + \sigma_y^M$$

As previously mentioned, the states of stress belonging to the limit surface of the N-T domain are those producing a principal tensile stress, σ_1, equal to the tensile strength of the concrete, f_{ctd}. Hence, in the equation, f_{ctd} has to replace σ_1.

The equation at the base of the construction of the N-T domain is the following:

$$\sigma_y^N = \frac{{\tau_{xy}}^2}{f_{ctd}} - f_{ctd} + \sigma_y^M$$

It can be also:

$$\tau_{xy} = \sqrt{\left(\sigma_y^M - \sigma_y^N\right) f_{ctd} + {f_{ctd}}^2}$$

For a given value of σ_y^M, depending on the acting bending moment, varying τ_{xy}, the relationship gives the corresponding value of σ_y^N such that, stress states defined by the couple (σ_y^N, τ_{xy}) generate σ_1 equal to f_{ctd}.

Also in this case, the set of couples $({\sigma_x}^{(i)}, {\tau_{xy}}^{(i)})$ defines the interaction domain in terms of stresses, not forces.

To obtain the N-T diagram, stresses need to be integrated on the cross section area of the element considered. For what concerns the axial force, for rectangular elements:

$$N^{(i)} = {\sigma_x}^{(i)}\, b\, h$$

Concerning the shear force, Jourawsky's formulae was employed to move from stresses to forces. The relationship between tangential stresses and shear force given by Jourawsky is the following:

$$\tau_{xy} = \frac{T\, S}{I\, b}$$

Where:

- T is the shear force related to tangential stress τ_{xy};
- S corresponds to the static moment of the cross section;
- I represents the moment of inertia of the element;
- b is the base of the cross section.

Jourawsky's equation solved for T:

$$T = \frac{\tau_{xy}\, I\, b}{S}$$

Considering a rectangular cross section element the formulae simplifies:

$$T = \frac{\tau_{xy}\, b\, h^3}{6\left(\frac{h^2}{4} - y^2\right)}$$

With:

- h is the height of the cross section;
- y corresponds to the y-coordinate of the fiber considered with respect to the centroid.

Considering the fiber in correspondence of the centroid where tangential stresses reach the maximum value, the equation simplifies further:

$$T = \frac{2}{3}\,\tau_{xy}\,b\,h$$

Thus, to pass from the generic tangential stress, ${\tau_{xy}}^{(i)}$, to the shear force, $T^{(i)}$, the formulation employed is the following one:

$$T^{(i)} = \frac{2}{3}\,{\tau_{xy}}^{(i)}\,b\,h$$

The set of triples $(N^{(i)}, T^{(i)}, M_{fixed})$ defines the axial force-shear-bending moment interaction domain.

Considering different values of the acting moment, the two-dimensional domain turns into a tri-dimensional surface described by the points $(N^{(i)}, T^{(i)}, M^{(i)})$.

3.2.1.2. Half Cross-Section Subjected to Compression Force related to the Moment

This paragraph considers the half cross section under the additional compression force due to the presence of the bending moment.

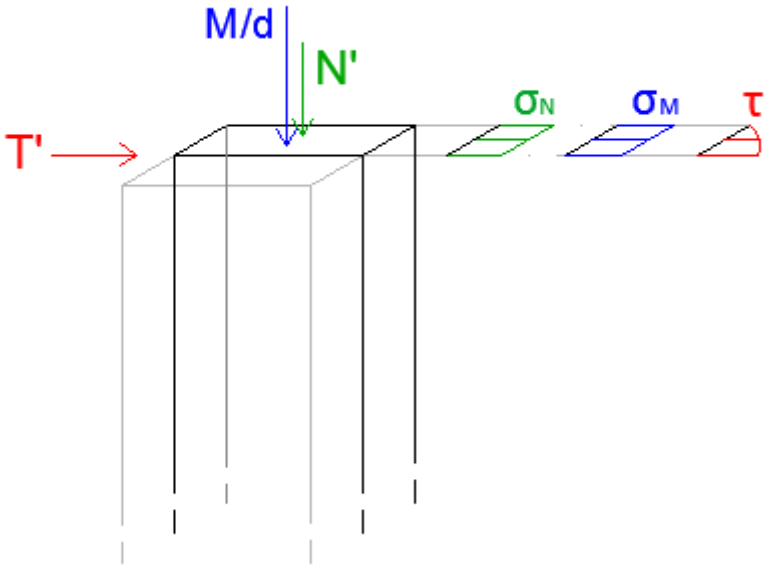

Figure 3.2.1.2.1 – Half cross-section under the traction force related to the bending moment

Therefore, the half cross section is generally subjected to external shear and axial force, T and N, and a concentrated force due to the bending moment that in this case produces compression, $F_C^{M_{act}}$.

Once again, considering an infinitesimal portion of the element in correspondence of the centroid of the half cross section, it is submitted to tangential stresses, τ_{xy}, produced by T, normal stresses, σ_x, related to the sum of $F_C^{M_{act}}$ and N.

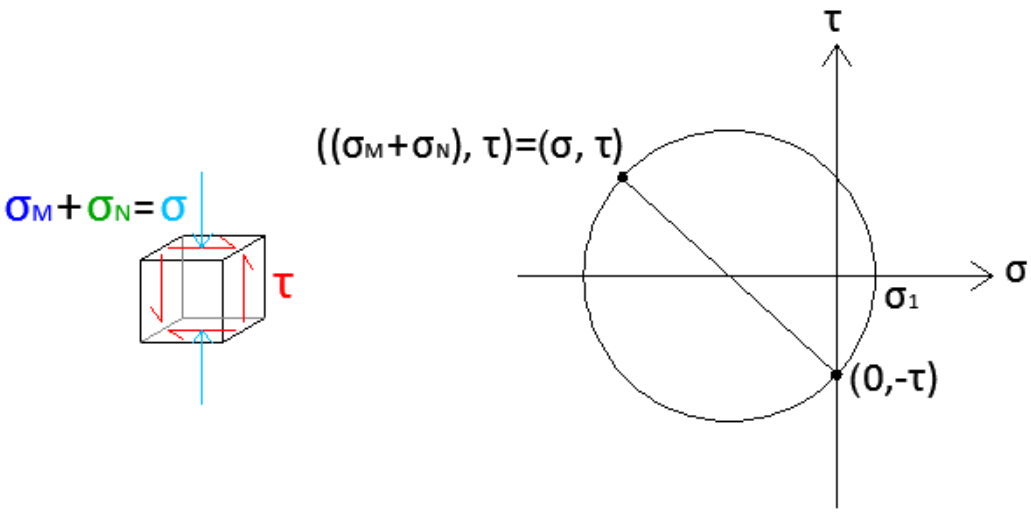

Figure 3.2.1.2.2 – Infinitesimal element subjected to stresses due to N, T and $F_C^{M_{act}}$

Hence, the infinitesimal element is stresses by the following actions:

- On the horizontal face of the infinitesimal element:
  - Normal stresses defined as:

$$\sigma_y^N = \frac{N}{A}$$

$$\sigma_y^M = \frac{F_C^{M_{act}}}{A}$$

$$\sigma_y = -\sigma_y^N - \sigma_y^M = -\frac{N}{A} - \frac{F_C^{M_{act}}}{A}$$

  - Tangential stresses defined as, τ_{xy}.
- On the vertical surface of the infinitesimal element:
  - Only tangential stress, τ_{xy}.

As already explained in previous paragraphs, since elements considered are columns, subjected to no axial force in the direction perpendicular to the axis of the column, the corresponding stress states are characterised by one normal stress equal to zero. This involves that the generic state of stress on the Mohr's plane is always identified by a couple of points, whose, one of them, lays on the vertical axis.

Therefore, the point representing the vertical surface defines through the coordinates $(0, -\tau_{xy})$, while the point standing for the horizontal edge corresponds to $\left((\sigma_y^N + \sigma_y^M), \tau_{xy}\right)$. In this case σ_y^N and σ_y^M have the same signs, both negative producing compression: this means that the two

contributions sum up in the negative portion of the Mohr's plane. As a consequence, the presence of the bending moment, for what concerns the half cross section under the corresponding compression force, compared with the condition of only axial and shear force acting, produces a translation of the point standing for the horizontal surface towards compression normal stresses. This corresponds to a rotation of the Mohr's circle towards negative normal stresses.
To conclude, the presence of the compression force related to the bending moment reduces the principal tensile stress. This results in a translation of the N-T interaction domain towards the right portion of the diagram.
It produces exactly the opposite effect of the half cross section subjected to traction.

Hence, this half element, under additional compression is less restrictive than the other portion. Anyway, the basic equation for the realization of N-T diagrams has obtained in following lines.

Once again, it has to impose principal tensile stress, σ_1, equal to the tensile strength of concrete, f_{ctd}, expressed as a function of the stresses acting on the element, σ_x and τ_{xy}. This concept can be obtained by equating two different expression of the radius of the Mohr's circle.

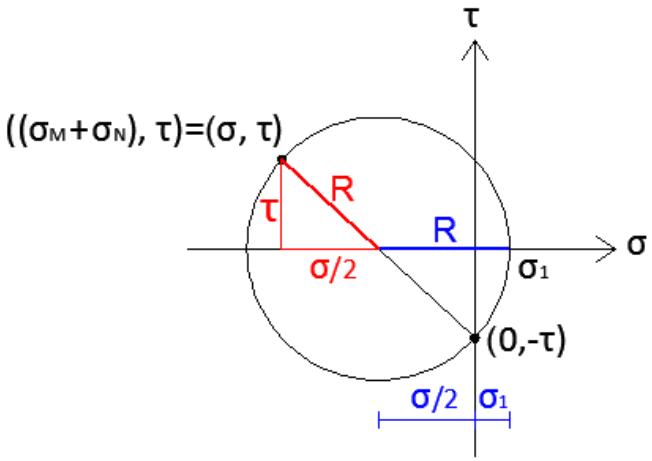

Figure 3.2.1.2.3 – Geometrical evidences

$$\begin{cases} R = \sqrt{{\tau_{xy}}^2 + \left(\dfrac{\sigma_y^N + \sigma_y^M}{2}\right)^2} \\ R = \dfrac{\left|\sigma_y^N + \sigma_y^M\right|}{2} + \sigma_1 \end{cases}$$

Equating the two formulation of the radius:

$$\sqrt{{\tau_{xy}}^2 + \left(\frac{\sigma_y^N + \sigma_y^M}{2}\right)^2} = \frac{\left|\sigma_y^N + \sigma_y^M\right|}{2} + \sigma_1$$

$${\tau_{xy}}^2 + \frac{\left(\sigma_y^N + \sigma_y^M\right)^2}{4} = \left(\frac{\left|\sigma_y^N + \sigma_y^M\right|}{2} + \sigma_1\right)^2$$

$${\tau_{xy}}^2 + \frac{\left(\sigma_y^N + \sigma_y^M\right)^2}{4} = \frac{\left(\sigma_y^N + \sigma_y^M\right)^2}{4} + 2\,\frac{\left|\sigma_y^N + \sigma_y^M\right|}{2}\,\sigma_1 + {\sigma_1}^2$$

$$\tau_{xy}{}^2 + \frac{\left(\sigma_y^N + \sigma_y^M\right)^2}{4} - \frac{\left(\sigma_y^N + \sigma_y^M\right)^2}{4} - \left(\sigma_y^N + \sigma_y^M\right)\sigma_1 - \sigma_1{}^2 = 0$$

$$\tau_{xy}{}^2 - \left(\sigma_y^N + \sigma_y^M\right)\sigma_1 - \sigma_1{}^2 = 0$$

$$\left(\sigma_y^N + \sigma_y^M\right)\sigma_1 = \tau_{xy}{}^2 + \sigma_1{}^2$$

$$\left(\sigma_y^N + \sigma_y^M\right) = \frac{\tau_{xy}{}^2 + \sigma_1{}^2}{\sigma_1}$$

$$\sigma_y^N = \frac{\tau_{xy}{}^2}{\sigma_1} + \sigma_1 - \sigma_y^M$$

Again, in the equation, f_{ctd} has to replace σ_1:

$$\sigma_y^N = \frac{\tau_{xy}{}^2}{f_{ctd}} + f_{ctd} - \sigma_y^M$$

It can be also:

$$\tau_{xy} = \sqrt{\left(\sigma_y^N + \sigma_y^M\right)f_{ctd} - f_{ctd}{}^2}$$

For a given value of σ_y^M, depending on the acting bending moment, varying τ_{xy}, the relationship gives the corresponding value of σ_y^N such that, stress states defined by the couple (σ_y^N, τ_{xy}) generate σ_1 equal to f_{ctd}.

To obtain the N-T diagram, stresses need to be integrated on the cross section area of the element considered. For what concerns the axial force, for rectangular elements:

$$N^{(i)} = \sigma_x{}^{(i)}\, b\, h$$

Concerning the shear force, Jourawsky's formulae was employed to move from stresses to forces. For rectangular cross sections:

$$T^{(i)} = \frac{2}{3}\,\tau_{xy}{}^{(i)}\, b\, h$$

The set of triples $(N^{(i)}, T^{(i)}, M_{fixed})$ defines the axial force-shear-bending moment interaction domain.

Considering different values of the acting moment, the two-dimensional domain turns into a tri-dimensional surface described by the points $(N^{(i)}, T^{(i)}, M^{(i)})$.

The more restrictive case corresponds to the half cross section submitted to the additional traction force due to the bending moment. Thus, in the following paragraph, the Matlab implementation concerns that more critical case.

3.2.1.3. Matlab Implementation

The procedure explained, aimed at constructing the interaction domain of axial force, shear and bending moment, for a fixed, assigned value of the last one, has implemented on the software Matlab to facilitate computations.

3.2.1.4. Problem Definition

The first step always provide the definition of the considered problem in terms of geometrical and material properties.
Geometrical properties:

- b, the base of the cross section of the structural element considered;
- h is the height of the cross section;
- c, the clear cover of steel reinforcement;

Properties of the material:

- f_{cd} corresponds to the design compressive strength of the concrete;
- f_{ctd}, the design tensile strength of the concrete.

From those parameters, derive some relevant quantities: the maximum tensile and compressive axial force, function of the cross section area and design strengths of the concrete:

$$N_{c,max} = f_{cd}\, A_{cls} = f_{cd}\frac{b\,h}{2}$$

$$N_{t,max} = f_{ctd}\, A_{cls} = f_{ctd}\frac{b\,h}{2}$$

In this case the area of concrete corresponds to a half of the total cross section area of the column because, as previously explained, this simplification model the bending moment as a couple of concentrated force, each one of them applied to a half of the cross section.
Those two terms define the boundaries of the interaction domain.
Also tangential stresses has to be bounded: the maximum value for τ_{xy} is the one corresponding to the highest compressive normal stress, $\sigma_x = f_{cd}$. It results from equations explained

$$\tau_{xy,max} = \sqrt{(f_{cd})\, f_{ctd} - {f_{ctd}}^2}$$

The minimum value of tangential stress correspond to $\tau_{xy,min} = -\tau_{xy,max}$.

Normal stress due to the bending moment can be defined once established the geometry. The formulae used is the following:

$$F_T^{M_{act}} = \frac{M}{d} = \frac{M}{\frac{h}{2}} = \frac{2\,M}{h}$$

Obviously, it depends on the applied bending moment. A first, easiest implementation computes the N-T-M interaction diagram for a fixed value of the external moment: it result a two-dimensional

domain on the N-T plane, translated towards negative values of axial force because of the presence of σ_y^M.

A more precise approach, calculating the N-T-M domain for several values of the applied bending, obtains through the introduction of a *for-cycle* on the bending moment magnitude. Hence, the domain is no longer two but tri-dimensional.

3.2.1.5. Formulae Implementation

As previously explained, the equation that correlates normal to tangential stresses, producing principal tensile stress equal to the tensile strength of concrete, is the following:

$$\sigma_y^N = \frac{{\tau_{xy}}^2}{f_{ctd}} + f_{ctd} - \sigma_y^M$$

Normal stress related to the bending moment, σ_y^M, is already known, once defined the cross section geometry. It also depends on the modulus of the external moment, M, which can be a unique quantity or a series of values, changing from M_{min} to M_{max}. Depending on that, the result will be respectively a two or tri-dimensional diagram.

Once defined σ_y^M, to build the N-T-M domain, the code has to evaluate σ_x by means of a for-cycle with τ_{xy} changing from its minimum to its maximum value. Since *for-cycles* in Matlab work only with positive and integer values, in the script τ_{xy} varies from 1 to $\tau_{xy,max}$. The domain is then reflected with respect to the x-axis.
To complete the domain some additional points have to be added. The first one corresponds to zero tangential stress, it derives from the equation below:

$$\sigma_{\tau_0} = \sigma(\tau = 0) = -f_{ctd} + \sigma_y^M$$

Again, since *for-cycles* in Matlab work only with positive values, the code computes normal stresses for integer values of τ_{xy}; therefore, if the maximum compressive normal stress, $\sigma_{c,max} = f_{cd}$, correspond to a non-integer value of τ_{xy}, the diagram will not be complete. The ultimate point of the domain results from the following formulae:

$$(\sigma_{c,max}, \tau_{max}) = \left(f_{cd}, \sqrt{\left(f_{cd} - \sigma_y^M\right) f_{ctd} - {f_{ctd}}^2}\right)$$

The result consists in two vectors, σ and τ, containing values of the *for-cycle* and the missing ones, computed separately, as explained above, and added in the correct position of the vectors.

To translate the interaction domain in terms of stresses to the one in terms of forces, assuming rectangular cross-sections, the following formula implemented:

$$N = \sigma_x \, b \, h$$

$$T = \frac{2}{3} \, \tau_{xy} \, b \, h$$

Two additional points added to close the domain corresponding to $(N_{c,max}, 0)$ for the portion of domain resulting from positive values of $T^{(i)}$, $(N_{c,max}, 0)$ for the portion of domain resulting from negative values of $T^{(i)}$.

At the end, the plot of the vector N, for normal forces, as a function of vector T, shear forces.
The script also plots a point whose coordinates corresponds to the axial force and the shear force acting on the considered column: if the point falls inside the domain, the element is verified, otherwise is not.

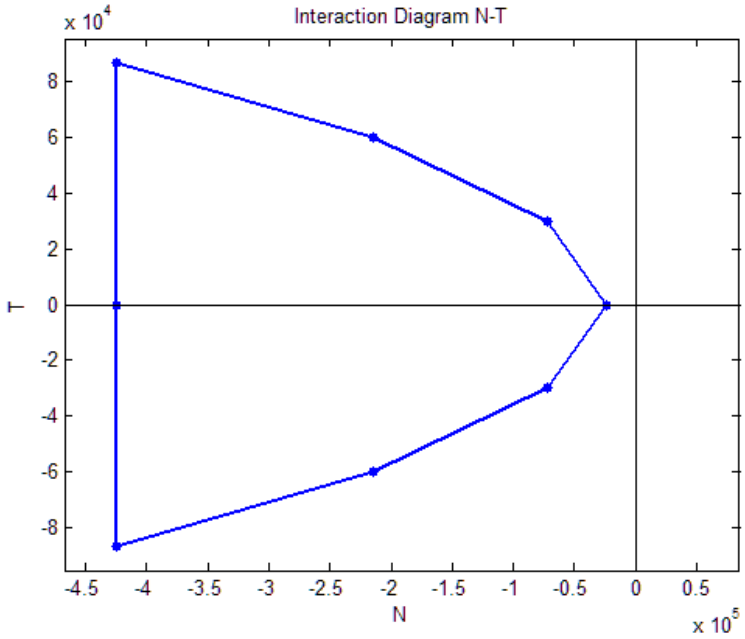

Figure 3.2.1.5.1 – N-T-M interaction domain using Matlab

3.2.2. Linear Distribution of Normal Stresses due to Bending

This second approach tries to detect the relationship between axial force, shear and bending, by employing Navier's formulation and the one given by Jourawsky: Navier's formula defines normal stresses corresponding to the simultaneous action of bending moment and axial force, Jourawsky's relationship relates to tangential stresses.

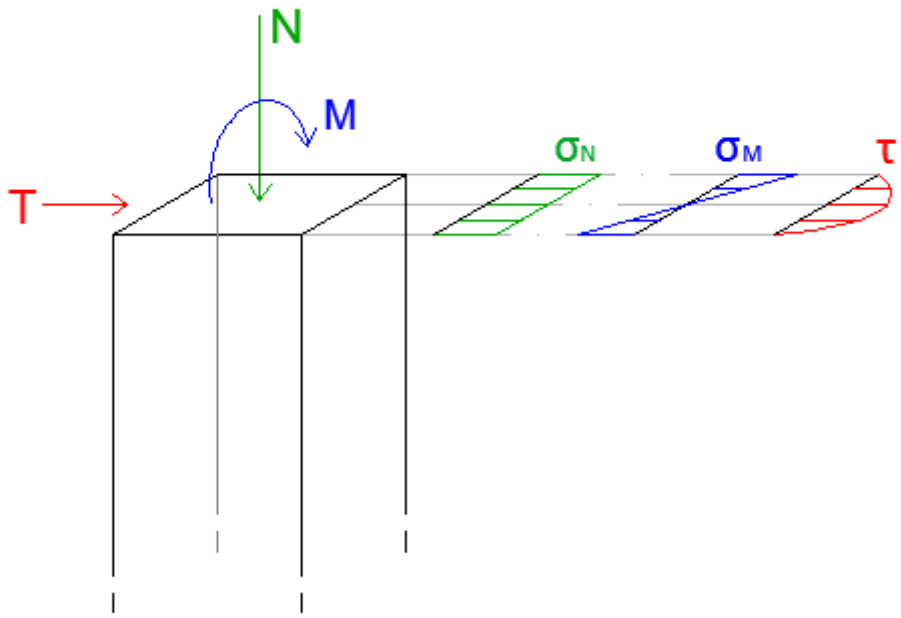

Figure 3.2.2.1 – Linear distribution of normal stresses due to bending

3.2.2.1. Hypotheses

This approach founds on some hypothesis:

- Perfect bound between concrete and steel reinforcements;
- Conservation of flat cross sections;
- Elastic behaviour of the materials;
- Homogenised cross section: the steel homogenised to concrete by means of the homogenisation coefficient, n;
- The concrete has assumed to work under traction if tensile stresses do not overcome the tensile strength of the material.

3.2.2.2. Navier's Formula

Considering bending moments acting parallel to the neutral axis, the equation defining the state of stress is the following:

$$\sigma = \frac{N}{A} \pm \frac{M}{I} y$$

Where:

- N is the axial force acting on the considered member;
- M corresponds to the acting bending moment;

- A represents the cross-section area of the element;
- I is the moment of inertia of the cross-section;
- y stands for the distance of the considered fiber from the neutral axis.

3.2.2.3. Jourawsky's Equation

The equation that expresses tangential stresses as a function of the acting shear force is given by the Jourawsky's formula:

$$\tau = \frac{T\,S}{I\,b}$$

Where:

- T is the shear force related to tangential stress τ;
- S corresponds to the static moment of the cross section under the considered fiber;
- I represents the moment of inertia of the element;
- b is the base of the cross section.

Those two equations determine tangential stresses and normal stresses along the height of the cross-section as a function of, respectively, T, N and M. Substituting those two relationship inside the failure criterion adopted, an equation relating axial forces, shears and bending moments that, acting together, produce the fracture of the element.

The failure criteria at the base of the construction of the domain have explained in the following pages.

3.2.2.4. Failure Criteria

Several failure criteria have considered accounting for all possible types of collapse that a reinforced concrete element can experience. The element could break because of the achievement of the concrete tensile strength, because of excessive compressive stresses on the concrete, greater than the compressive strength of the material; the collapse could be also related to the stresses in steel reinforcements, either compressive either tensile ones.

3.2.2.4.1. Achievement of the Tensile Strength of the Concrete

The first failure criterion considered relates to the tensile strength of the concrete. The aim is the definition of an equation able to identify the triplets (N,T,M) that generate principal tensile stress in the concrete equal to the tensile strength of the concrete.

$$(N,T,M) \qquad \text{Such that} \qquad \sigma_1 = f_{ctd}$$

This has obtained, once again, employing Mohr's circles. Since elements considered are columns, the state of stress acting on the generic infinitesimal element always defines as two points, whose, one of them, leys on the vertical axis of the Mohr's plane.

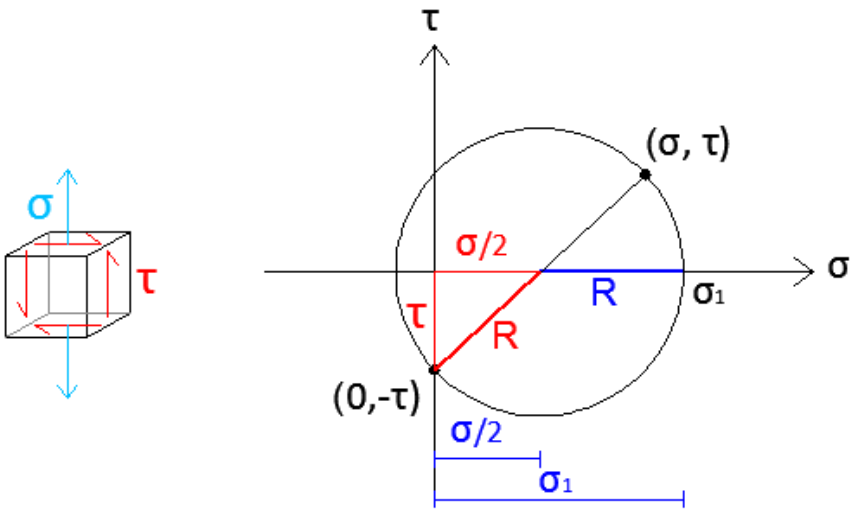

Figure 3.2.2.4.1.1 – Generic state of stress considered

The equation corresponding to the failure criterion imposes principal stress, σ_1, coincident with the tensile strength of concrete, f_{ctd}, expressed as a function of the stress state acting on the element, σ and τ. This has obtained by means of geometrical evidences related to the radius of the Mohr's circle. It can be seen as the sum of the principal tensile stress, σ_1, which has to be equal to $f_{ctd}$to satisfy the basic condition, and a half of the actual normal stress, but it can be also expressed as hypotenuse of the triangle described by the state of stress on the infinitesimal element, σ and τ.

$$\begin{cases} R = \sqrt{\tau^2 + \left(\frac{\sigma}{2}\right)^2} \\ R = \sigma_1 - \frac{|\sigma|}{2} = f_{ctd} - \frac{|\sigma|}{2} \end{cases}$$

As already explained in previous chapters, equating the two and simplifying, the failure criterion corresponding to the achievement of compressive strength of concrete comes out:

$$\sqrt{\tau^2 + \left(\frac{\sigma}{2}\right)^2} = f_{ctd} - \frac{|\sigma|}{2}$$

$$\tau^2 + \frac{\sigma^2}{4} = \left(f_{ctd} - \frac{|\sigma|}{2}\right)^2$$

$$\tau^2 + \frac{\sigma^2}{4} = {f_{ctd}}^2 - 2\,\frac{|\sigma|}{2}\,f_{ctd} + \frac{\sigma^2}{4}$$

$$\tau^2 + |\sigma|\,f_{ctd} - {f_{ctd}}^2 = 0$$

$$\boldsymbol{|\sigma| = f_{ctd} - \frac{\tau^2}{f_{ctd}}}$$

In this paragraph, criteria for the construction of *N-T-M* domain, are defined by using Navier and Jourawsky's equations. Therefore, substituting the relationship of normal stress given by Navier and Jourawsky's one for tangential stresses in the failure criterion reported above, derives the equation, function of N, T and M, describing the limit surface of the domain.
Navier and Jourawsky's formulae:

$$\sigma = \frac{N}{A} \pm \frac{M}{I} y$$

$$\tau = \frac{T\,S}{I\,b}$$

Substituting in the criterion:

$$\frac{N}{A} \pm \frac{M}{I} y = f_{ctd} - \frac{1}{f_{ctd}} \left(\frac{T\,S}{I\,b}\right)^2$$

Solving for N:

$$\boldsymbol{N = A\,f_{ctd} - \frac{A}{f_{ctd}} \left(\frac{T\,S}{I\,b}\right)^2 \mp \frac{A\,M}{I} y}$$

Varying T and M, the equation gives the corresponding value of N such that, stress states defined by the triplets (N, T, M), generate σ_1 equal to f_{ctd}, which means fracture of the concrete because of excessive tensile stresses.

The sets of N, T and M defined through that equation, describe a portion of the tri-dimensional *N-T-M* domain.

3.2.2.4.2. Achievement of the Compressive Strength of the Concrete

The second failure criterion relates to the compressive strength of the concrete. In this case, the equation has to define the triplets (N, T, M) generating a principal compressive stress equal to the compressive strength of the concrete. The equation that corresponds to the failure criterion imposes principal compressive stress, σ_2, coincident with the compressive strength of concrete, f_{cd}, defined as a function of the stress state acting on the element, σ and τ:

$$(N, T, M) \qquad \text{Such that} \qquad \sigma_2 = f_{cd}$$

Again, geometrical evidences of the Mohr's circle are at the base of the definition of the equation. The radius of the circle corresponds to the difference between principal compressive stress, σ_2, equal to f_{cd}, and a half of the actual normal stress, but it can be also expressed as the hypotenuse of the triangle described by the state of stress on the infinitesimal element, σ and τ.

$$\begin{cases} R = \sqrt{\tau^2 + \left(\frac{\sigma}{2}\right)^2} \\ R = \sigma_1 + \frac{|\sigma|}{2} = f_{cd} + \frac{|\sigma|}{2} \end{cases}$$

Equating the two and simplifying:

$$\sqrt{\tau^2 + \left(\frac{\sigma}{2}\right)^2} = f_{cd} + \frac{|\sigma|}{2}$$

$$\tau^2 + \frac{\sigma^2}{4} = \left(f_{cd} + \frac{|\sigma|}{2}\right)^2$$

$$\tau^2 + \frac{\sigma^2}{4} = \frac{\sigma^2}{4} + 2\,\frac{|\sigma|}{2}\,f_{cd} + {f_{cd}}^2$$

$$\tau^2 - |\sigma|\,f_{cd} - {f_{cd}}^2 = 0$$

$$\boldsymbol{|\sigma| = \frac{\tau^2}{f_{ctd}} - f_{cd}}$$

Substituting Navier and Jourawsky's formulations in the criterion just determined, the final expression of the equation derives.

$$\frac{N}{A} \pm \frac{M}{I} y = \frac{1}{f_{cd}} \left(\frac{T\,S}{I\,b}\right)^2 - f_{cd}$$

Solving for N:

$$\boldsymbol{N_c = \frac{A}{f_{cd}} \left(\frac{T\,S}{I\,b}\right)^2 - A\,f_{cd} \mp \frac{A\,M}{I} y}$$

Varying T and M, the equation returns the corresponding value of N such that, stress states due to the triplets (N, T, M), generate σ_2 equal to f_{cd}, which means failure of the concrete because of excessive compressive stresses.

The sets of N, T and M put into relation by means of that equation, describe a portion of the tri-dimensional N-T-M domain.

3.2.2.4.3. Achievement of the Tensile Strength of the Steel

The third criterion correspond to the failure of the steel under excessive tensile stresses. For what concerns steel reinforcements, it has assumed that tangential stresses do not affect the state of stress of the bars. Thus, only normal stresses have considered acting on the steel elements. The failure criterion corresponding to the tensile failure of rebar detects the states of stress generating a principal tensile stress in the steel equal to the tensile strength of the material:

$$(N,\ M) \qquad \text{Such that} \qquad \sigma_{1,s} = f_{yd}$$

In this case, the equation of the failure criterion only depends on the Navier's relationship, indeed:

$$\sigma_{1,s} = n\left(\frac{N}{A} \pm \frac{M}{I}y\right) = f_{yd}$$

Solving for N:

$$\boldsymbol{N_{st} = \frac{A\, f_{yd}}{n} \mp \frac{A\, M}{I} y}$$

Changing the value of M, the equation returns the corresponding value of N such that, stress states due to the couples (N,M), produce $\sigma_{1,s}$ equal to f_{yd}, corresponding to the failure of steel rebar because of excessive tensile stresses.

The sets of N and M in that equation, boundary the tri-dimensional N-T-M domain.

3.2.2.4.4. Achievement of the Compressive Strength of the Steel

The fourth and last criterion represents the failure of the steel because of excessive compressive stresses. Also in this case, it has assumed that tangential stresses do not affect the state of stress of the bars, only normal stresses have considered acting on them. This failure criterion detects the states of stress producing a principal tensile stress in the steel equal to the tensile strength of the material:

$$(N,\ M) \qquad \text{Such that} \qquad \sigma_{2,s} = f_{yd}$$

In this case, the equation of the failure criterion only depends on the Navier's relationship, indeed:

$$\sigma_{2,s} = n\left(\frac{N}{A} \mp \frac{M}{I}y\right) = f_{yd}$$

Solving for N:

$$\boldsymbol{N_{sc} = \frac{A\, f_{yd}}{n} \pm \frac{A\, M}{I} y}$$

Changing the value of M, the equation returns the corresponding value of N such that, stress states due to the couples (N, M), correspond to the failure of steel rebar because of excessive compressive stresses.

The sets of N and M in that equation, boundary the tri-dimensional N-T-M domain.

3.2.2.5. Discretization of the Cross Section

3.2.2.5.1. Main Quantities Definition

It can be observed in previous paragraphs, the fundamental equations to build up the interaction domain, depend on the considered y, thus, the considered fiber. Indeed:

- Failure criterion relating to the tensile strength of the concrete:

$$N = \frac{A}{f_{ctd}} \left(\frac{T\,S}{I\,b}\right)^2 - A\,f_{ctd} \mp \frac{A\,M}{I} y$$

- Achievement of the compressive strength of the concrete:

$$N_c = A\,f_{cd} - \frac{A}{f_{cd}} \left(\frac{T\,S}{I\,b}\right)^2 \mp \frac{A\,M}{I} y$$

- Tensile strength of the steel reinforcement:

$$N_{st} = \frac{A\,f_{yd}}{n} \mp \frac{A\,M}{I} y$$

- Failure criterion corresponding to the steel failure under compression:

$$N_{sc} = \frac{A\,f_{yd}}{n} \pm \frac{A\,M}{I} y$$

All those equations depend on y, distance of the considered fiber from the neutral axis; the failure criteria related to the concrete also depend on S, static moment of the cross section under the considered fiber, which is a function of y.
This means that the axial-shear-flexure interaction domain depends on the considered fiber. The domain has determined for several values of y.
The approach that has employed, assumes a fully reacting cross-section only when the considered fiber correspond to the one at the extremity of the element, which means y equal to $h/2$. For decreasing values of y, the reacting cross-section reduces with y; therefore, for a generic value of y, the reacting cross-section has a width equal to b, which does not change, and the height is equal to $\left(\frac{h}{2} + y\right)$.

The fiber model has obtained by dividing the height of the cross-section in a number of fiber, defined by the variable $2N$, the width of each fiber defines as follows:

$$w = \frac{h}{2\,N}$$

The domain has constructed for different reacting cross-sections, starting with an area fully working, then considering the height of the element reducing, iteration after iteration, consecutive fibers. The vector of the considered fiber defines as follows:

$$y = \left[\left(\frac{h}{2} - \frac{w}{2}\right),\ \left(\frac{h}{2} - w - \frac{w}{2}\right),\ \left(\frac{h}{2} - 2\,w - \frac{w}{2}\right)\ \ldots\ \left(\frac{h}{2} - (N-1)\,w - \frac{w}{2}\right)\right]$$

For each fiber, the following quantities, which appear in the strength criteria, change:

- The effective depth:

$$d = \left(\frac{h}{2} + y + \frac{w}{2}\right) - c$$

- The homogenized cross section into concrete:

$$A_{omog} = \left[b * \left(\frac{h}{2} + y + \frac{w}{2}\right)\right] + \left(n * A_{s,sup}\right) + \left(n * A_{s,inf}\right)$$

  Where n represents the homogenization coefficient, defined as the ratio between the young modulus of the steel over the one of the concrete;

- The position of the centroid of the cross section, expressed as its distance with respect to the lower edge of the element:

$$d_{g,inf} = \frac{S}{A_{omog}}$$

$$d_{g,sup} = h - d_{g,inf}$$

  Where:

  - S is the static moment of the cross section with respect to the lower edge:

$$S = \left\{b * \left(\frac{h}{2} + y + \frac{w}{2}\right) * \left[\frac{\left(\frac{h}{2} + y + \frac{w}{2}\right)}{2}\right]\right\} + \left[n\,A_{s,sup}\,\left(\frac{h}{2} - c\right)\right] + \left(n\,A_{s,inf}\,c\right)$$

- The moment of inertia of the reacting cross section:

$$I_{omog} = \left(\frac{b\,{d_{g,inf}}^3}{3}\right) + \left\{\frac{b\left[d_{g,sup} - \left(\frac{h}{2} - \left(y + \frac{w}{2}\right)\right)\right]^3}{3}\right\} + \left[n\,A_{s,sup}\left(d_{g,sup} - c\right)^2\right] + \left[n\,A_{s,inf}\left(d_{g,inf} - c\right)^2\right]$$

- The static moment of the portion of cross section under the centroidal fiber, corresponding to the maximum tangential stress:

$$S_{max,omog} = \left(b\,d_{g,inf}\,\frac{d_{g,inf}}{2}\right) + \left[n\,A_{s,inf}\left(d_{g,inf} - c\right)\right]$$

Considering the failure criteria related to the achievement of the compressive strength of the concrete, there would not be a progressive development of the crack, reducing the reacting cross section, thus reducing all the quantities defined above. The failure caused by excessive compressive stresses on the concrete, presents as a sudden crashing of the concrete once reached f_{cd}. This means that, in the equation corresponding to the compressive failure of the concrete, those terms remain constant, equal to their value at the first iteration, for $y = h/2$: $d^{1st-it}, A_{omog}{}^{1st-it}, d_{g,sup}{}^{1st-it}, d_{g,inf}{}^{1st-it}, I_{omog}{}^{1st-it}, S_{omog}{}^{1st-it}$.

Two terms remain to be defined: T and M, which are the acting shear force and bending moment. Since the objective is the construction of a tri-dimensional domain, T and M are vector, whose elements correspond to possible values of shear and bending acting on the member. Their elements varies from a minimum value to a maximum one, with step increment such that the two vectors have the same length. This has obtained as follows:

$$\bar{M} = [M_{min} : k : M_{max}]$$

$$\bar{T} = [T_{min} : q : T_{max}]$$

Given that:

- M_{min} and M_{max} are the minimum and maximum bending moment acting on the element, which depend on the considered case;
- T_{min} and T_{max} are the minimum and maximum external shear forces on the element, depending on the considered case;
- k and q are the step increment of the bending moment and shear vectors respectively. They have to be determined such that the two vectors, M and T, are characterised by the same length. Hence, given k, which should be imposed considering both the level of definition of the domain both the computational costs, the shear increment step defines as:

$$q = \frac{(T_{max} - T_{min})\, k}{(M_{max} - M_{min})}$$

3.2.2.5.2. Effect of the Axial Force not applied in the Centroid

Assuming a cross section that is reducing at each iteration, it needs to be accounted for the decentralized axial force. Indeed, at the beginning the whole cross section works, the axial force is applied at the centroid of the element; then, changing y, the cross section reduces, the axial force still applies at the same point, the centroid of the cross section fully working, but the centroid of the reacting cross section moved. This consists of a decentralized axial force, corresponding to the development of an additional bending moment working against the applied one.

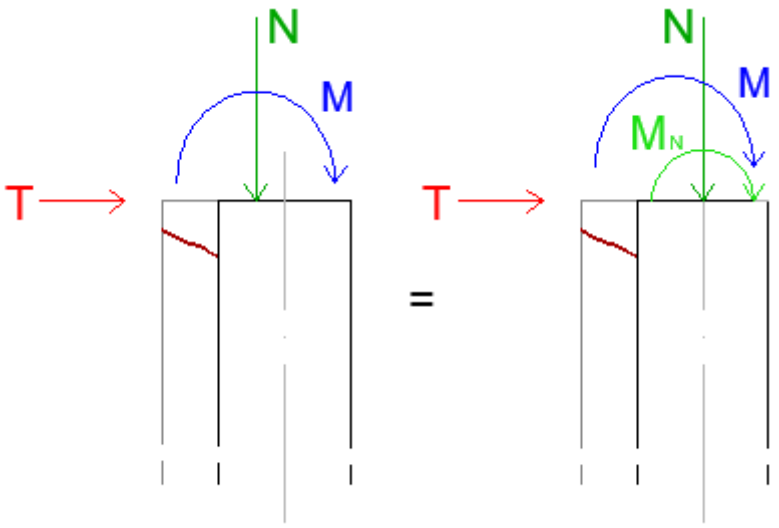

Figure 3.2.2.5.2.1 – Effect of the decentralized axial force

The moment that appears in the failure criteria previously mentioned is the difference between the applied one and the bending moment corresponding to the decentralized axial force:

$$M = \bar{M} - N\,e$$

Where e represent the distance between the initial centroid that, in case of symmetric reinforcements, lays at $h/2$, and the centroid of the element for a given considered fiber at y:

$$e = \frac{h}{2} - d_{g,sup}$$

Therefore, the failure criteria corresponding to the failure of concrete under traction becomes:

$$N = \frac{A}{f_{ctd}}\left(\frac{T\,S}{I\,b}\right)^2 - A\,f_{ctd} \mp \frac{A\,(\bar{M} - N\,e)}{I}\,y$$

Given that N is the vector of the previous iteration; imposing a very small width of the fiber, e.g. a very large number of fibers in which the element is divided into, the difference between the vector N at the i-th and the one at the $(i+1)$-th is very small, hence the error is negligible.

This aspect does not appear in the failure criteria related to the achievement of the compressive strength of the concrete because in that case the cross section does not undergo a progressive development of the crack, the concrete suddenly crashes once reached f_{cd}.

3.2.2.5.3. Stirrups Contribution

Up to now, no contribution of transversal reinforcement has considered.
Stirrups have taken into account assuming that the shear resistance of the whole element can be expressed as the sum of two contributions: the one related to the concrete and homogenized

longitudinal bars, determined through Jourawsky's theory, T_J, and the one related to stirrups, explained by the Ritter-Mörsch's theory, T_{RM}.
This approach assumes that the two shear resistances are complementary. When the cross section is not cracked, which correspond to the first iteration, when y is equal to $h/2$, it is assumed that the external shear is carried by the homogenised cross section through tangential stresses, as predicted by Jourawsky's model. When the crack affects the $2/3$ of the total height of the cross section, which means that the concrete still working corresponds only to $1/3$ of the total height, it is assumed that the remaining homogenised cross section is no longer able to carry shear force and the shear strength of the element is entirely provided by transvers reinforcement. For all intermediate conditions, between $y = h/2$ and $y = -2h/3$, the variation of T_J and T_{RM} is linear.

This has implemented through the formula below:

$$T_{tot} = \rho\, T_J + (1 - \rho)\, T_{RM}$$

In the script, T_J corresponds to the vector $\bar{T}$, which varies from T_{min} and T_{max}. The Ritter-Mörsch's shear resistance has determined by means of the formula given by the code:

$$T_{RM} = V_{Rd,s} = \frac{A_{sw}}{s}\, z\, f_{yd}\, cot\, \theta$$

Where:

- A_{sw} is the area of transversal reinforcement, corresponding to the product of the area of the single bar and the number of arms:

$$A_{sw} = n_{arms}\, A_{\Phi}$$

- $z = 0.9\, d$, the effective height;
- f_{yd}, the design strength of the steel;
- θ is the angle between the horizontal and the concrete strut.

Where ρ is a coefficient equal to 1 if the member is not cracked, equal to 0 when the crack affects the $2/3$ of the total height.

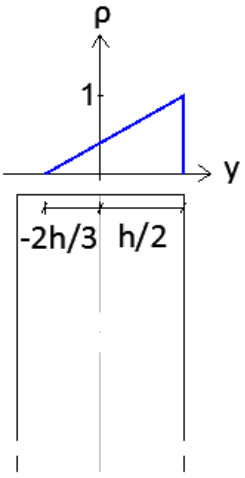

Figure 3.2.2.5.3.1 – Linear variation of the coefficient ρ

By means of the equation of a straight line through two points:

$$\frac{y-y_1}{y_2-y_1}=\frac{x-x_1}{x_2-x_1}$$

The equation of the coefficient ρ corresponds to the following one:

$$\frac{\rho-\rho_1}{\rho_2-\rho_1}=\frac{y-y_1}{y_2-y_1}$$

$$\frac{\rho-0}{1-1}=\frac{y-\left(-\frac{2}{3}\frac{h}{2}\right)}{\frac{h}{2}-\left(-\frac{2}{3}\frac{h}{2}\right)}$$

$$\frac{\rho-0}{1-1}=\frac{y+\frac{h}{3}}{\frac{h}{2}+\frac{h}{3}}$$

$$\rho=\frac{y+\frac{h}{3}}{\frac{5\,h}{6}}$$

$$\rho=\frac{6\,y+2\,h}{5\,h}$$

When the whole cross section works, thus $y=h/2$:

$$\rho=\frac{6\,\frac{h}{2}+2\,h}{5\,h}=\frac{5\,h}{5\,h}=1$$

$$T_{tot}=1*T_J+0*\,T_{RM}=T_J$$

Therefore, the shear resistance is entirely provided by the homogenised concrete, which corresponds to the shear resistance predicted by Jourawsky.

On the other hand, when the crack affects 2/3 of the whole cross section, thus $y=-h/3$:

$$\rho=\frac{6\,\left(-\frac{h}{3}\right)+2\,h}{5\,h}=\frac{0}{5\,h}=0$$

$$T_{tot}=0*T_J+1*\,T_{RM}=T_{RM}$$

Therefore, the shear resistance entirely derives from stirrups, which corresponds to the shear resistance of steel reinforcement defined by the Ritter-Mörsch's theory.

The shear that has to be inserted in the failure criteria to evaluate the corresponding N, is the Jourawsky's shear, T_j, because those equation base on the Jourawsky's theory. Once computed all the values of N describing, together with T and M, the domain, the plot of the interaction domain uses the total shear strength, given by the sum of the concrete shear resistance and the one provided by stirrups, T_{tot}.

To summarize, the failure criteria used to build the *N-T-M* domain, are the following:

- Failure criterion relating to the tensile strength of the concrete:

$$N = \frac{A_{omog}}{f_{ctd}} \left(\frac{\rho \, T_J \, S_{omog}}{I_{omog} \, b} \right)^2 - A_{omog} \, f_{ctd} \mp \frac{A_{omog} \, (\bar{M} - N \, e)}{I_{omog}} y$$

- Achievement of the compressive strength of the concrete:

$$N_c = {A_{omog}}^{1st-it} \, f_{cd} - \frac{{A_{omog}}^{1st-it}}{f_{cd}} \left(\frac{T_J \, {S_{omog}}^{1st-it}}{{I_{omog}}^{1st-it} \, b} \right)^2 \mp \frac{{A_{omog}}^{1st-it} \, M}{{I_{omog}}^{1st-it}} y$$

- Tensile strength of the steel reinforcement:

$$N_{st} = \frac{A_{omog} \, f_{yd}}{n} \mp \frac{A_{omog} \, M}{I_{omog}} y$$

- Failure criterion corresponding to the steel failure under compression:

$$N_{sc} = \frac{A_{omog} \, f_{yd}}{n} \pm \frac{A_{omog} \, M}{I_{omog}} y$$

3.2.2.6. Matlab Implementation

The procedure has implemented on Matlab to compute the *N-T-M* interaction domain for any value of y, avoiding computational efforts.

3.2.2.6.1. Input Data

The first step in the implementation of the procedure consists of the definition of input data. Information required, concerning both geometrical and material properties, have listed below.
Geometrical properties:

- b, the base of the cross section of the reinforced concrete element considered;
- h is the height of the cross section;
- c, the clear cover of steel reinforcement; therefore the effective depth derives:

$$d = h - c$$

- $A_{s,sup}$ defines the steel area of reinforcement in the upper part of the cross section;
- $A_{s,inf}$ is the steel area of reinforcement in the lower part of the cross section;
- Φ_{st} stands for the diameter of transvers reinforcement;
- n_{st} is the number of arms of transvers reinforcement;
- s_{st} represents the spacing of stirrups; thus, the cross sectional area of shear reinforcement:

$$A_{sw} = n_{st} \left[\pi \left(\frac{\Phi_{st}}{2} \right)^2 \right]$$

Properties of the materials:

- f_{cd} corresponds to the design compressive strength of the concrete;
- f_{ctd} characterises to the design tensile strength of the concrete, assumed equal to 0.1 f_{cd};
- f_{yd} is the design strength of steel reinforcements;
- E_c represents the Young's modulus of the concrete, computed as function of the design compressive strength of concrete, as prescribed by codes:

$$E_c = 22000 \left[\left(\frac{f_{cd}}{10}\right)^{0.3}\right]$$

- E_s is the elasticity modulus of the steel; hence, the homogenisation coefficient defines as:

$$n = \frac{E_c}{E_s}$$

3.2.2.6.2. Discretization of the cross section

The approach requires the subdivision of the cross section into fibers in order to consider a progressive reduction of the element because of the development of the crack.

This has obtained by defining the number of fibers in which a half cross section has to be divided into, deriving their width. The script needs those two information; the user decides the level of refinement. In this study, the subdivision has chosen in order to get the width of the fiber equal to 1 mm:

$$n_{fib} = \overline{n_{fib}}$$

$$w_{fib} = \frac{h/_2}{n_{fib}}$$

At each iteration, the member loses more fibers; at each iteration, the software compute all the quantities to build the domain, as a function of the extremity fiber, whose coordinate corresponds to the mid-point of the fiber itself. By means of a for-cycle, the y vector has determined:

$$for \quad i = \left[1{:}\left(n_{fib} - 1\right)\right]$$

$$\bar{y}(1) = \frac{h}{2} - \frac{w_{fib}}{2}$$

$$\bar{y}\,(i+1) = \frac{h}{2} - i * w_{fib} - \frac{w_{fib}}{2}$$

$$\bar{y} = [\bar{y}(1), \qquad \bar{y}(i+1)]$$

3.2.2.6.3. Main Quantities Definition

Once defined the vector y, all the terms depending on it, derive. The deriving terms have computed using a for-cycle too. The for-cycle evaluates those terms for all values of y:

$$for \quad y = \bar{y} = [\bar{y}(1), \qquad \bar{y}(i+1)]$$

$$d = \left(\frac{h}{2} + y + \frac{w}{2}\right) - c$$

$$A_{omog} = \left[b * \left(\frac{h}{2} + y + \frac{w}{2}\right)\right] + \left(n * A_{s,sup}\right) + \left(n * A_{s,inf}\right)$$

The position of the centroid of the cross section depends on y too; it has expressed as its distance with respect to the lower edge of the element:

$$S = \left\{ b * \left(\frac{h}{2} + y + \frac{w}{2}\right) * \left[\frac{\left(\frac{h}{2} + y + \frac{w}{2}\right)}{2}\right] \right\} + \left[n\, A_{s,sup}\, \left(\frac{h}{2} - c\right)\right] + \left(n\, A_{s,inf}\, c\right)$$

$$d_{g,inf} = \frac{S}{A_{omog}}$$

$$d_{g,sup} = h - d_{g,inf}$$

Once determined the position of the centroid of the reacting cross section, the evaluation of the moment of inertia and the static moment of the cross section under the centroidal fiber, follow:

$$I_{omog} = \left(\frac{b\, {d_{g,inf}}^3}{3}\right) + \left\{ \frac{b\, \left[d_{g,sup} - \left(\frac{h}{2} - \left(y + \frac{w}{2}\right)\right)\right]^3}{3} \right\} + \left[n\, A_{s,sup}\, \left(d_{g,sup} - c\right)^2\right] + \left[n\, A_{s,inf}\, \left(d_{g,inf} - c\right)^2\right]$$

$$S_{max,omog} = \left(b\, d_{g,inf}\, \frac{d_{g,inf}}{2}\right) + \left[n\, A_{s,inf}\, \left(d_{g,inf} - c\right)\right]$$

For what concerns the portion of the domain described by the failure criteria of the concrete under compression, the cross section has not assumed to reduce its height throughout the for-cycle. Excessive compression stresses do not generate cracks; the cross section maintains its initial height until ultimate stress, then the material crashes.

The script separately calculates all the quantities listed above for the failure criterion of the concrete under compression:

$$for \quad y = \bar{y}(1) = \frac{h}{2} - \frac{w}{2}$$

$$d^{1st-it} = \left(\frac{h}{2} + y + \frac{w}{2}\right) - c = \left(\frac{h}{2} + \frac{h}{2} - \frac{w}{2} + \frac{w}{2}\right) - c = h - c$$

$${A_{omog}}^{1st-it} = \left[b * \left(\frac{h}{2} + \frac{h}{2} - \frac{w}{2} + \frac{w}{2}\right)\right] + n\left(A_{s,sup} + A_{s,inf}\right) = (b\, h) + \left(n * A_{s,sup}\right) + \left(n * A_{s,inf}\right)$$

$${d_{g,inf}}^{1st-it} = {d_{g,sup}}^{1st-it} = \frac{h}{2}$$

$$I_{omog}{}^{1st-it} = \frac{b\,h^3}{12} + \left[n\,A_{s,sup}\,\left(\frac{h}{2} - c\right)^2\right] + \left[n\,A_{s,inf}\,\left(\frac{h}{2} - c\right)^2\right]$$

$$S_{max,omog}{}^{1-st} = \left(b\,h\frac{h}{2}\right) + \left[n\,A_{s,inf}\,\left(\frac{h}{2} - c\right)\right]$$

3.2.2.6.4. Moment Vector

As already explained in the previous chapter, failure criteria are all function of the external bending moment; therefore, to construct the domain, it has to define the vector of bending moments.
In Matlab this was obtained by imposing the limit values that the user wants to consider, then creating a vector containing the moments, whose value do not exceed the maximum and the minimum imposed, at a constant step increment.
From a practical point of view, the script first requires the limit values, then the step increment, which are all user's choices, depending on the desired refinement, than creates the vector:

$$M_{min} = \overline{M_{min}}$$
$$M_{max} = \overline{M_{max}}$$
$$k = \bar{k}$$
$$M' = [M_{min} : k : M_{max}]$$

This approach also considers the effects of the axial force not applied in the centroid of the cross section: iteration after iteration, the cross section decreases, the centroid of the reacting concrete moves but the external axial force remains applied in the geometrical centroid of the un-cracked element. This produces a moment acting against M'.
The script calculates, at each iteration, the distance between the geometrical centroid of the un-cracked cross section and the centroid of the reacting concrete, then evaluates the effective acting moments:

$$for \quad y = \bar{y} = [\bar{y}(1), \qquad \bar{y}(i+1)]$$

$$e = \frac{h}{2} - d_{g,inf}(y)$$
$$M = M' - e\,N$$

Where N corresponds to the vector of axial forces resulting from the previous iteration.

The elements of this vector are the values for which the domain is calculated.

3.2.2.6.5. Shear Vector

The same procedure adopted to define the vector of acting shear forces. The script needs the limit values that the user wants to consider, compute the step increment such that M and T have the same length, then creates the vector:

$$T_{min} = \overline{T_{min}}$$
$$T_{max} = \overline{T_{max}}$$
$$q = \frac{(T_{max} - T_{min})\, k}{(M_{max} - M_{min})}$$
$$T' = [T_{min} : q : T_{max}]$$

As already mentioned, the shear has assumed equal to the sum of two contributions, the concrete and transverse reinforcement resistances, which are complementary. Through the coefficient ρ, this has implemented. This coefficient is a function of y, therefore the script computes it at each iteration:

$$for \quad y = \bar{y} = [\bar{y}(1), \qquad \bar{y}(i+1)]$$
$$\rho = \frac{6\, y + 2\, h}{5\, h}$$

The transverse shear strength is simply:

$$V_{Rd,s} = \frac{A_{sw}}{s}\ 0.9\ d\ f_{yd}\ \cot\theta$$

The total shear has expressed in the script as reported below:

$$T = \rho\, T' + (1 - \rho)\, V_{Rd,s}$$

Thus, the shear resistance given by the concrete, which in previous chapters has indicated as T_J, the shear strength accounted by the Jourawsky's theory, corresponds to the vector T'.

3.2.2.6.6. Construction of the Domain

All variables involved in failure criteria have defined, the script can solve the problem.
First, the construction of the mesh, function of the vectors T and M:

$$M = [M_{min} : k : M_{max}]$$
$$T = [T_{min} : q : T_{max}]$$
$$[T, M] = meshgrid\ (T, M)$$

Failure criteria implementation evaluated for all values of y:

$$for \quad y = [\bar{y}(1), \qquad \bar{y}(i+1)]$$

$$N = \frac{A_{omog}}{f_{ctd}} \left(\frac{\rho \, T_J \, S_{omog}}{I_{omog} \, b} \right)^2 - A_{omog} \, f_{ctd} \mp \frac{A_{omog} \, (\bar{M} - N \, e)}{I_{omog}} y$$

$$N_c = {A_{omog}}^{1st-it} \, f_{cd} - \frac{{A_{omog}}^{1st-it}}{f_{cd}} \left(\frac{T_J \, {S_{omog}}^{1st-it}}{{I_{omog}}^{1st-it} \, b} \right)^2 \mp \frac{{A_{omog}}^{1st-it} \, M}{{I_{omog}}^{1st-it}} y$$

$$N_{st} = \frac{A_{omog} \, f_{yd}}{n} \mp \frac{A_{omog} \, M}{I_{omog}} y$$

$$N_{sc} = \frac{A_{omog} \, f_{yd}}{n} \pm \frac{A_{omog} \, M}{I_{omog}} y$$

3.2.2.6.7. Domains Refinement

For each failure criteria, the software draws a limit surface. Those limit surfaces assume value from T_{min} to T_{max} in the shear dimension, from M_{min} to M_{max} in the moment dimension. Nevertheless, this does not correspond to the N-T-M diagram. The interaction domain consists in the intersection of those surfaces: only the points standing below all the surfaces are admissible state of stress.

The final N-T-M diagram is the intersection of the surfaces corresponding to different failure criteria. In the script, this has obtained by cutting those surfaces in correspondence of their intersections.

First, the limit surface corresponding to the fracture of the concrete under traction has cut in correspondence of the intersection with the surface of the concrete compressive failure. This has obtained asking the software to find the element of the matrix N, which are smaller than the corresponding elements in the matrix N_c, putting them equal to Nan. In the script:

$$for \quad i = [1: size(N)]$$

$$for \quad j = [1: size(N)]$$

$$if \quad N(i,j) \leq N_c(i,j), \qquad N(i,j) = NaN$$

Once bounded the tensile limit surface, the compressive one requires the same process. In this case, the software has to detect the element of the new matrix N equal to Nan, and then put the corresponding elements of the matrix N_c equal to Nan as well. In the script, $isnan(N)$ returns a matrix of the same dimension of N whose elements are 0 or 1: 0 if the corresponding element in N is different from Nan, 1 if it is Nan.

$$Nan = isnan(N)$$

Then is necessary to know the rows and the columns of the elements equal to Nan:

$$[Nan_x, Nan_y] = find(Nan = 1)$$

$$v_{Nan} = [Nan_x, Nan_y]$$

The vector nan_x contains all the rows of all the elements equal to Nan in N; the vector nan_y contains all the columns of all the elements equal to Nan in N. Thus, the element $N\left(nan_x(i), nan_y(i)\right)$ is Nan. The corresponding elements of N_c needs to be replaced with Nan:

$$for \quad i = [1: size(nan_x)]$$

$$p = v_{Nan}\,(i: 1)$$

$$p_1(i) = p(1)$$

$$p_{end}(i) = p(end)$$

$$N_c\big(p_1(i), p_{end}(i)\big) = Nan$$

Only positive values of bending moment have considered in order to compare them with the N-M interaction diagram given by codes. In the script:

$$\left[M_{neg,x}, M_{neg,y}\right] = find(M \leq 0)$$

$$v_{M,neg} = \left[M_{neg,x}, M_{neg,y}\right]$$

$$for \quad i = \left[1: size\big(M_{neg,x}\big)\right]$$

$$o = v_{M,neg}\,(i: 1)$$

$$o_1(i) = o(1)$$

$$o_{end}(i) = o(end)$$

$$M\big(o_1(i), o_{end}(i)\big) = Nan$$

$$N\big(o_1(i), o_{end}(i)\big) = Nan$$

$$T\big(o_1(i), o_{end}(i)\big) = Nan$$

3.2.2.6.8. Plot of the Domain

The final step is the plot of the domains. This has performed by means of a tri-dimensional plot of the refined matrices N, T and M:

$$s = surf(N, T, M)$$

$$s_c = surf(N_c, T, M)$$

$$s_{st} = surf(N_{st}, T, M)$$

$$s_{sc} = surf(N_{sc}, T, M)$$

The verification consists in checking that the solicitation point, defined by the triplet $(N_{act}, T_{act}, M_{act})$, values of solicitation acting on the element, falls inside the domain. If it stays out of the domain means that the element is not verified.

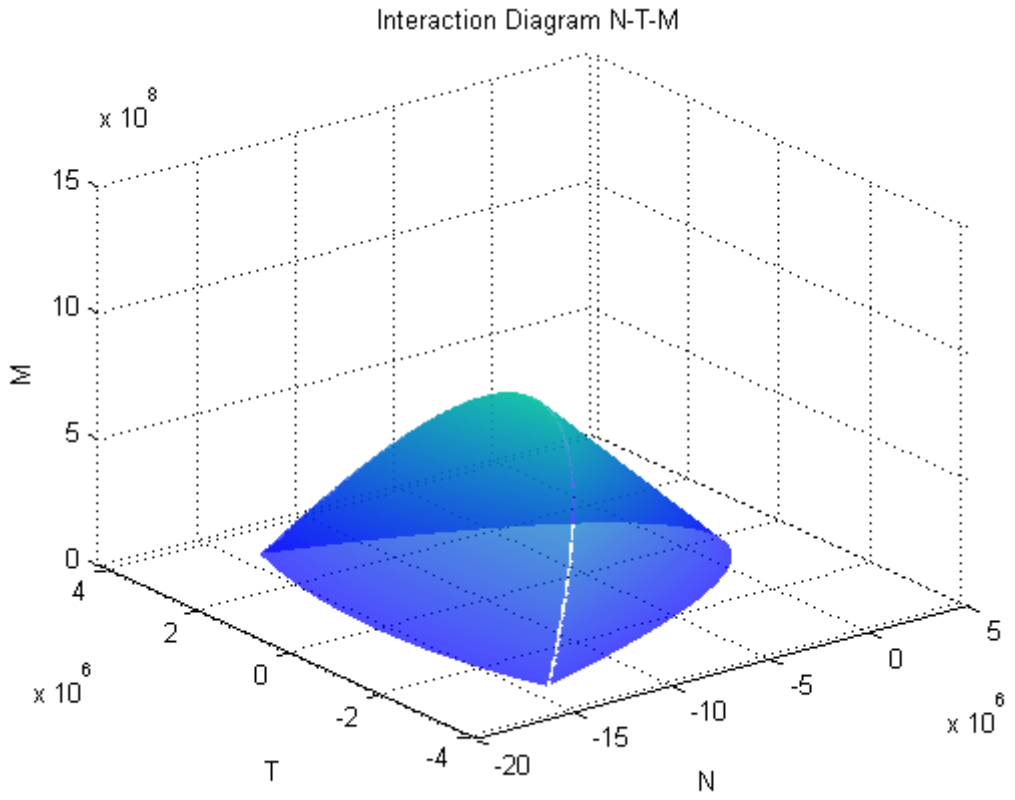

Figure 3.2.2.6.8.1 – Plot of the domain for the whole cross section working

This elastic limit surface has compared with the N-M domain. Certainly, they don't have to coincide, since the suggested diagram corresponds to an elastic condition while the N-M domain represents ultimate conditions. The comparison is just to underline the difference between the elastic limit surface and the ultimate one.

The N-M domain has plotted for all values of the shear in order to get a surface, not a line.

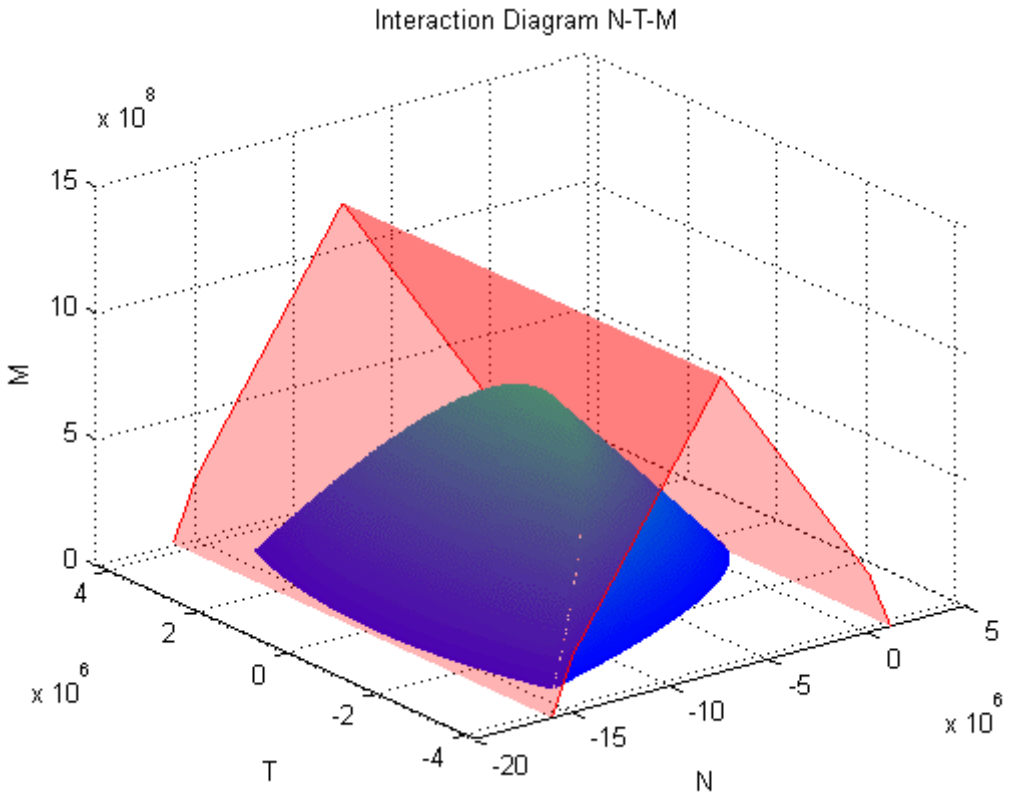

Figure 3.2.2.6.8.1 – Elastic domain inside the ultimate N-M domain

4. Nonlinear Evaluation of the Cross Section as a Sequence of Linear Analyses

This research continued with the development of a fiber model able to capture which type of failure affects the reinforced concrete member, how it evolves throughout the element, if it is possible to achieve an equilibrium condition under specified solicitations and, finally, according to all those aspects, reconstruct the interaction domain N-T-M.

The two failure modes considered are the achievement of the compressive strength of the concrete in correspondence of the most compressed fiber or the achievement of the tensile strength of the concrete in the tensest one.

This has obtained by dividing the cross section in a certain number of fiber, depending on the level of refinement that the user requires. According to the stress state on the element, two main scenarios are possible. The most compressed fiber overcomes the compressive strength of the material, it means that the concrete crushes and is no longer possible to understand how the failure develops. The other case happens when the tensest fiber reaches the tensile strength of the element: in this case, that fiber cracks, the reacting cross-section is no longer the initial one but reduced of that fiber. The stress state evaluation can be performed again on the reduced element: if stresses do not exceeds the tensile limit the procedure stops, otherwise, if tensile stress is still above the limit, another fiber cracks, the working cross section further reduces, the procedure goes on.

To summarize, the study proceeds through some main steps:

5. Evaluation of basic parameters necessary for following steps;
6. Computation of normal stresses on the cross section;
7. Tangential stresses distribution throughout the height of the cross section;
8. According to the stress state, evaluation of the cross section condition. If the acting forces do not produce critical conditions, such as tensile stresses above the tensile strength of the concrete or compressive stresses exceeding the compressive strength of the material, the procedure stops; otherwise, according to the critical condition affecting the element, the analysis studies how the failure mode develops.

4.1. Basic Quantities Definition

Even in this case, the analysis begins with the definition of geometrical and material properties, which are listed below:

- b, the base of the cross section of the reinforced concrete element considered;
- h is the height of the cross section;
- c, the clear cover of steel reinforcement; therefore the effective depth derives:

$$d = h - c$$

- $A_{s,sup}$ defines the steel area of reinforcement in the upper part of the cross section;
- $A_{s,inf}$ is the steel area of reinforcement in the lower part of the cross section;
- Φ_{st} stands for the diameter of transvers reinforcement;
- n_{st} is the number of arms of transvers reinforcement;
- s_{st} represents the spacing of stirrups; thus, the cross sectional area of shear reinforcement:

$$A_{sw} = n_{st} \left[\pi \left(\frac{\Phi_{st}}{2} \right)^2 \right]$$

- f_{cd} corresponds to the design compressive strength of the concrete;
- f_{ctd} characterises to the design tensile strength of the concrete, assumed equal to $0.1\, f_{cd}$;
- f_{yd} is the design strength of steel reinforcements;
- E_c represents the Young's modulus of the concrete, computed as function of the design compressive strength of concrete, as prescribed by codes:

$$E_c = 22000 \left[\left(\frac{f_{cd}}{10} \right)^{0.3} \right]$$

- E_s is the elasticity modulus of the steel; hence, the homogenisation coefficient defines as:

$$n = \frac{E_c}{E_s}$$

As already mentioned, the fiber model has obtained by dividing the height of the cross-section in a number of fiber, thus, to compute following quantities, is necessary to first define the mesh. This has obtained by dividing the height of the cross section, h, in a certain number of fiber defined by the variable $2N$, the width of each fiber defines as follows:

$$w = \frac{h}{2\,N}$$

Then the vector of the considered fiber:

$$y = \left[\left(\frac{h}{2} - \frac{w}{2} \right),\ \left(\frac{h}{2} - w - \frac{w}{2} \right),\ \left(\frac{h}{2} - 2\,w - \frac{w}{2} \right)\ \ldots\ \left(\frac{h}{2} - (N-1)\,w - \frac{w}{2} \right) \right]$$

For each fiber, the following quantities, which appear in the strength criteria, change:

- The effective depth:

$$d = \left(\frac{h}{2} + y + \frac{w}{2} \right) - c$$

- The homogenized cross section into concrete:

$$A_{omog} = \left[b * \left(\frac{h}{2} + y + \frac{w}{2}\right)\right] + \left(n * A_{s,sup}\right) + \left(n * A_{s,inf}\right)$$

Where n represents the homogenization coefficient, defined as the ratio between the young modulus of the steel over the one of the concrete;

- The position of the centroid of the cross section, expressed as its distance with respect to the lower edge of the element:

$$d_{g,inf} = \frac{S}{A_{omog}}$$

$$d_{g,sup} = h - d_{g,inf}$$

Where:

- S is the static moment of the cross section with respect to the lower edge:

$$S = \left\{b * \left(\frac{h}{2} + y + \frac{w}{2}\right) * \left[\frac{\left(\frac{h}{2} + y + \frac{w}{2}\right)}{2}\right]\right\} + \left[n\, A_{s,sup}\, \left(\frac{h}{2} - c\right)\right] + \left(n\, A_{s,inf}\, c\right)$$

- The moment of inertia of the reacting cross section:

$$I_{omog} = \left(\frac{b\, {d_{g,inf}}^3}{3}\right) + \left\{\frac{b\left[d_{g,sup} - \left(\frac{h}{2} - \left(y + \frac{w}{2}\right)\right)\right]^3}{3}\right\} + \left[n\, A_{s,sup}\, \left(d_{g,sup} - c\right)^2\right] + \left[n\, A_{s,inf}\, \left(d_{g,inf} - c\right)^2\right]$$

- The static moment of the portion of cross section under the centroidal fiber, corresponding to the maximum tangential stress:

$$S_{max,omog} = \left(b\, d_{g,inf}\, \frac{d_{g,inf}}{2}\right) + \left[n\, A_{s,inf}\, \left(d_{g,inf} - c\right)\right]$$

4.2. Hypotheses

Also in this case, the analysis founds on some main hypothesis:

- Perfect bound between concrete and steel reinforcements;
- Conservation of flat cross sections;
- Elastic behaviour of the materials;
- Homogenised cross section: the steel homogenised to concrete by means of the homogenisation coefficient, n;
- The concrete has assumed to work under traction if tensile stresses do not exceed the tensile strength of the material.

4.3. Evaluation of Normal Stresses Distribution on the Cross-Section

To calculate the distribution of normal stresses along the cross section, the Navier's formulation has used. Since this method assumes the concrete working under traction if stresses stay below the limit value, fibers subjected to traction under the tensile strength of the concrete have to be accounted.

First, the definition of the neutral axis position by evaluating the y-coordinate, with respect to the geometrical centroid of the entirely working cross section, where the normal stress due to both axial force and bending moments, is null. The Navier's formula, for σ equal to zero, solved for the coordinate y, gives the neutral axis position with respect to the centroid of the cross-section:

$$0 = \frac{N_{act}}{A_{omog}} \pm \frac{M_{act} - (N_{act}\, e)}{I_{omog}} y_{n.a.}$$

Where:

- N_{act} is the axial force acting on the considered member;
- M_{act} corresponds to the acting bending moment;
- A_{omog} represents the homogenised cross-section area of the element;
- I_{omog} is the moment of inertia of the homogenised cross-section;
- y stands for the distance of the considered fiber from the neutral axis.

As it can observed from the equation, the effect of the decentralized axial force has considered: if tensile stresses overcomes the tensile strength of the concrete, the cross section reduces, the axial force still applies at the same point, the centroid of the cross section fully working, but the centroid of the reacting cross section moves. This consists of a decentralized axial force, considered in the procedure by reducing the acting bending by means of the acting axial force, N_{act}, multiplied by the eccentricity, e, defined as the distance between the centroid of the initial cross section, $\frac{h}{2}$, and the actual position of the centroid, $d_{g,sup}$:

$$e = \frac{h}{2} - d_{g,sup}$$

Solving for y:

$$y_{n.a.} = \pm \frac{N_{act}}{M_{act} - (N_{act}\, e)} \frac{A_{omog}}{I_{omog}}$$

Knowing the neutral axis position, the normal stresses diagram is a linear distribution from the most compressed to the tensest fiber, passing through zero in correspondence of the neutral axis. It has evaluated by means of the Navier's equation, where y^i corresponds to the distance from the neutral axis:

$$\sigma^i = \frac{N_{act}}{A_{omog}} \pm \frac{M_{act} - (N_{act}\, e)}{I_{omog}} y^i$$

4.4. Evaluation of Tangential Stresses Distribution on the Cross-Section

The tangential stresses diagram has computed by means of the Jourawsky's formula:

$$\tau = \frac{T_{act}\, S_{omog}}{I_{omog}\, b}$$

Where:

- T_{act} is the acting shear force;
- S_{omog} corresponds to the static moment of the homogenised cross section under the considered fiber;
- I_{omog} represents the moment of inertia of the element;
- b is the base of the cross section.

Jourawsky's equation gives a parabolic distribution of stresses along the height of the element, null in correspondence of the lower and upper edge of the cross section, maximum for the centroidal fiber, if the member is no to cracked. If the crack propagates up to the steel reinforcement, the distribution is parabolic throughout the reacting height, null in correspondence of the upper compressed edge of the element and the lower un-cracked fiber, maximum in the centroid of the working element. Finally, if the crack develops beyond the steel rebar, the tangential stresses distribution is null at the upper compressed fiber, parabolic until the last un-cracked one. The distribution is characterised by a maximum value in correspondence of the centroid of the reacting cross-section, then it decreases until the last un-cracked fiber where tangential stress is different from zero. The distribution is then constant up to the position of steel reinforcements. This derives from the fact that, even if the concrete is cracked beyond the steel bars position, longitudinal steel reinforcement are still working, which means that the static moment goes to zero only below reinforcement.

The formulae used for the static moment depend on the considered fiber. Defining the position of the considered fiber as i, the distance from the upper edge:

- If $i \leq c$: $S_{omog} = b\, i\, (d_{g,sup} - {}^{i}/_{2})$;
- If $c < i \leq (h - c)$: $S_{omog} = b\, i\, \left(d_{g,sup} - {}^{i}/_{2}\right) + n\, A_{s,sup}\, \left(d_{g,sup} - c\right)$;
- If $i \geq (h - c)$: $S_{omog} = b\, i\, \left(d_{g,sup} - {}^{i}/_{2}\right) + n\, A_{s,sup}\, \left(d_{g,sup} - c\right) - n\, A_{s,inf}\, \left(d_{g,inf} - c\right)$;

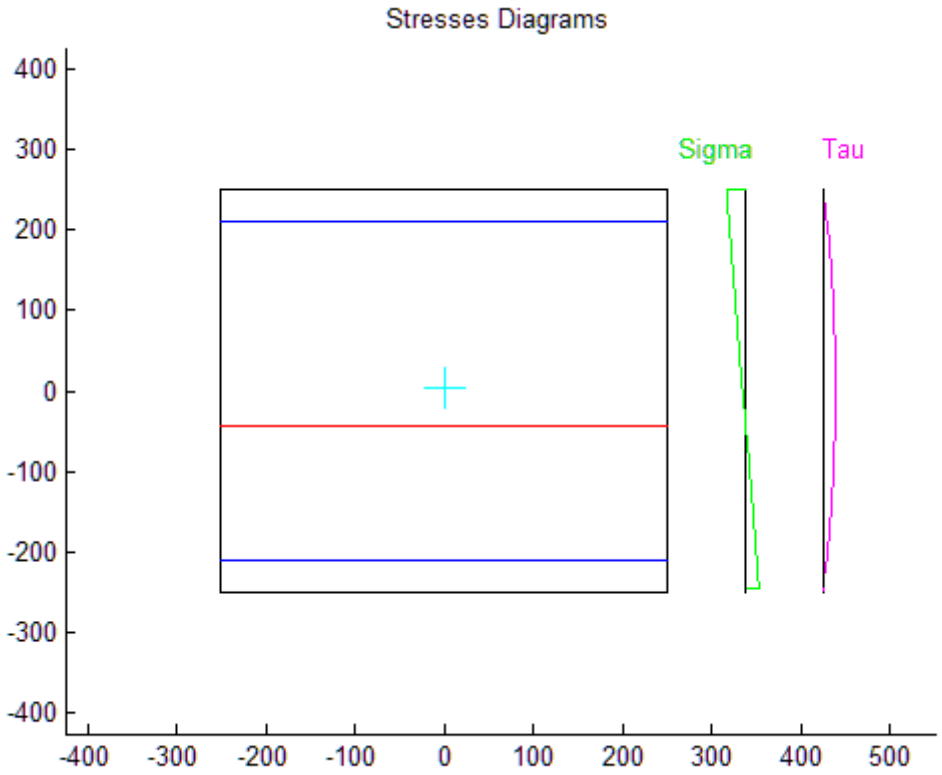

Figure 4.4.1 – State of stress of the generic cross-section

4.5. Analysis of the Condition of the Cross Section

Once computed both the normal and tangential stress distributions is then possible to analyse the condition of the cross section and understand what kind of damages develops on the member. The two types of failure correspond to the crushing of the concrete because of excessive compressive stresses, above the compressive strength of the material, or the cracking of the concrete due to tensile stress above the tensile strength of the concrete.

If the distribution of normal stresses shows that, in correspondence of the upper edge of the cross section, the fiber is subjected to a compressive stress that is higher than the compressive strength of the material, a local crushing of the fiber happens. In this case is no longer possible to proceed with the analysis because there are no formulae able to capture how the crushing develops along the member.

If the distribution of stresses shows, in correspondence of the lower edge of the element, a tensile stress higher than the maximum one, the concrete fiber cracks. In this case is possible to proceed with the analysis indeed, according to the value of normal stress, σ_{crack}, and the tangential one, τ_{crack}, acting on that fiber, the inclination of the crack derives:

$$\theta_{crack} = \frac{1}{2} \tan^{-1}\left(\frac{2\,\tau_{crack}}{\sigma_{crack}}\right)$$

Since the last fiber is cracked, that portion of the cross section is no longer working. To move on in the evaluation of the development of this type of failure, the following iteration consists in computing again the stress state, both normal both tangential, on a reduced member, corresponding to the initial one without the cracked fiber. Also at this second iteration, the crack inclination comes out as a function of the state of stress on the fiber. The reduction of the cross sections, and therefore the iterations, continue until the normal stress acting on the last un-cracked fiber results lower than the tensile strength of the material.

At the end of the iteration, the development of the failure has obtained, consisting in the drawing of the crack along the element, function of the normal stress state, due to axial force, N, and bending moment, M, and tangential stress related to the acting shear force, T.

By means of this procedure the interaction between the axial force, shear ad bending moment has considered at a fiber level, resulting in a N-T-M interaction on the crack development throughout the cross section.

The script returns the vector of normal stresses and the one of tangential stresses on the remaining reacting cross section at the equilibrium condition, which corresponds to the state of stress having both the upper compressed edge and the last un-cracked fiber subjected to stresses below the limits. It also gives a plot of the cracked element.

5. Suggested Procedure

Once separately considered the construction of the *N-T-M* interaction domain, based on the Mohr's theory, Navier and Jourawsky's equations, and the fiber model analysing the development of the type of failure, this two studies have joined. The result is a procedure able to capture how the interaction between axial force, shear and bending, affects a column element and which type of failure results on the member.

What has to be determined first is the state of stress on the cross section element. Following the procedure explained in the previous chapter, it can be computed the maximum compressive stress acting on the fiber corresponding to the upper edge of the cross section and the maximum tensile stress on the lowest fiber of the element. All the possible scenarios are the four following ones:

1. $\sigma_1^{upper\ edge} < f_{ctm}$ and $\sigma_2^{lower\ edge} < f_{cm}$: this corresponds to an admissible stress state, the cross section does not crush neither crack, it elastically carries the external forces;
2. $\sigma_1^{upper\ edge} < f_{ctm}$ and $\sigma_2^{lower\ edge} > f_{cm}$: the fiber at the lowest extremity of the element is subjected to tensile stresses below the tensile strength of the material but the highest compressed fiber is solicited by stresses greater than the compressive strength of the concrete. This produce a local crushing of the fiber;
3. $\sigma_1^{upper\ edge} > f_{ctm}$ and $\sigma_2^{lower\ edge} > f_{cm}$: this case is characterised by the overcoming of both the tensile strength in the lowest fiber and the compressive strength of the concrete in the highest one, which means local cracking of the lowest fiber and local crushing of the highest one.
4. $\sigma_1^{upper\ edge} > f_{ctm}$ and $\sigma_2^{lower\ edge} < f_{cm}$: this scenario corresponds to the achievement of the tensile strength of the concrete at the lowest fiber under traction but admissible stresses at the upper compressed fiber. In this case, the tensest fiber cracks. The final condition of the cross section has to be determined by proceeding with the iteration: the cross section reduces, the cracked fiber at the extremity has no longer considered, the tangential and normal stresses distributions change.
   The new state of stress may fall inside all the scenarios mentioned above.

According to the type of failure experienced, it can appear a local failure or a global one: the cracking could affect a limited portion of the cross section or it could develop throughout the element. They correspond respectively to local and global cracking of the element considered. As for the cracking,

the crushing could be limited only to a portion of the cross section, when a fiber exceeds the compressive strength but, as a whole, the element withstands the forces acting on it, which means that the *N-M* domains verification is satisfied. On the other hand it could happen a global crushing, when the fiber at the extremity of the cross section reaches the compressive strength of the material and the *N-M* domains verification is not satisfied.

Following this procedure is possible to understand how the element responds to external solicitation, what kind of damage affects the member and how this damage propagates, the type of condition the member experience, elastic or ultimate, or, if the elements fails, which type of failure derives.

The suggested procedure is summarised by a flow chart reported below.

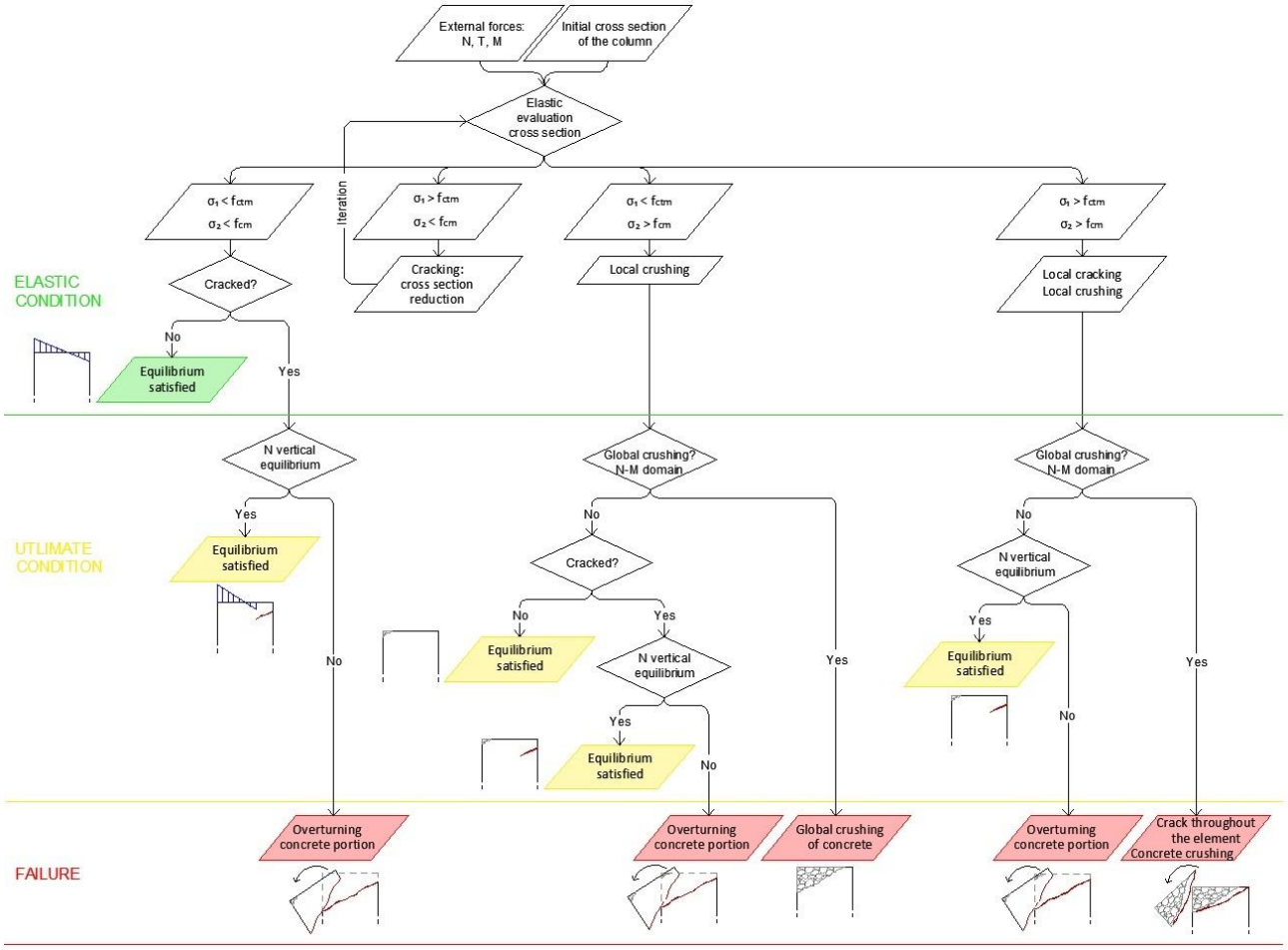

Figure 5.1 – Flow chart, suggested procedure

5.1. Input Data

The procedure requires the definition of some input data. This information are:

- *b*, the base of the cross section of the reinforced concrete element considered;

- h is the height of the cross section;
- c, the clear cover of steel reinforcement; therefore the effective depth derives:

$$d = h - c$$

- $A_{s,sup}$ defines the steel area of reinforcement in the upper part of the cross section;
- $A_{s,inf}$ is the steel area of reinforcement in the lower part of the cross section;
- Φ_{st} stands for the diameter of transvers reinforcement;
- n_{st} is the number of arms of transvers reinforcement;
- s_{st} represents the spacing of stirrups; thus, the cross sectional area of shear reinforcement:

$$A_{sw} = n_{st} \left[\pi \left(\frac{\Phi_{st}}{2} \right)^2 \right]$$

- f_{cd} corresponds to the design compressive strength of the concrete;
- f_{ctd} characterises to the design tensile strength of the concrete, assumed equal to 0.1 f_{cd};
- f_{yd} is the design strength of steel reinforcements;
- E_c represents the Young's modulus of the concrete, computed as function of the design compressive strength of concrete, as prescribed by codes:

$$E_c = 22000 \left[\left(\frac{f_{cd}}{10} \right)^{0.3} \right]$$

- E_s is the elasticity modulus of the steel; hence, the homogenisation coefficient defines as:

$$n = \frac{E_c}{E_s}$$

5.2. Elastic Evaluation of the Cross Section

5.2.1. Basic Quantities Evaluation

Since the procedure derives from the combination of the fiber model that analyses the stress state of the cross section and the model that construct the interaction domain, also in this case the subdivision of the cross section into fibers is the first step.

Even in this case the discretization of the domain has obtained by dividing the height of the cross section, h, in a number of fiber defined by the variable $2N$, the width of each fiber derives as follows:

$$w = \frac{h}{2\,N}$$

Then the vector of the coordinate of the generic considered fiber:

$$y = \left[\left(\frac{h}{2} - \frac{w}{2} \right),\ \left(\frac{h}{2} - w - \frac{w}{2} \right),\ \left(\frac{h}{2} - 2\,w - \frac{w}{2} \right)\ \ldots\ \left(\frac{h}{2} - (N-1)\,w - \frac{w}{2} \right) \right]$$

Depending on those two terms, some basic quantities that appear in Navier's equation and Jourawsky's formula, therefore necessary to calculate the stress state diagrams derive.

This corresponds to the first step of the procedure. The elastic evaluation of the cross section consists in the computation of those basic quantities:

- The effective depth:

$$d = \left(\frac{h}{2} + y + \frac{w}{2}\right) - c$$

- The homogenized cross section into concrete:

$$A_{omog} = \left[b * \left(\frac{h}{2} + y + \frac{w}{2}\right)\right] + \left(n * A_{s,sup}\right) + \left(n * A_{s,inf}\right)$$

  Where n represents the homogenization coefficient, which corresponds to the ratio between the young modulus of the steel over the one of the concrete;

- The position of the centroid of the cross section, expressed as its distance with respect to the lower edge of the element:

$$d_{g,inf} = \frac{S}{A_{omog}}$$

$$d_{g,sup} = h - d_{g,inf}$$

  Where:

  - S is the static moment of the cross section with respect to the lower edge:

$$S = \left\{b * \left(\frac{h}{2} + y + \frac{w}{2}\right) * \left[\frac{\left(\frac{h}{2} + y + \frac{w}{2}\right)}{2}\right]\right\} + \left[n\, A_{s,sup}\, \left(\frac{h}{2} - c\right)\right] + \left(n\, A_{s,inf}\, c\right)$$

- The moment of inertia of the reacting cross section:

$$I_{omog} = \left(\frac{b\, {d_{g,inf}}^3}{3}\right) + \left\{\frac{b\left[d_{g,sup} - \left(\frac{h}{2} - \left(y + \frac{w}{2}\right)\right)\right]^3}{3}\right\} + \left[n\, A_{s,sup}\, \left(d_{g,sup} - c\right)^2\right] + \left[n\, A_{s,inf}\, \left(d_{g,inf} - c\right)^2\right]$$

- The static moment of the portion of cross section under the centroidal fiber, corresponding to the maximum tangential stress:

$$S_{max,omog} = \left(b\, d_{g,inf}\, \frac{d_{g,inf}}{2}\right) + \left[n\, A_{s,inf}\, \left(d_{g,inf} - c\right)\right]$$

5.2.2. Normal Stresses Distribution

As already mentioned in the previous chapter, to calculate the distribution of normal stresses along the cross section, the Navier's formulation has used. The assumption of the concrete working under traction until the tensile strength of the material requires the definition of the neutral axis at first.

It is obtained from the Navier's formula imposing σ equal to zero and solving for the coordinate y. This gives the neutral axis position with respect to the centroid of the cross-section:

$$0 = \frac{N_{act}}{A_{omog}} \pm \frac{M_{act} - (N_{act}\, e)}{I_{omog}} y_{n.a.}$$

Where:

- N_{act} is the axial force acting on the considered member;
- M_{act} corresponds to the acting bending moment;
- A_{omog} represents the homogenised cross-section area of the element;
- I_{omog} is the moment of inertia of the homogenised cross-section;
- y stands for the distance of the considered fiber from the neutral axis.

As already explained, the effect of the decentralized axial force has considered by reducing the acting bending by means of the acting axial force, N_{act}, multiplied by the eccentricity, e, defined as the distance between the centroid of the initial cross section, $\frac{h}{2}$, and the actual position of the centroid, $d_{g,sup}$:

$$e = \frac{h}{2} - d_{g,sup}$$

Solving for y:

$$y_{n.a.} = \pm \frac{N_{act}}{M_{act} - (N_{act}\, e)} \frac{A_{omog}}{I_{omog}}$$

Once computed the neutral axis position, the normal stresses diagram is a linear distribution from the most compressed to the tensest fiber, passing through zero in correspondence of the neutral axis. It has evaluated by means of the Navier's equation, where y^i corresponds to the distance from the neutral axis:

$$\sigma^i = \frac{N_{act}}{A_{omog}} \pm \frac{M_{act} - (N_{act}\, e)}{I_{omog}} y^i$$

5.2.3. Tangential Stresses Diagram

The tangential stresses diagram has computed by means of the Jourawsky's formula:

$$\tau = \frac{T_{act}\, S_{omog}}{I_{omog}\, b}$$

Where:

- T_{act} is the acting shear force;
- S_{omog} corresponds to the static moment of the homogenised cross section under the considered fiber;

- I_{omog} represents the moment of inertia of the element;
- b is the base of the cross section.

Jourawsky's equation gives a parabolic distribution of stresses along the height of the element, null in correspondence of the lower and upper edge of the cross section, maximum for the centroidal fiber, if the member is not cracked. If the crack propagates up to the steel reinforcement, the distribution is parabolic throughout the reacting height, null in correspondence of the upper compressed edge of the element and the lower un-cracked fiber, maximum in the centroid of the working element. Finally, if the crack develops beyond the steel rebar, the tangential stresses distribution is null at the upper compressed fiber, parabolic until the last un-cracked one. The distribution is characterised by a maximum value in correspondence of the centroid of the reacting cross-section, then it decreases until the last un-cracked fiber where tangential stress is different from zero. The distribution is then constant up to the position of steel reinforcements. This derives from the fact that, even if the concrete is cracked beyond the steel bars position, longitudinal steel reinforcement are still working, which means that the static moment goes to zero only below reinforcement.

The formulae used for the static moment depend on the considered fiber. Defining the position of the considered fiber as i, the distance from the upper edge:

- If $i \leq c$: $S_{omog} = b\, i\, (d_{g,sup} - {}^{i}/_{2})$;
- If $c < i \leq (h - c)$: $S_{omog} = b\, i\, \left(d_{g,sup} - {}^{i}/_{2}\right) + n\, A_{s,sup}\, \left(d_{g,sup} - c\right)$;
- If $i \geq (h - c)$: $S_{omog} = b\, i\, \left(d_{g,sup} - {}^{i}/_{2}\right) + n\, A_{s,sup}\, \left(d_{g,sup} - c\right) - n\, A_{s,inf}\, \left(d_{g,inf} - c\right)$;

5.3. Possible Alternative Scenarios

The evaluation of the normal and tangential stresses diagrams corresponds to the elastic analysis of the cross section, which is the first step of the procedure. At this point, the flow chart divides in four possible scenarios, depending on the stress state, which are:

1. $\sigma_1^{lower\ edge} < f_{ctm}$ and $\sigma_2^{upper\ edge} < f_{cm}$: this corresponds to an admissible stress state, the cross section does not crush neither crack, it elastically carries the external forces;
2. $\sigma_1^{lower\ edge} < f_{ctm}$ and $\sigma_2^{upper\ edge} > f_{cm}$: the fiber at the lowest extremity of the element is subjected to tensile stresses below the tensile strength of the material but the highest compressed fiber is solicited by stresses greater than the compressive strength of the concrete. This produce a local crushing of the fiber;
3. $\sigma_1^{lower\ edge} > f_{ctm}$ and $\sigma_2^{upper\ edge} > f_{cm}$: this case is characterised by the overcoming of both the tensile strength in the lowest fiber and the compressive strength of the concrete in the highest one, which means local cracking of the lowest fiber and local crushing of the highest one.

4. $\sigma_1^{lower\ edge} > f_{ctm}$ and $\sigma_2^{upper\ edge} < f_{cm}$: this scenario corresponds to the achievement of the tensile strength of the concrete at the lowest fiber under traction but admissible stresses at the upper compressed fiber. In this case, the tensest fiber cracks. The final condition of the cross section has to be determined by proceeding with the iteration: the cross section reduces, the cracked fiber at the extremity has no longer considered, the tangential and normal stresses distributions change.
   The new state of stress may fall inside all the scenarios mentioned above.

The only alternative that allows the iteration is the one corresponding to principal tensile stress greater than its limit and admissible principal compressive stress, $\sigma_1^{upper\ edge} > f_{ctm}$ and $\sigma_2^{lower\ edge} < f_{cm}$. In this case, according the state of stress is possible to reconstruct the development of the crack, since that fiber is no longer working, the procedure goes on, the cross section reduces and the elastic evaluation of the cross section repeats.

One scenario, $\sigma_1^{lower\ edge} < f_{ctm}$ and $\sigma_2^{upper\ edge} < f_{cm}$, correspond to an equilibrium condition, thus the procedure stops.

The remaining two scenarios, corresponding to the crushing of the compressed concrete, cannot be further analysed in terms of damage development. There cannot be any iteration.

Therefore, the possible paths throughout the flow chart are six; they are deeply explained in following paragraphs.

5.3.1. First Scenario

The first elastic evaluation of the cross section shows a stress state such that both principal tensile stress at the lowest fiber and principal compressive stress at the upper edge stand below respective limits:

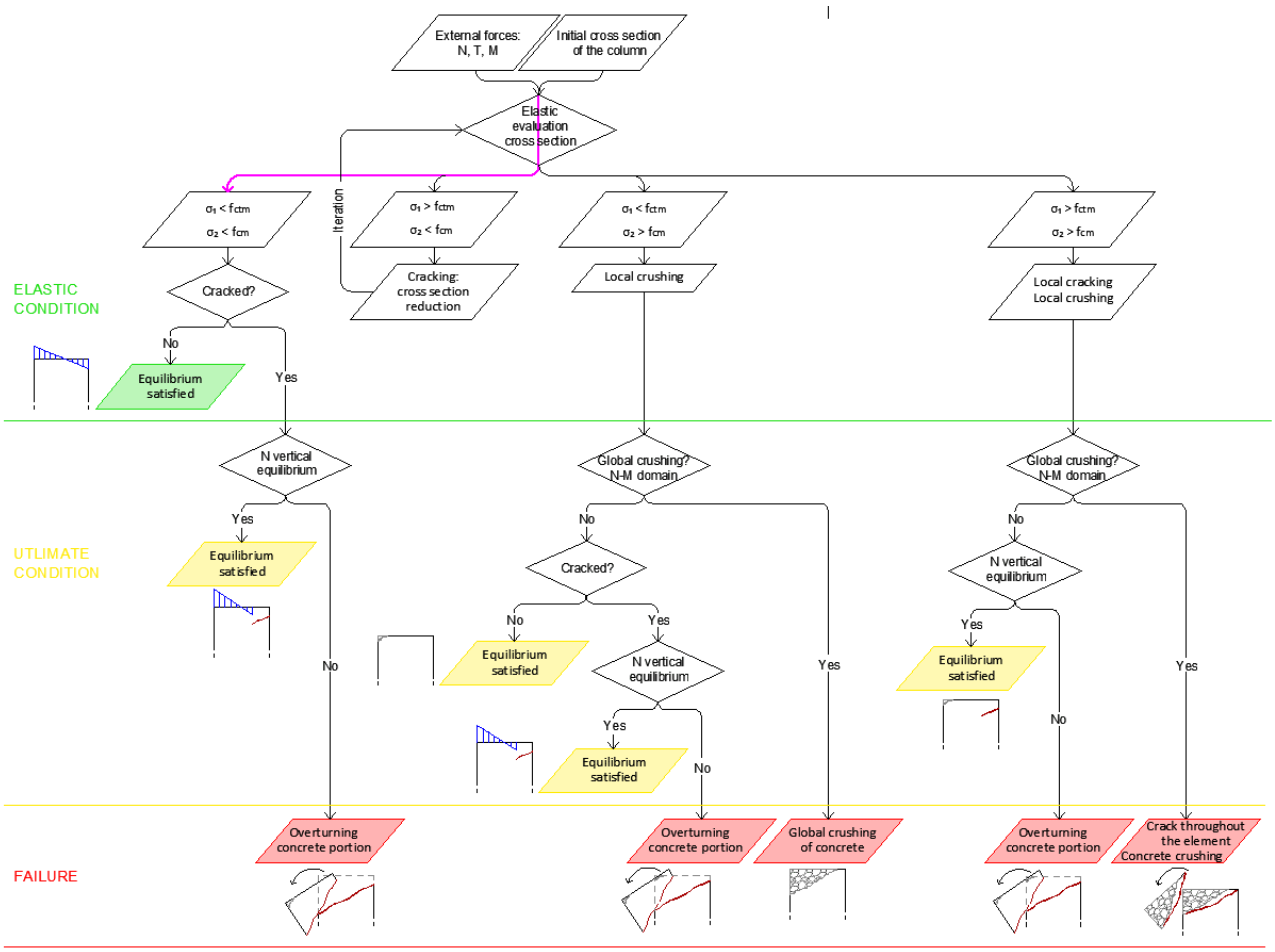

Figure 5.3.1.1 – Path corresponding to the first scenario in the flow chart

$$\left(\sigma_1^{lower\ edge}\right)^{1st\ it.} < f_{ctd}$$

$$\left(\sigma_2^{upper\ edge}\right)^{1st\ it.} < f_{cd}$$

This means that the cross section does not crack, it is able to carry external forces in elastic condition.

Since the element does not crack, there is no need for further verifications.

5.3.2. Second Scenario

At the first elastic evaluation of the cross section, the stress state is characterised by the principal tensile stress at the lowest fiber smaller than its limit value and the principal compressive stress at the upper edge below the compressive strength of the concrete:

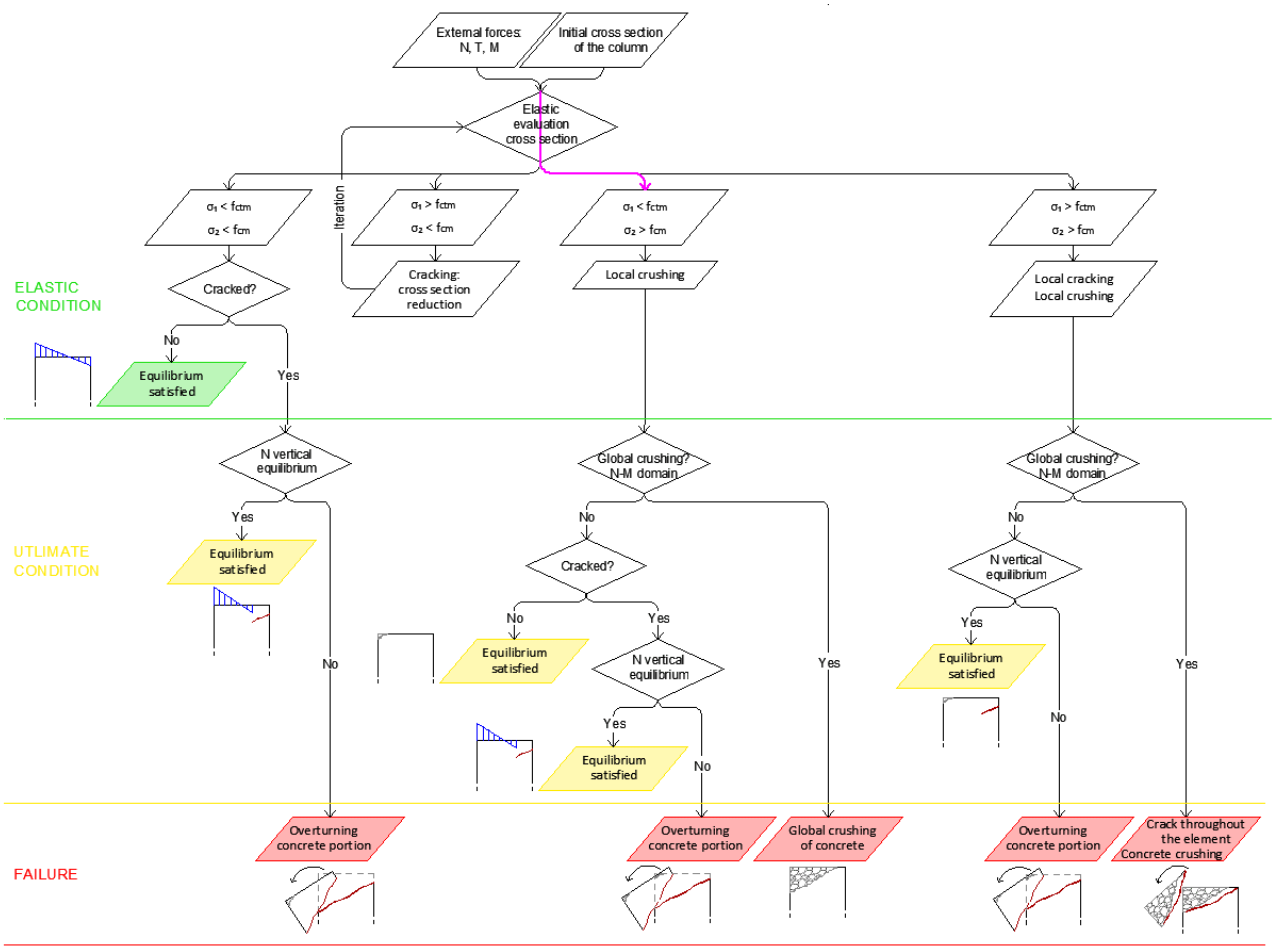

Figure 5.3.2.1 – Path corresponding to the second scenario in the flow chart

$$\left(\sigma_1^{lower\ edge}\right)^{1st\ it.} < f_{ctd}$$

$$\left(\sigma_2^{upper\ edge}\right)^{1st\ it.} > f_{cd}$$

It corresponds to admissible tensile stresses, thus no openings of cracks, but the too high compressive stress produces the crushing of the concrete.

In this case, it is not possible to investigate further the damage development because no theory captures it.

What can be analysed is the type of crushing: local or global. A local damage is certainly happening, but it could also affect the whole element. It could be limited only to a portion of the cross section, when a fiber exceeds the compressive strength but, as a whole, the element withstands the forces

acting on it. On the other hand, it could happen a global crushing, when the element is not able to carry external forces.

This information can be deduced from traditional *N-M* interaction domains. If the solicitation point falls inside the domain, it could conclude that, as a whole, the column withstands the external force, it does not entirely crash. If the point falls out means that the member fails under those actions, thus the crushing is not limited to a fiber but it involves the entire element.

5.3.3. Third Scenario

At the first elastic evaluation of the cross section, the stress state is such that both the principal tensile stress at the lowest fiber and the principal compressive stress at the highest edge exceed their respective limit values:

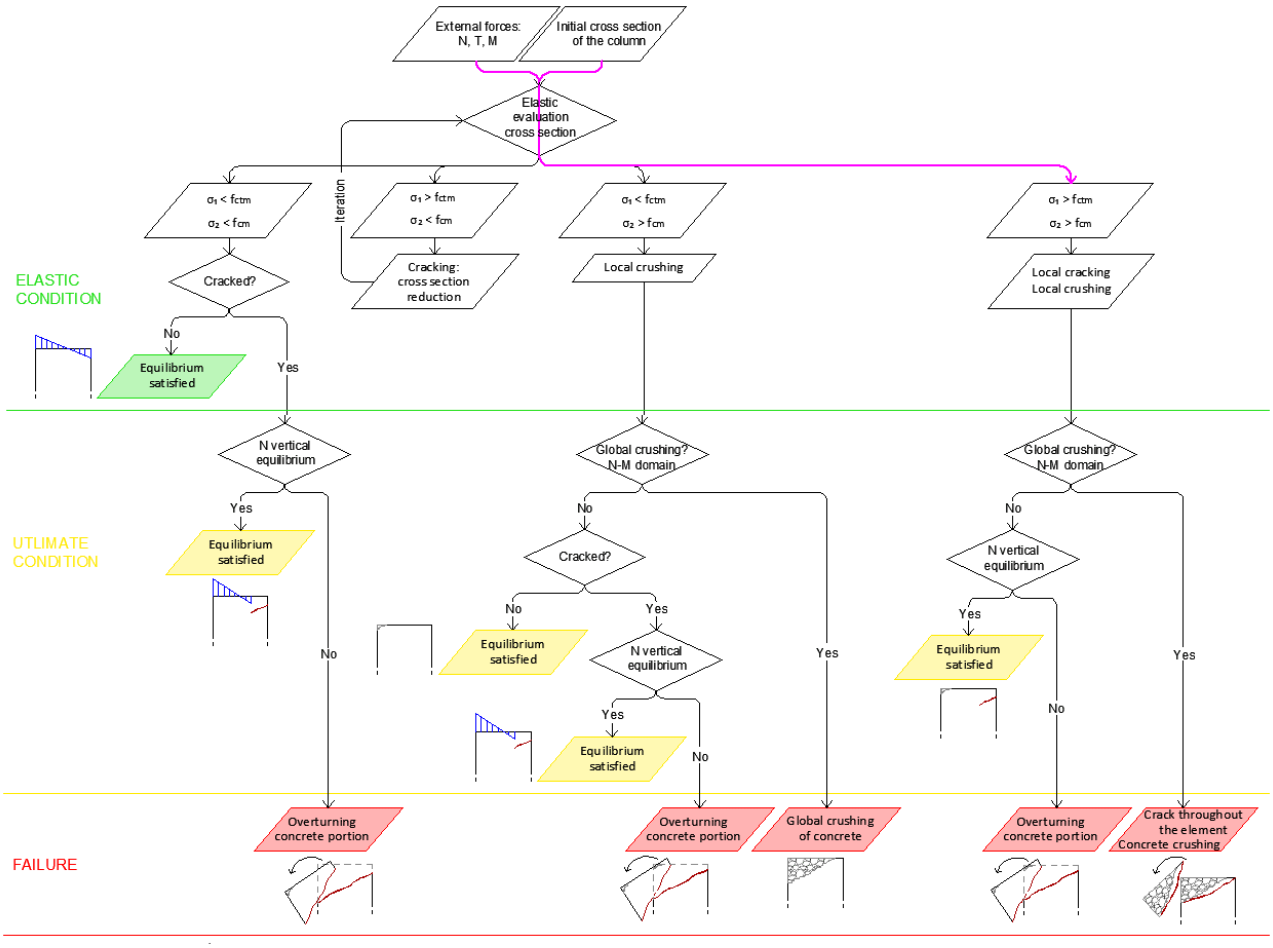

Figure 5.3.3.1 – Path corresponding to the third scenario in the flow chart

$$\left(\sigma_1^{lower\ edge}\right)^{1st\ it.} > f_{ctd}$$

$$\left(\sigma_2^{upper\ edge}\right)^{1st\ it.} > f_{cd}$$

At the very first analysis, both failure criteria overcame. Even in this case no further study of the development of the damage. It can be defined the type of crushing, basing on the traditional N-M interaction domains: if the point falls out, the whole element crushes, hence the entire element fails; if the N-M domain verification is satisfied, the crushing of the concrete affects only a limited portion of the element and the analysis can deepen by checking the N vertical equilibrium. It can be satisfied, in that case, the column is locally crushed on one side and locally cracked on the other one, but the element does not entirely fail. If it is not, the crushing is local but the cracking affects the whole element, thus it fails because of the overturning of the portion of concrete above the crack.

5.3.4. Fourth Scenario

The first elastic evaluation of the cross section shows a stress state such that the principal tensile stress at the lowest fiber overcomes the tensile strength of the material and principal compressive stress at the upper edge stand below its limit:

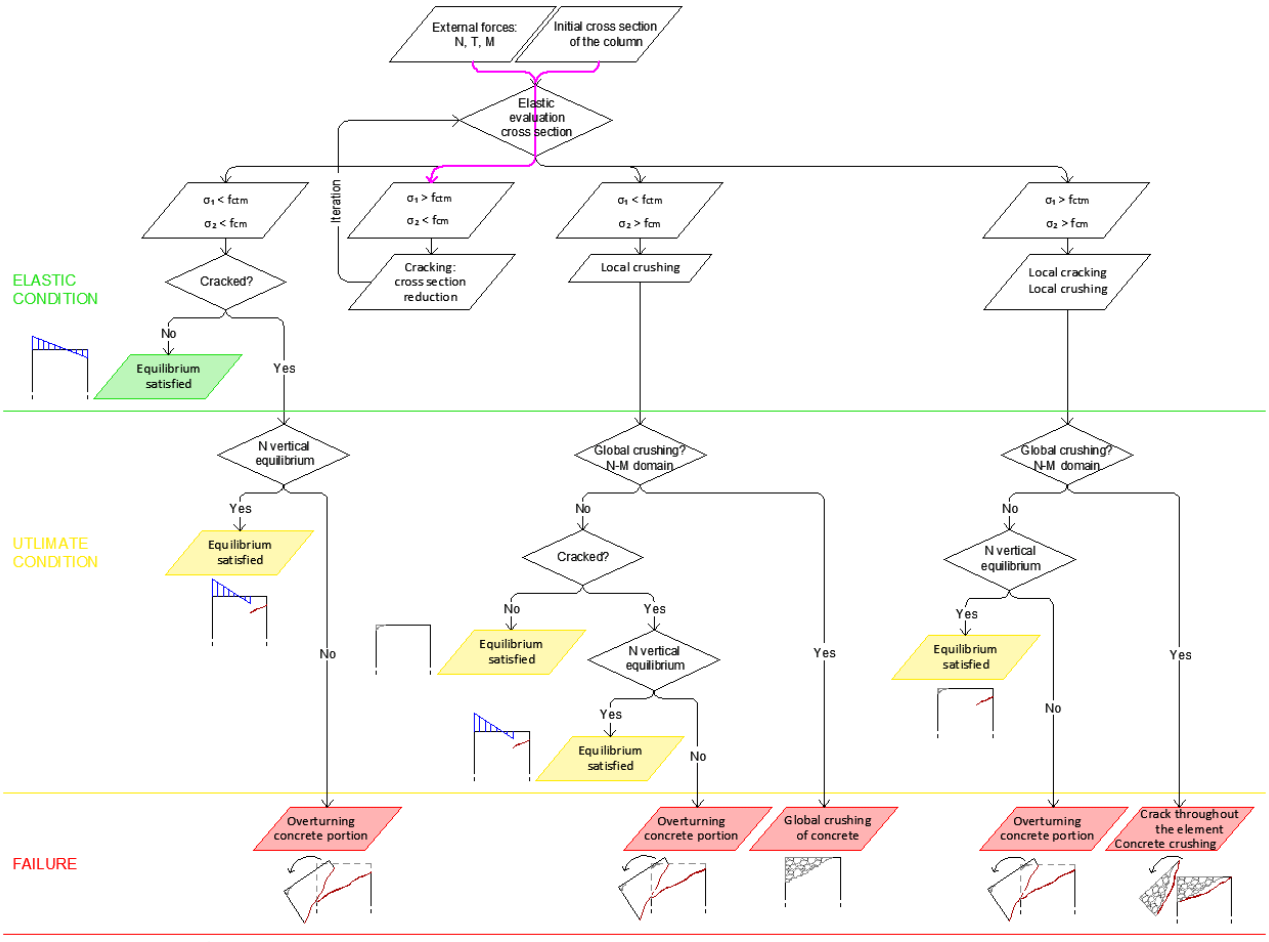

Figure 5.3.4.1 – Path corresponding to the fourth scenario in the flow chart

$$\left(\sigma_1^{lower\ edge}\right)^{1st\ it.} > f_{ctd}$$

$$\left(\sigma_2^{upper\ edge}\right)^{1st\ it.} < f_{cd}$$

In this case, the analysis does not stop but proceeds with the iteration. The fiber at the extremity of the cross section cracks, according to the stress state the computation of the crack inclination derives.

Then the flow chart shows that the procedure gets back the first step, the evaluation of the column cross section. Since the last fiber is no longer working, the elastic evaluation of the cross section needs to repeat: all the basic quantities recomputed, a new normal stresses diagram and a new tangential stress distribution follow.

Since the state of stress changed, the principal tensile stress at the lowest fiber and the principal compressive stress at the upper edge changed as well. So now, the procedure can take three different branches:

- $\sigma_1^{lower\ edge} < f_{ctm}$ and $\sigma_2^{upper\ edge} < f_{cm}$
- $\sigma_1^{lower\ edge} < f_{ctm}$ and $\sigma_2^{upper\ edge} > f_{cm}$
- $\sigma_1^{upper\ edge} > f_{ctm}$ and $\sigma_2^{lower\ edge} > f_{cm}$

Let us consider first the case where, after the first iteration, the state of stress shows both principal tensile stress at the lower extremity and principal compressive stress at the upper edge, smaller than their respective limit values. Thus, this case can be summarised as:

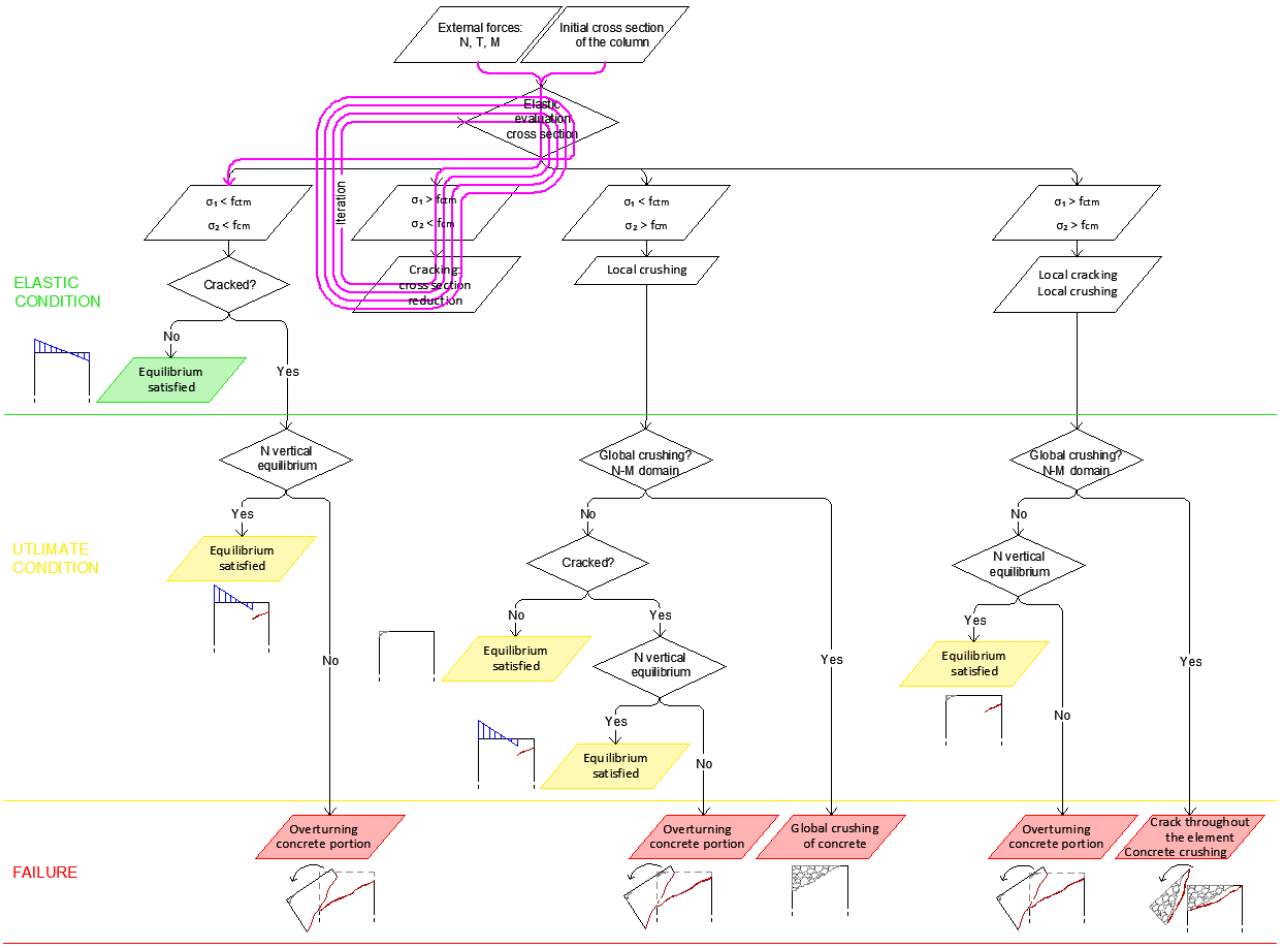

Figure 5.3.4.2 – Path corresponding to the fourth scenario in the flow chart

$$1^{st}\ iteration: \begin{cases} \left(\sigma_1^{lower\ edge}\right)^{1st\ it.} > f_{ctd} \\ \left(\sigma_2^{upper\ edge}\right)^{1st\ it.} < f_{cd} \end{cases}$$

$$2^{nd}\ iteration: \begin{cases} \left(\sigma_1^{lower\ edge}\right)^{2nd\ it.} < f_{ctd} \\ \left(\sigma_2^{upper\ edge}\right)^{2nd\ it.} < f_{cd} \end{cases}$$

Alternatively, the same case derives if:

$$1^{st}\ iteration: \begin{cases} \left(\sigma_1^{lower\ edge}\right)^{1st\ it.} > f_{ctd} \\ \left(\sigma_2^{upper\ edge}\right)^{1st\ it.} < f_{cd} \end{cases}$$

...

$$i^{th}\ iteration: \begin{cases} \left(\sigma_1^{lower\ edge}\right)^{i-th\ it.} > f_{ctd} \\ \left(\sigma_2^{upper\ edge}\right)^{i-th\ it.} < f_{cd} \end{cases}$$

...

$$n^{th}\ iteration: \begin{cases} \left(\sigma_1^{lower\ edge}\right)^{n-th\ it.} < f_{ctd} \\ \left(\sigma_2^{upper\ edge}\right)^{n-th\ it.} < f_{cd} \end{cases}$$

This means that, after the propagation of the crack, thus after one or some iterations, which reduce the cross section because of the cracking of one or more fibers, then the element finds an equilibrium condition. In that condition, both the principal tensile stress at the lowest un-cracked fiber and the principal compressive stress at the upper edge of the cross section, stand below their limit values.

In this case, the development of the damage could be observed. The crack develops up to a certain fiber, and then stops when the element finds an equilibrium condition.

In the flow chart, this alternative is represented by the path that follows "*Yes*" to the question "*Cracked?*". The crack can be drawn, the last verification checks the N vertical equilibrium. Since the element is cracked, it has to be verified if, in the damaged condition, the element is in equilibrium condition for what concerns N. If it is satisfied, it means that the locally cracked column withstands the external forces. On the other hand, if the N vertical equilibrium is not satisfied, the column fails because of the overturning of the portion of concrete above the crack.

5.3.5. Fifth Scenario

Another possible scenario is the following:

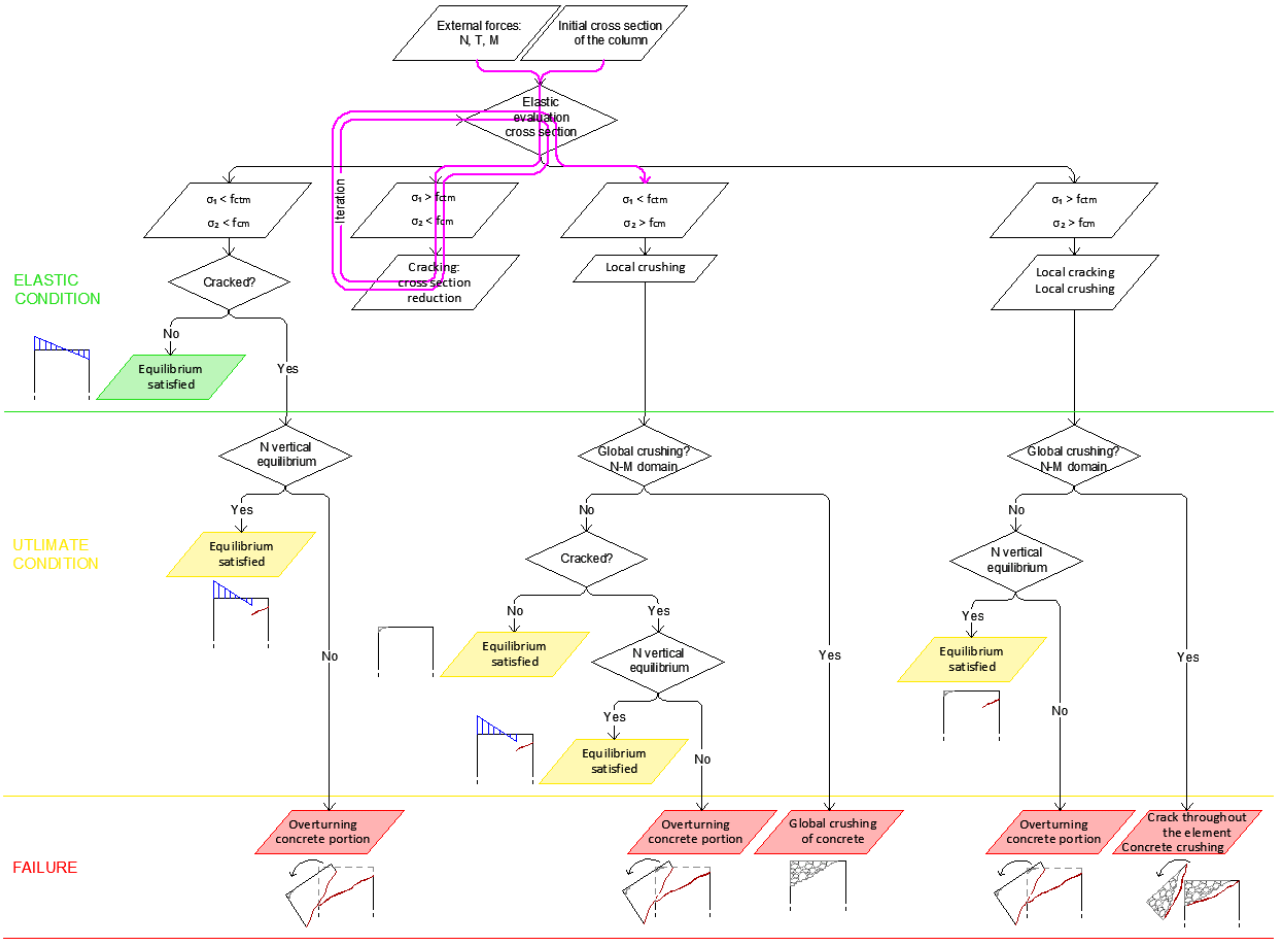

Figure 5.3.5.1 – Path corresponding to the fifth scenario in the flow chart

$$1^{st}\ iteration: \begin{cases} \left(\sigma_1^{lower\ edge}\right)^{1st\ it.} > f_{ctd} \\ \left(\sigma_2^{upper\ edge}\right)^{1st\ it.} < f_{cd} \end{cases}$$

...

$$i^{th}\ iteration: \begin{cases} \left(\sigma_1^{lower\ edge}\right)^{i-th\ it.} > f_{ctd} \\ \left(\sigma_2^{upper\ edge}\right)^{i-th\ it.} < f_{cd} \end{cases}$$

...

$$n^{th}\ iteration: \begin{cases} \left(\sigma_1^{lower\ edge}\right)^{n-th\ it.} < f_{ctd} \\ \left(\sigma_2^{upper\ edge}\right)^{n-th\ it.} > f_{cd} \end{cases}$$

This case correspond to an initial development of the crack because the principal tensile stress at the lowest fiber exceeds the tensile strength of the concrete but, after a certain number of iterations, it becomes smaller than the limit and, simultaneously, the principal compressive stress at the upper edge overcomes the compressive strength of the concrete. Thus, after the development of the crack on the tensile side, the element also crushes.

In this case, what has to be defined first is the type of crushing: a local damage is certainly happened, but it could also affect the whole element. This information arises from traditional *N-M* interaction domains: if the point falls out, the whole element crushes, hence the entire element fails, there is no need for further investigations; if the *N-M* domain verification is satisfied, the crushing of the concrete affects only a limited portion of the element and the analysis can deepen by checking the *N* vertical equilibrium. It can be satisfied, in that case, the column is locally crushed on one side and locally cracked on the other one, but the element does not entirely fail. If it is not, the crushing is local but the cracking affects the whole element, thus it fails because of the overturning of the portion of concrete above the crack.

5.3.6. Sixth Scenario

The last case corresponds to the following case:

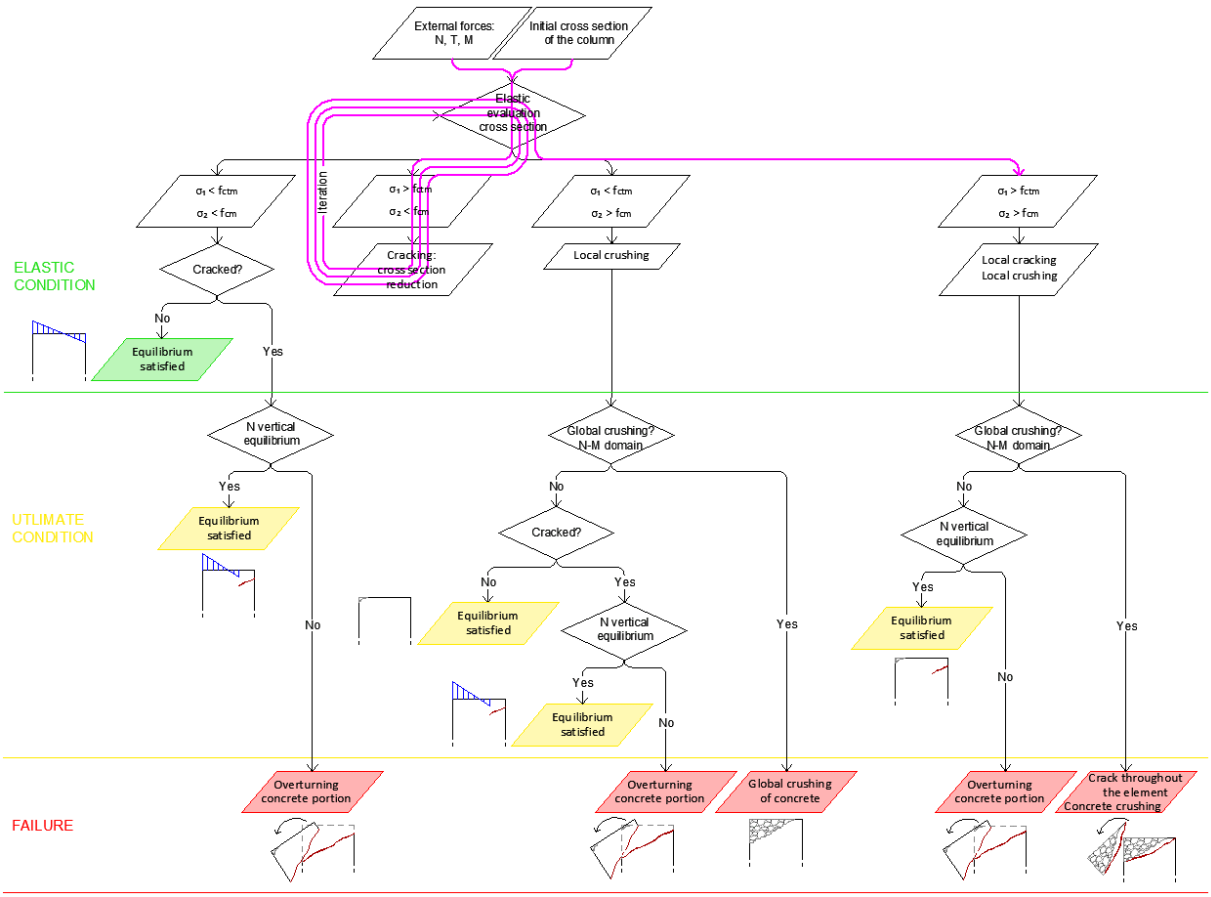

Figure 5.3.6.1 – Path corresponding to the sixth scenario in the flow chart

$$1^{st}\ iteration: \begin{cases} \left(\sigma_1^{lower\ edge}\right)^{1st\ it.} > f_{ctd} \\ \left(\sigma_2^{upper\ edge}\right)^{1st\ it.} < f_{cd} \end{cases}$$

...

$$i^{th}\ iteration: \begin{cases} \left(\sigma_1^{lower\ edge}\right)^{i-th\ it.} > f_{ctd} \\ \left(\sigma_2^{upper\ edge}\right)^{i-th\ it.} < f_{cd} \end{cases}$$

...

$$n^{th}\ iteration: \begin{cases} \left(\sigma_1^{lower\ edge}\right)^{n-th\ it.} > f_{ctd} \\ \left(\sigma_2^{upper\ edge}\right)^{n-th\ it.} > f_{cd} \end{cases}$$

Also this case correspond to an initial development of the crack because the principal tensile stress at the lowest fiber exceeds the tensile strength of the concrete and, after a certain number of iterations, also the principal compressive stress at the upper edge overcomes the compressive strength of the concrete. Thus, after the development of the crack on the tensile side, the element also crushes.

In this case, what has to be defined first is the type of crushing: a local damage is certainly happened, but it could also affect the whole element. This information arises from traditional *N-M* interaction domains: if the point falls out, the whole element crushes, hence the entire element fails, there is no need for further investigations; if the *N-M* domain verification is satisfied, the crushing of the concrete affects only a limited portion of the element and the analysis can deepen by checking the *N* vertical equilibrium. It can be satisfied, in that case, the column is locally crushed on one side and locally cracked on the other one, but the element does not entirely fail. If it is not, the crushing is local but the cracking affects the whole element, thus it fails because of the overturning of the portion of concrete above the crack.

6. Applicative Examples

6.1. Practical Example of the Fourth Scenario

In order to understand clearly how the procedure works, some practical example have considered. This first case takes into account of a real existing column, external forces acting on it are reduced lightly in order to test the procedure and obtain the first scenario explained in the previous paragraph.

6.1.1. Input Data

The information that the procedure requires has listed below:

- $b = 500\,mm$;
- $h = 500\,mm$;
- $c = 40\,mm$;
- $d = 260\,mm$;
- $A_{s,sup} = 2\,\Phi\,24 = 904\,mm^2$;
- $A_{s,inf} = 2\,\Phi\,24 = 904\,mm^2$;
- $\Phi_{st} = \Phi\,6 = 6\,mm$;
- $n_{st} = 2$;
- $s_{st} = 200\,mm$:
- $f_{cd} = 60\,MPa$;
- $f_{ctd} = 0.1\,f_{cd} = 6\,MPa$;
- $f_{yd} = 600\,MPa$;
- $E_c = 22000\left[\left(\frac{f_{cd}}{10}\right)^{0.3}\right] = 37659\,MPa$;
- $E_s = 210000\,MPa$;
- $n = {E_c}/{E_s} = 5.58$;
- $N_{act} = -400000\,N$;

- $T_{act} = 400000\ N$;
- $M_{act} = 200000000\ N\ mm$;

Once defined input data, the script subdivides a half cross section into fibers, in this case it has decided to obtain a width of the fiber equal to one centimetre, considered as a good balance between computational costs and accuracy. The vector of the fiber considered is the following one:

$$y = [245,\ 235,\ 225,\ 215,\ 205,\ 195,\ 185,\ 175,\ 165,\ 155,\ 145,\ 135,\ 125,\ 115, \ldots$$

$$\ldots\ 105,\ 95,\ 85,\ 75,\ 65,\ 55,\ 45,\ 35,\ 25,\ 15,\ 5]$$

The basic quantities that are necessary to evaluate the stress state distribution depend on the iteration; at each iteration, they are computed.

6.1.2. 1st Elastic Evaluation of the Cross Section

The procedure has represented on the flow chart as a purple line that follows the steps the analysis goes through. This first iteration corresponds to the beginning of the iteration; it has drawn in the following picture.

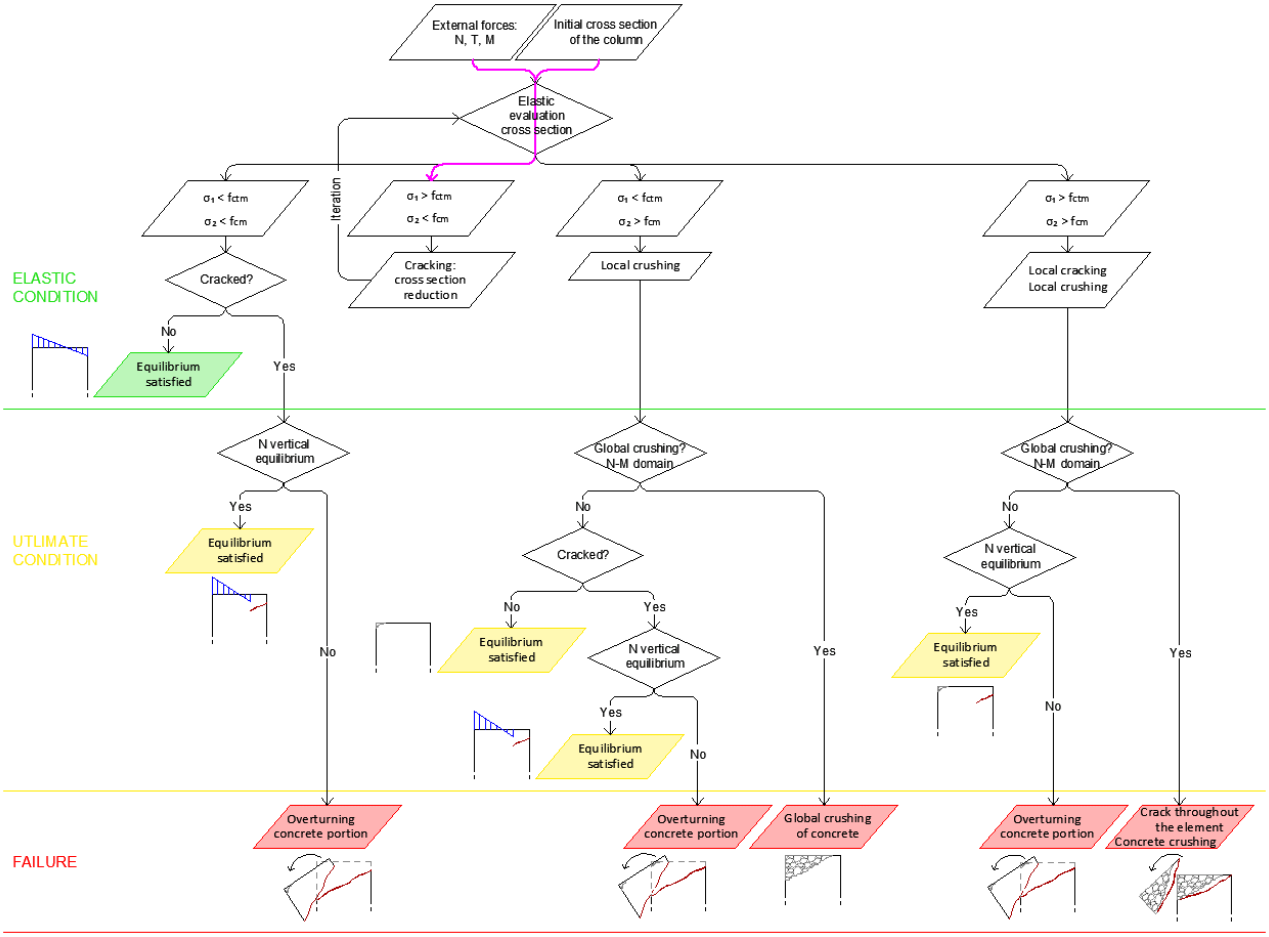

Figure 6.1.2.1 – 1st iteration of the procedure represented in the flow chart

6.1.2.1. Basic Quantities

The first step of the procedure consists in the elastic evaluation of the initial cross section of the column. This corresponds to the computation of some basic quantities, such as the effective depth, the homogenised cross section area, the homogenised moment of inertia and the homogenised static moment, and then it is possible to proceed with the normal and tangential stresses diagram.

All those parameters depend on the cross section considered; the first iteration correspond to the initial configuration, e.g. the whole cross section reacting. This case identifies by the coordinate of the last fiber, the one at the extremity of the reacting cross section, that is:

$$y^{1st\ it.} = y(1) = 245\ mm$$

All other quantities have expressed as a function of it, thus, at each iteration, if the cross section cracks, and therefore it reduces, the script computes them depending on the y coordinate:

- The effective depth at the 1st iteration, when the entire cross section works, $y = 245\ mm$:

$$d^{1st\ it.} = \left(\frac{h}{2} + y^{1st\ it.} + \frac{w}{2}\right) - c = \left(\frac{500}{2} + 245 + \frac{10}{2}\right) - 40 = 460\ mm$$

- The homogenized cross section into concrete:

$$A_{omog}{}^{1st\ it.} = \left[b * \left(\frac{h}{2} + y^{1st\ it.} + \frac{w}{2}\right)\right] + \left(n * A_{s,sup}\right) + \left(n * A_{s,inf}\right)$$

$$= \left[500 * \left(\frac{500}{2} + 245 + \frac{10}{2}\right)\right] + (5.58 * 904) + (5.58 * 904)$$

$$= 260088\ mm^2$$

- S is the static moment of the cross section with respect to the lower edge:

$$S^{1st\ it.} = \left\{b * \left(\frac{h}{2} + y^{1st\ it.} + \frac{w}{2}\right) * \left[\frac{\left(\frac{h}{2} + y^{1st\ it.} + \frac{w}{2}\right)}{2}\right]\right\} + \left[n\ A_{s,sup}\ \left(\frac{h}{2} - c\right)\right] + \left(n\ A_{s,inf}\ c\right)$$

$$= \left\{500\ \left(\frac{500}{2} + 245 + \frac{10}{2}\right)\left[\frac{\left(\frac{500}{2} + 245 + \frac{10}{2}\right)}{2}\right]\right\} + \left[5.58 * 904\ \left(\frac{500}{2} - 40\right)\right] + (5.58 * 904 * 40)$$

$$= 63760259\ mm^3$$

- The position of the centroid of the cross section, expressed as its distance with respect to the upper edge of the element:

$$d_{g,sup}{}^{1st\ it.} = \frac{S^{1st\ it.}}{A_{omog}{}^{1st\ it.}} = 245$$

$$d_{g,inf}{}^{1st\ it.} = h - d_{g,sup}{}^{1st\ it.} = 255$$

- The moment of inertia of the reacting cross section:

$$I_{omog}{}^{1st\ it.} = \left(\frac{b\ d_{g,inf}{}^{1st\ it.3}}{3}\right) + \left\{\frac{b\left[d_{g,sup} - \left(\frac{h}{2} - \left(y^{1st\ it.} + \frac{w}{2}\right)\right)\right]^3}{3}\right\}$$

$$+ \left[n\ A_{s,sup}\left(d_{g,sup} - c\right)^2\right] + \left[n\ A_{s,inf}\left(d_{g,inf} - c\right)^2\right]$$

$$= \left(\frac{500 * 245^3}{3}\right) + \left\{\frac{500\left[255 - \left(\frac{500}{2} - \left(245 + \frac{10}{2}\right)\right)\right]^3}{3}\right\} + [5.58 * 904\ (255 - 40)^2]$$

$$+ [5.58 * 904\ (245 - 40)^2]$$

$$= 5659059309\ mm^4$$

6.1.2.2. Normal Stresses Distribution

The position of the neutral axis can be determined as the y coordinate where normal stresses are equal to zero; hence, solving for y:

$$y_{n.a.}{}^{1st\ it.} = \frac{N_{act}}{M_{act} - \left(N_{act}\left(\frac{h}{2} - d_{g,sup}{}^{1st\ it.}\right)\right)} \frac{A_{omog}{}^{1st\ it.}}{I_{omog}{}^{1st\ it.}} = \frac{-400000}{200000000 - \left(-400000\left(\frac{500}{2} - 255\right)\right)} \frac{260088}{5659059309}$$

$$= -43\ mm$$

Once computed the neutral axis position, the normal stresses diagram is a linear distribution from the most compressed to the tensest fiber, passing through zero in correspondence of the neutral axis. It has evaluated by means of the Navier's equation, where y^i corresponds to the distance from the neutral axis:

$$\sigma^i = \frac{N_{act}}{A_{omog}{}^{1st\ it.}} \pm \frac{M_{act} - (N_{act}\ e)}{I_{omog}{}^{1st\ it.}} y^i$$

Using Navier's equation, the vector containing the value of normal stress for each fiber is computed. This vector also contains the stress acting on the most compressed fiber, the one at the upper extremity, $y^{max\ comp.1st\ it.} = 250\ mm$, solicited by a compressive stress equal to:

$$\sigma^{\max comp.\ 1st\ it.} = \frac{-400000}{260088} - \frac{200000000 - \left(400000\left(\frac{500}{2} - 245\right)\right)}{5659059309} 250 = -10.459\ MPa$$

It also contains the stress on the tensest fiber, the one at the lower extremity, corresponding to $y^{max\ tens.\ 1st\ it} = -245\ mm$:

$$\sigma^{\max tens.\ 1st\ it} = \frac{-400000}{260088} - \frac{200000000 - \left(-400000\left(\frac{500}{2} - 255\right)\right)}{5659059309}(-245) = 7.426\ MPa$$

These two values are the maximum compressive and tensile stresses acting on the cross section, to evaluate the principal tensile stress at the lowest fiber and the principal compressive stress at the upper edge, the values of the corresponding tangential stresses are required.

6.1.2.3. Tangential Stress Distribution

As previously explained, tangential stresses derive from the Jourawsky's formula:

$$\tau = \frac{T_{act}\, S_{omog}{}^{1st\ it.}}{I_{omog}{}^{1st\ it.}\, b}$$

Where the homogenised static moment varies throughout the height of the cross section.

The script computes the tangential stresses for all the fiber of the cross section. Since the procedure works on the base of the fiber at the lowest extremity of the working cross section and the one at the highest extremity of the reacting cross section, the two values that the script requires to proceed are the one in correspondence of the upper compressed edge and the one for $y^{1st\ it.} = 145\ mm$. At the compressed fiber, tangential stress is always null, at the tensest fiber, depends if it stays below reinforcement or not. In this case, y falls below reinforcement, therefore tangential stresses are equal to zero for the tensest fiber too:

$$\tau^{\max comp.\ 1st\ it.} = 0\ MPa$$

$$\tau^{\max tens.\ 1st\ it.} = 0\ MPa$$

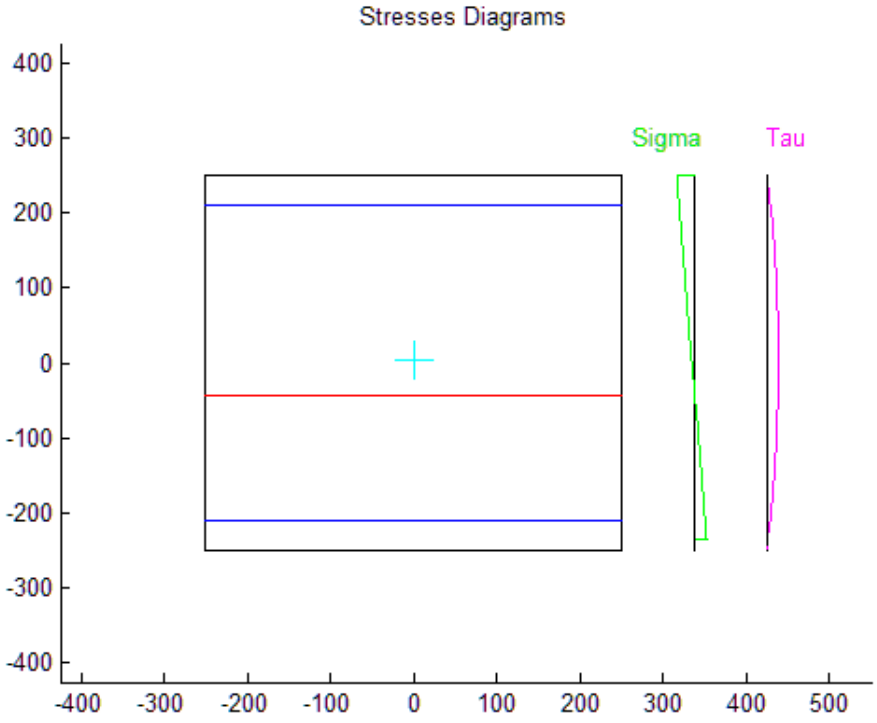

Figure 6.1.2.3.1 – Tangential and normal stresses distributions

6.1.2.4. Principal Stresses

The failure criteria depend on the principal stresses at the extremities of the working cross section; they can be evaluated as a function of the normal and tangential stresses listed in the two previous paragraphs.

For the compressed fiber, the equation that returns the value of the principal compressive stress as a function of the normal and tangential stresses is the following:

$$\sigma_1{}^{\max comp.\ 1st\ it.} = \frac{\sigma^{\max comp.\ 1st\ it.} - \sqrt{\sigma^{\max comp.\ 1st\ it.{}^2} + 4\,\tau^{\max comp.\ 1st\ it.}}}{2} = -10.459\ MPa$$

On the other hand, for the tensile fiber:

$$\sigma_1{}^{\max tens.} = \frac{\sigma^{\max tens.\ 1st\ it.} + \sqrt{\sigma^{\max tens.\ 1st\ it.{}^2} + 4\,\tau^{\max tens.\ 1st\ it.}}}{2} = 7.426\ MPa$$

Since tangential stresses are both null, principal stresses coincide with the maximum normal ones.

Depending on those two terms, the procedure follows a specific path. Depending on those two terms, four possible alternative paths. In this case, at the first iteration the situation is:

$$\sigma_1{}^{\max comp.\ 1st\ it.} = |\mathbf{-10.459}|\ \boldsymbol{MPa} < \boldsymbol{f_{cd}} = |-60|\ MPa$$

$$\sigma_1{}^{\max tens.\ 1st\ it.} = \mathbf{7.462MPa} > \boldsymbol{f_{ctd}} = 6\ MPa$$

It means that, at the end of the first iteration, principal tensile stress exceeds the tensile strength of the concrete in the lowest fiber but the principal compressive stress at the upper edge stays below the limit, and therefore the scenario is:

$$\left(\sigma_1^{lower\ edge}\right)^{1st\ it.} > f_{ctd}$$

$$\left(\sigma_2^{upper\ edge}\right)^{1st\ it.} < f_{cd}$$

This means that the last fiber subjected to traction cracks. The script proceeds returning at the first step, revaluating the cross section now reduced of that one fiber and computing again the state of stress.

6.1.3. 2nd Elastic Evaluation of the Cross Section

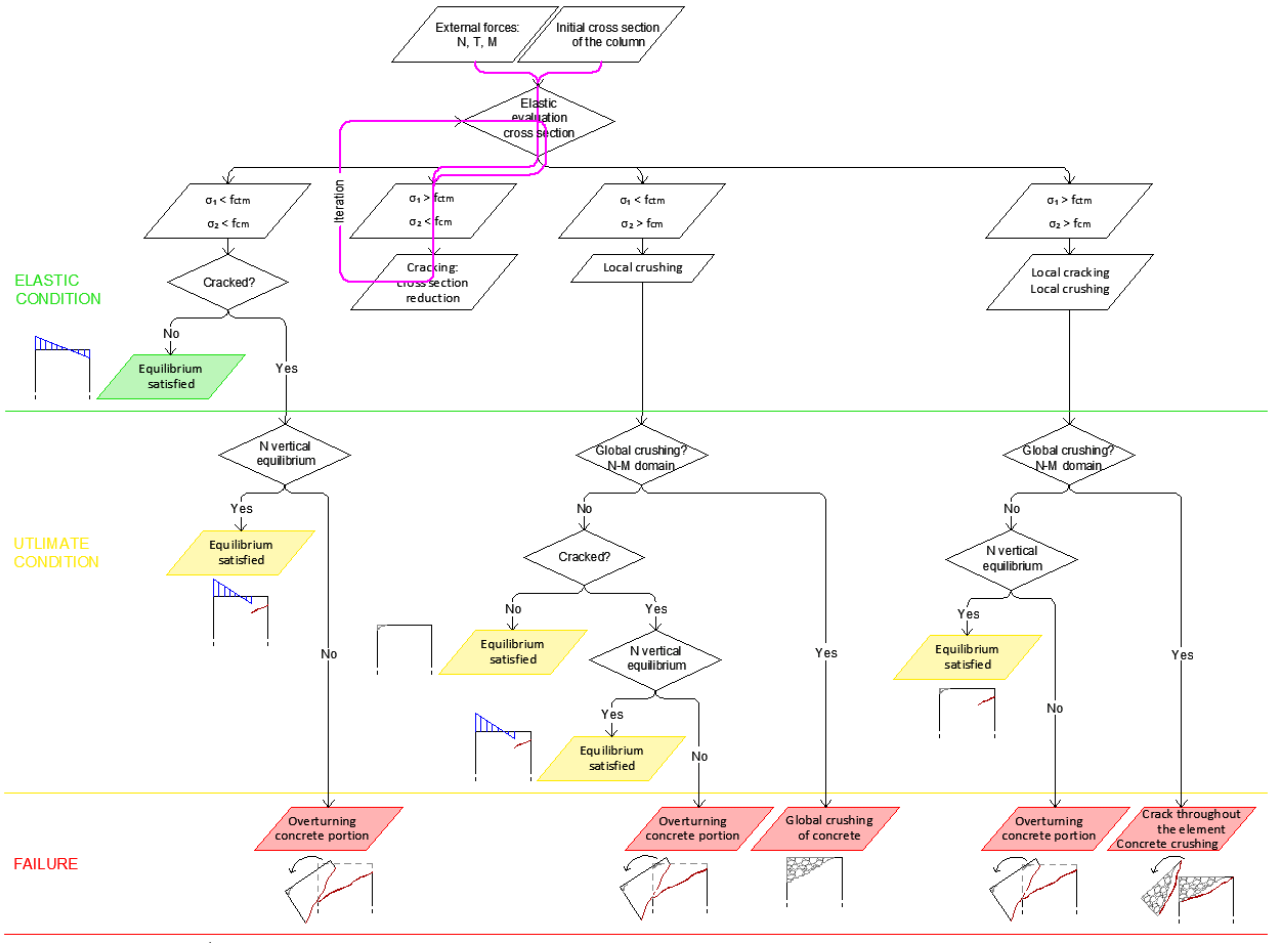

Figure 6.1.3.1 – 2nd iteration of the procedure represented in the flow chart

At the end of the first elastic evaluation of the cross section, the principal tensile stress exceeds the tensile strength of the concrete in the lowest fiber but the principal compressive stress at the upper edge stays below the limit. This means that the fiber at the extremity of the cross section subjected to traction, cracks. Consequently, the procedure returns at the first step, which involves the revaluation of the changed cross section, the initial one without the last cracked fiber.

Hence, at this second iteration, what changes is the coordinate of the last working fiber, the one at the extremity of the reacting cross section that is in this case is

$$y^{2nd\ it.} = y(2) = 235\ mm$$

Now the procedure repeats exactly as for the first iteration, the only parameter that changed is y.

All basic quantities computed at the first step, depending on y, have to be computed again, since the coordinate changed, but the equation are the same mentioned for the first iteration:

$$d^{2nd\ it.} = 450\ mm$$

$$A_{omog}{}^{2nd\ it.} = 255082\ mm^2$$

$$S^{2nd\ it.} = 61285259\ mm^3$$

$$d_{g,sup}{}^{2nd\ it.} = \frac{S}{A_{omog}} = 240\ mm$$

$$d_{g,inf}{}^{2nd\ it.} = h - d_{g,inf} = 260\ mm$$

$$I_{omog}{}^{2nd\ it.} = 5677641020\ mm^4$$

The position of the neutral axis is straightforward:

$$y_{a.n.}{}^{2nd\ it.} = -44\ mm$$

Once computed the neutral axis position, Navier's equation gives the normal stresses distribution. The sigma value that the procedure is interested in, is the one related to the upper edge under compression, corresponding to $y^{\max comp.} = 250\ mm$:

$$\sigma^{\max comp.\ 2nd\ it.} = -10.546\ MPa$$

Even the one acting on the tensest fiber, the one at the lower extremity, corresponding to $y^{max\ tens.} = -235\ mm$:

$$\sigma^{\max tens.\ 2nd\ it.} = 7.063\ MPa$$

Tangential stresses are still equal to zero because the considered fiber is below steel rebar:

$$\tau^{\max comp.\ 2nd\ it.} = 0\ MPa$$

$$\tau^{\max tens.\ 2nd\ it.} = 0\ MPa$$

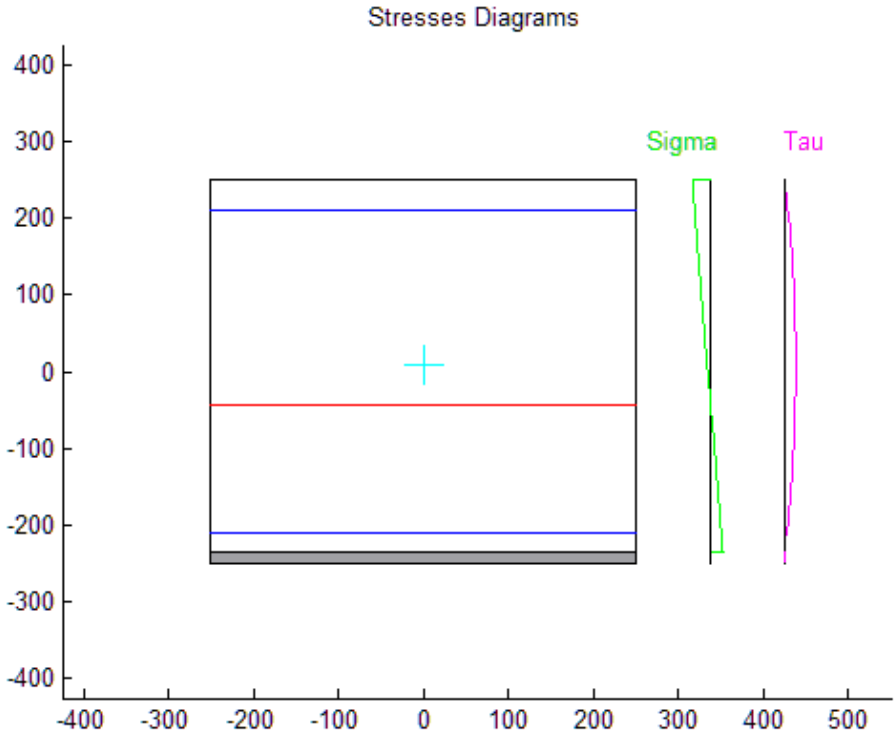

Figure 6.1.3.2 - Tangential and normal stresses distributions

Also in this case, considering that tangential stresses are null, principal stresses are equal to normal ones:

$$\sigma_1{}^{\max comp.\ 2nd\ it.} = -10.546\ MPa$$

For the tensile fiber:

$$\sigma_1{}^{\max tens.\ 2nd\ it.} = 7.063\ MPa$$

At the end of the second iteration, the procedure falls again in the fourth scenario:

$$\sigma_1{}^{\max comp.\ 2nd\ it.} = |\mathbf{-10.546}|\ \boldsymbol{MPa} < \boldsymbol{f_{cd}} = |-60|\ MPa$$

$$\sigma_1{}^{\max tens.\ 2nd\ it.} = \mathbf{7.063\ MPa} > \boldsymbol{f_{ctd}} = 6\ MPa$$

At the end of the second iteration, once again, principal tensile stress exceeds the tensile strength of the concrete in the lowest fiber but the principal compressive stress at the upper edge stays below the limit, and therefore the scenario is:

$$\left(\sigma_1^{lower\ edge}\right)^{2nd\ it.} > f_{ctd}$$

$$\left(\sigma_2^{upper\ edge}\right)^{2nd\ it.} < f_{cd}$$

The last fiber subjected to traction cracks. The script proceeds returning at the first step, revaluating the cross section now reduced of that one fiber and computing again the state of stress.

6.1.4. 3rd Elastic Evaluation of the Cross Section

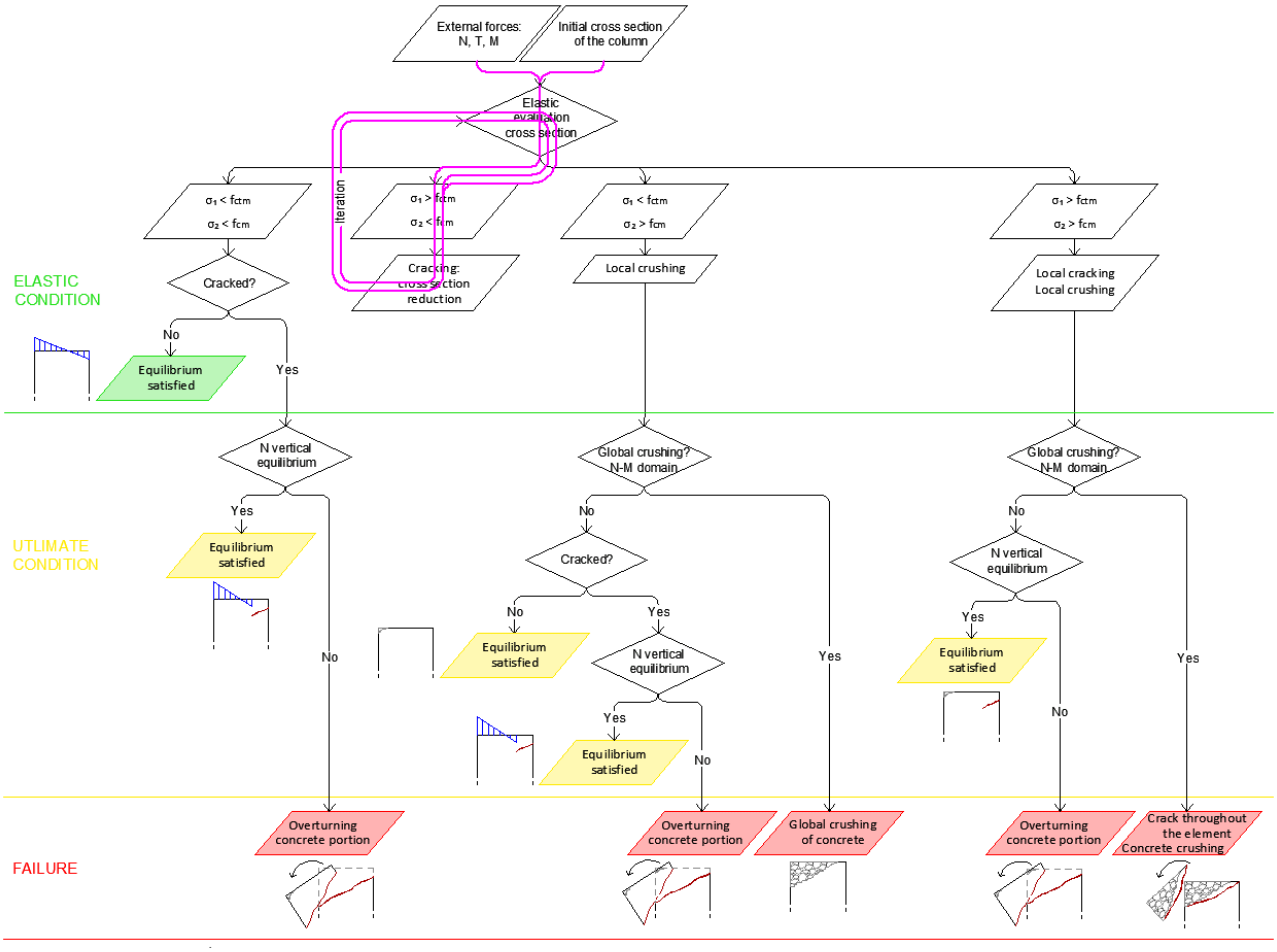

Figure 6.1.4.1 – 3rd iteration of the procedure represented in the flow chart

At the third iteration, the coordinate of the last working fiber, the one at the extremity of the reacting cross section, changes again:

$$y^{3rd\ it.} = y(3) = 225\ mm$$

All basic quantities computed at previous steps, depending on y, have to be calculated again using same equations. They are necessary to evaluate the stress distribution, which at this iteration are characterised by the following maximum values:

$$\sigma^{\max comp.\ 3rd\ it.} = -10.615\ MPa$$

$$\sigma^{\max tens.\ 3rd\ it.} = 6.756\ MPa$$

The corresponding tangential stresses are still null:

$$\tau^{\max comp.\ 3rd\ it.} = 0\ MPa$$

$$\tau^{\max tens.\ 3rd\ it.} = 0\ MPa$$

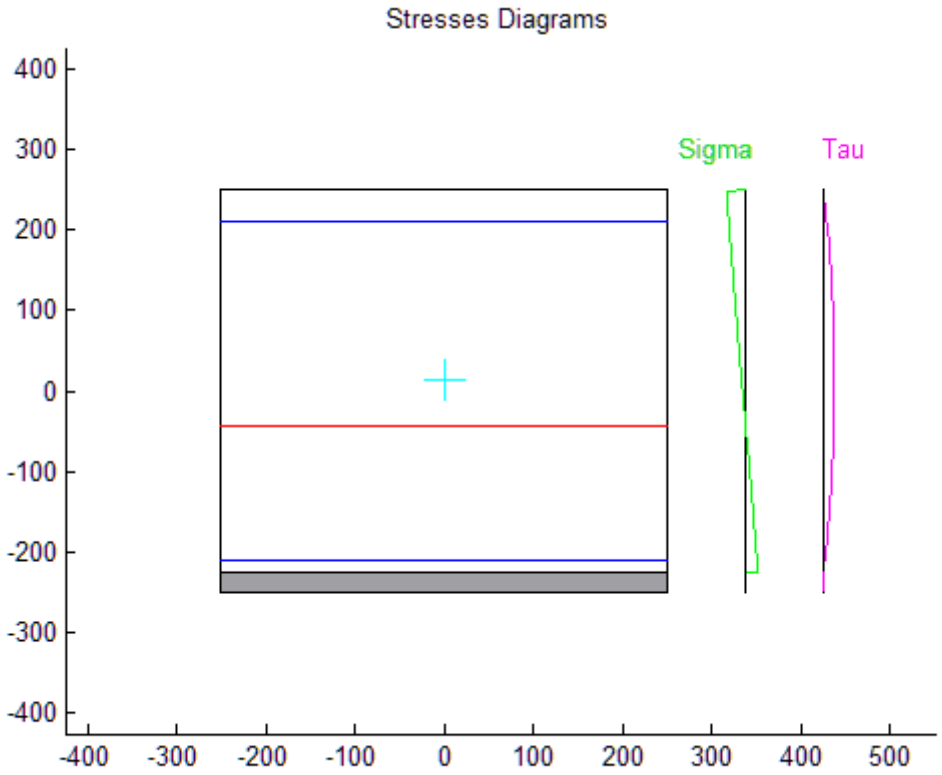

Figure 6.1.4.2 - Tangential and normal stresses distributions

Using same equations of the first iteration, the principal compressive stress at the most compressed fiber is:

$$\sigma_1{}^{\max comp.\ 3rd\ it.} = -10.615\ MPa$$

For the tensile fiber:

$$\sigma_1{}^{\max tens.\ 3rd\ it.} = 6.756\ MPa$$

At the end of the third iteration, the procedure falls again in the fourth scenario: principal tensile stress exceeds the tensile strength of the concrete in the lowest fiber but the principal compressive stress at the upper edge stays below the limit, and therefore the scenario is:

$$\sigma_1{}^{\max comp.\ 3rd\ it.} = |\mathbf{-10.615}|\ \boldsymbol{MPa} < \boldsymbol{f_{cd}} = |-60|\ MPa$$

$$\sigma_1{}^{\max tens.\ 3rd\ it.} = \mathbf{6.756\ MPa} > \boldsymbol{f_{ctd}} = 6\ MPa$$

Thus:

$$\left(\sigma_1^{lower\ edge}\right)^{3rd\ it.} > f_{ctd}$$

$$\left(\sigma_2^{upper\ edge}\right)^{3rd\ it.} < f_{cd}$$

The script revaluates again the cross section reduced.

6.1.5. 4th Elastic Evaluation of the Cross Section

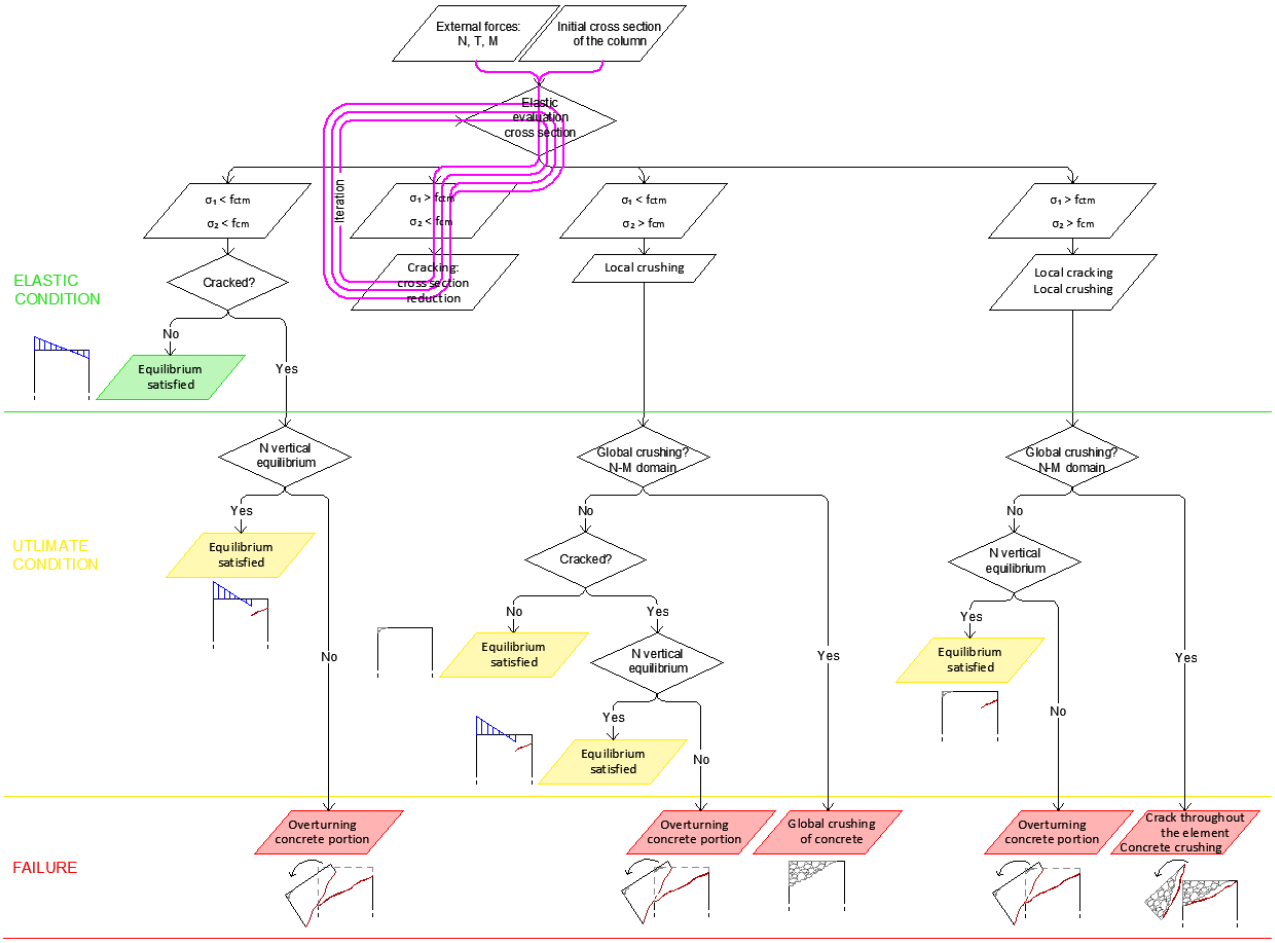

Figure 6.1.5.1 – 4th iteration of the procedure represented in the flow chart

At the fourth iteration:

$$y^{4th\ it.} = y(4) = 215\ mm$$

$$\sigma^{\max comp.\ 4th\ it.} = -10.664\ MPa$$

$$\sigma^{\max tens.\ 4th\ it.} = 6.365\ MPa$$

$$\tau^{\max comp.\ 4th\ it.} = 0\ MPa$$

$$\tau^{\max tens.\ 4th\ it.} = 0\ MPa$$

$$\sigma_1{}^{\max comp.\ 4th\ it.} = -10.664\ MPa$$

$$\sigma_1{}^{\max tens.\ 4th\ it.} = 6.365\ MPa$$

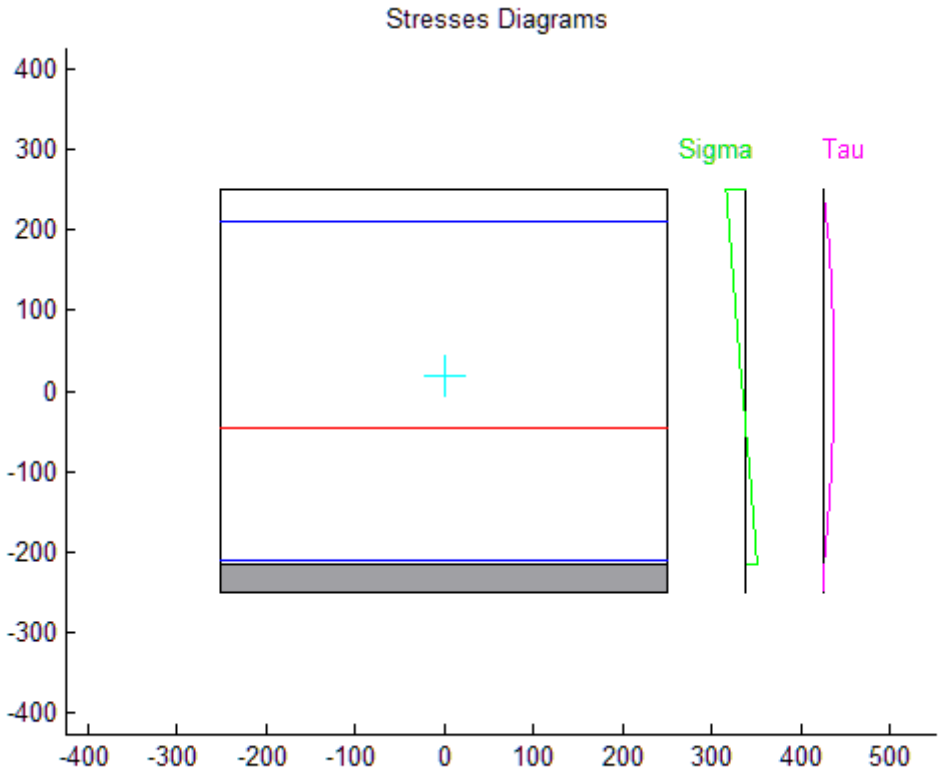

Figure 6.1.5.2 - Tangential and normal stresses distributions

At the end of the fourth iteration, the procedure falls again in the fourth scenario:

$$\sigma_1{}^{\max comp.\ 4th\ it.} = |\mathbf{-10.664}|\ \boldsymbol{MPa} < \boldsymbol{f_{cd}} = |-60|\ MPa$$

$$\sigma_1{}^{\max tens.\ 4th\ it.} = \mathbf{6.356}\ \boldsymbol{MPa} > \boldsymbol{f_{ctd}} = 6\ MPa$$

6.1.6. 5th Elastic Evaluation of the Cross Section

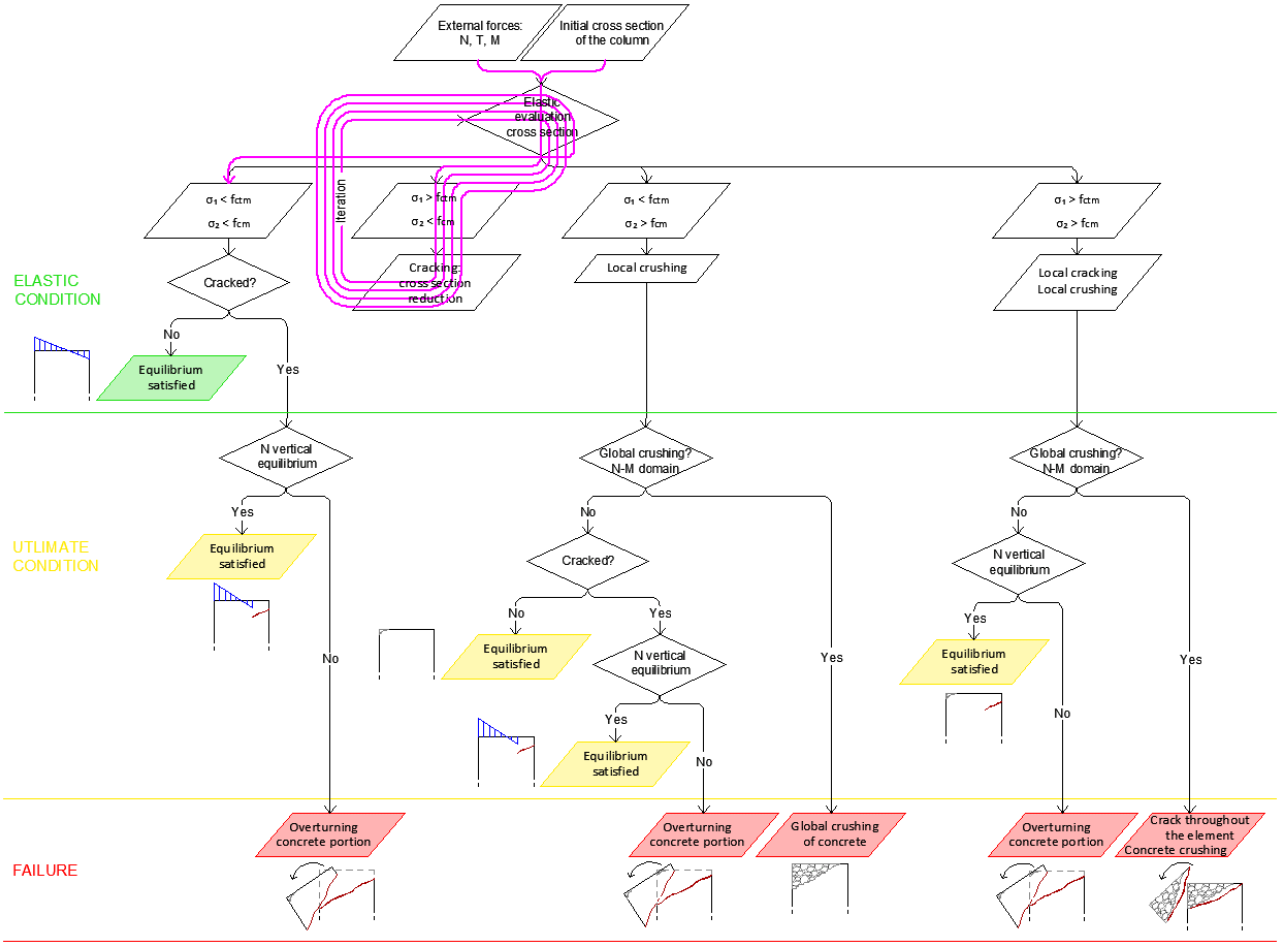

Figure 6.1.6.1 – 5th iteration of the procedure represented in the flow chart

$$y^{5th\ it.} = y(5) = 205\ mm$$

$$\sigma^{\max comp.\ 5th\ it.} = -10.695\ MPa$$

$$\sigma^{\max tens.\ 5th\ it.} = 5.964\ MPa$$

$$\tau^{\max comp.\ 5ht\ it.} = 0\ MPa$$

$$\tau^{\max tens.\ 5th\ it.} = 0.069\ MPa$$

$$\sigma_1{}^{\max comp.\ 5th\ it.} = -10.702\ MPa$$

$$\sigma_1{}^{\max tens.\ 5th\ it.} = 5.976\ MPa$$

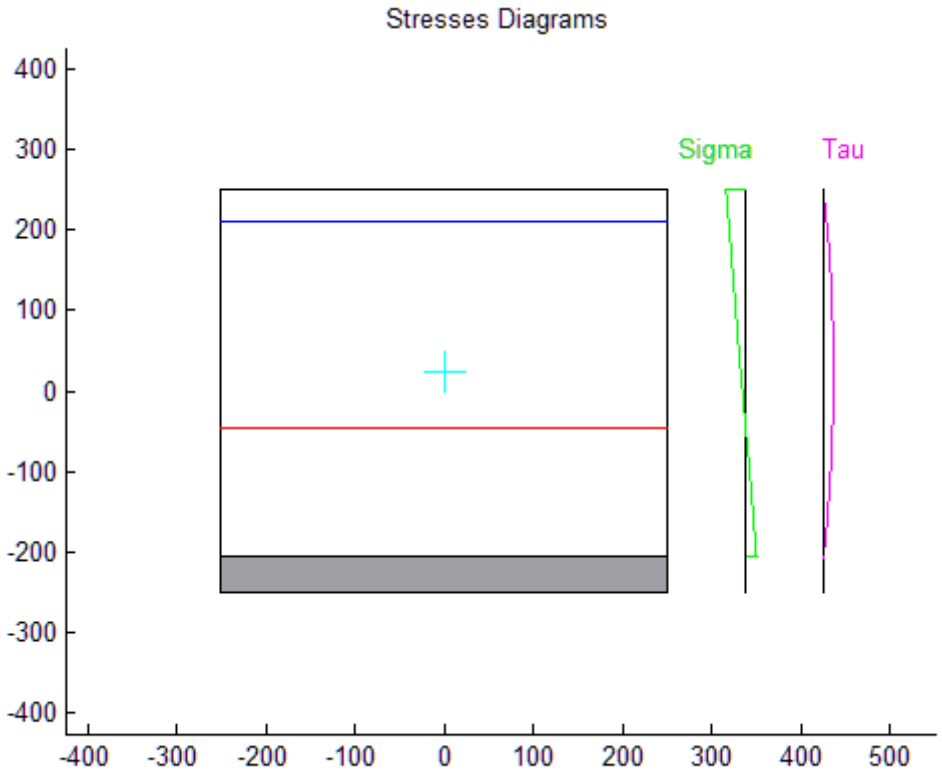

Figure 6.1.6.2 - Tangential and normal stresses distributions

At the end of the fifth iteration, the procedure falls again in the first scenario:

$$\sigma_1{}^{\max comp.\,5th\,it.} = |\mathbf{-10.695}|\ \boldsymbol{MPa} < \boldsymbol{f_{cd}} = |-60|\ MPa$$

$$\sigma_1{}^{\max tens.\ 5th\,it.} = \mathbf{5.964}\ \boldsymbol{MPa} < \boldsymbol{f_{ctd}} = 6\ MPa$$

Both the principal compressive stress on the most compressed fiber and the principal tensile stress on the tensest fiber are lower than their limit. The last un-cracked fiber does not crack. The cross section is now in equilibrium conditions. The interaction domain is the final one.

At the end of the fifth iteration, the analysis ends up in the first scenario. Now the procedure can take two alternative ways: the un-cracked case, which could happen only if the first scenario happens at the first iteration, or the cracked condition. Since this is the fifth iteration, the path has to follow the cracked condition.

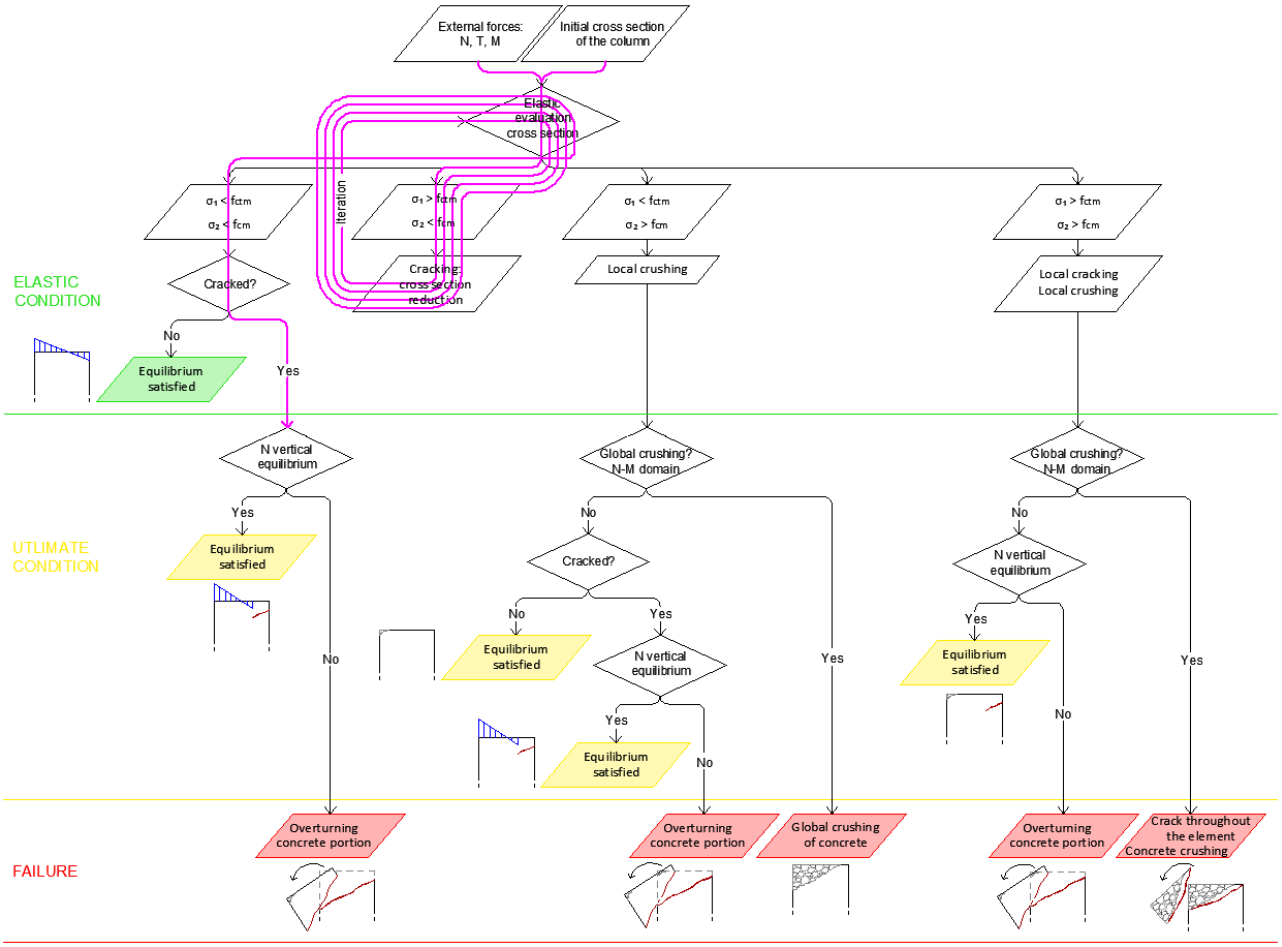

Figure 6.1.6.3 – Path on the flow chart

Since the column has cracked, it has to be verified the vertical equilibrium of the element: the verification consists in checking that the friction force acting on the crack, assumed to maintain the same average inclination throughout the cross section, is capable of carrying the external axial load. In this case, it was satisfied. In this case, the script plots “The vertical equilibrium is satisfied”.

The procedure ends with an equilibrium achieved in ultimate conditions.

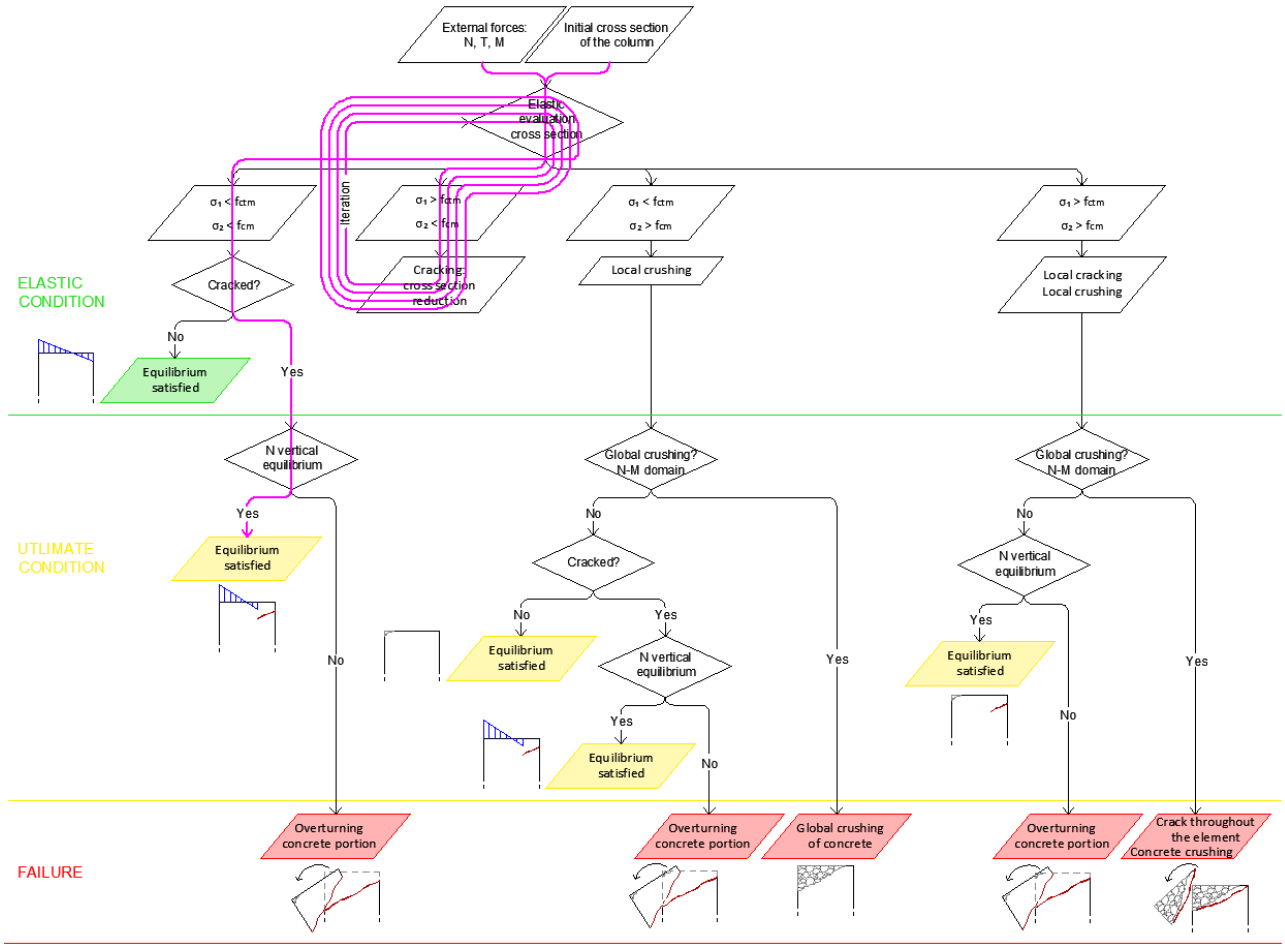

Figure 6.1.6.4 – Complete path on the flow chart

The script also plots how the crack developed through the column.

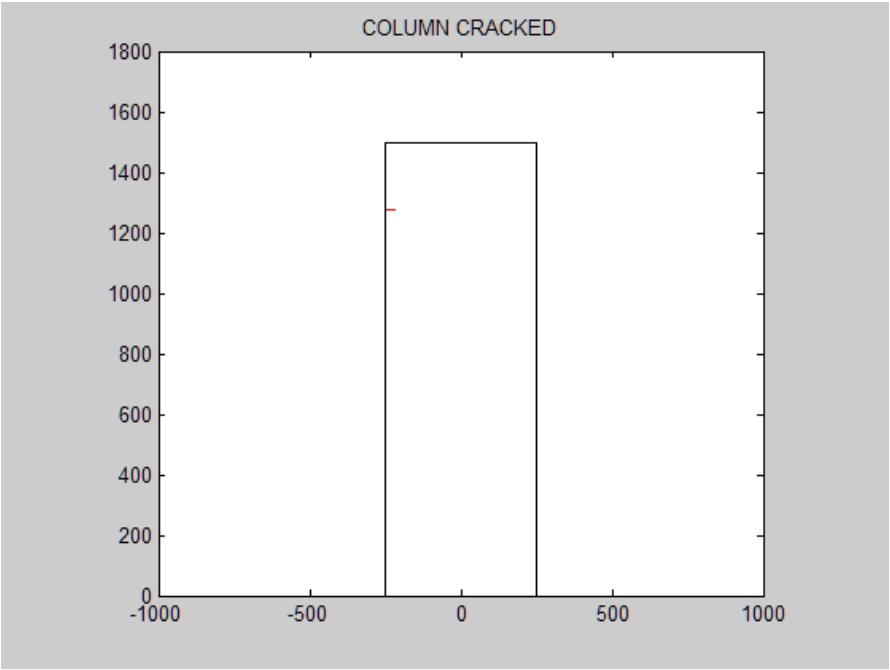

Figure 6.1.6.5 – Cracked Cross section

As it can observed in the figure above, the length of the crack is very small, in fact, the element finds an equilibrium condition at the fifth iteration, which means that four fibers crack before obtaining the final condition; since the width of each fiber is one centimetre, and the crack develops only for four centimetres. Besides, considering that all the fibers cracked stay below steel reinforcements, tangential stresses in the fibers at extremities are null, and therefore the inclination of the crack is horizontal.

6.2. Practical Example of the Fifth Scenario

In this paragraph a practical example that evolves in the fifth scenario. Even in this case a real column has considered, its geometrical and material properties have inserted, only external forces have lightly reduced in order to test the procedure and obtain the fifth scenario explained.

6.2.1. Input Data

The procedure requires input data that follow:

- $b = 300\,mm$;
- $h = 300\,mm$;
- $c = 30\,mm$;
- $d = 270\,mm$;
- $A_{s,sup} = 2\,\Phi\,10 = 157\,mm^2$;
- $A_{s,inf} = 2\,\Phi\,10 = 157\,mm^2$;
- $\Phi_{st} = \Phi\,6 = 6\,mm$;
- $n_{st} = 2$;
- $s_{st} = 100\,mm$:
- $f_{cd} = 9.4\,MPa$;
- $f_{ctd} = 0.1\,f_{cd} = 0.94\,MPa$;
- $f_{yd} = 447.8\,MPa$;
- $E_c = 22000\left[\left(\frac{f_{cd}}{10}\right)^{0.3}\right] = 28821\,MPa$;
- $E_s = 210000\,MPa$;
- $n = {E_c}/{E_s} = 7.29$;
- $N_{act} = -330000\,N$;
- $T_{act} = 500000\,N$;
- $M_{act} = 24000000\,N\,mm$.

The script divides a half cross section in fifteen fibers in order to get the width of each fiber equal to one centimetre, as in the previous example.
The vector of the fiber considered is the following one:

$$y = [145,\ 135,\ 125,\ 115,\ 105,\ 95,\ 85,\ 75,\ 65,\ 55,\ 45,\ 35,\ 25,\ 15,\ 5]$$

The basic quantities that are necessary to evaluate the stress state distribution depend on the iteration; at each iteration, they are computed. These quantities are the effective depth, the homogenised cross section, the position of the centroid of the homogenised area, the homogenised moment of inertia and the homogenised static moment, as in the example reported in the previous paragraph. Since formulae do not change, the computation has not reported in this case because it has already explained in the previous example. Only relevant terms are mentioned, those that are necessary to understand why the procedure follows a specific path.

6.2.2. 1st Elastic Evaluation of the Cross Section

The procedure begins with the first elastic evaluation of the initial cross section, as shown in the flow chart.

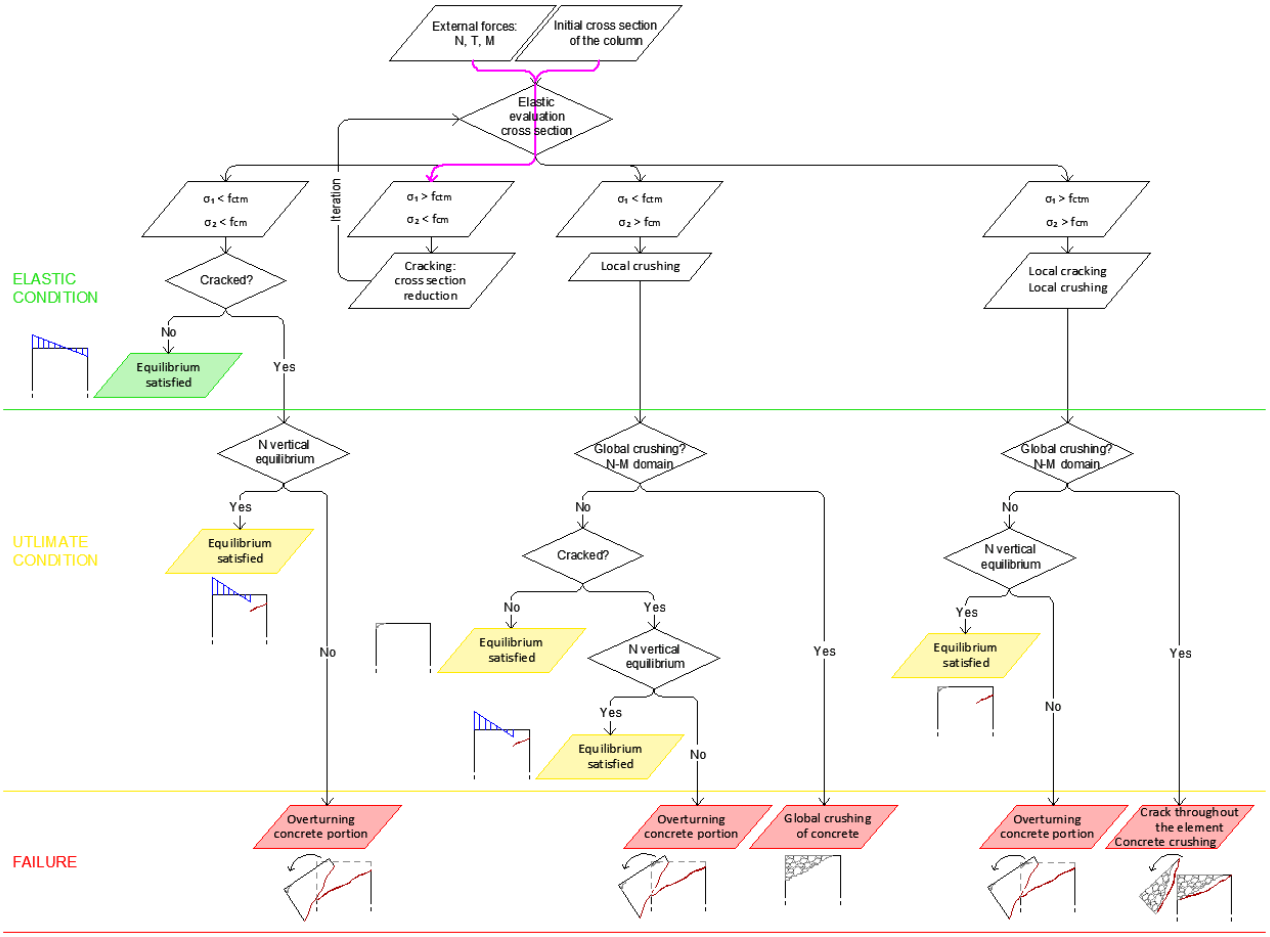

Figure 6.2.2.1 – 1st iteration of the procedure represented in the flow chart

The coordinate of the last un-cracked fiber, the one at the extremity of the reacting cross section, is:

$$y^{1st\ it.} = y(1) = 145\ mm$$

The basic terms necessary to compute the stresses diagrams are the following ones:

$$d^{1st\ it.} = 270\ mm$$

$$A_{omog}{}^{1st\ it.} = 92289\ mm^2$$

$$S^{1st\ it.} = 13671659\ mm^3$$

$$d_{g,sup}{}^{1st\ it.} = \frac{S}{A_{omog}} = 148\ mm$$

$$d_{g,inf}{}^{1st\ it.} = h - d_{g,inf} = 152\ mm$$

$$I_{omog}{}^{1st\ it.} = 708277858\ mm^4$$

The position of the neutral axis, imposing stress equal to zero in the Navier's equation and solving for the y coordintae:

$$y_{a.n.}{}^{1st\ it.} = -103\ mm$$

Once computed the neutral axis position, Navier's equation gives the normal stresses distribution. The sigma value that the procedure requires is the one related to the upper edge under compression, corresponding to $y^{\max comp.} = 150\ mm$:

$$\sigma^{\max comp.\ 1st\ it.} = -8.789\ MPa$$

Even the one acting on the tensest fiber, the one at the lower extremity, corresponding to $y^{max\ tens.} = -145\ mm$:

$$\sigma^{\max tens.\ 1st\ it.} = 1.491\ MPa$$

Tangential stresses are equal to zero because the considered fiber is below steel rebar, where the static moment gets to zero:

$$\tau^{\max comp.\ 1st\ it.} = 0\ MPa$$

$$\tau^{\max tens.\ 1st\ it.} = 0\ MPa$$

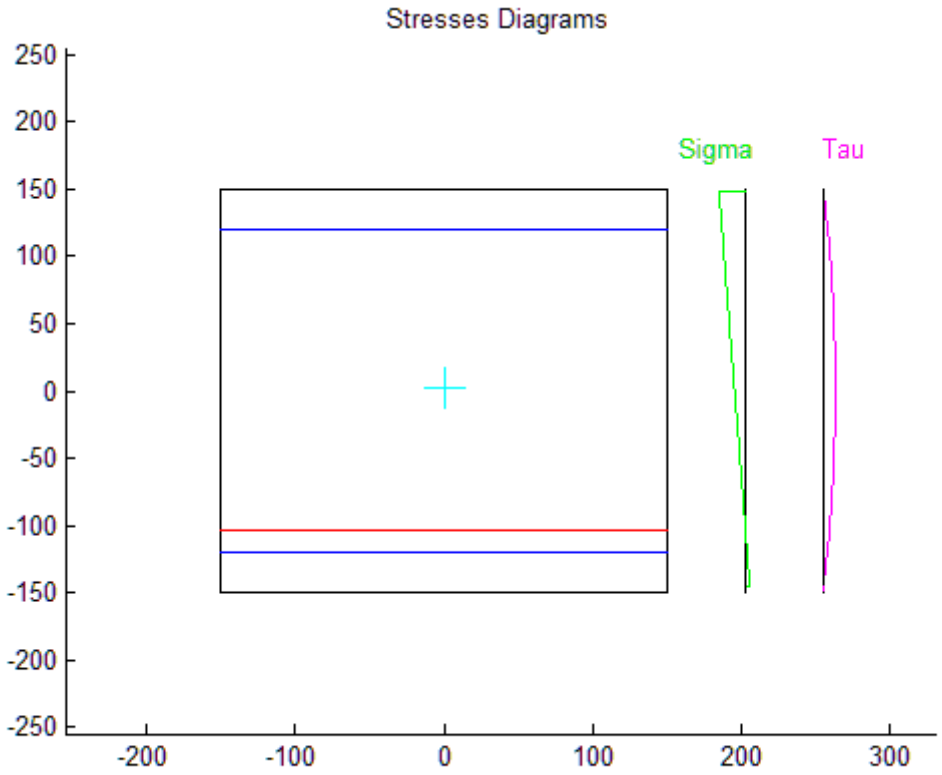

Figure 6.2.2.2 - Tangential and normal stresses distributions

Also in this case, considering that tangential stresses are null, principal stresses are equal to normal ones:

$$\sigma_1{}^{\max comp.\ 1st\ it.} = -8.789\ MPa$$

For the tensile fiber:

$$\sigma_1{}^{\max tens.\ 1st\ it.} = 1.491\ MPa$$

At the end of the first iteration, the procedure falls again in the fourth scenario:

$$\sigma_1{}^{\max comp.\ 1st\ it.} = |\mathbf{-8.798}|\ \boldsymbol{MPa} < \boldsymbol{f_{cd}} = |-9.4|\ MPa$$

$$\sigma_1{}^{\max tens.\ 1st\ it.} = \mathbf{1.491\ MPa} > \boldsymbol{f_{ctd}} = 0.94\ MPa$$

At the end of the first iteration, principal tensile stress exceeds the tensile strength of the concrete in the lowest fiber but the principal compressive stress at the upper edge stays below the limit, and therefore the scenario is:

$$\left(\sigma_1^{lower\ edge}\right)^{1st\ it.} > f_{ctd}$$

$$\left(\sigma_2^{upper\ edge}\right)^{1st\ it.} < f_{cd}$$

The last fiber subjected to traction cracks. The script returns at the beginning of the procedure, revaluates the cross section now reduced of that one fiber and computes again the state of stress.

6.2.3. 2nd Elastic Evaluation of the Cross Section

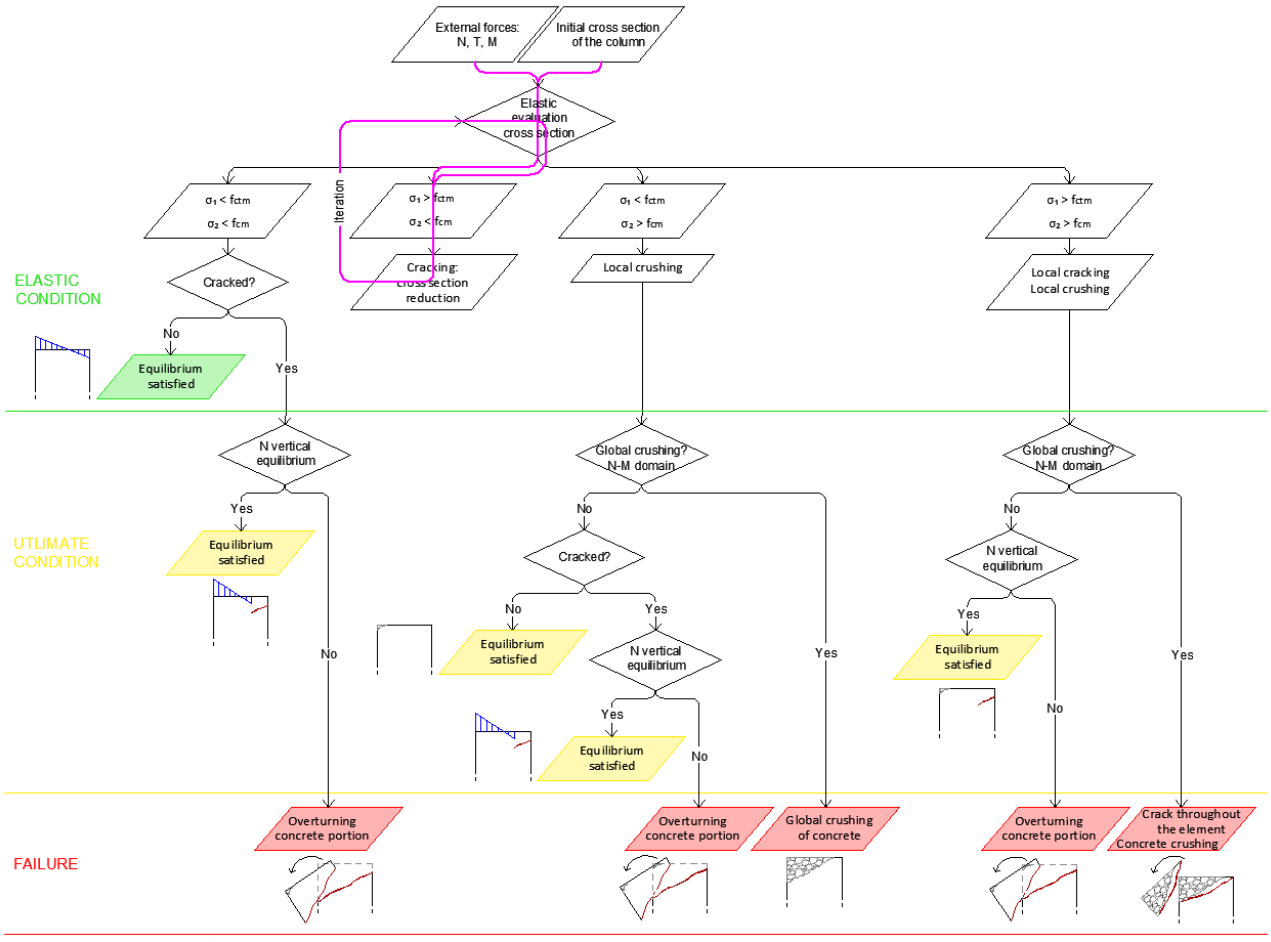

Figure 6.2.3.1 – 2nd iteration of the procedure represented in the flow chart

At the end of the first elastic evaluation of the cross section, the principal tensile stress exceeds the tensile strength of the concrete in the lowest fiber but the principal compressive stress at the upper edge stays below the limit. This means that the fiber at the extremity of the cross section subjected to traction, cracks. Consequently, the procedure returns at the first step, which involves the revaluation of the changed cross section, the initial one without the last cracked fiber.

Hence, at this second iteration, what changes is the coordinate of the last working fiber, the one at the extremity of the reacting cross section that is in this case is

$$y^{2nd\ it.} = y(2) = 135\ mm$$

Now the procedure repeats exactly as for the first iteration, the only parameter that changed is y.

All basic quantities computed at the first step, depending on y, have to be computed again, since the coordinate changed, but the equation are the same mentioned for the first iteration:

$$d^{2nd\ it.} = 260\ mm$$

$$A_{omog}{}^{2nd\ it.} = 89289\ mm^2$$

$$S^{2nd\ it.} = 12786659\ mm^3$$

$$d_{g,sup}{}^{2nd\ it.} = 143\ mm$$

$$d_{g,inf}{}^{2nd\ it.} = 157\ mm$$

$$I_{omog}{}^{2nd\ it.} = 712218912\ mm^4$$

The position of the neutral axis:

$$y_{a.n.}{}^{2nd\ it.} = -100\ mm$$

Then, Navier's equation gives the normal stresses distribution. The sigma value that the procedure is interested in, is the one related to the upper edge under compression, corresponding to $y^{\max comp.} = 150\ mm$:

$$\sigma^{\max comp.\ 2nd\ it.} = -9.223\ MPa$$

Even the one acting on the tensest fiber, the one at the lower extremity, corresponding to $y^{max\ tens.} = 135\ mm$:

$$\sigma^{\max tens.\ 2nd\ it.} = 1.117\ MPa$$

Tangential stresses are still equal to zero:

$$\tau^{\max comp.\ 2nd\ it.} = 0\ MPa$$

$$\tau^{\max tens.\ 2nd\ it.} = 0\ MPa$$

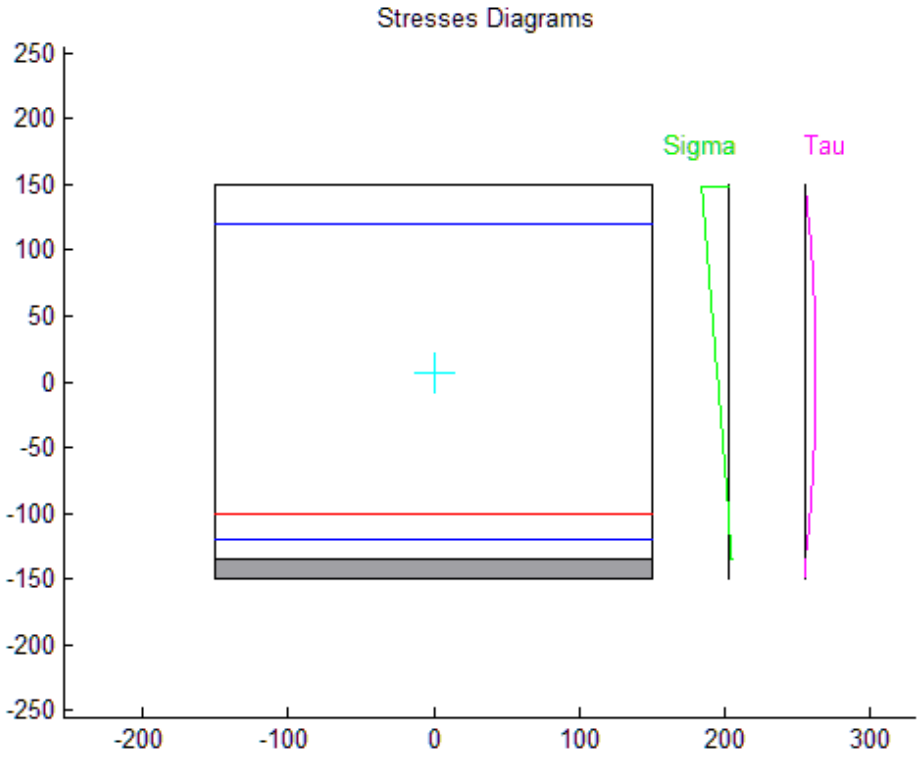

Figure 6.2.3.2 - Tangential and normal stresses distributions

Also in this case, considering that tangential stresses are null, principal stresses are equal to normal ones:

$$\sigma_1{}^{\max comp.\ 2nd\ it.} = -9.223\ MPa$$

For the tensile fiber:

$$\sigma_1{}^{\max tens.\ 2nd\ it.} = 1.117\ MPa$$

At the end of the second iteration, the procedure falls again in the fourth scenario:

$$\sigma_1{}^{\max comp.\ 2nd\ it.} = |\mathbf{-9.223}|\ \boldsymbol{MPa} < \boldsymbol{f_{cd}} = |-9.4|\ MPa$$

$$\sigma_1{}^{\max tens.\ 2nd\ it.} = \mathbf{1.117\ MPa} > \boldsymbol{f_{ctd}} = 0.94\ MPa$$

At the end of the second iteration, once again, principal tensile stress exceeds the tensile strength of the concrete in the lowest fiber but the principal compressive stress at the upper edge stays below the limit, and therefore the scenario is:

$$\left(\sigma_1^{lower\ edge}\right)^{2nd\ it.} > f_{ctd}$$

$$\left(\sigma_2^{upper\ edge}\right)^{2nd\ it.} < f_{cd}$$

The last un-cracked fiber subjected to traction cracks. The script proceeds returning at the first step, revaluating the cross section now reduced of that one fiber and computing again the state of stress.

6.2.4. 3rd Elastic Evaluation of the Cross Section

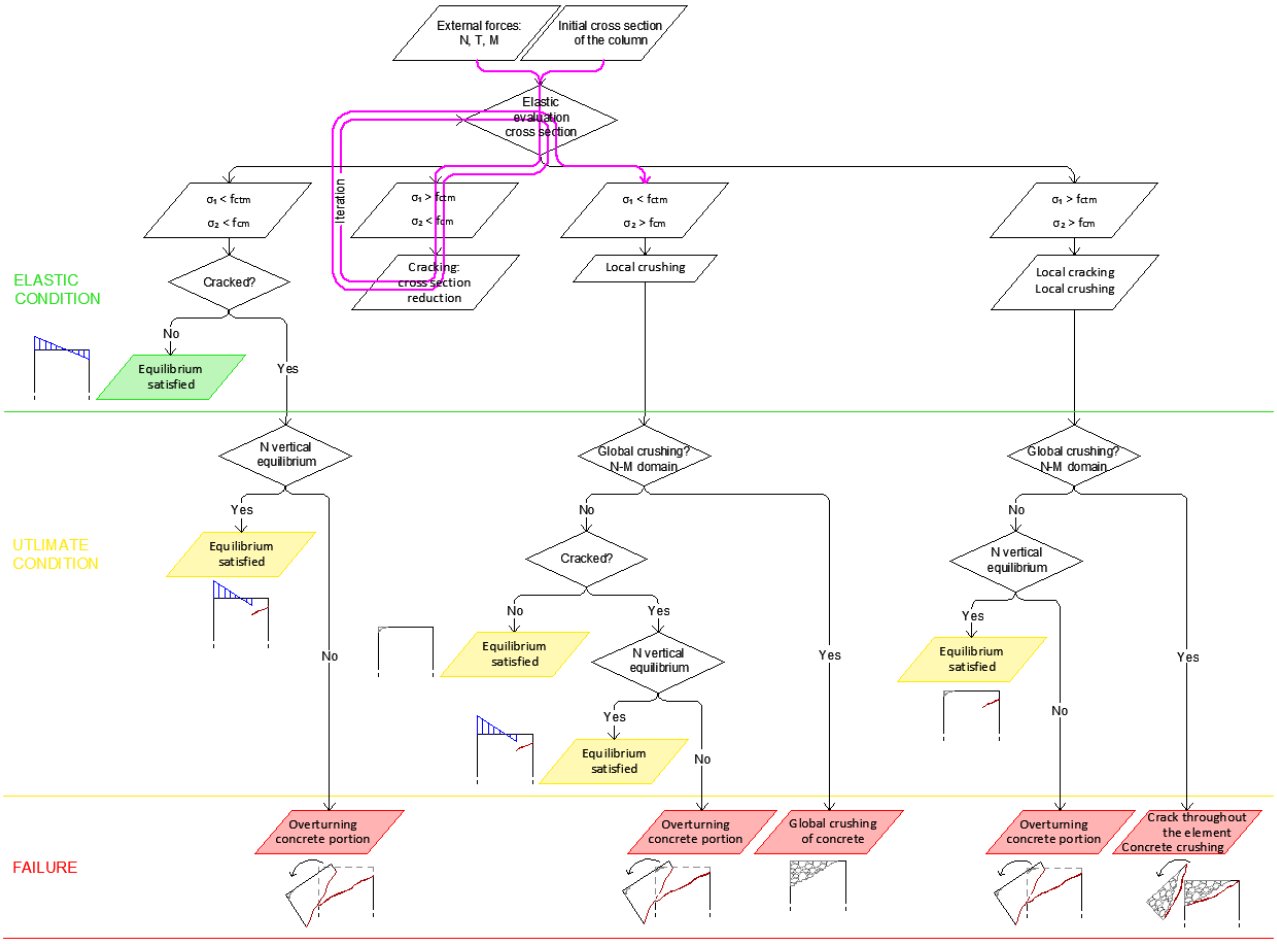

Figure 6.2.4.1 – 3rd iteration of the procedure represented in the flow chart

At the third iteration, the coordinate of the last working fiber, the one at the extremity of the reacting cross section, changes again:

$$y^{3rd\ it.} = y(3) = 125\ mm$$

All basic quantities computed at previous steps, depending on y, have to be calculated again using same equations. They are necessary to evaluate the stress distribution, which at this iteration are characterised by the following maximum values:

$$\sigma^{\max comp.\ 3rd\ it.} = -9.625\ MPa$$

$$\sigma^{\max tens.\ 3rd\ it.} = 0.731\ MPa$$

The corresponding tangential stresses are still null:

$$\tau^{\max comp.\ 3rd\ it.} = 0\ MPa$$

$$\tau^{\max tens.\ 3rd\ it.} = 0\ MPa$$

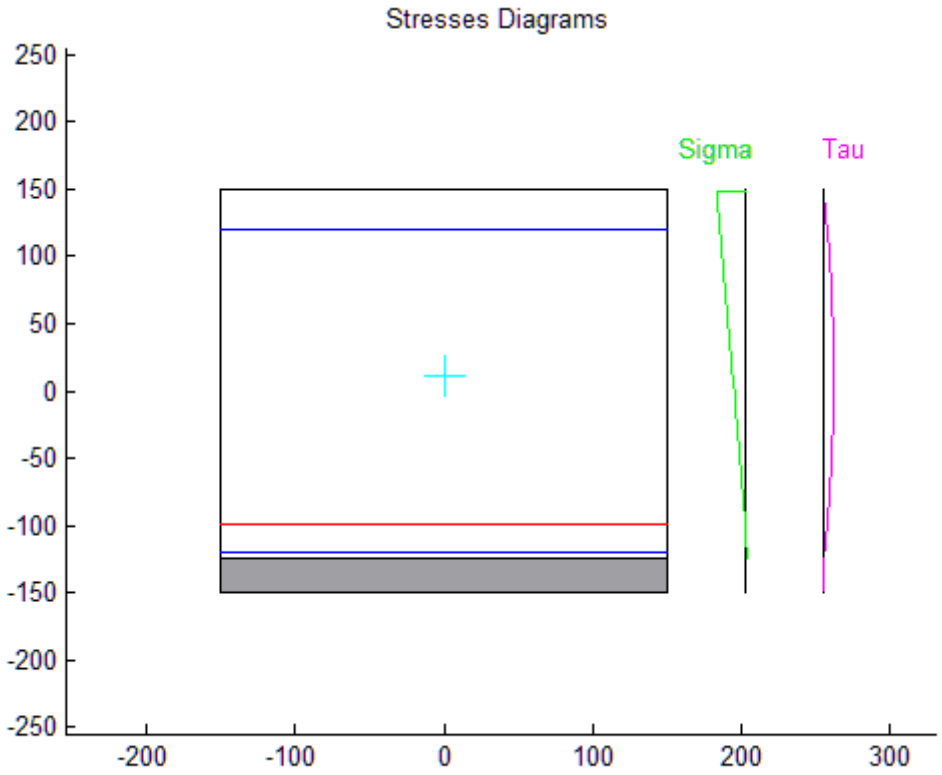

Figure 6.2.4.2 - Tangential and normal stresses distributions

Using same equations of the first iteration, the principal compressive stress at the most compressed fiber is:

$$\sigma_1{}^{\max comp.\ 3rd\ it.} = -9.625\ MPa$$

For the tensile fiber:

$$\sigma_1{}^{\max tens.\ 3rd\ it.} = 0.731\ MPa$$

At the end of the third iteration, the procedure falls again in the second scenario: principal tensile stress is lower than the tensile strength of the concrete in the lowest fiber but the principal compressive stress at the upper edge exceeds the limit, and therefore the scenario is:

$$\sigma_1{}^{\max comp.\ 3rd\ it.} = |\mathbf{-9.625}|\ \boldsymbol{MPa} > \boldsymbol{f_{cd}} = |-9.4|\ MPa$$

$$\sigma_1{}^{\max tens.\ 3rd\ it.} = \mathbf{0.731\ MPa} < \boldsymbol{f_{ctd}} = 0.94\ MPa$$

Thus:

$$\left(\sigma_1^{lower\ edge}\right)^{3rd\ it.} < f_{ctd}$$

$$\left(\sigma_2^{upper\ edge}\right)^{3rd\ it.} > f_{cd}$$

At the end of the third iteration, the principal tensile stress on the tensest fiber is lower than the tensile strength of the concrete while the principal compressive stress on the most compressed fiber exceeds its limit. This means that the crack stops developing but the most compressed fiber crushes.

The development of the crushing of the concrete is not possible to define, what can be established is if the cross section is subjected to a local or a global crushing. Considering that the most compressed fiber has already crushed, a local damage is certain; it has to be analysed if the crushing affects the whole cross section or not. It can be determined through an N-M domain verification. If the point representing the external forces falls inside the domain, it can be expected that the column is able to withstand solicitations, therefore, even if a portion of the concrete crushed, the whole element is capable of carrying external loads; this corresponds to a local crushing. If the point is out of the domain, it means that the member fails under such actions, thus it fails because of a global crushing.

Once the procedure coincides with the second scenario, the script has to control if the crushing is global, which means verifying the cross section by means of the N-M interaction domain.

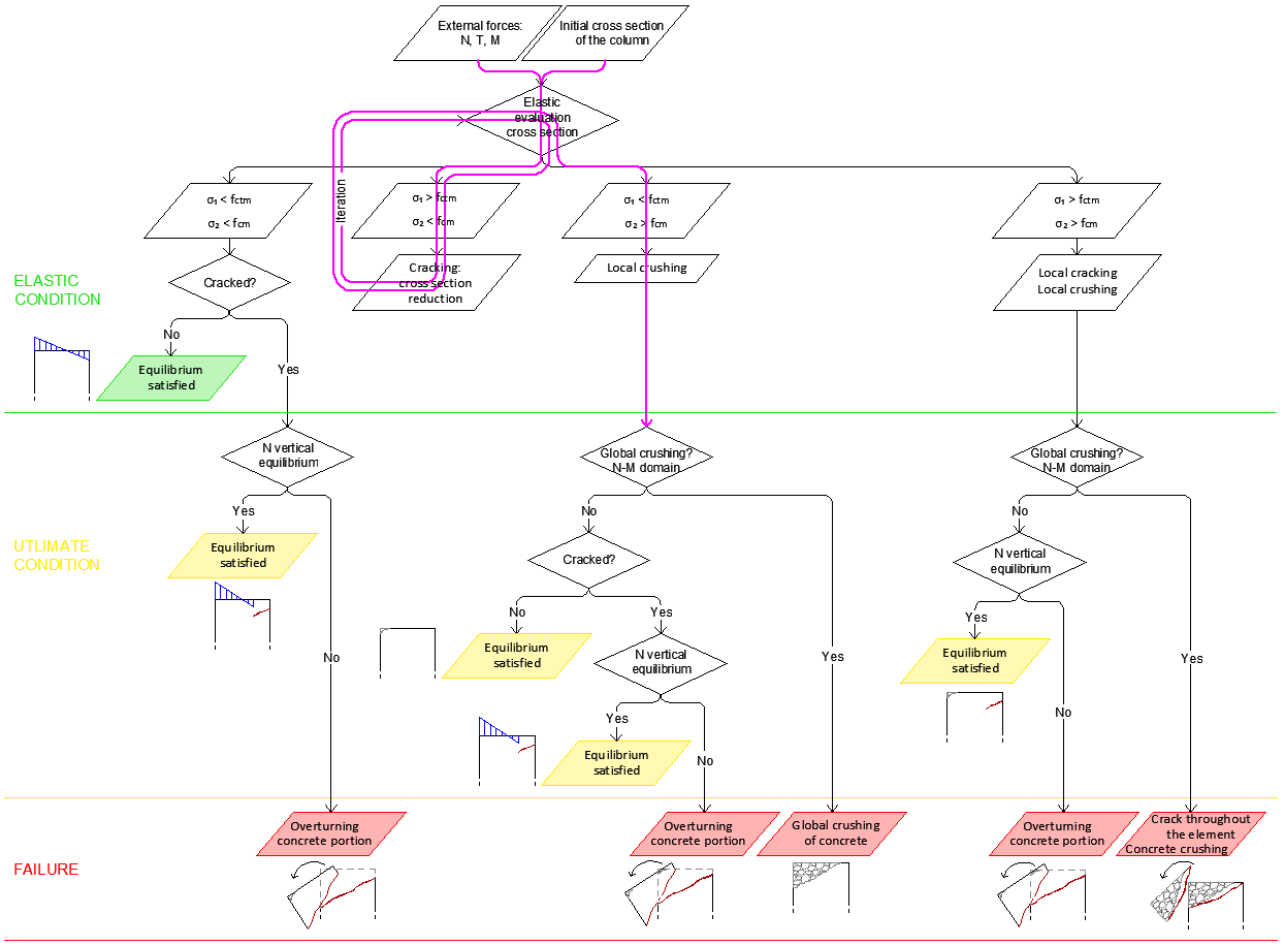

Figure 6.2.4.3 – Path on the flow chart: global crushing verification

At the end of the global crushing verification, the plot of the N-M domain and the point representing the external forces on the column. In this case, the point falls inside the interaction diagram; the script returns " The verification of the N-M domain is satisfied, no global crushing of the element".

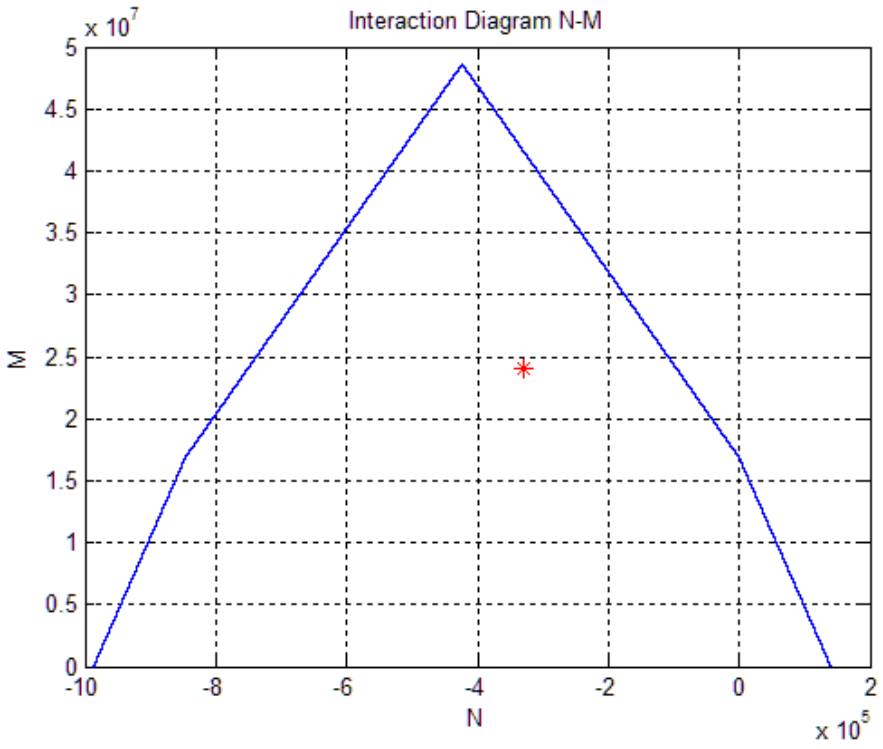

Figure 5.2.4.4 – N-M interaction domain

Since the global crushing is not happening, the path on the flow charts follows the *"No"* alternative, which proceeds with another analysis: the cracking of the concrete. If the concrete is not cracked, which could happen only if the second scenario appears at the very first iteration, there is no need for further checking. On the other hand, if the crushing of most compressed fiber, e.g. the second scenario, happens after some iterations, for sure a portion of the cross section has cracked. In this example, since the crushing arrives at the third iteration, two fibers on the tense side has cracked. This means that the path advances through the cracked condition.

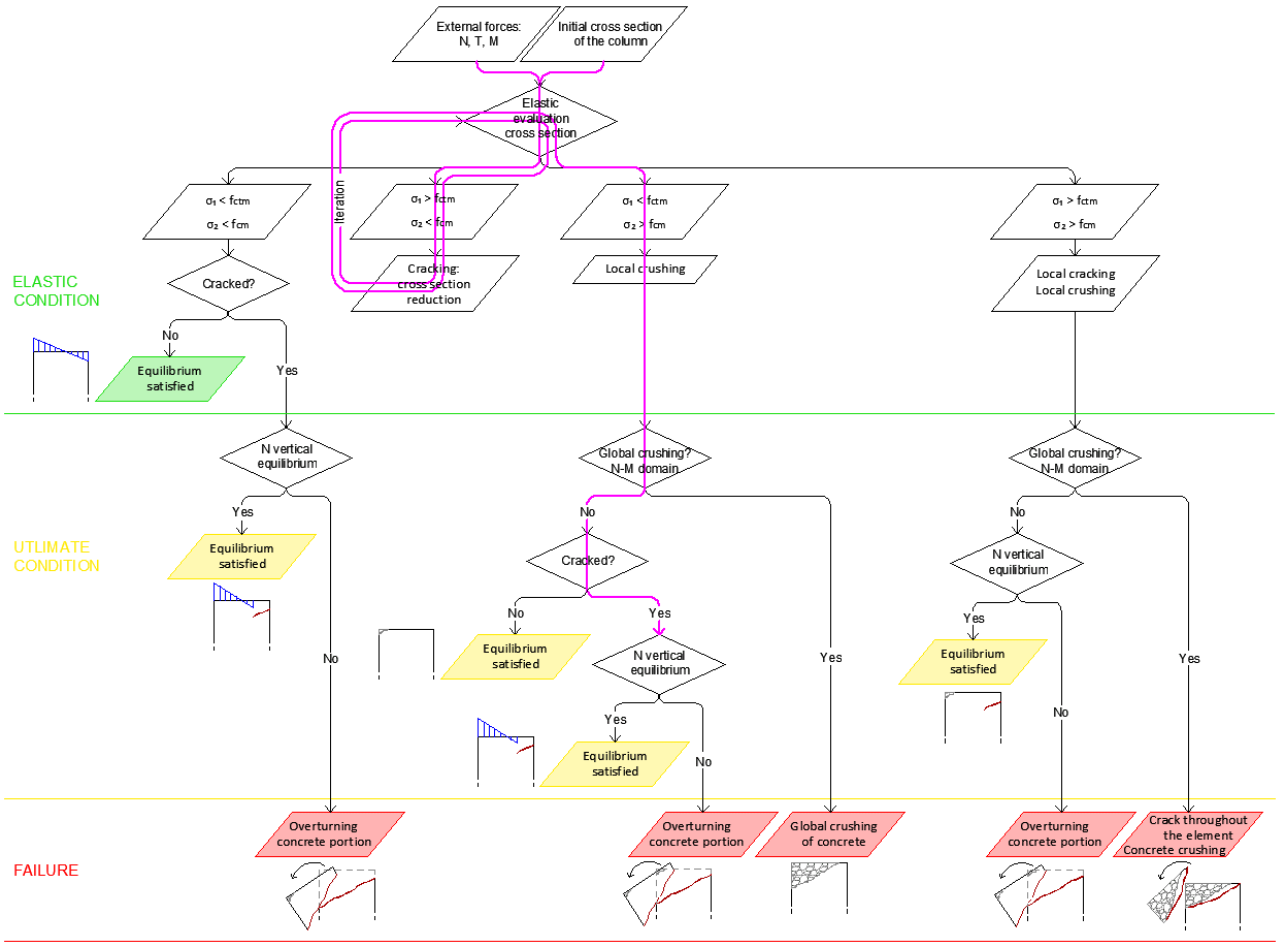

Figure 6.2.4.5 – Path on the flow chart: cracked condition

The analysis goes on with the verification of the crack that is the verification of the N vertical equilibrium. It consists in checking that the friction force acting on the crack, assumed to maintain the same average inclination throughout the cross section, is capable of carrying the external axial load. In this case, it was satisfied; the script plots “The vertical equilibrium is satisfied”.

The procedure ends with the plot of the crack on the column.

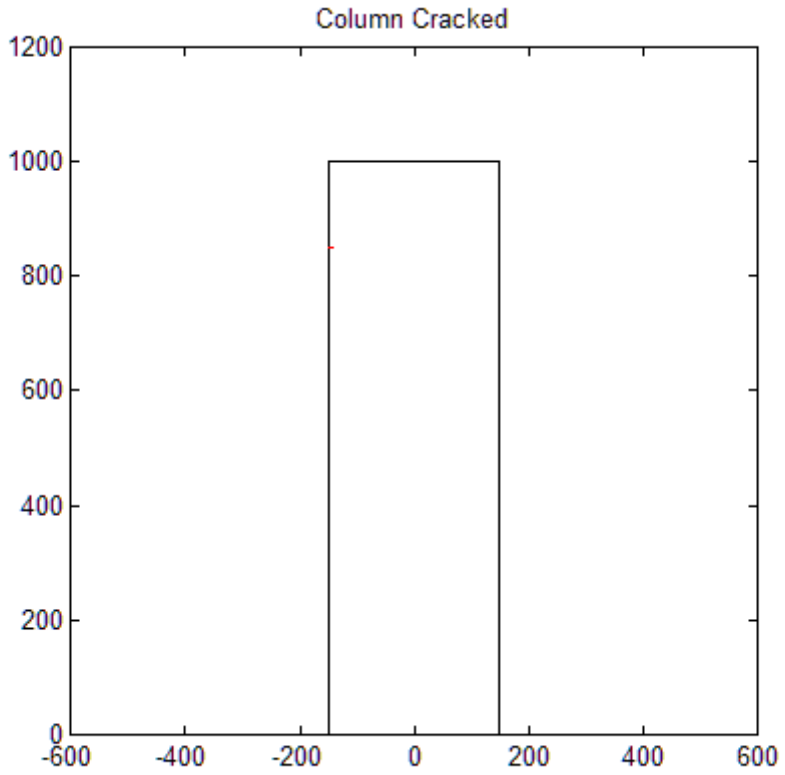

Figure 6.2.4.6 – Cracked Cross section

Even in this case, the length of the crack is very small, in fact, the element finds an equilibrium condition at the third iteration, which means that only two fibers crack before obtaining the final condition; thus, the crack develops only for two centimetres. Besides, all the fibers cracked stay below steel reinforcements, therefore the inclination of the crack is horizontal.

6.3. Practical Example of the Sixth Scenario

In this paragraph a practical example that evolves in the sixth scenario. A real column has considered, its geometrical and material properties have inserted, only external forces have lightly reduced in order to test the procedure and obtain the sixth scenario explained.

6.3.1. Input Data

Required information is:

- $b = 600\,mm$;
- $h = 800\,mm$;
- $c = 40\,mm$;

- $d = 760\ mm$;
- $A_{s,sup} = 2\ \Phi\ 22 = 760\ mm^2$;
- $A_{s,inf} = 2\ \Phi\ 22 = 760\ mm^2$;
- $\Phi_{st} = \Phi\ 6 = 8\ mm$;
- $n_{st} = 2$;
- $s_{st} = 100\ mm$:
- $f_{cd} = 45\ MPa$;
- $f_{ctd} = 0.1\ f_{cd} = 4.5\ MPa$;
- $f_{yd} = 580\ MPa$;
- $E_c = 22000\ \left[\left(\frac{f_{cd}}{10}\right)^{0.3}\right] = 34545\ MPa$;
- $E_s = 210000\ MPa$;
- $n = {E_c}/{E_s} = 6.08$;
- $N_{act} = -7000000\ N$;
- $T_{act} = 800000\ N$;
- $M_{act} = 1800000000\ N\ mm$.

The script divides a half cross section in twenty fibers in order to get the width of each fiber equal to two centimetres.
The vector of the fiber considered is the following one:

$$y = [390,\ 370,\ 350,\ 330,\ 310,\ 290,\ 270,\ 250,\ 230,\ 210,\ 190,\ 170,\ 150,\ 130, \ldots$$

$$\ldots\ 110,\ 90,\ 70,\ 50,\ 30,\ 10]$$

The basic quantities that are necessary to evaluate the stress state distribution depend on the iteration; at each iteration, they are computed. These quantities are the effective depth, the homogenised cross section, the position of the centroid of the homogenised area, the homogenised moment of inertia and the homogenised static moment, as in the example reported in the previous paragraph. Since formulae do not change, the computation has not reported in this case because it has already explained in the first example. Only relevant terms are mentioned, those that are necessary to understand why the procedure follows a specific path.

6.3.2. 1st Elastic Evaluation of the Cross Section

The procedure begins with the first elastic evaluation of the initial cross section, as shown in the flow chart.

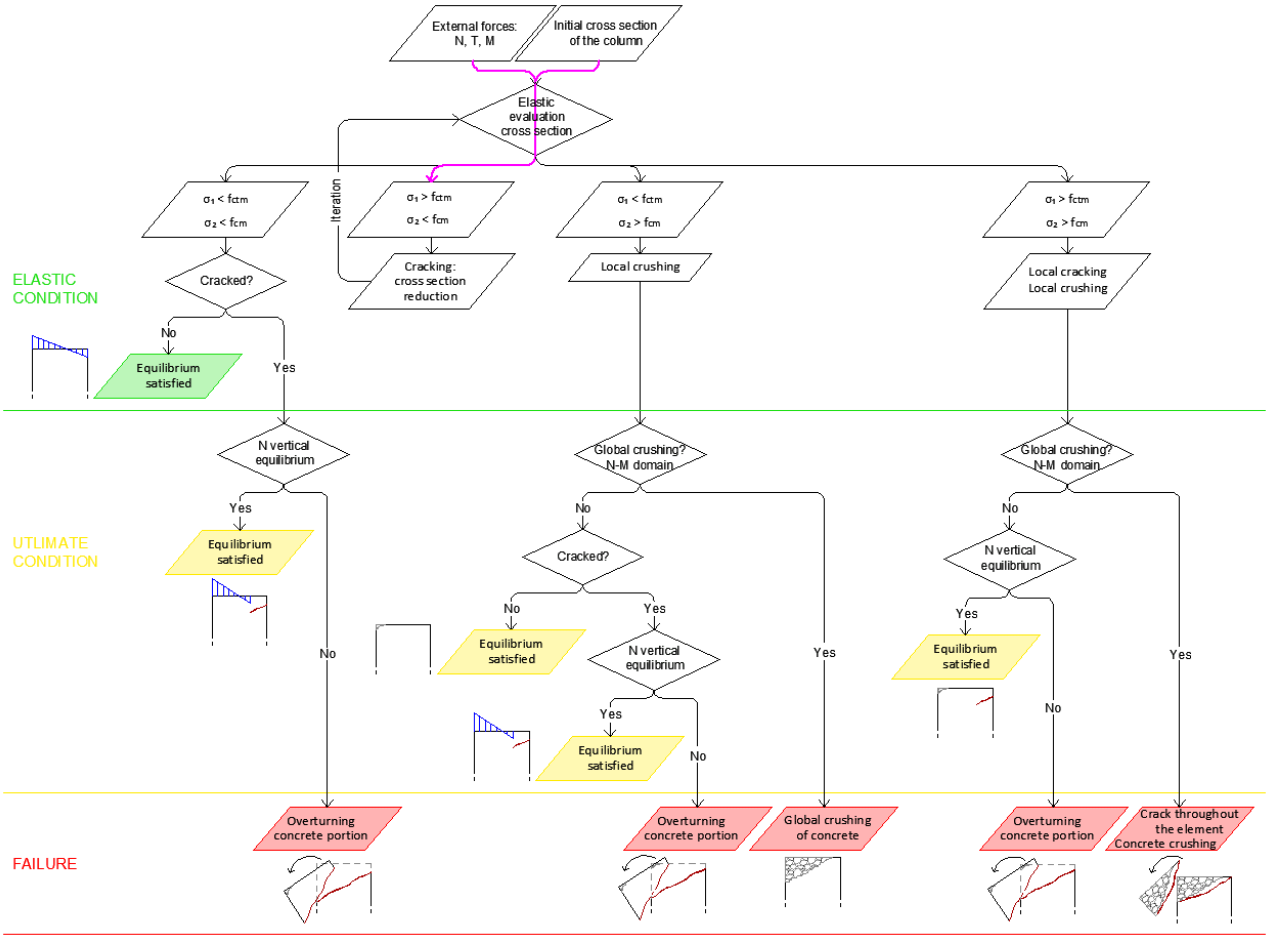

Figure 6.3.2.1 – 1st iteration of the procedure represented in the flow chart

The coordinate of the last un-cracked fiber, the one at the extremity of the working cross section, is:

$$y^{1st\ it.} = y(1) = 390\ mm$$

The basic terms necessary to compute the stresses diagrams are the following ones:

$$d^{1st\ it.} = 760\ mm$$

$$A_{omog}{}^{1st\ it.} = 489240\ mm^2$$

$$S^{1st\ it.} = 193848019\ mm^3$$

$$d_{g,sup}{}^{1st\ it.} = 396\ mm$$

$$d_{g,inf}{}^{1st\ it.} = 404\ mm$$

$$I_{omog}{}^{1st\ it.} = 26804496912\ mm^4$$

The position of the neutral axis, imposing stress equal to zero in the Navier's equation and solving for the y coordintae:

$$y_{a.n.}{}^{1st\ it.} = -210\ mm$$

The sigma value required by the procedure is the one related to the upper edge under compression, corresponding to $y^{\max comp.} = 400\ mm$:

$$\sigma^{\max comp.\ 1st\ it.} = -41.564\ MPa$$

Even the one acting on the tensest fiber, the one at the lower extremity, corresponding to $y^{max\ tens.} = -390\ mm$:

$$\sigma^{\max tens.\ 1st\ it.} = 12.604\ MPa$$

Tangential stresses are equal to zero because the considered fiber is below steel rebar, where the static moment gets to zero:

$$\tau^{\max comp.\ 1st\ it.} = 0\ MPa$$

$$\tau^{\max tens.\ 1st\ it.} = 0\ MPa$$

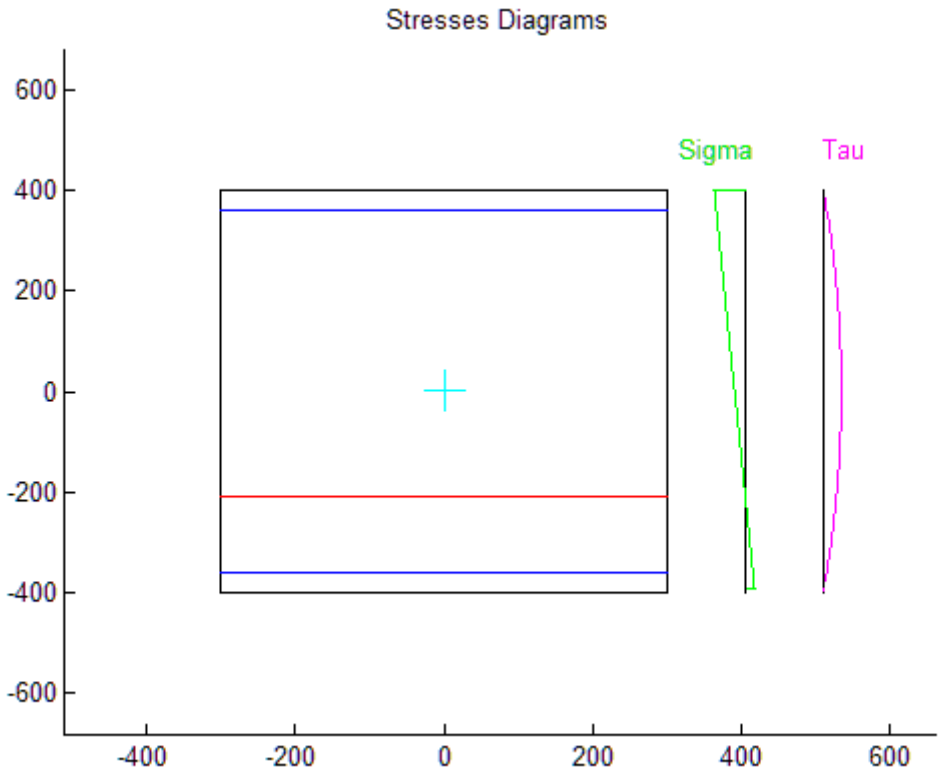

Figure 6.3.2.2 - Tangential and normal stresses distributions

Also in this case, considering that tangential stresses are null, principal stresses are equal to normal ones:

$$\sigma_1{}^{\max comp.\ 1st\ it.} = -41.564\ MPa$$

For the tensile fiber:

$$\sigma_1{}^{\max tens.\ 1st\ it.} = 12.604\ MPa$$

At the end of the first iteration, the procedure falls in the fourth scenario: principal tensile stress exceeds the tensile strength of the concrete in the lowest fiber but the principal compressive stress at the upper edge stays below the limit:

$$\sigma_1{}^{\max comp.\ 1st\ it.} = |\mathbf{-41.564}|\ \boldsymbol{MPa} < \boldsymbol{f_{cd}} = |-45|\ MPa$$

$$\sigma_1{}^{\max tens.\ 1st\ it.} = \mathbf{12.604}\ \boldsymbol{MPa} > \boldsymbol{f_{ctd}} = 4.5\ MPa$$

That is:

$$\left(\sigma_1^{lower\ edge}\right)^{1st\ it.} > f_{ctd}$$

$$\left(\sigma_2^{upper\ edge}\right)^{1st\ it.} < f_{cd}$$

The last fiber subjected to traction cracks. The script returns at the beginning of the procedure, revaluates the cross section now reduced of that one fiber and computes again the state of stress.

6.3.3. 2nd Elastic Evaluation of the Cross Section

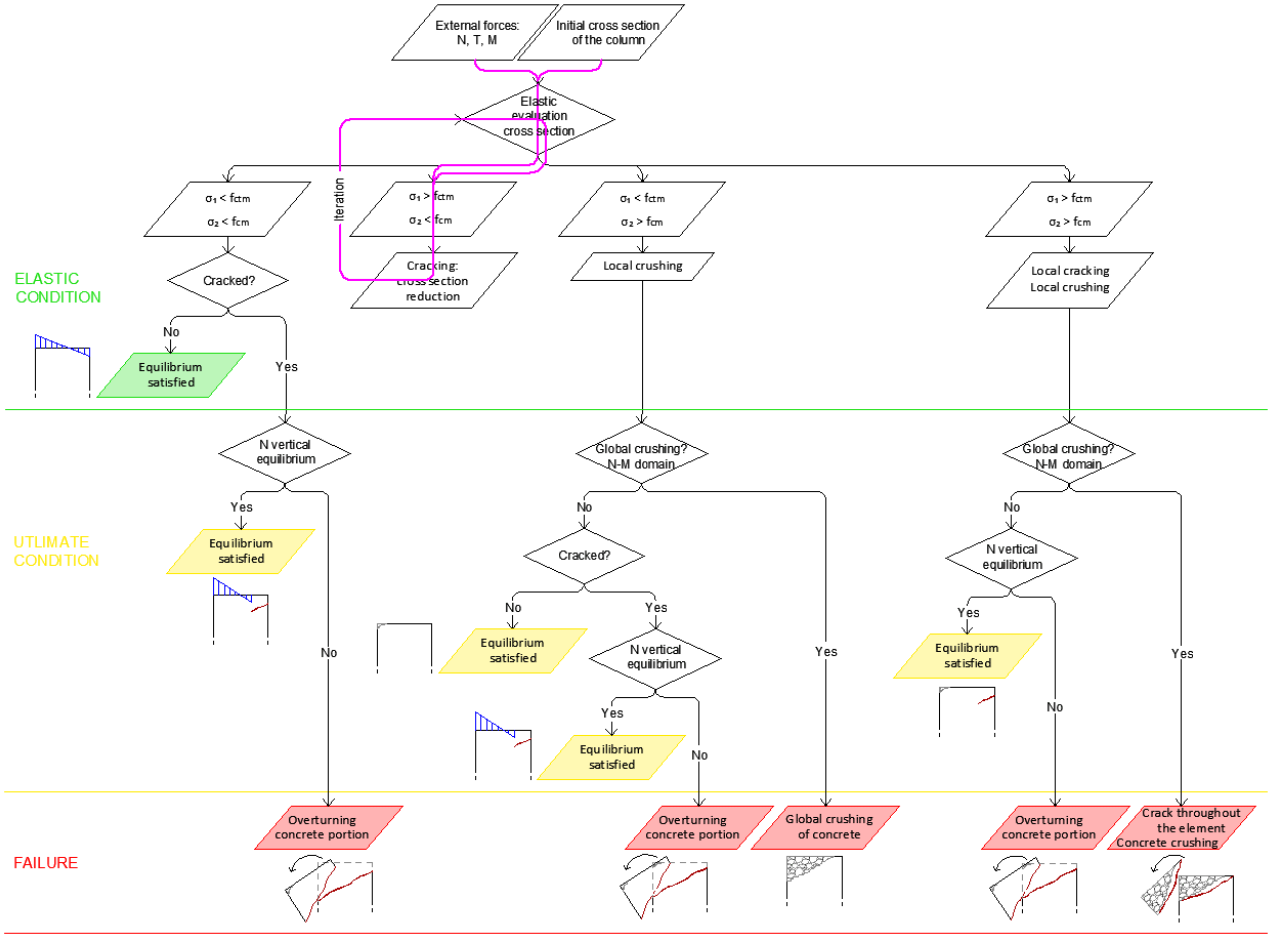

Figure 6.3.3.1 – 2nd iteration of the procedure represented in the flow chart

At the end of the first iteration, the fiber at the extremity of the cross section subjected to traction, cracks. Hence, at this second iteration, the coordinate of the last working fiber, the one at the extremity of the reacting cross section is:

$$y^{2nd\ it.} = y(2) = 370\ mm$$

Basic quantities that have to be computed again, since the coordinate changed, are:

$$d^{2nd\ it.} = 260\ mm$$

$$A_{omog}{}^{2nd\ it.} = 477240\ mm^2$$

$$S^{2nd\ it.} = 184368019\ mm^3$$

$$d_{g,sup}{}^{2nd\ it.} = 386\ mm$$

$$d_{g,inf}{}^{2nd\ it.} = 414\ mm$$

$$I_{omog}{}^{2nd\ it.} = 26889056367\ mm^4$$

The position of the neutral axis:

$$y_{a.n.}{}^{2nd\ it.} = -208\ mm$$

The sigma value that the procedure is interested in, is the one related to the upper edge under compression, corresponding to $y^{\max comp.} = 400\ mm$:

$$\sigma^{\max comp.\ 2nd\ it.} = -42.869\ MPa$$

Even the one acting on the tensest fiber, the one at the lower extremity, corresponding to $y^{max\ tens.} = -370\ mm$:

$$\sigma^{\max tens.\ 2nd\ it.} = 11.495\ MPa$$

Tangential stresses are still equal to zero:

$$\tau^{\max comp.\ 2nd\ it.} = 0\ MPa$$

$$\tau^{\max tens.\ 2nd\ it.} = 0\ MPa$$

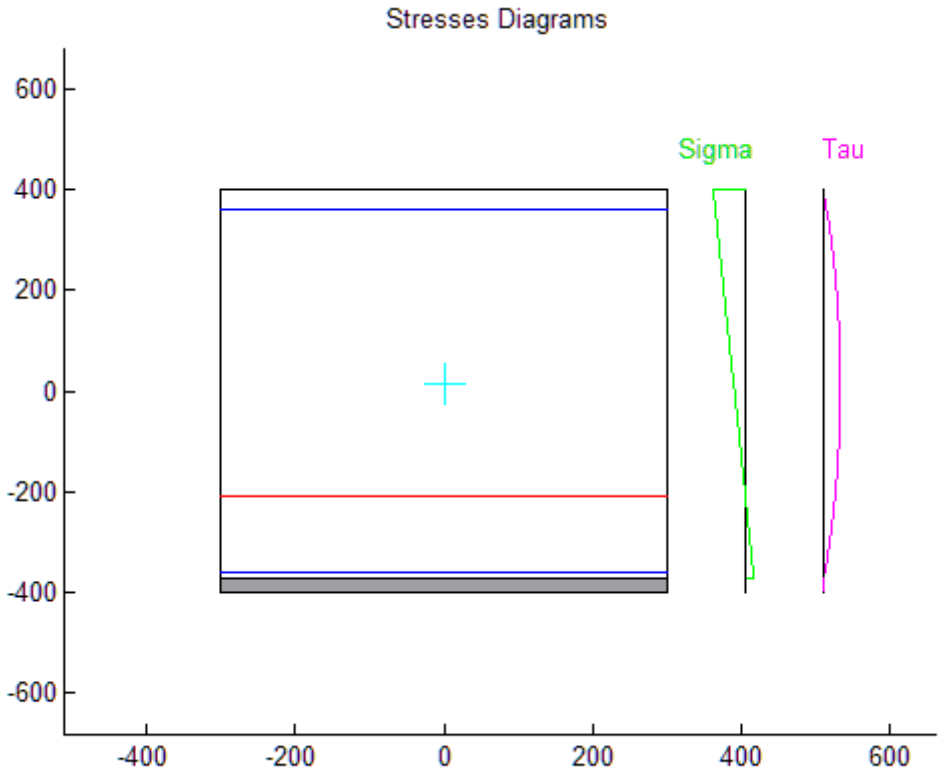

Figure 6.3.3.2 - Tangential and normal stresses distributions

Also in this case, considering that tangential stresses are null, principal stresses are equal to normal ones:

$$\sigma_1{}^{\max comp.\ 2nd\ it.} = -41.381\ MPa$$

For the tensile fiber:

$$\sigma_1{}^{\max tens.\ 2nd\ it.} = 10.060\ MPa$$

At the end of the second iteration, the procedure falls again in the fourth scenario:

$$\sigma_1{}^{\max comp.\ 2nd\ it.} = |\mathbf{-41.381}|\ \boldsymbol{MPa} < \boldsymbol{f_{cd}} = |-45|\ MPa$$

$$\sigma_1{}^{\max tens.\ 2nd\ it.} = \mathbf{10.060\ MPa} > \boldsymbol{f_{ctd}} = 4.5\ MPa$$

At the end of the second iteration, once again, the fourth scenario:

$$\left(\sigma_1^{lower\ edge}\right)^{2nd\ it.} > f_{ctd}$$

$$\left(\sigma_2^{upper\ edge}\right)^{2nd\ it.} < f_{cd}$$

The last un-cracked fiber subjected to traction cracks. The script proceeds returning at the first step, revaluating the cross section now reduced of that one fiber and computing again the state of stress.

6.3.4. 3rd Elastic Evaluation of the Cross Section

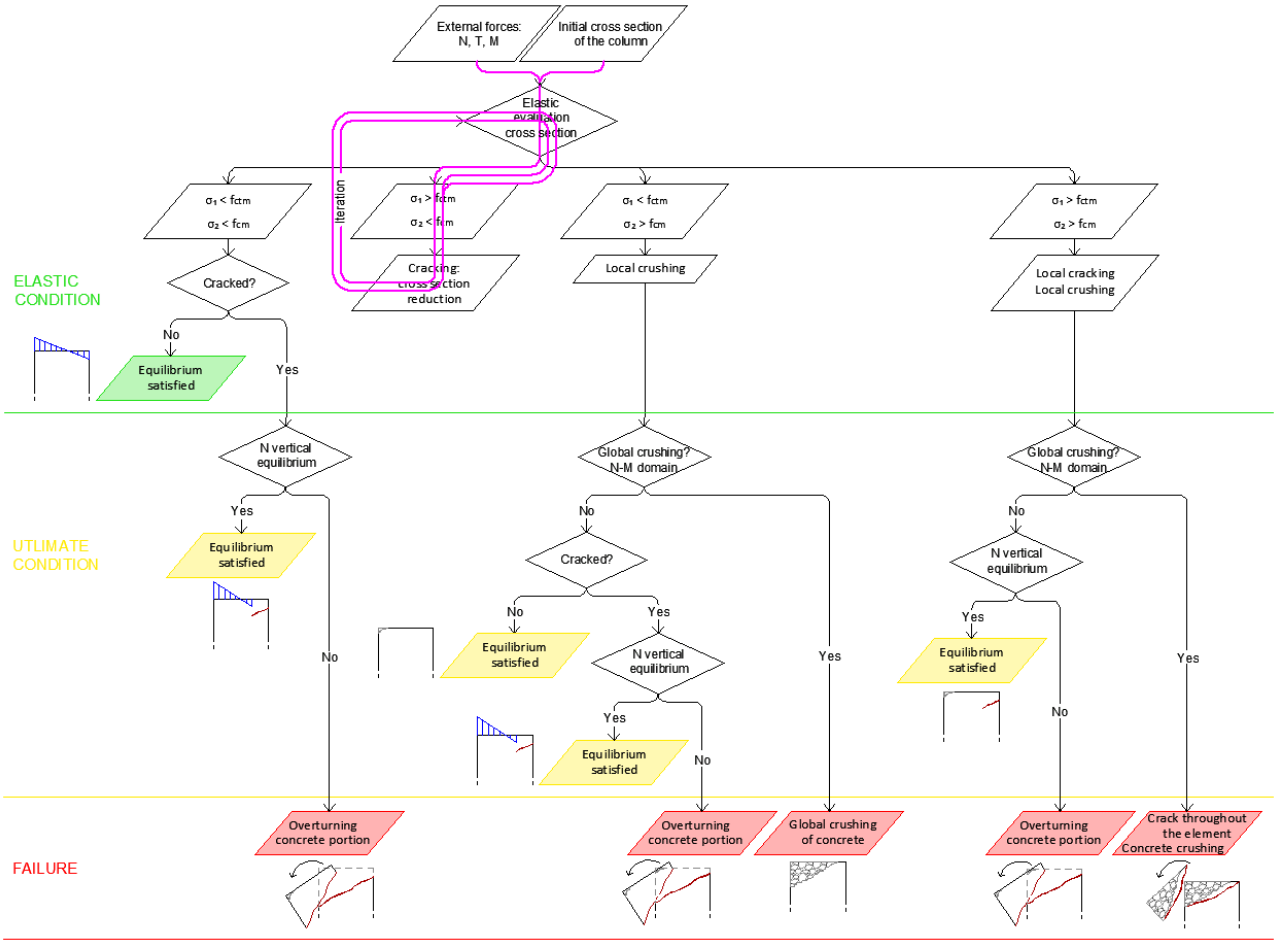

Figure 6.3.4.1 – 3rd iteration of the procedure represented in the flow chart

At the third iteration, the coordinate of the last working fiber, the one at the extremity of the reacting cross section, changes again:

$$y^{3rd\ it.} = y(3) = 350\ mm$$

All basic quantities computed at previous steps, depending on y, have to be calculated again using same equations. They are necessary to evaluate the stress distribution, which at this iteration are characterised by the following maximum values:

$$\sigma^{\max comp.\ 3rd\ it.} = -44.083\ MPa$$

$$\sigma^{\max tens.\ 3rd\ it.} = 10.328\ MPa$$

The considered fiber lays below reinforcements and therefore corresponding tangential stresses are different from zero:

$$\tau^{\max comp.\ 3rd\ it.} = 0\ MPa$$

$$\tau^{\max tens.\ 3rd\ it.} = 0.108\ MPa$$

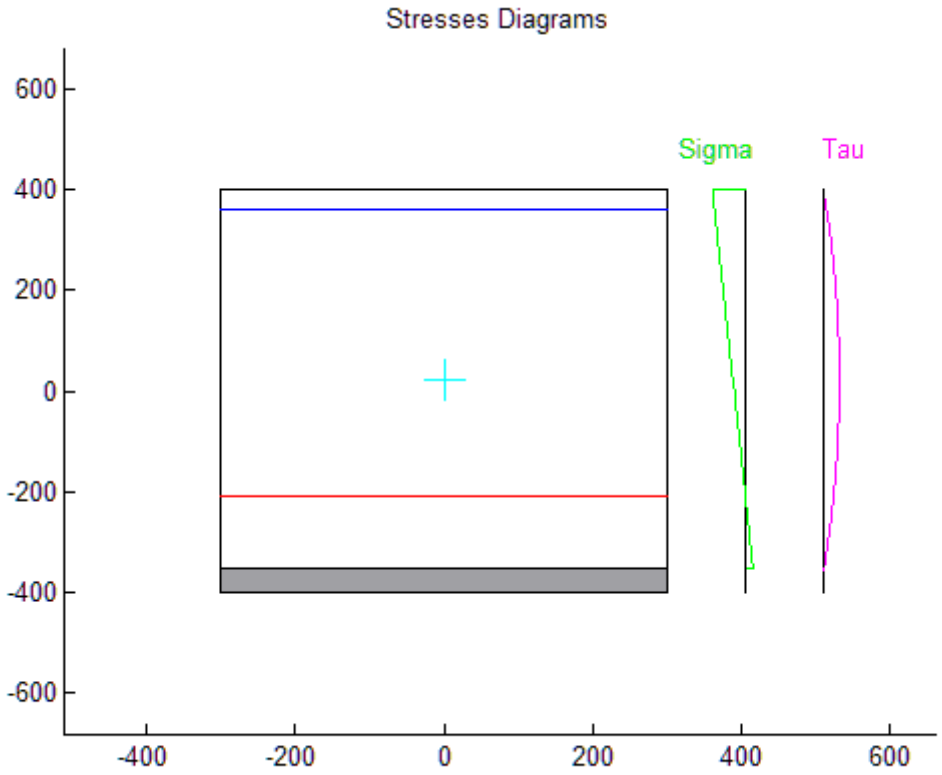

Figure 6.3.4.2 - Tangential and normal stresses distributions

The principal compressive stress at the most compressed fiber is determined through the following equation:

$$\sigma_1{}^{\max comp.\ 3rd\ it.} = \frac{\sigma^{\max comp.\ 3rd\ it.} - \sqrt{\sigma^{\max comp.\ 3rd\ it.{}^2} + 4\,\tau^{\max comp.\ 3rd\ it.}}}{2} = -44.085\ MPa$$

For the tensile fiber:

$$\sigma_1{}^{\max tens.\ 3rd\ it.} = \frac{\sigma^{\max comp.\ 3rd\ it.} + \sqrt{\sigma^{\max comp.3rd\ it.{}^2} + 4\,\tau^{\max comp.\ 3rd\ it.}}}{2} = 10.338\ MPa$$

At the end of the third iteration, the procedure falls again in the fourth scenario:

$$\sigma_1{}^{\max comp.\ 3rd\ it.} = |\mathbf{-44.085}|\ \boldsymbol{MPa} < \boldsymbol{f_{cd}} = |-45|\ MPa$$

$$\sigma_1{}^{\max tens.\ 3rd\ it} = \mathbf{10.338\ MPa} > \boldsymbol{f_{ctd}} = 4.5\ MPa$$

The last tensest fiber cracks, the procedure returns at the beginning and recalculates the new cross section.

6.3.5. 4th Elastic Evaluation of the Cross Section

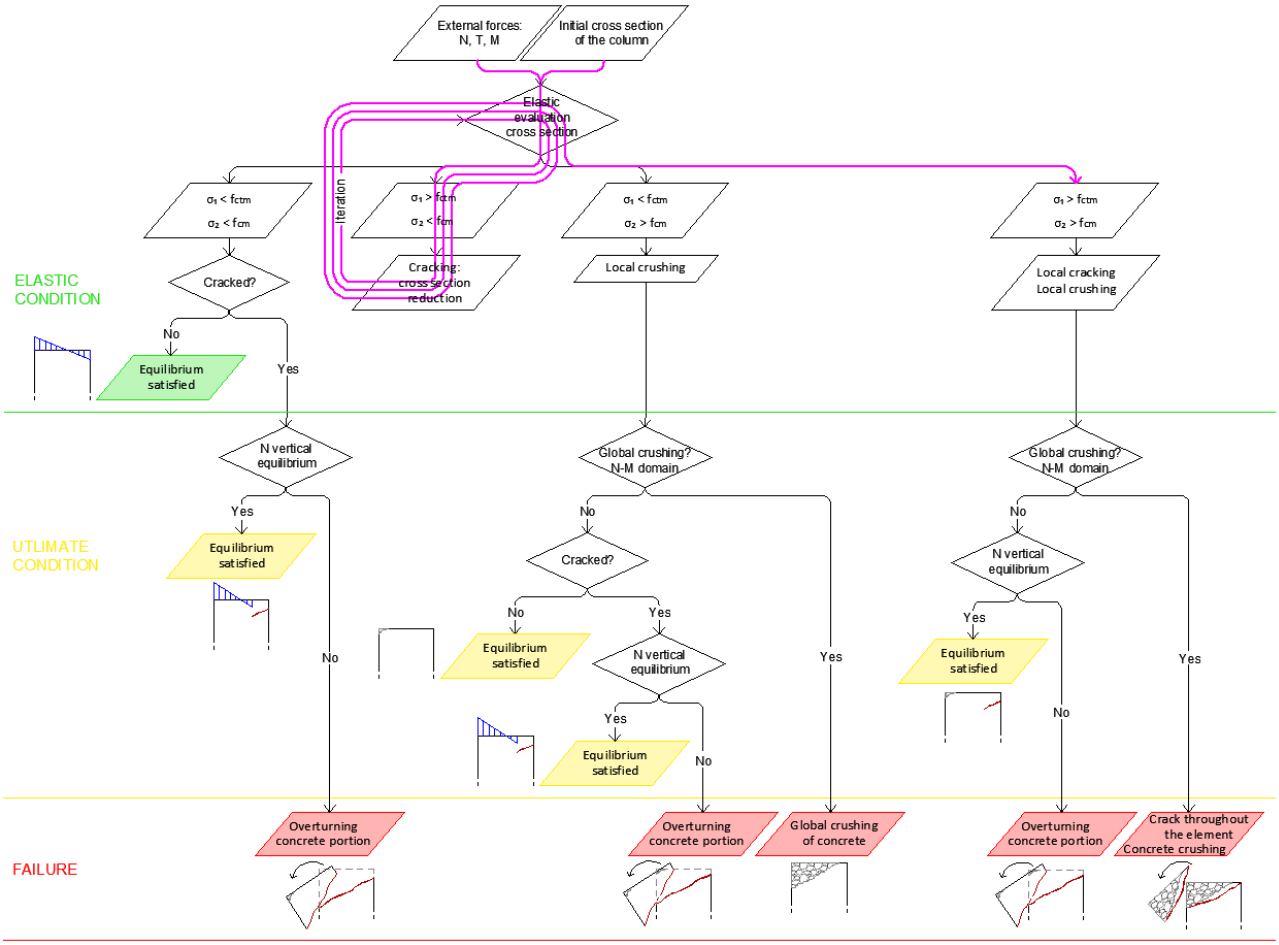

Figure 6.3.5.1 – 4th iteration of the procedure represented in the flow chart

At the sixth iteration, the coordinate of the last working fiber is:

$$y^{4th\ it.} = y(3) = 290\ mm$$

The stress distribution is now characterised by the following maximum values:

$$\sigma^{\max comp.\ 4th\ it.} = -45.208\ MPa$$

$$\sigma^{\max tens.\ 4th\ it.} = 9.121\ MPa$$

The considered fiber lays below reinforcements and therefore corresponding tangential stresses are different from zero:

$$\tau^{\max comp.\ 4th\ it.} = 0\ MPa$$

$$\tau^{\max tens.\ 4th\ it.} = 0.106\ MPa$$

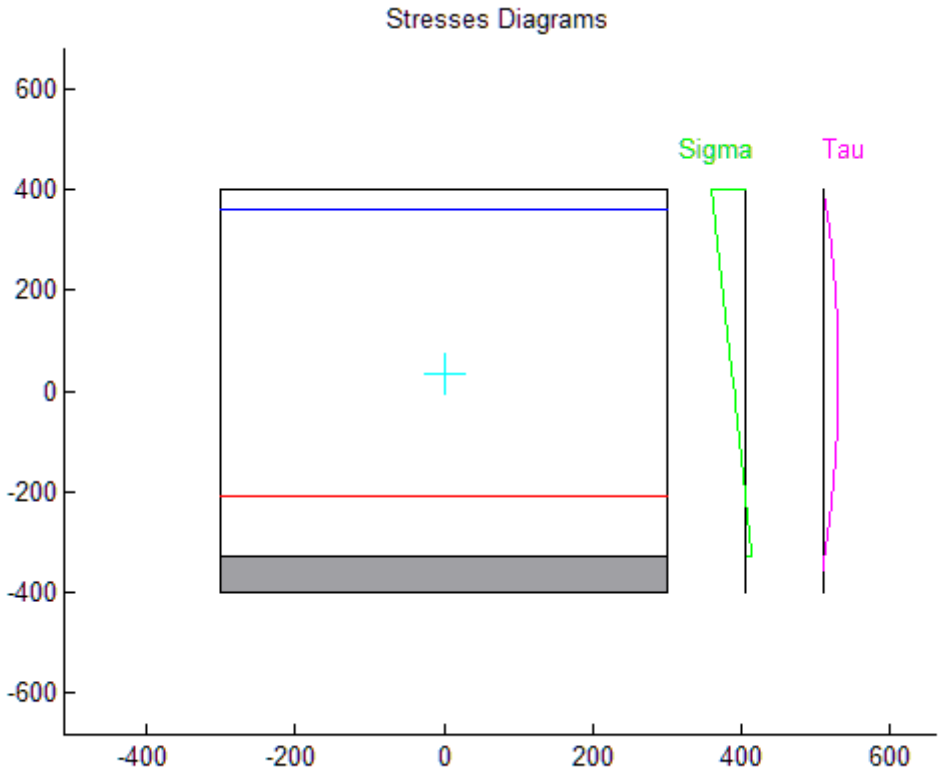

Figure 6.3.5.2 - Tangential and normal stresses distributions

The principal compressive stresses:

$$\sigma_1{}^{\max comp.\ 4th\ it.} = -45.203\ MPa$$

For the tensile fiber:

$$\sigma_1{}^{\max tens.\ 4th\ it.} = 9.133\ MPa$$

At the end of the third iteration, the procedure falls in the sixth scenario:

$$\sigma_1{}^{\max comp.\ 4th\ it.} = |\mathbf{-45.203}|\ \boldsymbol{MPa} > \boldsymbol{f_{cd}} = |-45|\ MPa$$

$$\sigma_1{}^{\max tens.\ 4th\ it.} = \mathbf{9.133\ MPa} > \boldsymbol{f_{ctd}} = 4.5\ MPa$$

At the end of the sixth iteration, both principal tensile stress on the tensest fiber and principal compressive stress on the most compressed fiber exceed their limits. This means that the crack continues developing and the most compressed fiber crushes. Both a local cracking and a local crushing happened. It has to verify if they affect the whole cross section.
The procedure starts analysing the crushing of the concrete: the type of crushing, local or global, can be determined through an N-M domain verification. If the point representing the external forces falls inside the domain, the column is able to withstand solicitations, therefore, even if a portion of the concrete crushes, the whole element is capable of carrying external loads; this corresponds to a

local crushing. If the point is out of the domain, it means that the member fails under such actions, thus it fails because of a global crushing.
Once the procedure coincides with the second scenario, the script has to control if the crushing is global, which means verifying the cross section by means of the N-M interaction domain.

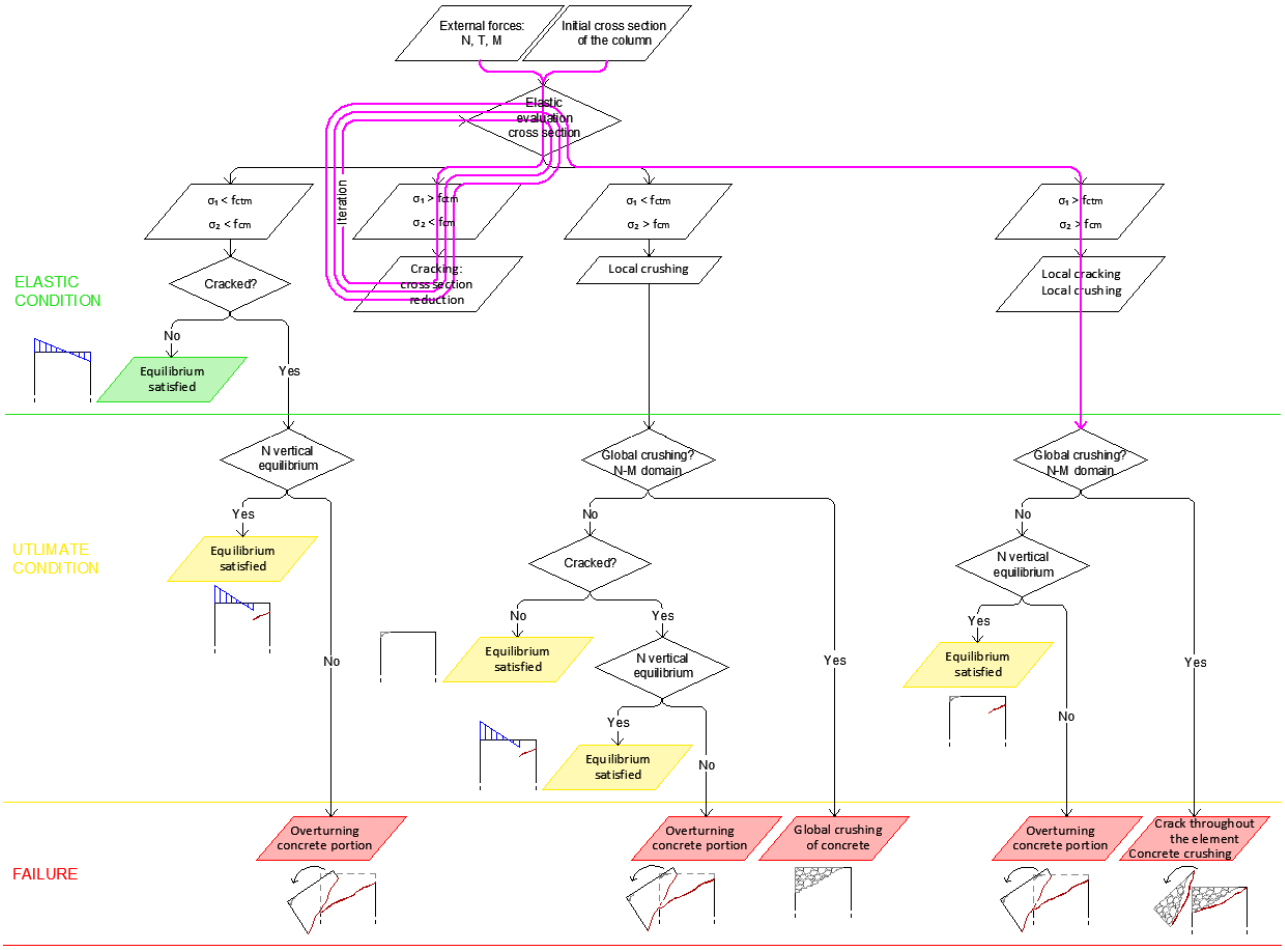

Figure 6.3.5.3 – Path on the flow chart: global crushing verification

At the end of the global crushing verification, the plot of the N-M domain and the point representing the external forces on the column. In this case, the point is outside the interaction diagram; the script returns “The verification of the N-M domain is not satisfied, global crushing of the element”.

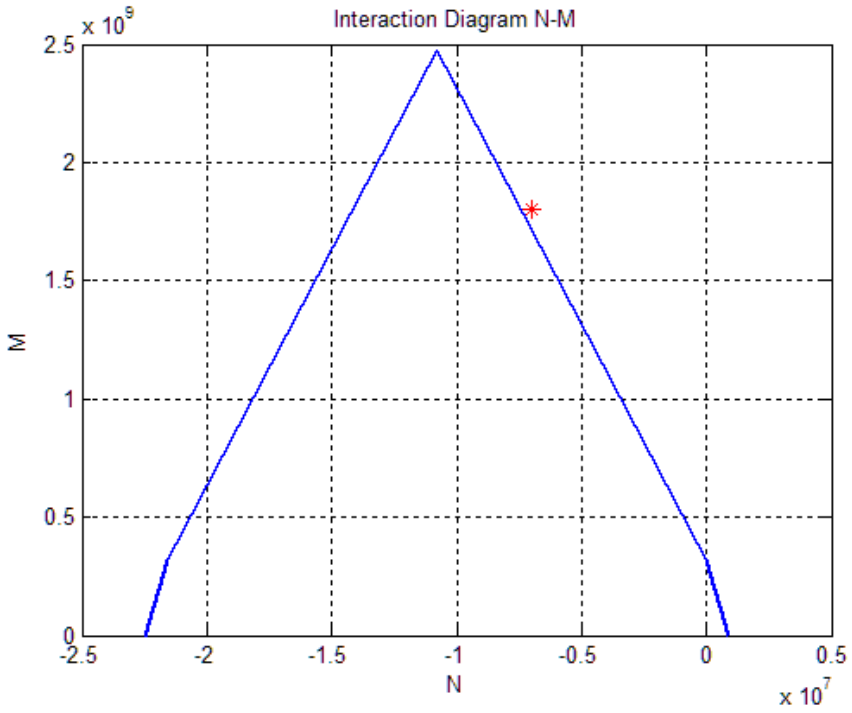

Figure 6.3.5.4 – N-M interaction domain

The whole element crushes; the path on the flow chart follow the *"Yes"* alternative. Since the column has already failed because of the crushing, the verification of the crack is worthless.

The procedure ends with the failure of the column. The script returns "The crack develops throughout the cross section and global crushing of the column".

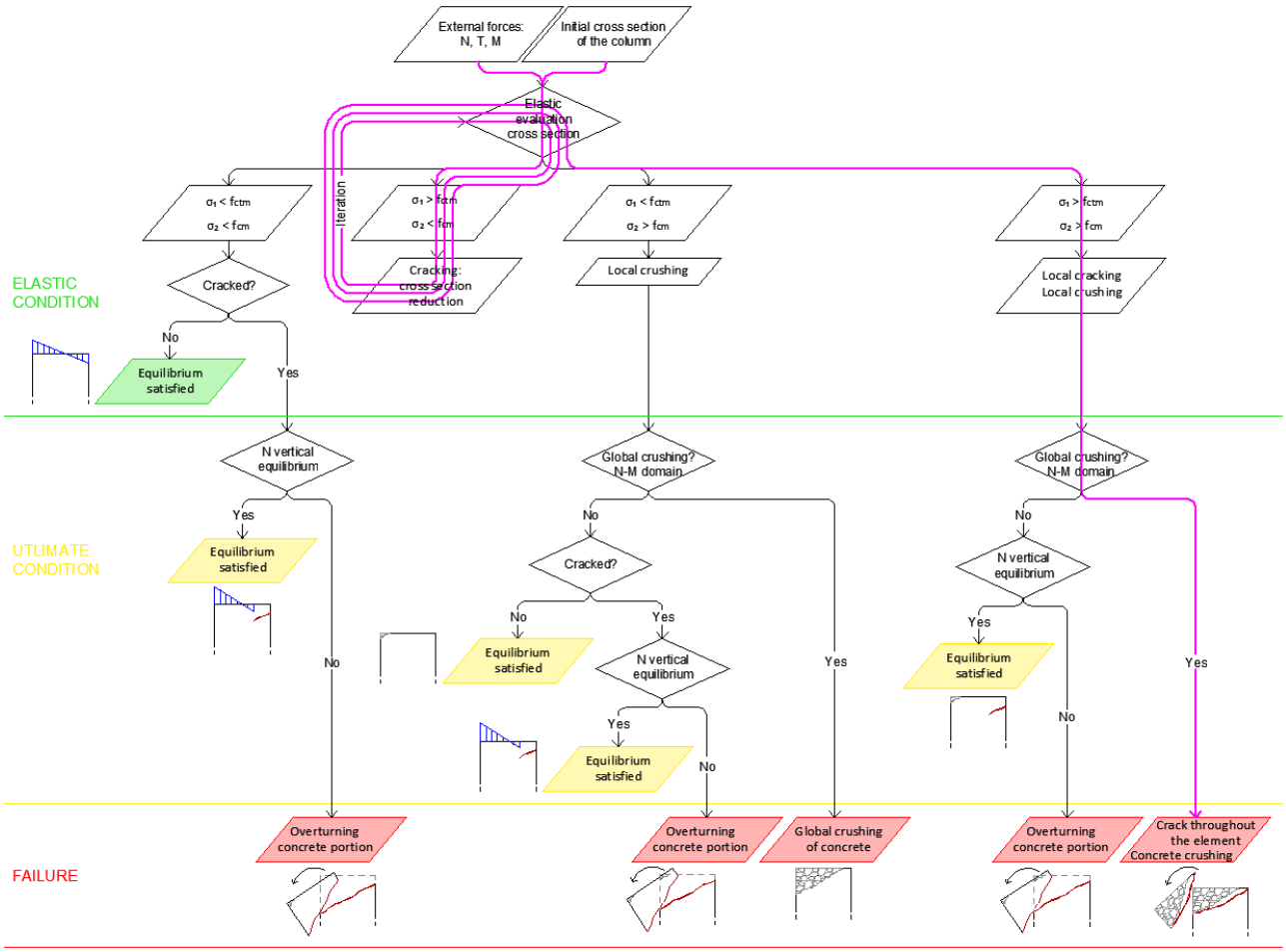

Figure 6.3.5.5 – Path on the flow chart: end of the procedure

6.4. Application of the Procedure to Real Cases

The procedure has also applied to three real cases, thus, in addition to geometrical properties and material ones, also external forces correspond to the values acting on the element when it collapsed.

6.4.1. Case 1

The information required by the procedure, corresponding to geometrical ad material properties of a real column, are:

- $b = 300\ mm$;
- $h = 300\ mm$;
- $c = 30\ mm$;
- $d = 270\ mm$;
- $A_{s,sup} = 2\ \Phi\ 10 = 157\ mm^2$;
- $A_{s,inf} = 2\ \Phi\ 10 = 157\ mm^2$;
- $\Phi_{st} = \Phi\ 6 = 6\ mm$;

- $n_{st} = 2$;
- $s_{st} = 100\ mm$:
- $f_{cd} = 9.4\ MPa$;
- $f_{ctd} = 0.1\ f_{cd} = 0.94\ MPa$;
- $f_{yd} = 447.8\ MPa$;
- $E_c = 22000\ \left[\left(\frac{f_{cd}}{10}\right)^{0.3}\right] = 28821\ MPa$;
- $E_s = 210000\ MPa$;
- $n = {E_c}/{E_s} = 7.29$;
- $N_{act} = -300000\ N$;
- $T_{act} = 30000\ N$;
- $M_{act} = 60000000\ N\ mm$.

A half cross section has subdivided in fifteen fibers in order to get the width of each fiber equal to one centimetre.
The vector of the fiber considered is the following one:

$$y = [145,\ 135,\ 125,\ 115,\ 105,\ 95,\ 85,\ 75,\ 65,\ 55,\ 45,\ 35,\ 25,\ 15,\ 5]$$

The fundamental quantities necessary to determine both tangential and normal stresses distributions are, as in previous examples, the effective depth, the homogenised cross section, the position of the centroid of the homogenised area, the homogenised moment of inertia and the homogenised static moment. Formulae have already explained in the first example of the procedure, hence, they will not repeat in this case. Only the values that those terms assume have reported.

6.4.1.1. 1st Elastic Evaluation of the Cross Section

The procedure starts with the first elastic evaluation of the initial cross section, as shown in the flow diagram.

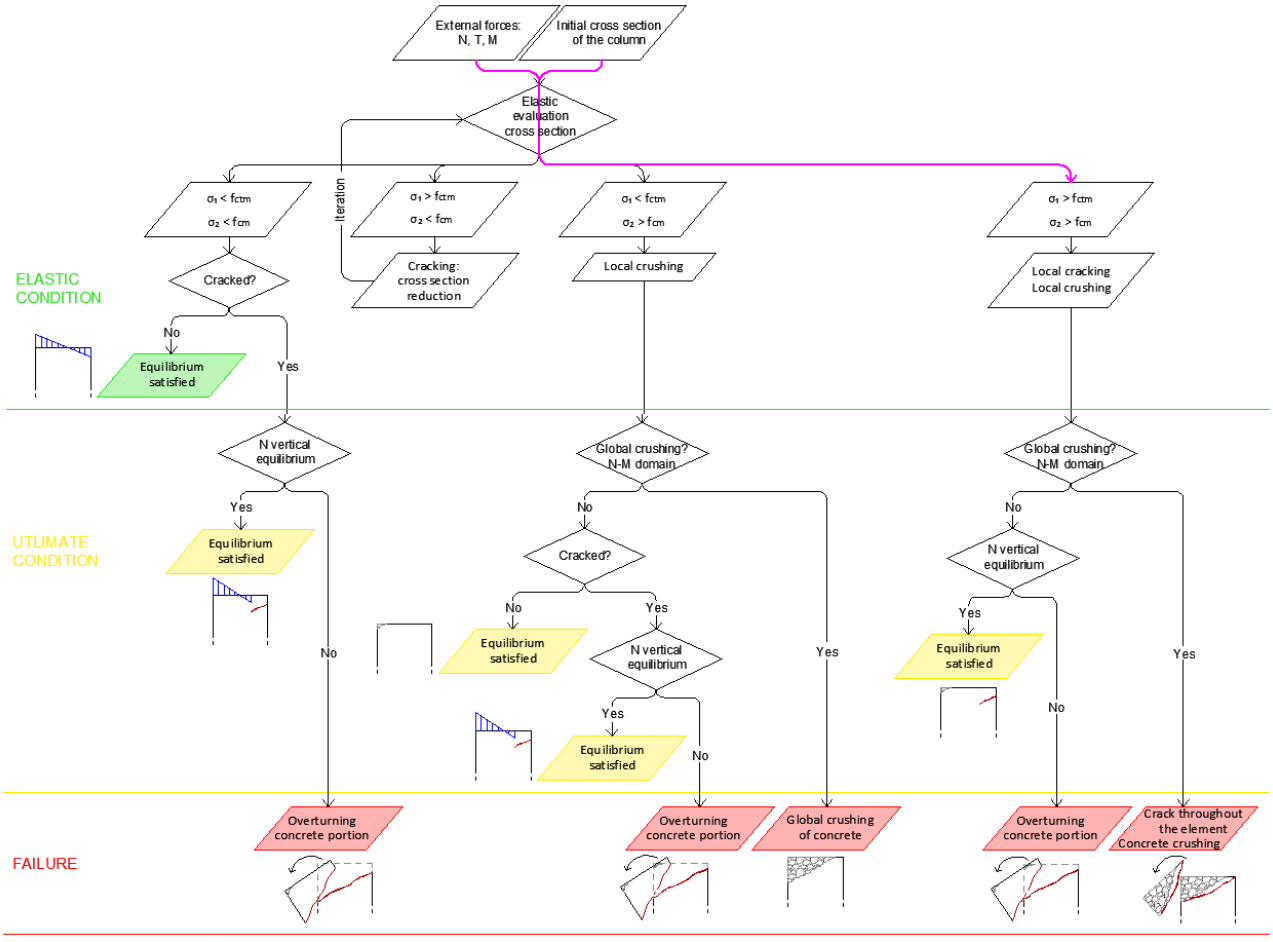

Figure 6.4.1.1.1 – 1st iteration of the procedure represented in the flow chart

The coordinate of the last un-cracked fiber, the one at the extremity of the working cross section, is:

$$y^{1st\ it.} = y(1) = 145\ mm$$

The basic terms necessary to compute the stresses diagrams are the following ones:

$$d^{1st\ it.} = 270\ mm$$

$$A_{omog}{}^{1st\ it.} = 92289\ mm^2$$

$$S^{1st\ it.} = 13671659\ mm^3$$

$$d_{g,sup}{}^{1st\ it.} = 148\ mm$$

$$d_{g,inf}{}^{1st\ it.} = 152\ mm$$

$$I_{omog}{}^{1st\ it.} = 708277858\ mm^4$$

The position of the neutral axis, imposing stress equal to zero in the Navier's equation and solving for the y coordintae:

$$y_{a.n.}{}^{1st\ it.} = -38\ mm$$

The sigma value required by the procedure is the one related to the upper edge under compression, corresponding to $y^{\max comp.} = 150\ mm$:

$$\sigma^{\max comp.\ 1st\ it.} = -16.076\ MPa$$

Even the one acting on the tensest fiber, the one at the lower extremity, corresponding to $y^{max\ tens.} = -145\ mm$:

$$\sigma^{\max tens.\ 1st\ it.} = 9.492\ MPa$$

Tangential stresses are equal to zero because the considered fiber is below steel rebar, where the static moment gets to zero:

$$\tau^{\max comp.\ 1st\ it.} = 0\ MPa$$

$$\tau^{\max tens.\ 1st\ it.} = 0\ MPa$$

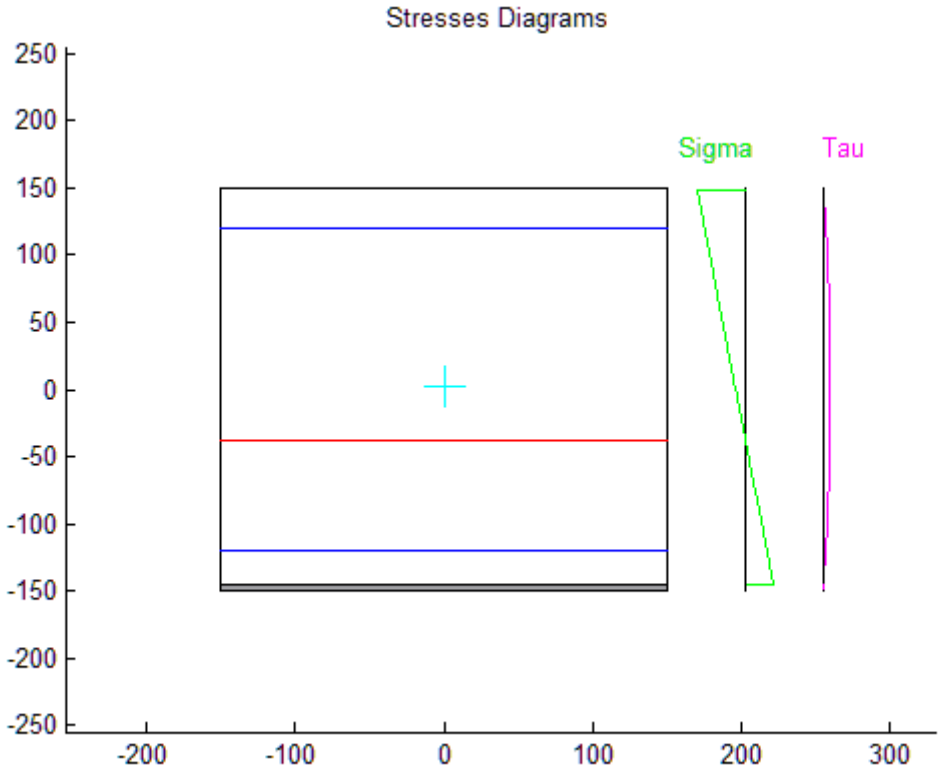

Figure 6.4.1.1.2 - Tangential and normal stresses distributions

Also in this case, considering that tangential stresses are null, principal stresses are equal to normal ones:

$$\sigma_1{}^{\max comp.\ 1st\ it.} = -16.076\ MPa$$

For the tensile fiber:

$$\sigma_1{}^{\max tens.\ 1st\ it.} = 9.492\ MPa$$

At the end of the first iteration, the procedure follows the third scenario: both principal tensile stress in the lowest fiber both principal compressive stress at the upper edge are greater than the tensile and the compressive strength of the concrete, respectively:

$$\sigma_1{}^{\max comp.\ 1st\ it.} = |\mathbf{-16.076}|\ \boldsymbol{MPa} > \boldsymbol{f_{cd}} = |-9.4|\ MPa$$

$$\sigma_1{}^{\max tens.\ 1st\ it.} = \mathbf{9.492}\ \boldsymbol{MPa} > \boldsymbol{f_{ctd}} = 0.94\ MPa$$

The scenario is:

$$\left(\sigma_1^{lower\ edge}\right)^{1st\ it.} > f_{ctd}$$

$$\left(\sigma_2^{upper\ edge}\right)^{1st\ it.} > f_{cd}$$

This means that the crack continues developing and the most compressed fiber crushes. Both a local cracking and a local crushing certainly happened. The analysis proceeds considering first the crushing of the concrete: the type of crushing, local or global, can be determined through an N-M domain verification. If the solicitation point lays inside the domain, the column is able to withstand external actions and therefore the crushing is local. If the point is out of the domain, it means that the member fails under such actions, thus it fails because of a global crushing.

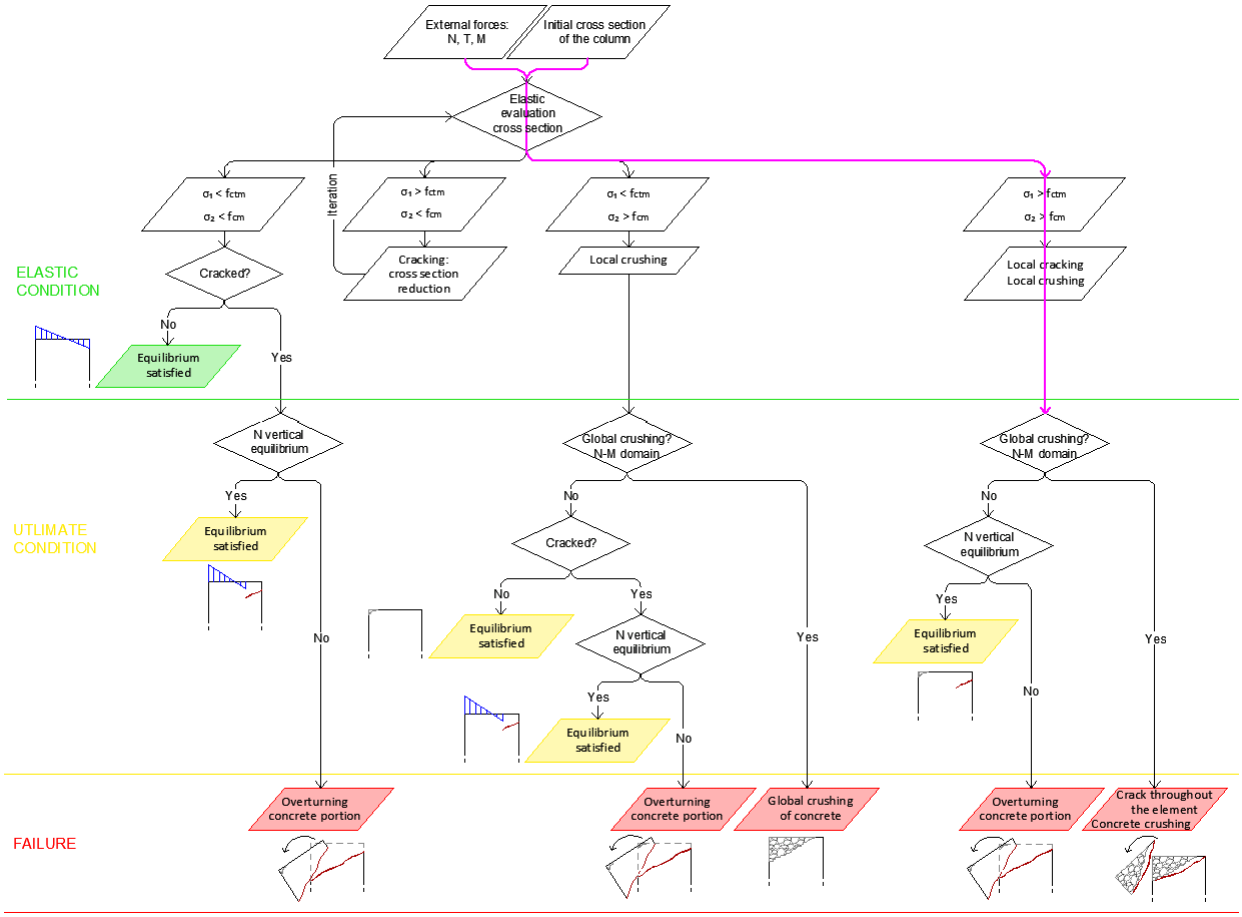

Figure 6.4.1.1.3 – Path on the flow chart: global crushing verification

The script goes on with the N-M domain verification.

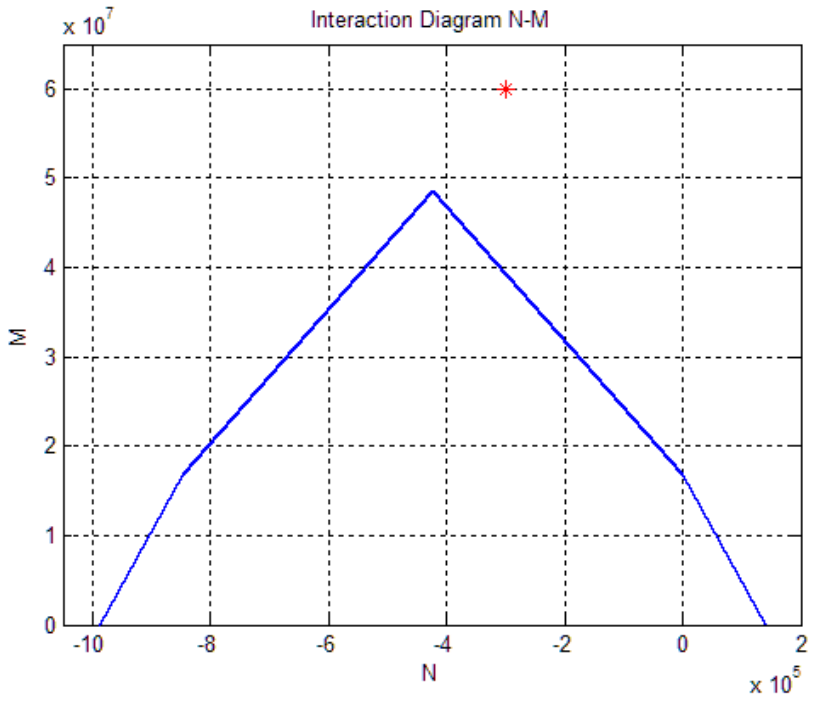

Figure 6.4.1.1.4 – N-M interaction domain

As shown in the figure, the point is outside the interaction diagram; the script returns "The verification of the N-M domain is not satisfied, global crushing of the element". The whole element crushes; the path on the flow chart follow the *"Yes"* alternative. Since the column has already failed because of the crushing, the verification of the crack is worthless.

The procedure ends with the failure of the column. The script returns "The crack develops throughout the cross section and global crushing of the column".

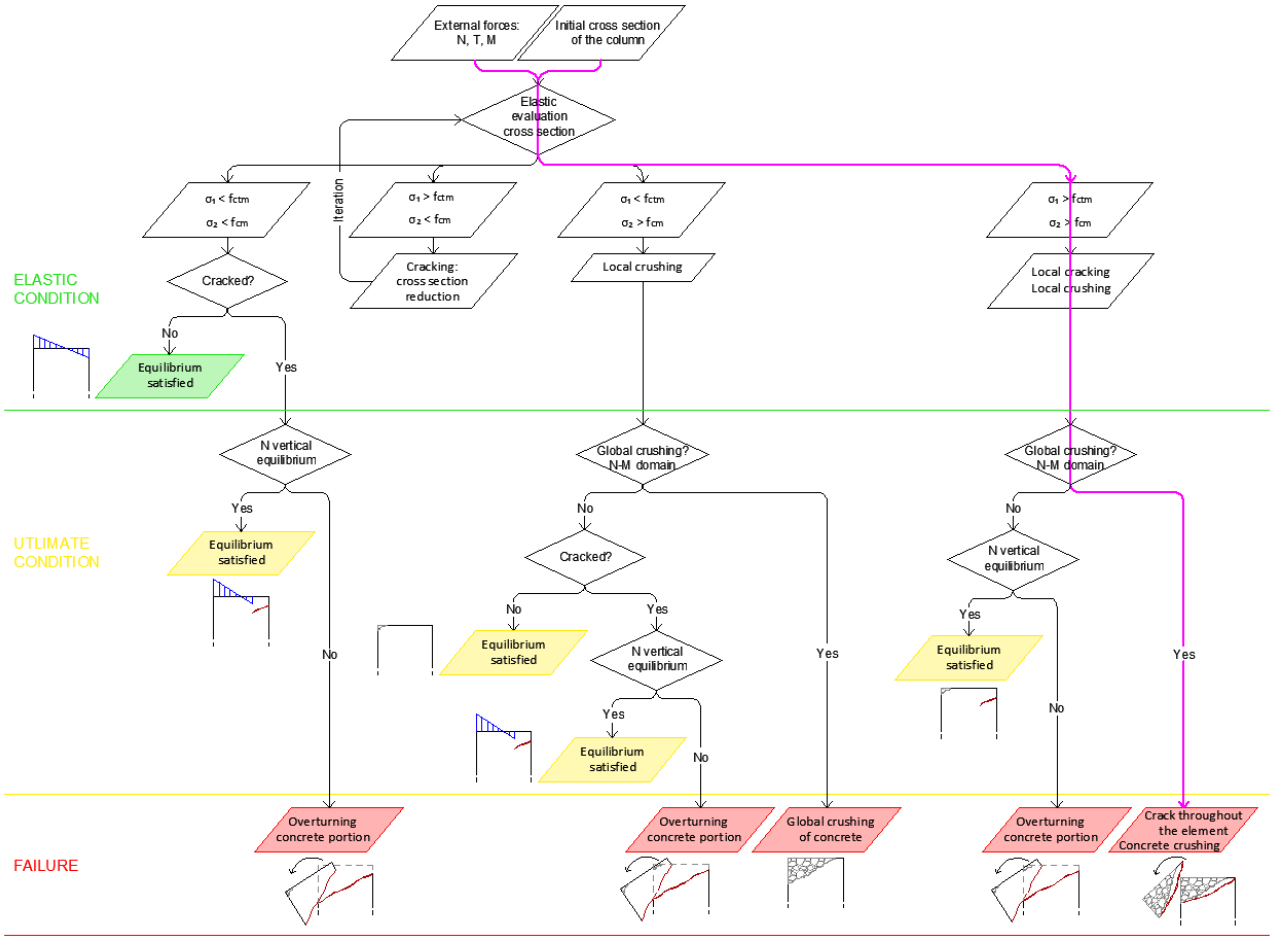

Figure 6.4.1.1.6 – Path on the flow chart: end of the procedure

6.4.2. Case 2

The information that the procedure requires has listed below:

- $b = 500\ mm$;
- $h = 500\ mm$;
- $c = 40\ mm$;
- $d = 260\ mm$;
- $A_{s,sup} = 2\ \Phi\ 24 = 904\ mm^2$;
- $A_{s,inf} = 2\ \Phi\ 24 = 904\ mm^2$;
- $\Phi_{st} = \Phi\ 6 = 6\ mm$;
- $n_{st} = 2$;
- $s_{st} = 200\ mm$:
- $f_{cd} = 60\ MPa$;
- $f_{ctd} = 0.1\ f_{cd} = 6\ MPa$;
- $f_{yd} = 600\ MPa$;

- $E_c = 22000 \left[\left(\frac{f_{cd}}{10}\right)^{0.3}\right] = 37659\ MPa$;
- $E_s = 210000\ MPa$;
- $n = {}^{E_c}/_{E_s} = 5.58$;
- $N_{act} = -660000\ N$;
- $T_{act} = 180000\ N$;
- $M_{act} = 290000000\ N\ mm$;

A half cross section has subdivided into twenty-five fibers, in order to get the width of each fiber equal to one centimetre. The vector of the fiber considered is the following one:

$$y = [245,\ 235,\ 225,\ 215,\ 205,\ 195,\ 185,\ 175,\ 165,\ 155,\ 145,\ 135,\ 125,\ 115, \ldots$$

$$\ldots\ 105,\ 95,\ 85,\ 75,\ 65,\ 55,\ 45,\ 35,\ 25,\ 15,\ 5]$$

6.4.2.1. 1st Elastic Evaluation of the Cross Section

The procedure starts with the first elastic evaluation of the initial cross section.

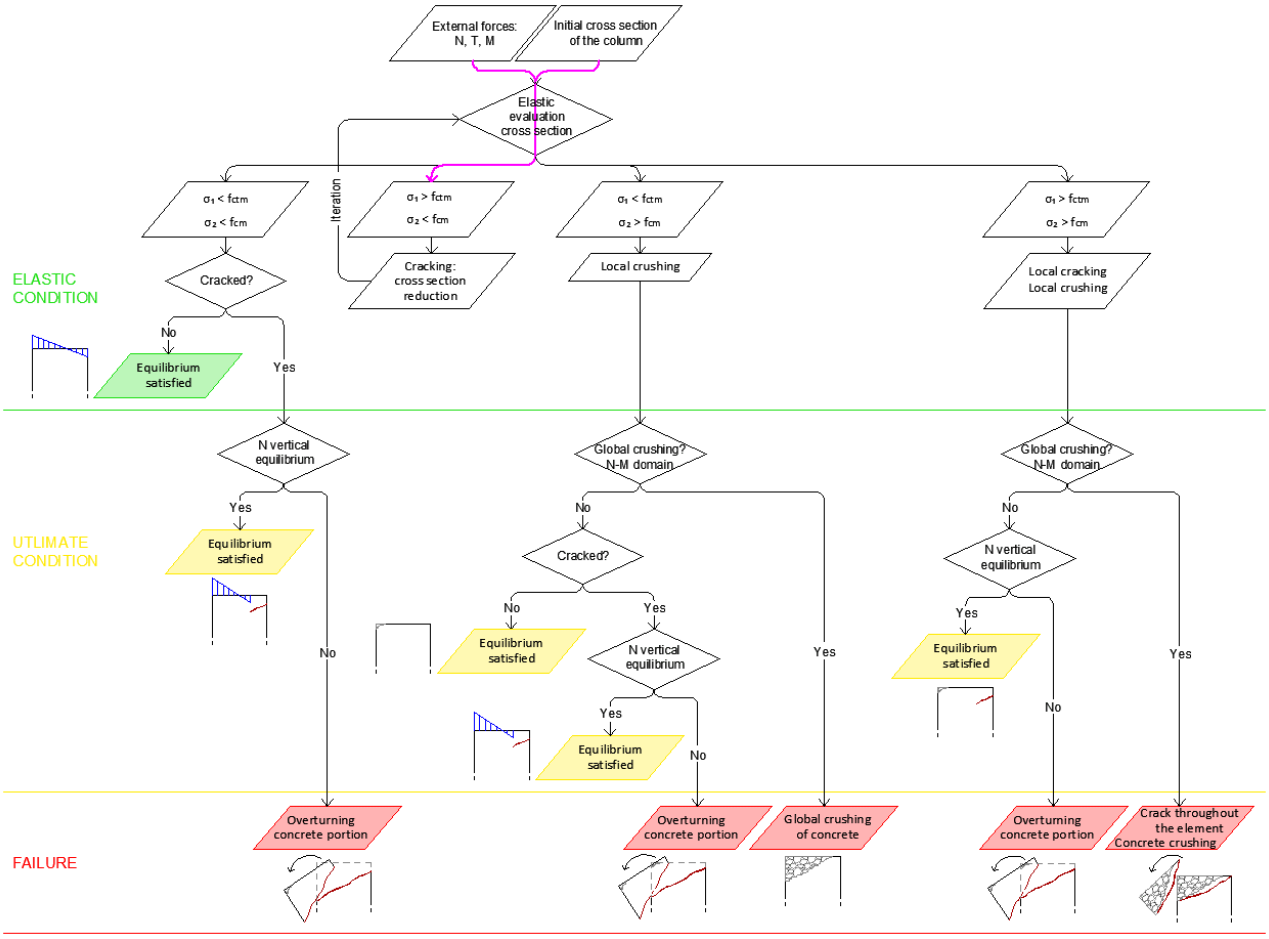

Figure 6.4.2.1.1 – 1st iteration of the procedure represented in the flow chart

The coordinate of the last un-cracked fiber, the one at the extremity of the working cross section, is:

$$y^{1st\ it.} = y(1) = 245\ mm$$

The basic terms necessary to compute the stresses diagrams are the following ones:

$$d^{1st\ it.} = 470\ mm$$

$$A_{omog}{}^{1st\ it.} = 260082\ mm^2$$

$$S^{1st\ it.} = 63760259\ mm^3$$

$$d_{g,sup}{}^{1st\ it.} = 245\ mm$$

$$d_{g,inf}{}^{1st\ it.} = 255\ mm$$

$$I_{omog}{}^{1st\ it.} = 5702412206\ mm^4$$

The position of the neutral axis, imposing stress equal to zero in the Navier's equation and solving for the y coordintae:

$$y_{a.n.}{}^{1st\ it.} = -49\ mm$$

The sigma value required by the procedure is the one related to the upper edge under compression, corresponding to $y^{\max comp.} = 250\ mm$:

$$\sigma^{\max comp.\ 1st\ it.} = -15.392\ MPa$$

Even the one acting on the tensest fiber, the one at the lower extremity, corresponding to $y^{max\ tens.} = -245\ mm$:

$$\sigma^{\max tens.\ 1st\ it.} = 10.919\ MPa$$

Tangential stresses are equal to zero because the considered fiber is below steel rebar, where the static moment gets to zero:

$$\tau^{\max comp.\ 1st\ it.} = 0\ MPa$$

$$\tau^{\max tens.\ 1st\ it.} = 0\ MPa$$

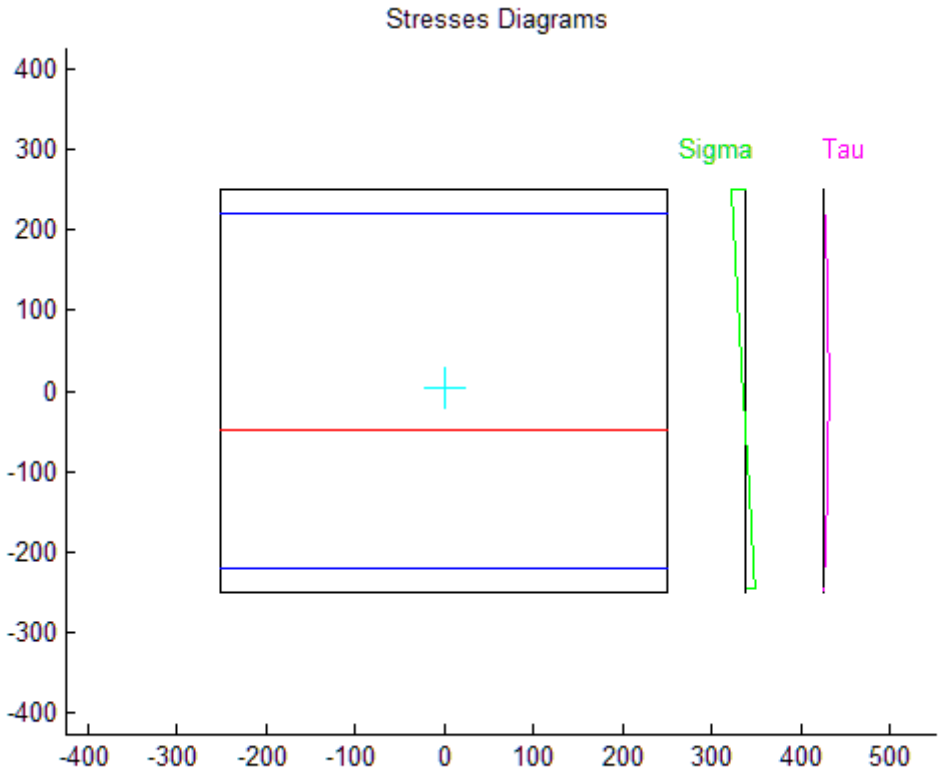

Figure 6.4.2.1.2 - Tangential and normal stresses distributions

Also in this case, considering that tangential stresses are null, principal stresses are equal to normal ones:

$$\sigma_1{}^{\max comp.\ 1st\ it.} = -15.392\ MPa$$

For the tensile fiber:

$$\sigma_1{}^{\max tens.\ 1st\ it.} = 10.919\ MPa$$

At the end of the first iteration, the procedure follows the fourth scenario:

$$\sigma_1{}^{\max comp.\ 1st\ it.} = |\mathbf{-15.392}|\ \boldsymbol{MPa} < \boldsymbol{f_{cd}} = |-60|\ MPa$$

$$\sigma_1{}^{\max tens.\ 1st\ it.} = \mathbf{10.919\ MPa} > \boldsymbol{f_{ctd}} = 6\ MPa$$

The procedure returns at the beginning of the analysis, recalculates the cross section and the state of stress. A second iteration follow this first one.

6.4.2.2. 2nd Elastic Evaluation of the Cross Section

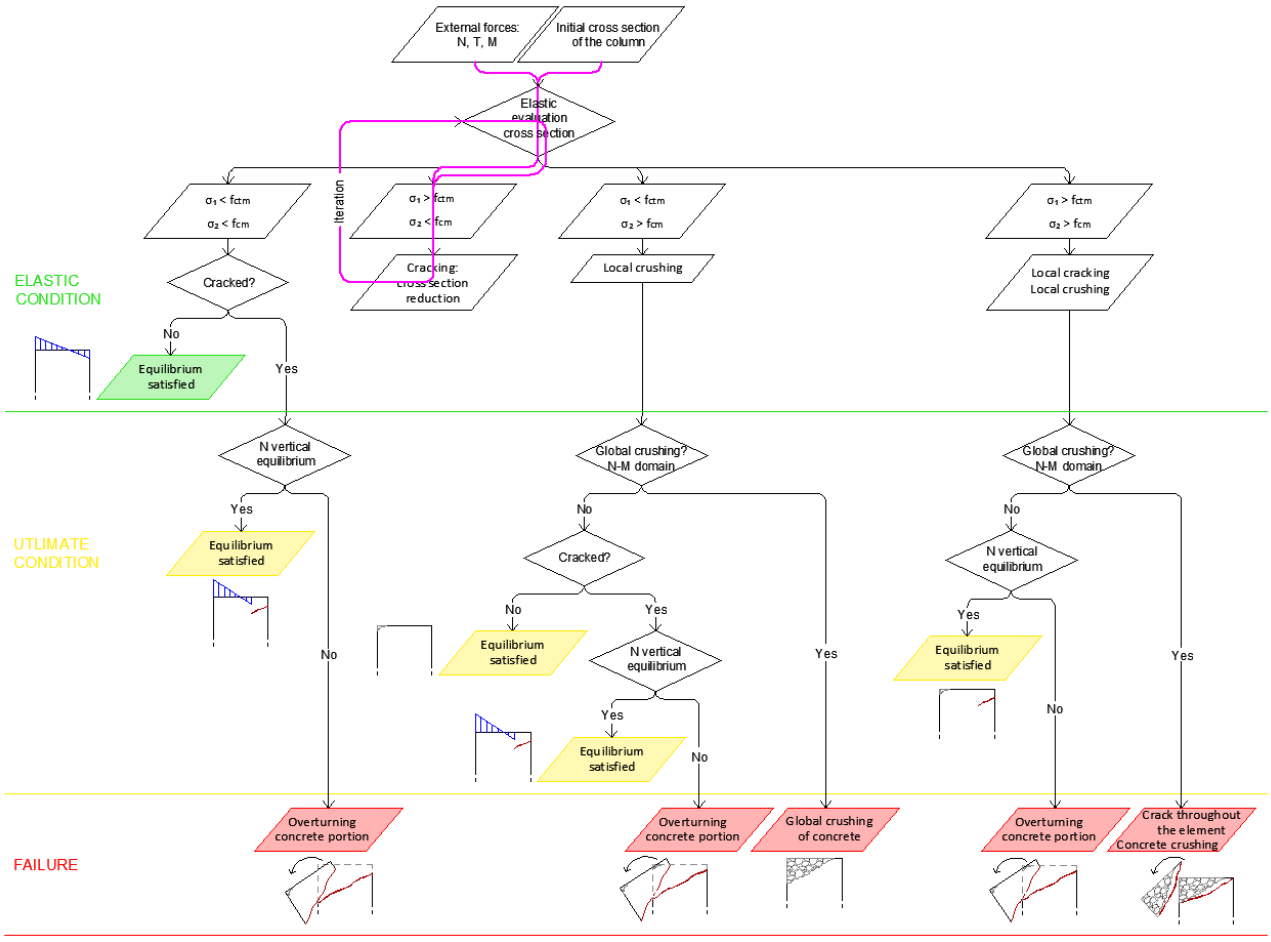

Figure 6.4.2.2.1 – 2nd iteration of the procedure represented in the flow chart

The fiber at the extremity of the initial cross section cracked hence the element has reduced. The coordinate of the last un-cracked fiber, is:

$$y^{2nd\ it.} = y(2) = 235\ mm$$

Fundamental terms necessary to compute the stresses diagrams are the following ones:

$$d^{2nd\ it.} = 460\ mm$$

$$A_{omog}{}^{2nd\ it.} = 255082\ mm^2$$

$$S^{2nd\ it.} = 61285259\ mm^3$$

$$d_{g,sup}{}^{2nd\ it.} = 240\ mm$$

$$d_{g,inf}{}^{2nd\ it.} = 260\ mm$$

$$I_{omog}{}^{2nd\ it.} = 5720993917\ mm^4$$

The position of the neutral axis, imposing stress equal to zero in the Navier's equation and solving for the y coordintae:

$$y_{a.n.}{}^{2nd\ it.} = -50\ mm$$

The sigma value required by the procedure is the one related to the upper edge under compression, corresponding to $y^{\max comp.} = 250\ mm$:

$$\sigma^{\max comp.\ 2nd\ it.} = -15.541\ MPa$$

Even the one acting on the tensest fiber, the one at the lower extremity, corresponding to $y^{max\ tens.} = -235\ mm$:

$$\sigma^{\max tens.\ 2nd\ it.} = 10.411\ MPa$$

Tangential stresses are equal to zero because the considered fiber is below steel rebar, where the static moment gets to zero:

$$\tau^{\max comp.\ 2nd\ it.} = 0\ MPa$$

$$\tau^{\max tens.\ 2nd\ it.} = 0\ MPa$$

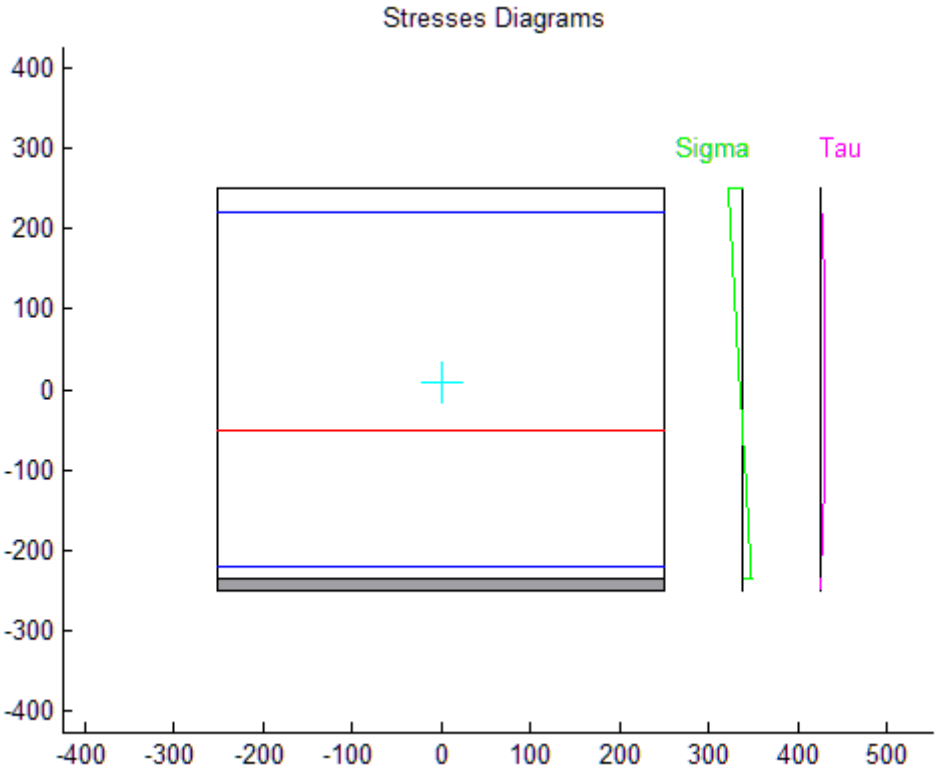

Figure 6.4.2.2.2 - Tangential and normal stresses distributions

Also in this case, considering that tangential stresses are null, principal stresses are equal to normal ones:

$$\sigma_1{}^{\max comp.\ 2nd\ it.} = -15.541\ MPa$$

For the tensile fiber:

$$\sigma_1{}^{\max tens.\ 2nd\ it.} = 10.411\ MPa$$

At the end of the second iteration, the procedure falls into the fourth scenario:

$$\sigma_1{}^{\max comp.\ 2nd\ it.} = |-\mathbf{15.541}|\ \boldsymbol{MPa} < \boldsymbol{f_{cd}} = |-60|\ MPa$$

$$\sigma_1{}^{\max tens.\ 2nd\ it.} = \mathbf{10.411}\ \boldsymbol{MPa} > \boldsymbol{f_{ctd}} = 6\ MPa$$

Also at the end of the second iteration the procedure returns in the fourth scenario, the last fiber cracks and the analysis goes back to the beginning of the procedure and revaluates the stresses acting on the cross section.

6.4.2.3. 3rd Elastic Evaluation of the Cross Section

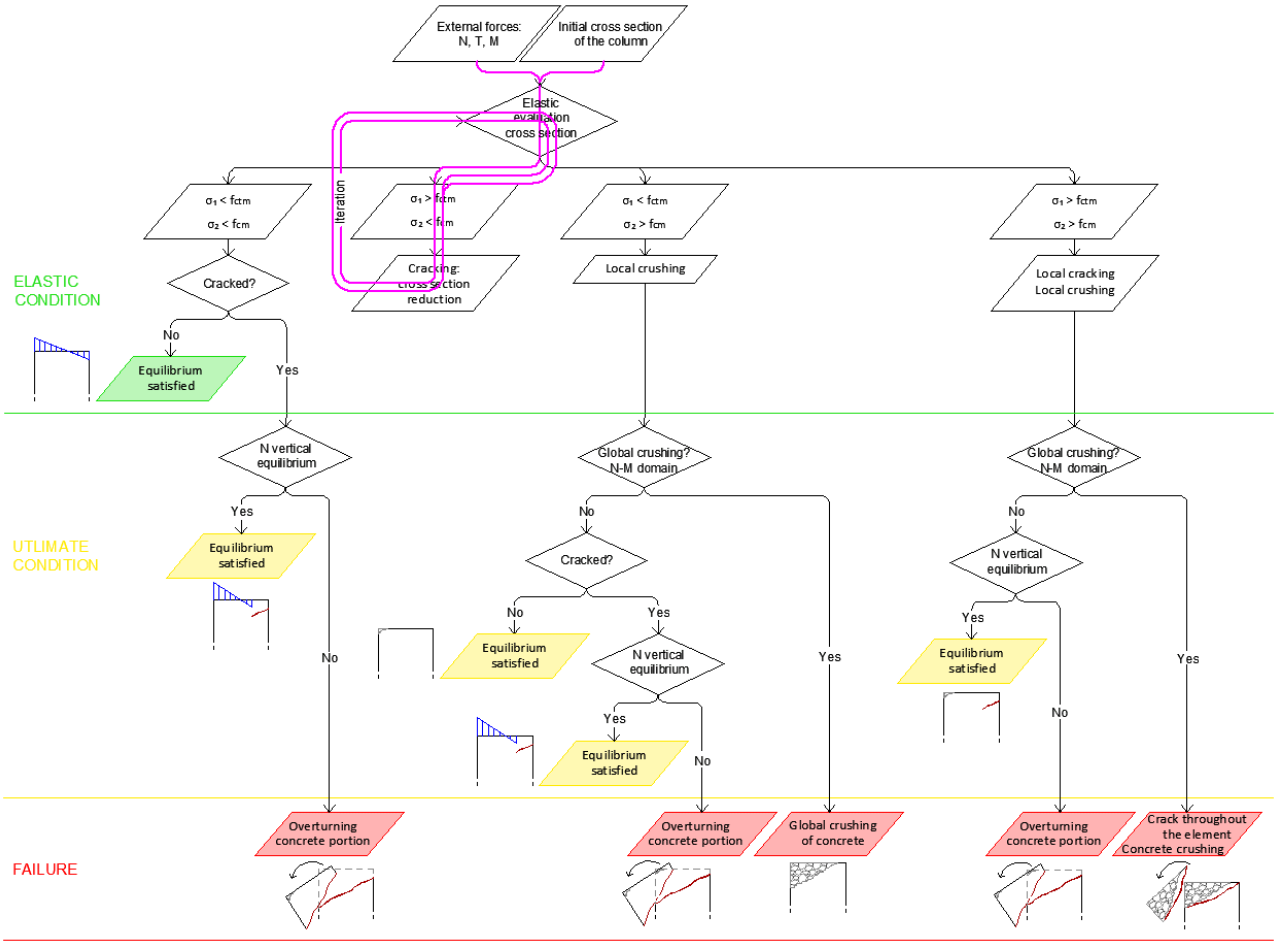

Figure 6.4.2.3.1 – 3rd iteration of the procedure represented in the flow chart

At the third iteration, the coordinate of the last un-cracked fiber, is:

$$y^{3rd\ it.} = y(3) = 225\ mm$$

The basic terms necessary to compute the stresses diagrams have to recalculate, since the y coordinate has changed.
The position of the neutral axis from Navier's equation:

$$y_{a.n.}{}^{3rd\ it.} = -51\ mm$$

The sigma value required by the procedure is the one related to the upper edge under compression, corresponding to $y^{\max comp.} = 250\ mm$:

$$\sigma^{\max comp.\ 3rd\ it.} = -15.663\ MPa$$

Even the one acting on the tensest fiber, the one at the lower extremity, corresponding to $y^{max\ tens.} = -225\ mm$:

$$\sigma^{\max tens.\ 3rd\ it.} = 9.881\ MPa$$

Tangential stresses are equal to zero because the considered fiber is below steel rebar, where the static moment gets to zero:

$$\tau^{\max comp.\ 3rd\ it.} = 0\ MPa$$

$$\tau^{\max tens.\ 3rd\ it.} = 0.108\ MPa$$

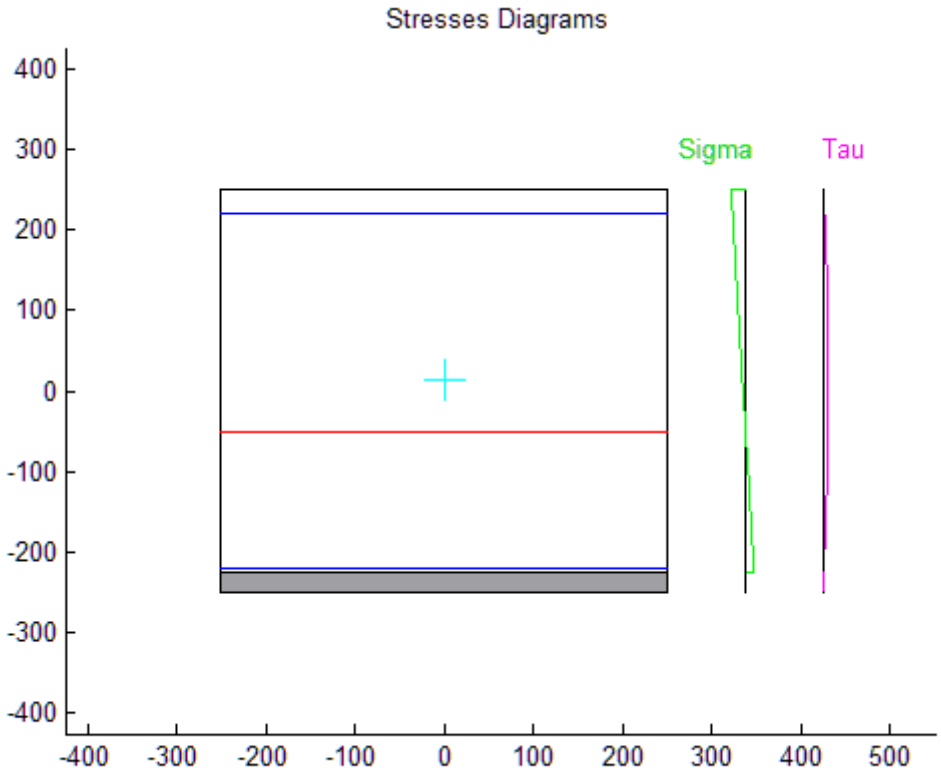

Figure 6.4.2.3.2 - Tangential and normal stresses distributions

Principal compressive stress, depending on both normal and tangential stresses:

$$\sigma_1{}^{\max comp.\ 3rd\ it.} = -15.663\ MPa$$

For the tensile fiber:

$$\sigma_1^{\max tens.\ 3rd\ it.} = 9.881\ MPa$$

At the end of the second iteration, the procedure returns the fourth scenario:

$$\sigma_1^{\max comp.\ 3rd\ it.} = |-\mathbf{15.663}|\ \boldsymbol{MPa} < \boldsymbol{f_{cd}} = |-60|\ MPa$$

$$\sigma_1^{\max tens.\ 3rd\ it.} = \mathbf{9.881}\ \boldsymbol{MPa} > \boldsymbol{f_{ctd}} = 6\ MPa$$

Also at the end of the second iteration the procedure returns in the fourth scenario, the procedure repeats

6.4.2.4. 4th Elastic Evaluation of the Cross Section

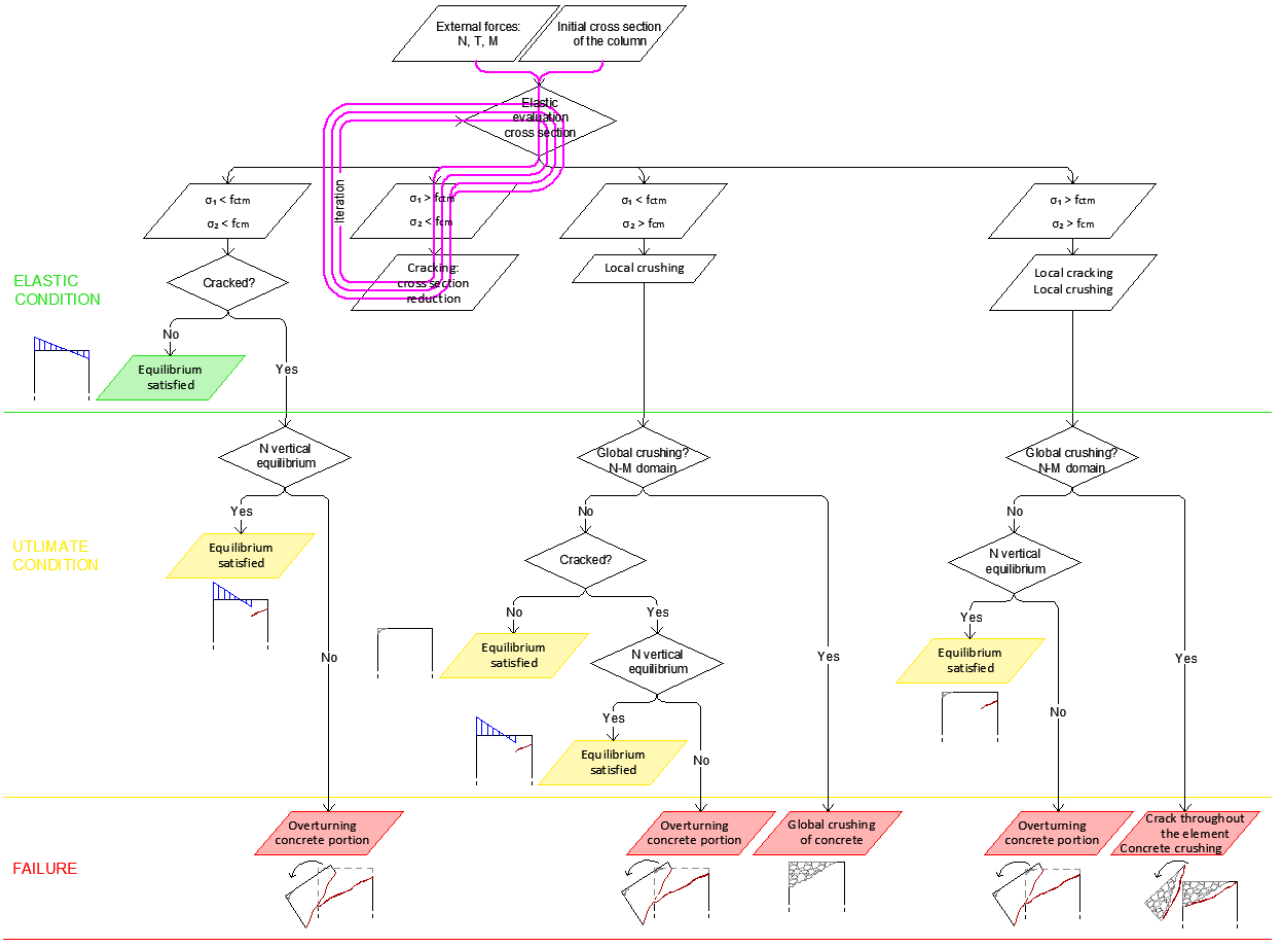

Figure 6.4.2.4.1 – 4th iteration of the procedure represented in the flow chart

For the fourth iteration, the coordinate of the last un-cracked fiber, is:

$$y^{4th\ it.} = y(4) = 215\ mm$$

The position of the neutral axis from Navier's equation:

$$y_{a.n.}^{\ 4th\ it.} = -52\ mm$$

The sigma value required by the procedure is the one related to the upper edge under compression, corresponding to $y^{\max comp.} = 250\ mm$:

$$\sigma^{\max comp.\ 4th\ it.} = -15.759\ MPa$$

And the one at the lower extremity, corresponding to $y^{max\ tens.} = -215\ mm$:

$$\sigma^{\max tens.\ 4th\ it.} = 9.330\ MPa$$

Tangential stresses:

$$\tau^{\max comp.\ 4th\ it.} = 0\ MPa$$

$$\tau^{\max tens.\ 4th\ it.} = 0.0335\ MPa$$

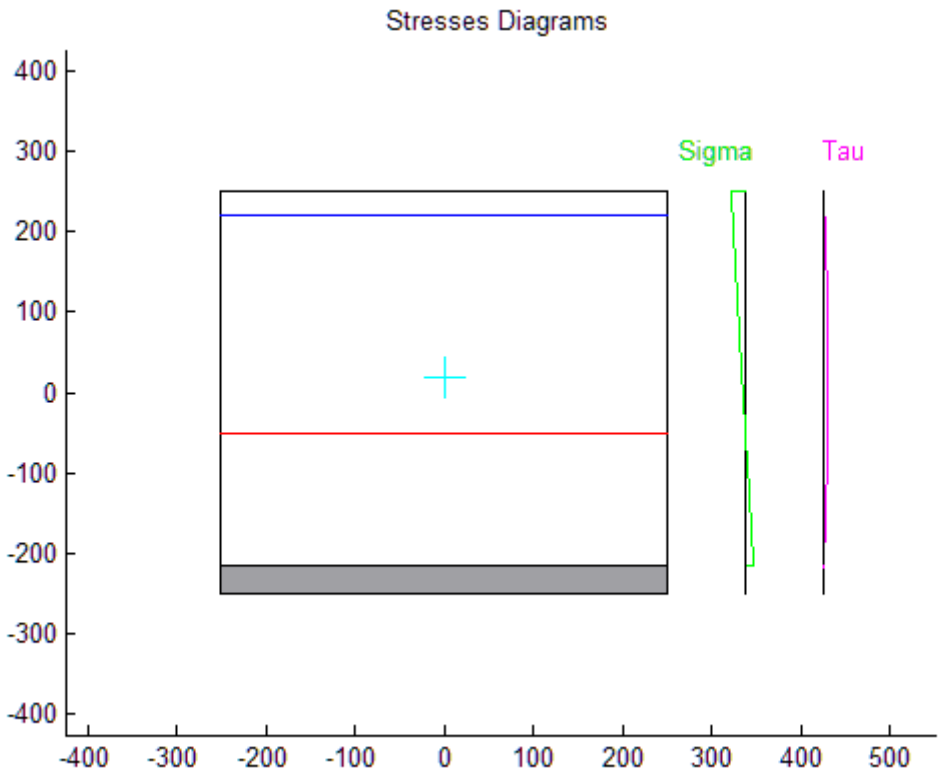

Figure 6.4.2.4.2 - Tangential and normal stresses distributions

Principal stresses are function of both normal and tangential stresses:

$$\sigma_1{}^{\max comp.\ 4th\ it.} = -15.761\ MPa$$

For the tensile fiber:

$$\sigma_1{}^{\max tens.\ 4th\ it.} = 9.33\ MPa$$

At the end of the fourth iteration, the procedure follows the fourth scenario:

$$\sigma_1{}^{\max comp.\ 4th\ it.} = |\mathbf{-15.761}|\ \boldsymbol{MPa} > \boldsymbol{f_{cd}} = |-60|\ MPa$$

$$\sigma_1{}^{\max tens.\ 4th\ it.} = \mathbf{9.33\ MPa} > \boldsymbol{f_{ctd}} = 6\ MPa$$

6.4.2.5. 5th Elastic Evaluation of the Cross Section

For the fifth iteration, the coordinate of the last un-cracked fiber, is:

$$y^{5th\ it.} = y(5) = 205\ mm$$

The position of the neutral axis from Navier's equation:

$$y_{a.n.}{}^{5th\ it.} = -53\ mm$$

The sigma value required by the procedure is the one related to the upper edge under compression, corresponding to $y^{\max comp.} = 250\ mm$:

$$\sigma^{\max comp.\ 5th\ it.} = -15.828\ MPa$$

And the one at the lower extremity, corresponding to $y^{max\ tens.} = -205\ mm$:

$$\sigma^{\max tens.\ 5th\ it.} = 8.765\ MPa$$

Tangential stresses are now equal to::

$$\tau^{\max comp.\ 5th\ it.} = 0\ MPa$$

$$\tau^{\max tens.\ 5th\ it.} = 0.0339\ MPa$$

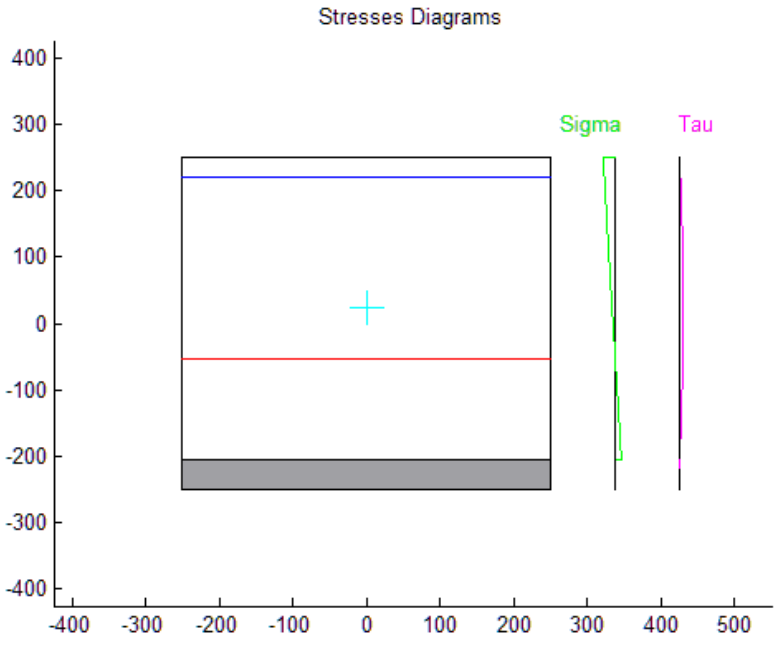

Figure 6.4.2.5.1 - Tangential and normal stresses distributions

Principal stresses are function of both normal and tangential stresses:

$$\sigma_1{}^{\max comp.\ 5th\ it.} = -15.830\ MPa$$

For the tensile fiber:

$$\sigma_1{}^{\max tens.\ 5th\ it.} = 8.769\ MPa$$

At the end of the fifth iteration, the procedure corresponds to the fourth scenario:

$$\sigma_1{}^{\max comp.\ 5th\ it.} = |\mathbf{-15.830}|\ \boldsymbol{MPa} > \boldsymbol{f_{cd}} = |-60|\ MPa$$

$$\sigma_1{}^{\max tens.\ 5th\ it.} = \mathbf{8.769\ MPa} > \boldsymbol{f_{ctd}} = 6\ MPa$$

6.4.2.6. 6th Elastic Evaluation of the Cross Section

For the sixth iteration: $y^{6th\ it.} = y(6) = 195\ mm$

The position of the neutral axis from Navier's equation:

$$y_{a.n.}{}^{6th\ it.} = -54\ mm$$

The sigma value required by the procedure is the one related to the upper edge under compression, corresponding to $y^{\max comp.} = 250\ mm$:

$$\sigma^{\max comp.\ 6th\ it.} = -15.872\ MPa$$

And the one at the lower extremity, corresponding to $y^{max\ tens.} = -195\ mm$:

$$\sigma^{\max tens.\ 6th\ it.} = 8.19\ MPa$$

Tangential stresses correspond to:

$$\tau^{\max comp.\ 6th\ it.} = 0\ MPa$$

$$\tau^{\max tens.\ 6th\ it.} = 0.0343\ MPa$$

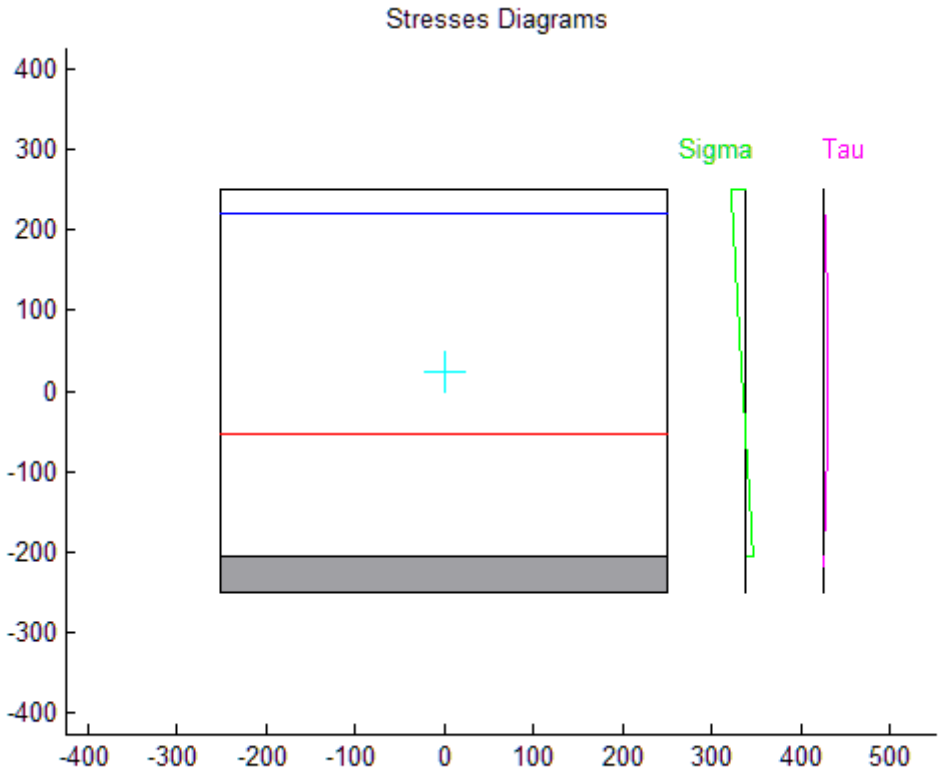

Figure 6.4.2.6.1 - Tangential and normal stresses distributions

Principal stresses are function of both normal and tangential stresses:

$$\sigma_1{}^{\max comp.\ 6th\ it.} = -15.874\ MPa$$

For the tensile fiber:

$$\sigma_1{}^{\max tens.\ 6th\ it.} = 8.194\ MPa$$

At the end of the sixth iteration, the analysis proceeds with the fourth scenario, again:

$$\sigma_1{}^{\max comp.\ 6th\ it.} = |\mathbf{-15.874}|\ \boldsymbol{MPa} > \boldsymbol{f_{cd}} = |-60|\ MPa$$

$$\sigma_1{}^{\max tens.\ 6th\ it.} = \mathbf{8.194\ MPa} > \boldsymbol{f_{ctd}} = 6\ MPa$$

6.4.2.7. 7th Elastic Evaluation of the Cross Section

For the seventh iteration, the coordinate of the last un-cracked fiber, is:

$$y^{7th\ it.} = y(7) = 185\ mm$$

The position of the neutral axis from Navier's equation:

$$y_{a.n.}{}^{7th\ it.} = -55\ mm$$

The sigma value required by the procedure is the one related to the upper edge under compression, corresponding to $y^{\max comp.} = 250\ mm$:

$$\sigma^{\max comp.\ 7th\ it.} = -15.892\ MPa$$

And the one at the lower extremity, corresponding to $y^{max\ tens.} = -185\ mm$:

$$\sigma^{\max tens.\ 7th\ it.} = 7.609\ MPa$$

Tangential stresses are now different from zero because the considered fiber is no longer below reinforcements:

$$\tau^{\max comp.\ 7th\ it.} = 0\ MPa$$

$$\tau^{\max tens.\ 7th\ it.} = 0.0345\ MPa$$

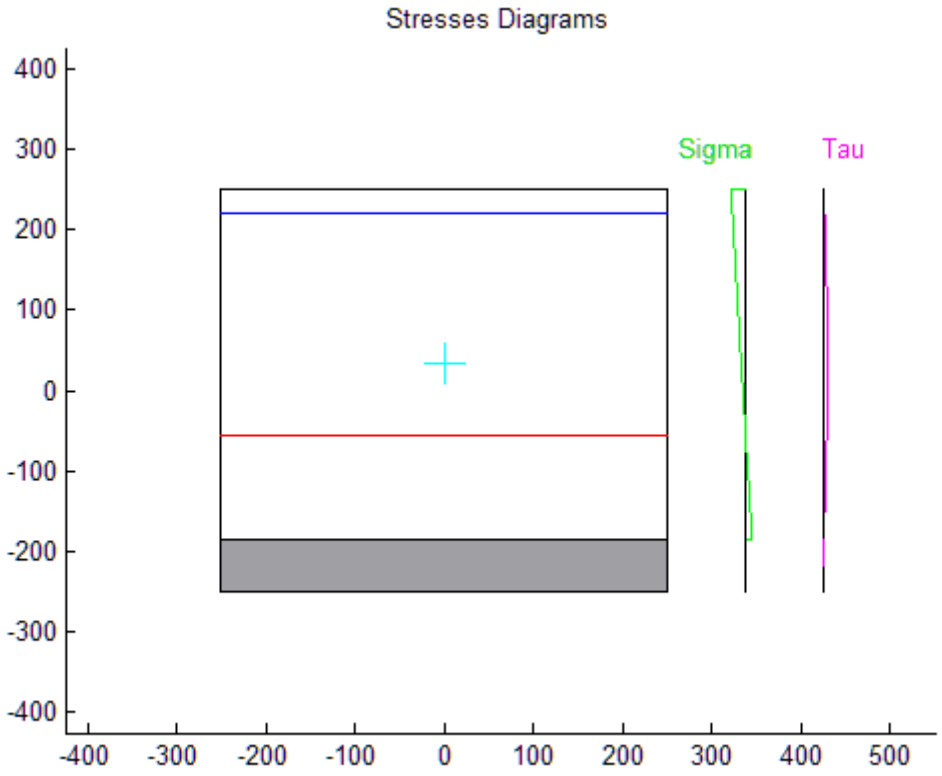

Figure 6.4.2.7.1 - Tangential and normal stresses distributions

Principal stresses are function of both normal and tangential stresses:

$$\sigma_1{}^{\max comp.\ 7th\ it.} = -15.894\ MPa$$

For the tensile fiber:

$$\sigma_1{}^{\max tens.\ 7th\ it.} = 7.614\ MPa$$

At the end of the seventh iteration, the path follows the fourth scenario:

$$\sigma_1{}^{\max comp.\ 7th\ it.} = |\mathbf{-15.894}|\ \boldsymbol{MPa} > \boldsymbol{f_{cd}} = |-60|\ MPa$$

$$\sigma_1^{\max tens.\,7th\,it.} = \mathbf{7.614\ MPa} > \boldsymbol{f_{ctd}} = 6\ MPa$$

6.4.2.8. 8th Elastic Evaluation of the Cross Section

For the eighth iteration, the coordinate of the last un-cracked fiber, is:

$$y^{8th\,it.} = y(8) = 175\ mm$$

The position of the neutral axis from Navier's equation:

$$y_{a.n.}^{8th\,it.} = -57\ mm$$

The sigma value required by the procedure is the one related to the upper edge under compression, corresponding to $y^{\max comp.} = 250\ mm$:

$$\sigma^{\max comp.\ 8th\,it.} = -15.889\ MPa$$

And the one at the lower extremity, corresponding to $y^{max\ tens.} = -175\ mm$:

$$\sigma^{\max tens.\ 8th\,it.} = 6.923\ MPa$$

Tangential stresses are now different from zero because the considered fiber is no longer below reinforcements:

$$\tau^{\max comp.\ 8th\,it.} = 0\ MPa$$

$$\tau^{\max tens.\ 8th\,it.} = 0.0347\ MPa$$

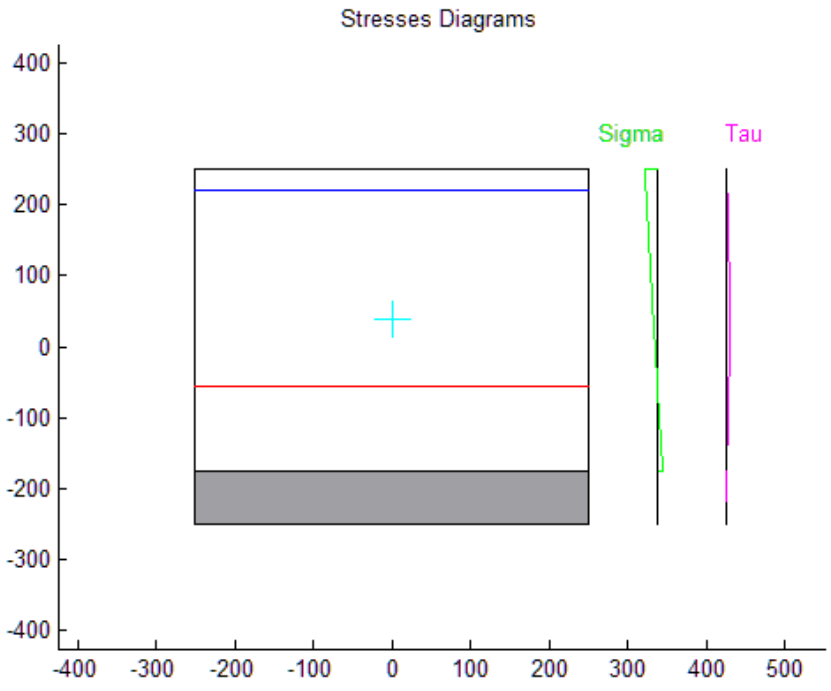

Figure 6.4.2.8.1 - Tangential and normal stresses distributions

Principal stresses are function of both normal and tangential stresses:

$$\sigma_1{}^{\max comp.\ 8th\ it.} = -15.891\ MPa$$

For the tensile fiber:

$$\sigma_1{}^{\max tens.\ 8th\ it.} = 6.928\ MPa$$

At the end of the eighth iteration, the procedure follows the fourth scenario:

$$\sigma_1{}^{\max comp.\ 8th\ it.} = |\mathbf{-15.891}|\ \boldsymbol{MPa} > \boldsymbol{f_{cd}} = |-60|\ MPa$$

$$\sigma_1{}^{\max tens.\ 8th\ it.} = \mathbf{6.928\ MPa} > \boldsymbol{f_{ctd}} = 6\ MPa$$

6.4.2.9. 9th Elastic Evaluation of the Cross Section

For the ninth iteration, the coordinate of the last un-cracked fiber, is:

$$y^{9th\ it.} = y(9) = 165\ mm$$

The position of the neutral axis from Navier's equation:

$$y_{a.n.}{}^{9th\ it.} = -58\ mm$$

The sigma value required by the procedure is the one related to the upper edge under compression, corresponding to $y^{\max comp.} = 250\ mm$:

$$\sigma^{\max comp.\ 9th\ it.} = -15.866\ MPa$$

And the one at the lower extremity, corresponding to $y^{max\ tens.} = -165\ mm$:

$$\sigma^{\max tens.\ 9th\ it.} = 6.344\ MPa$$

Tangential stresse::

$$\tau^{\max comp.\ 9th\ it.} = 0\ MPa$$

$$\tau^{\max tens.\ 9th\ it.} = 0.0348\ MPa$$

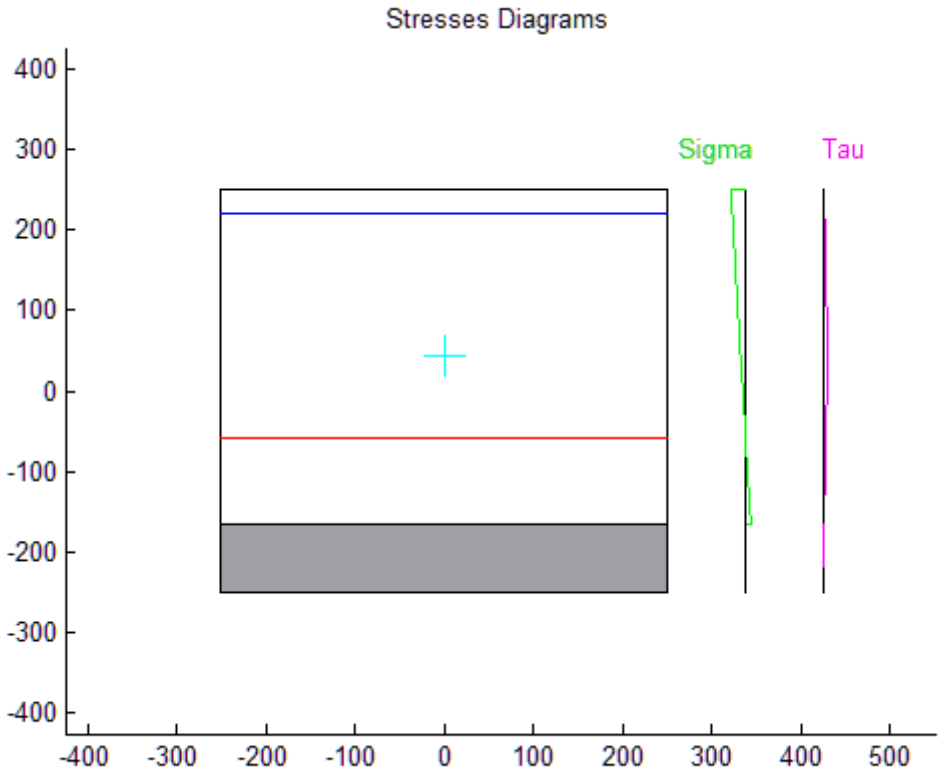

Figure 6.4.2.9.1 - Tangential and normal stresses distributions

Principal stresses are function of both normal and tangential stresses:

$$\sigma_1{}^{\max comp.\ 9th\ it.} = -15.891\ MPa$$

For the tensile fiber:

$$\sigma_1{}^{\max tens.\ 9th\ it.} = 6.350\ MPa$$

At the end of the ninth iteration, the procedure follows the again fourth scenario:

$$\sigma_1{}^{\max comp.\ 9th\ it.} = |\mathbf{-15.868}|\ \boldsymbol{MPa} > \boldsymbol{f_{cd}} = |-60|\ MPa$$

$$\sigma_1{}^{\max tens.\ 9th\ it.} = \mathbf{6.350\ MPa} > \boldsymbol{f_{ctd}} = 6\ MPa$$

5.4.2.10 10th Elastic Evaluation of the Cross Section

For the tenth iteration, the coordinate of the last un-cracked fiber, is:

$$y^{10th\ it.} = y(10) = 155\ mm$$

The position of the neutral axis from Navier's equation:

$$y_{a.n.}{}^{10th\ it.} = -60\ mm$$

The sigma value required by the procedure is the one related to the upper edge under compression, corresponding to $y^{\max comp.} = 250\ mm$:

$$\sigma^{\max comp.\ 10th\ it.} = -15.824\ MPa$$

And the one at the lower extremity, corresponding to $y^{max\ tens.} = -155\ mm$:

$$\sigma^{\max tens.\ 10th\ it.} = 5.671\ MPa$$

Tangential stresses are equal to::

$$\tau^{\max comp.\ 10th\ it.} = 0\ MPa$$

$$\tau^{\max tens.\ 10th\ it.} = 0.0348\ MPa$$

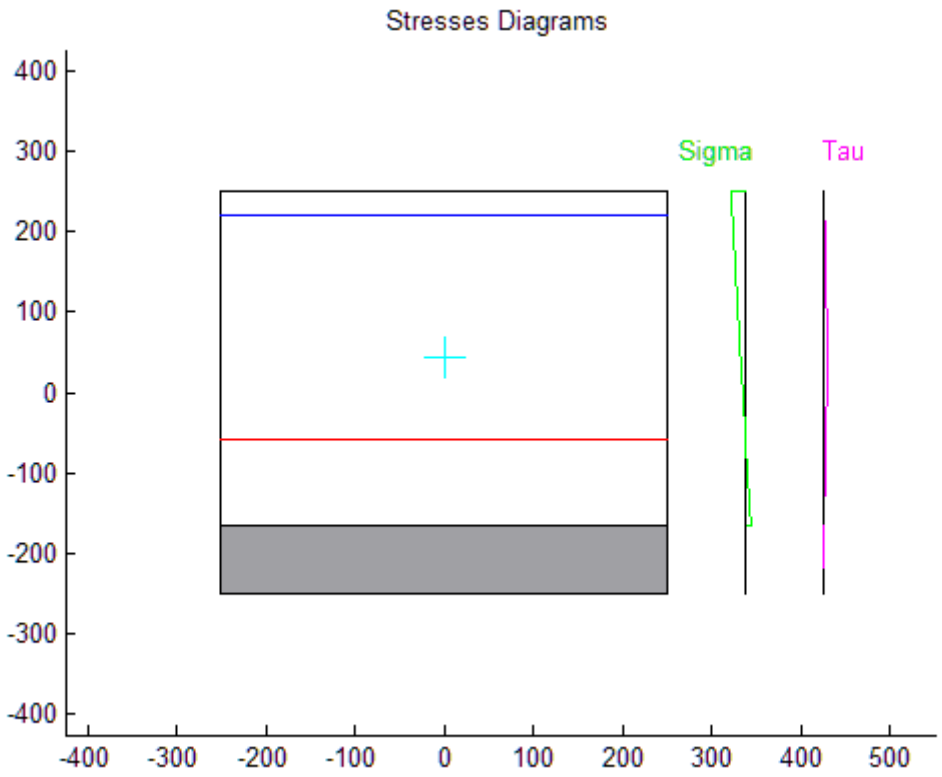

Figure 6.4.2.10.1 - Tangential and normal stresses distributions

Principal stresses are function of both normal and tangential stresses:

$$\sigma_1{}^{\max comp.\ 10th\ it.} = -15.826\ MPa$$

For the tensile fiber:

$$\sigma_1{}^{\max tens.\ 10th\ it.} = 5.678\ MPa$$

At the end of the tenth iteration, the procedure follows the second scenario:

$$\sigma_1{}^{\max comp.\ 10th\ it.} = |-\mathbf{15.826}|\ \boldsymbol{MPa} > \boldsymbol{f_{cd}} = |-60|\ MPa$$

$$\sigma_1{}^{\max tens.\ 10th\ it.} = \mathbf{5.678}\ \boldsymbol{MPa} < \boldsymbol{f_{ctd}} = 6\ MPa$$

Both the principal compressive stress on the most compressed fiber and the principal tensile stress on the tensest fiber are lower than their limits. The last un-cracked fiber does not crack. The cross section is now in equilibrium conditions.

At the end of the tenth iteration, the analysis ends up in the first scenario and follows the cracked condition. In this case, it was satisfied and the script plots “The vertical equilibrium is satisfied”.

The procedure ends with an equilibrium achieved in ultimate conditions.

The script also plots how the crack developed through the column.

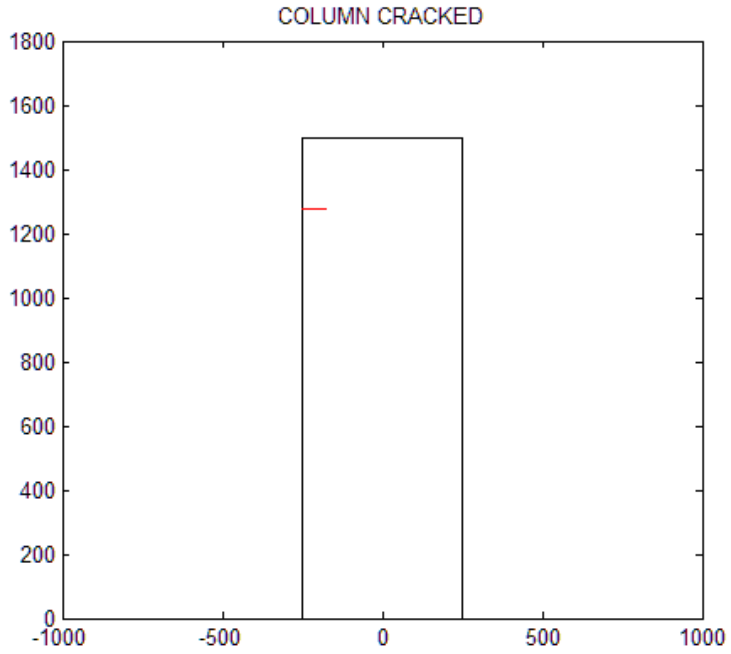

Figure 5.4.2.10.2 – Cracked Cross section

6.4.3. Case 3

Information necessary to use the procedure listed below:

- $b = 600\ mm$;
- $h = 800\ mm$;
- $c = 40\ mm$;
- $d = 760\ mm$;
- $A_{s,sup} = 2\ \Phi\ 22 = 760\ mm^2$;
- $A_{s,inf} = 2\ \Phi\ 22 = 760\ mm^2$;
- $\Phi_{st} = \Phi\ 6 = 8\ mm$;
- $n_{st} = 2$;
- $s_{st} = 100\ mm$:

- $f_{cd} = 45\ MPa$;
- $f_{ctd} = 0.1\ f_{cd} = 4.5\ MPa$;
- $f_{yd} = 580\ MPa$;
- $E_c = 22000\ \left[\left(\frac{f_{cd}}{10}\right)^{0.3}\right] = 34545\ MPa$;
- $E_s = 210000\ MPa$;
- $n = {E_c}/{E_s} = 6.08$;
- $N_{act} = -1500000\ N$;
- $T_{act} = 800000\ N$;
- $M_{act} = 3500000000\ N\ mm$.

The script divides a half cross section in twenty fibers in order to get the width of each fiber equal to two centimetres.
The vector of the fiber considered is the following one:

$$y = [390,\ 370,\ 350,\ 330,\ 310,\ 290,\ 270,\ 250,\ 230,\ 210,\ 190,\ 170,\ 150,\ 130, \ldots$$

$$\ldots\ 110,\ 90,\ 70,\ 50,\ 30,\ 10]$$

6.4.3.1. 1st Elastic Evaluation of the Cross Section

The procedure starts with the first elastic evaluation of the initial cross section.

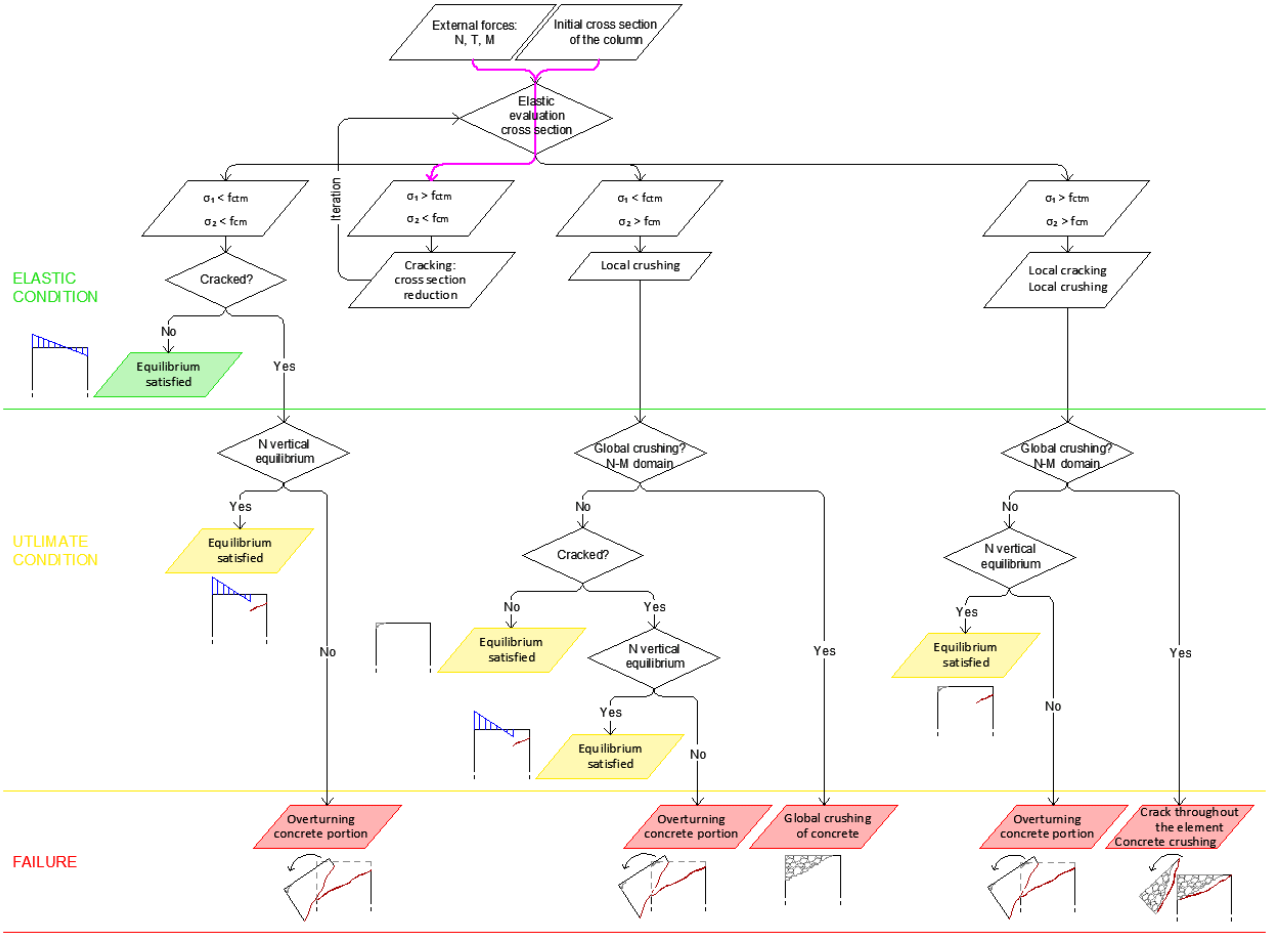

Figure 6.4.3.1.1 – 1st iteration of the procedure represented in the flow chart

The coordinate of the last un-cracked fiber, the one at the extremity of the working cross section, is:

$$y^{1st\ it.} = y(1) = 390\ mm$$

The basic terms necessary to compute the stresses diagrams are the following ones:

$$d^{1st\ it.} = 760\ mm$$

$$A_{omog}{}^{1st\ it.} = 489240\ mm^2$$

$$S^{1st\ it.} = 193848019\ mm^3$$

$$d_{g,sup}{}^{1st\ it.} = 396\ mm$$

$$d_{g,inf}{}^{1st\ it.} = 404\ mm$$

$$I_{omog}{}^{1st\ it.} = 26804496912\ mm^4$$

The position of the neutral axis, imposing stress equal to zero in the Navier's equation and solving for the y coordintae:

$$y_{a.n.}{}^{1st\ it.} = -210\ mm$$

The sigma value required by the procedure is the one related to the upper edge under compression, corresponding to $y^{\max comp.} = 400\ mm$:

$$\sigma^{\max comp.\ 1st\ it.} = -41.564\ MPa$$

Even the one acting on the tensest fiber, the one at the lower extremity, corresponding to $y^{max\ tens.} = -390\ mm$:

$$\sigma^{\max tens.\ 1st\ it.} = 12.604\ MPa$$

Tangential stresses are equal to zero because the considered fiber is below steel rebar, where the static moment gets to zero:

$$\tau^{\max comp.\ 1st\ it.} = 0\ MPa$$

$$\tau^{\max tens.\ 1st\ it.} = 0\ MPa$$

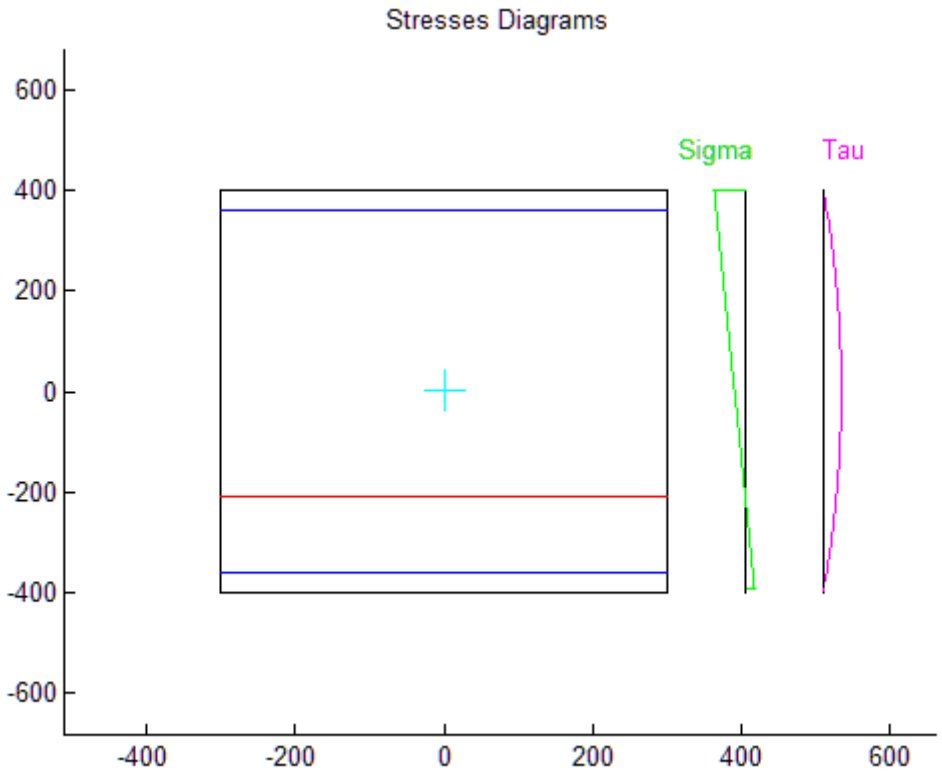

Figure 6.4.3.1.2 - Tangential and normal stresses distributions

Also in this case, considering that tangential stresses are null, principal stresses are equal to normal ones:

$$\sigma_1{}^{\max comp.\ 1st\ it.} = -41.564\ MPa$$

For the tensile fiber:

$$\sigma_1^{\max tens.\ 1st\ it.} = 12.604\ MPa$$

At the end of the first iteration, the scenario corresponds to the fourth::

$$\sigma_1^{\max comp.\ 1st\ it.} = |\mathbf{-41.564}|\ \boldsymbol{MPa} < \boldsymbol{f_{cd}} = |-45|\ MPa$$

$$\sigma_1^{\max tens.\ 1st\ it.} = \mathbf{12.604\ MPa} > \boldsymbol{f_{ctd}} = 4.5\ MPa$$

The procedure returns at the beginning of the analysis, recalculates the cross section and the state of stress. A second iteration follow this first one.

6.4.3.2. 2nd Elastic Evaluation of the Cross Section

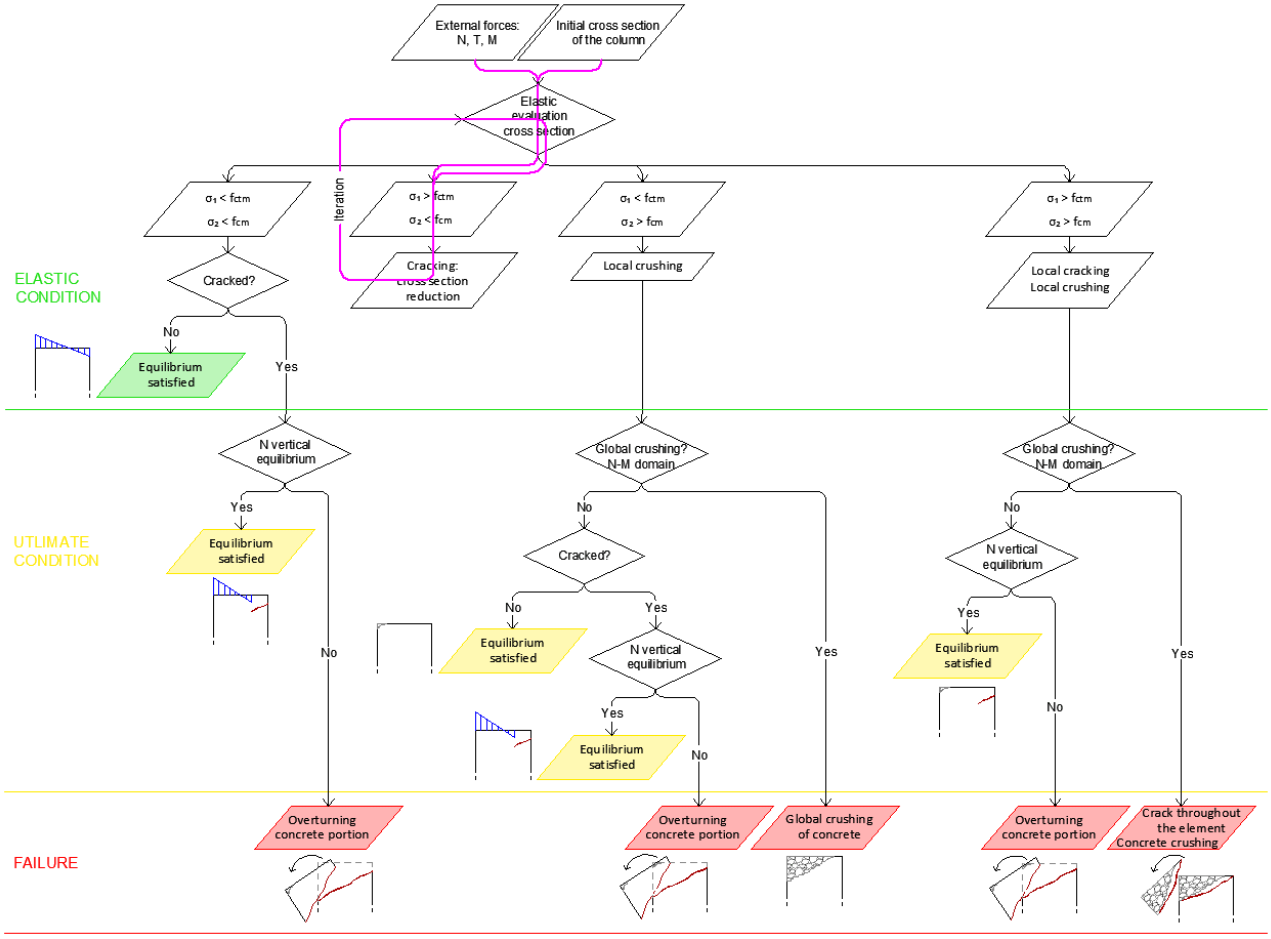

Figure 6.4.3.2.1 – 2nd iteration of the procedure represented in the flow chart

The fiber at the extremity of the initial cross section cracked hence the element has reduced. The coordinate of the last un-cracked fiber, is:

$$y^{2nd\ it.} = y(1) = 370\ mm$$

Fundamental terms necessary to compute the stresses diagrams are the following ones:

$$d^{2nd\ it.} = 740\ mm$$

$$A_{omog}{}^{2nd\ it.} = 477240\ mm^2$$

$$S^{1st\ it.} = 184368019\ mm^3$$

$$d_{g,sup}{}^{2nd\ it.} = 386\ mm$$

$$d_{g,inf}{}^{2nd\ it.} = 414\ mm$$

$$I_{omog}{}^{2nd\ it.} = 26889056367\ mm^4$$

The position of the neutral axis, imposing stress equal to zero in the Navier's equation and solving for the y coordintae:

$$y_{a.n.}{}^{2nd\ it.} = -208\ mm$$

The sigma value required by the procedure is the one related to the upper edge under compression, corresponding to $y^{\max comp.} = 400\ mm$:

$$\sigma^{\max comp.\ 2nd\ it.} = -42.869\ MPa$$

Even the one acting on the tensest fiber, the one at the lower extremity, corresponding to $y^{max\ tens.} = -370\ mm$:

$$\sigma^{\max tens.\ 2nd\ it.} = 11.495\ MPa$$

Tangential stresses are still equal to zero because the considered fiber is below steel rebar, where the static moment gets to zero:

$$\tau^{\max comp.\ 2nd\ it.} = 0\ MPa$$

$$\tau^{\max tens.\ 2nd\ it.} = 0\ MPa$$

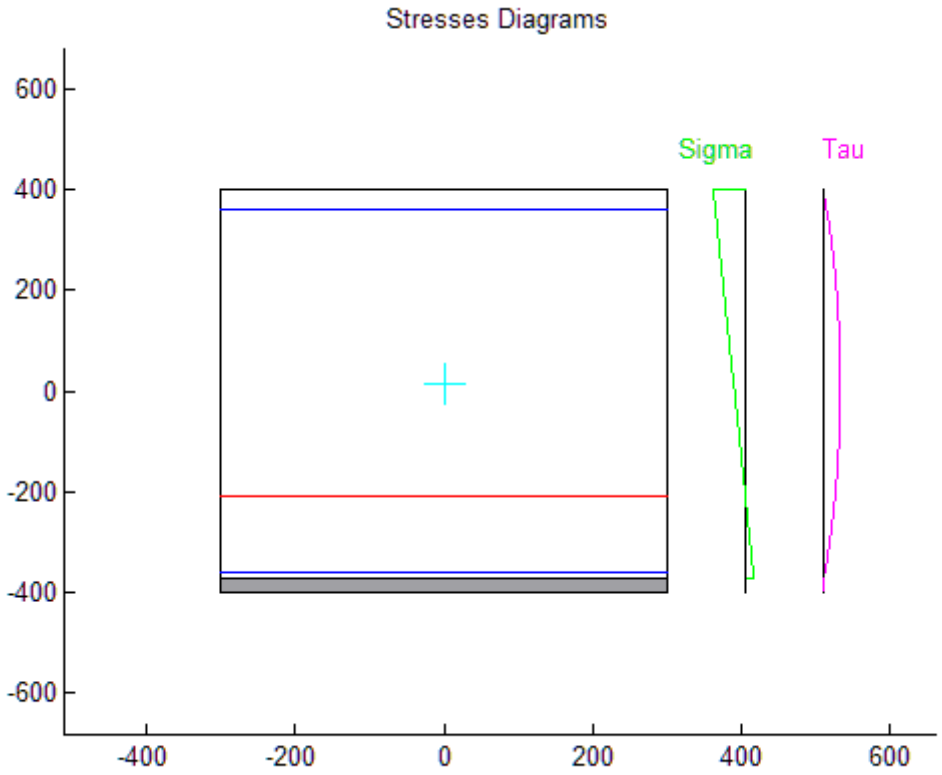

Figure 6.4.3.2.2 - Tangential and normal stresses distributions

Also in this case, considering that tangential stresses are null, principal stresses are equal to normal ones:

$$\sigma_1{}^{\max comp.\ 2nd\ it.} = -42.869\ MPa$$

For the tensile fiber:

$$\sigma_1{}^{\max tens.\ 2nd\ it.} = 11.495\ MPa$$

At the end of the second iteration, the procedure follows the fourth scenario:

$$\sigma_1{}^{\max comp.\ 2nd\ it.} = |\mathbf{-42.869}|\ \boldsymbol{MPa} < \boldsymbol{f_{cd}} = |-45|\ MPa$$

$$\sigma_1{}^{\max tens.\ 2nd\ it.} = \mathbf{11.495\ MPa} > \boldsymbol{f_{ctd}} = 4.5\ MPa$$

Also at the end of the second iteration the procedure returns in the fourth scenario, the last fiber cracks and the analysis goes back to the beginning of the procedure and revaluates the stresses acting on the cross section.

6.4.3.3. 3rd Elastic Evaluation of the Cross Section

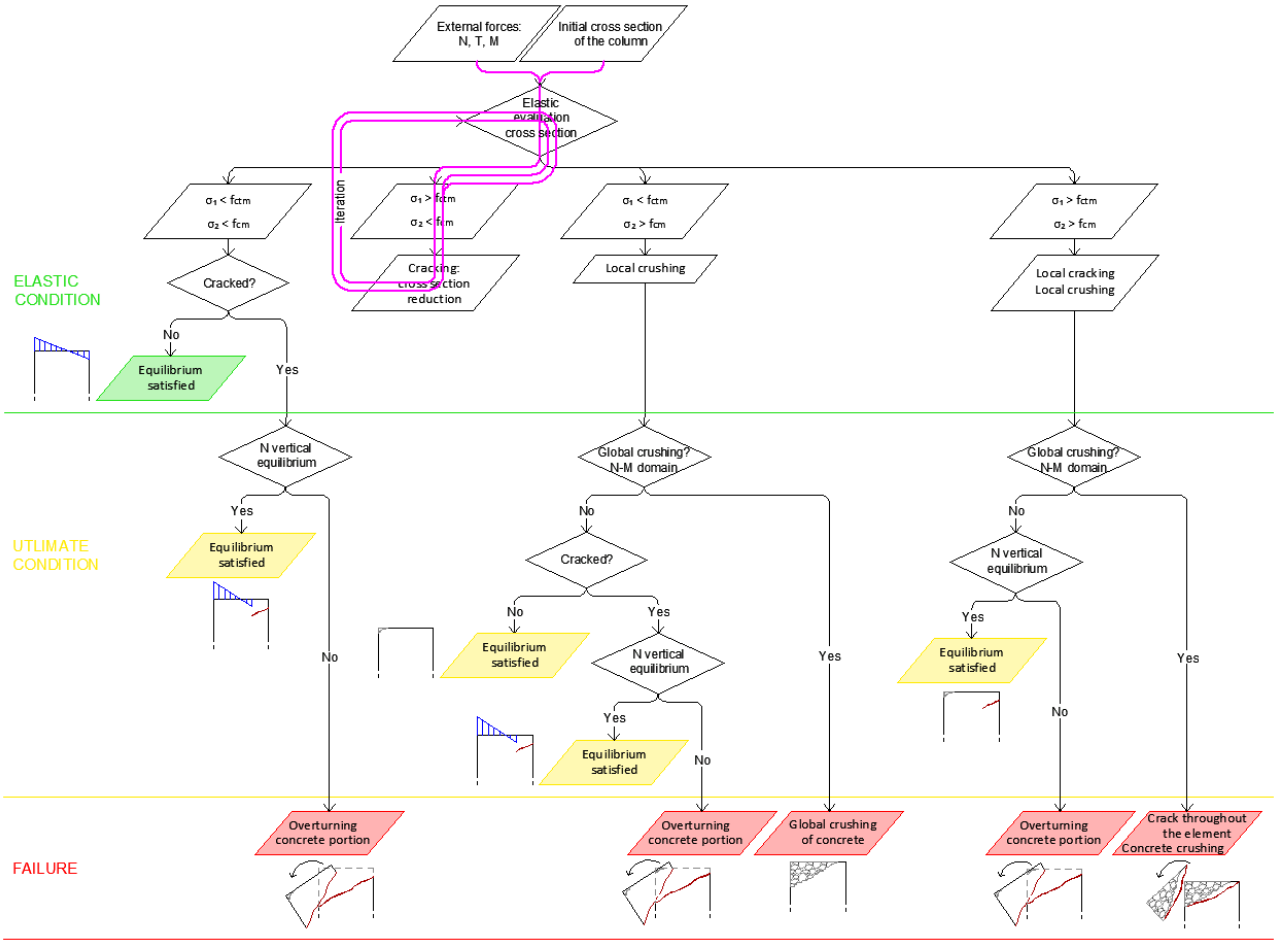

Figure 6.4.3.3.1 – 3rd iteration of the procedure represented in the flow chart

At the third iteration:

$$y^{3rd\ it.} = y(1) = 350\ mm$$

The basic terms necessary to compute the stresses diagrams have to recalculate, since the y coordinate has changed.

The position of the neutral axis from Navier's equation:

$$y_{a.n.}{}^{3rd\ it.} = -207\ mm$$

The sigma value required by the procedure is the one related to the upper edge under compression, corresponding to $y^{\max comp.} = 400\ mm$:

$$\sigma^{\max comp.\ 3rd\ it.} = -42.869\ MPa$$

Even the one acting on the tensest fiber, the one at the lower extremity, corresponding to $y^{max\ tens.} = -350\ mm$:

$$\sigma^{\max tens.\ 3rd\ it.} = 11.495\ MPa$$

Tangential stresses are different from zero because the considered fiber stays above steel rebar, and therefore:

$$\tau^{\max comp.\ 3rd\ it.} = 0\ MPa$$

$$\tau^{\max tens.\ 3rd\ it.} = 0.108\ MPa$$

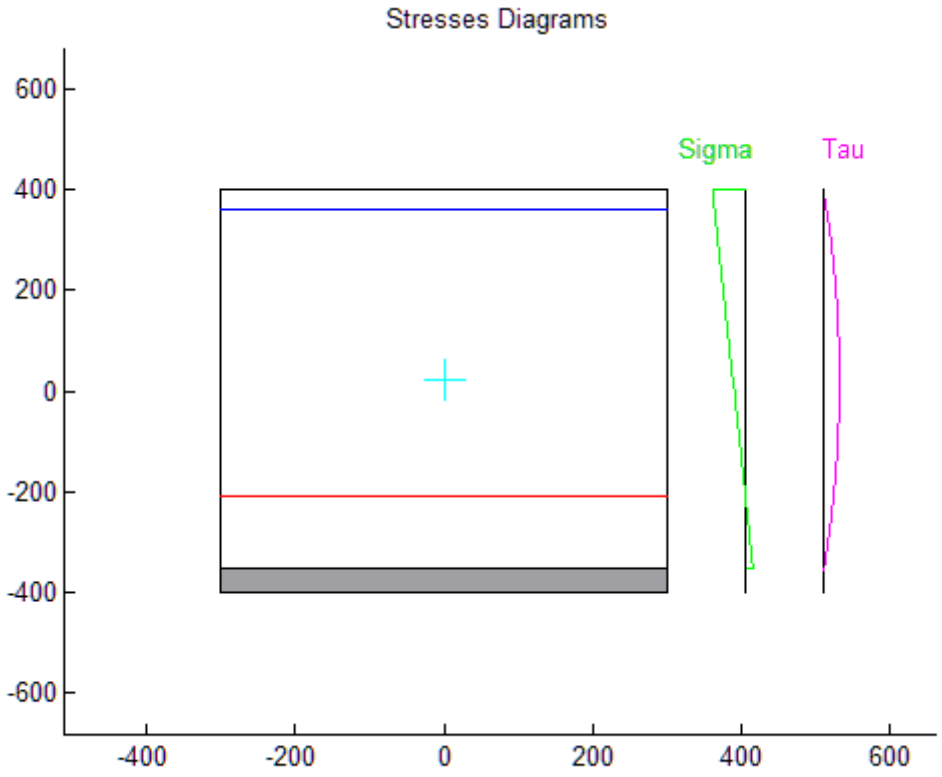

Figure 6.4.3.3.2 - Tangential and normal stresses distributions

Principal compressive stress, depending on both normal and tangential stresses:

$$\sigma_1{}^{\max comp.\ 3rd\ it.} = -44.085\ MPa$$

For the tensile fiber:

$$\sigma_1{}^{\max tens.\ 3rd\ it.} = 10.338\ MPa$$

At the end of the second iteration, the procedure follows the fourth scenario:

$$\sigma_1{}^{\max comp.\ 3rd\ it.} = |\mathbf{-44.085}|\ \boldsymbol{MPa} < \boldsymbol{f_{cd}} = |-45|\ MPa$$

$$\sigma_1{}^{\max tens.\ 3rd\ it.} = \mathbf{10.338}\ \boldsymbol{MPa} > \boldsymbol{f_{ctd}} = 4.5\ MPa$$

Also at the end of the third iteration the procedure returns in the fourth scenario and the analysis repeats.

6.4.3.4. 4th Elastic Evaluation of the Cross Section

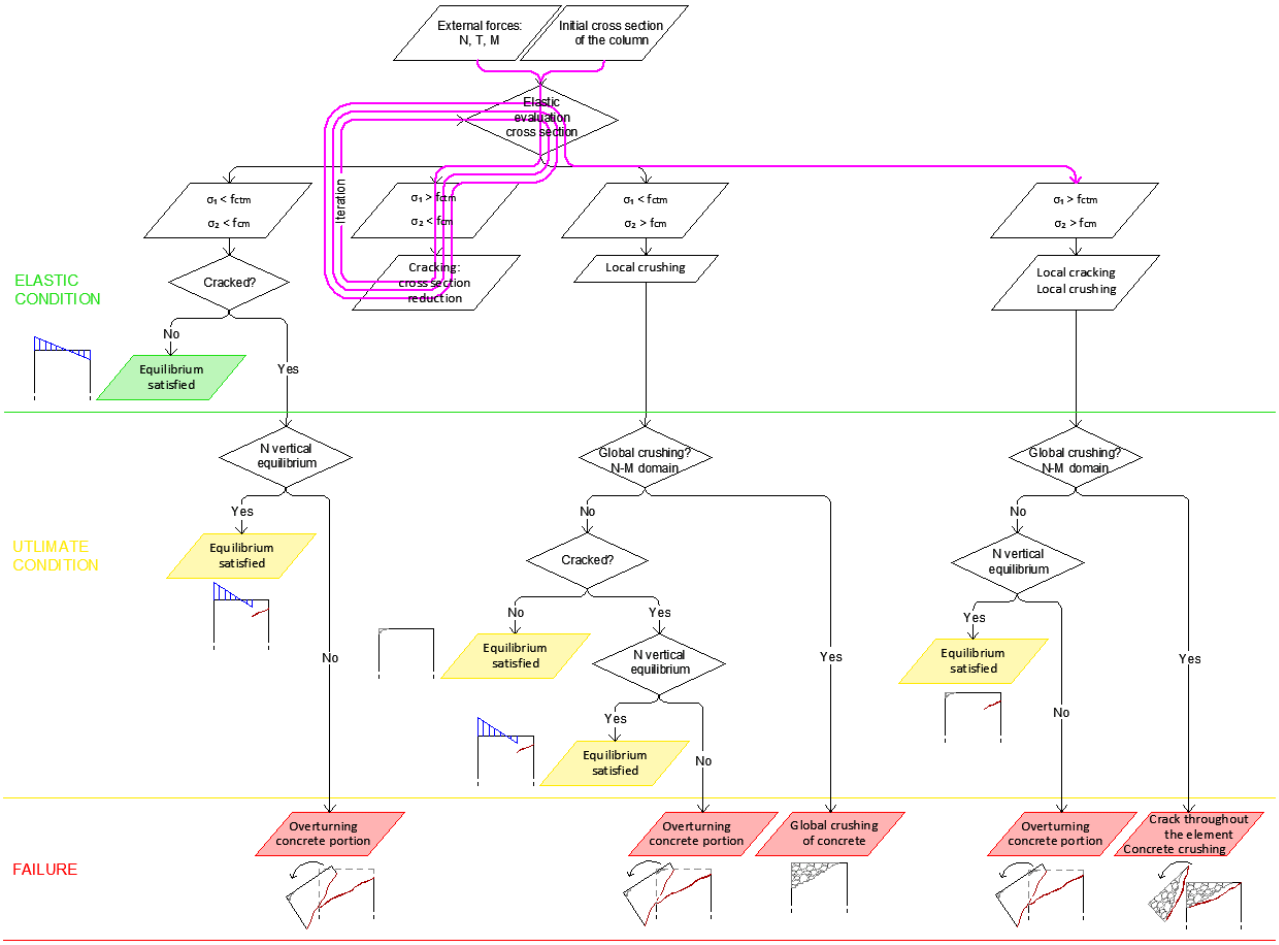

Figure 6.4.3.4.1 – 4th iteration of the procedure represented in the flow chart

For the fourth iteration:

$$y^{4th\ it.} = y(4) = 330\ mm$$

The position of the neutral axis from Navier's equation:

$$y_{a.n.}{}^{4th\ it.} = -208\ mm$$

The sigma value required by the procedure is the one related to the upper edge under compression, corresponding to $y^{\max comp.} = 400\ mm$:

$$\sigma^{\max comp.\ 4th\ it.} = -45.201\ MPa$$

And the one at the lower extremity, corresponding to $y^{max\ tens.} = -330\ mm$:

$$\sigma^{\max tens.\ 4th\ it.} = 9.121\ MPa$$

Tangential stresses are equal to:

$$\tau^{\max comp.\ 3rd\ it.} = 0\ MPa$$

$$\tau^{\max tens.\ 3rd\ it.} = 0.106\ MPa$$

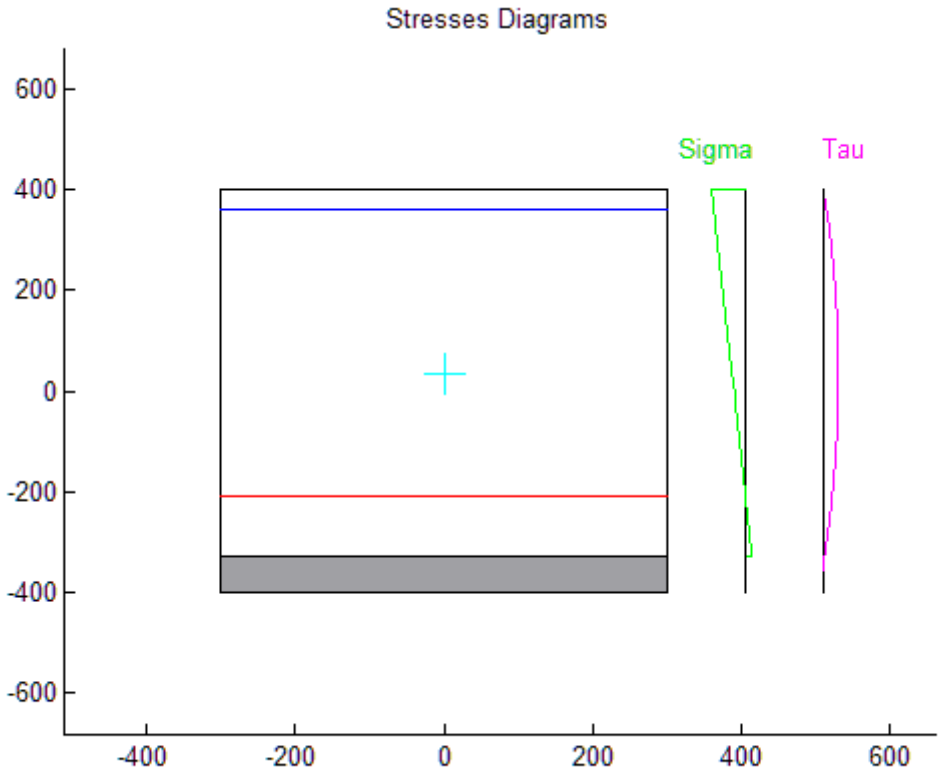

Figure 6.4.3.4.2 - Tangential and normal stresses distributions

Principal stresses are function of both normal and tangential stresses:

$$\sigma_1{}^{\max comp.\ 4th\ it.} = -45.203\ MPa$$

For the tensile fiber:

$$\sigma_1{}^{\max tens.\ 4th\ it.} = 9.133\ MPa$$

At the end of the fourth iteration, the procedure follows the second scenario:

$$\sigma_1{}^{\max comp.\ 4th\ it.} = |\mathbf{-45.203}|\ \boldsymbol{MPa} > \boldsymbol{f_{cd}} = |-45|\ MPa$$

$$\sigma_1{}^{\max tens.\ 4th\ it.} = \mathbf{9.133\ MPa} > \boldsymbol{f_{ctd}} = 4.5\ MPa$$

The crack continues developing and the most compressed fiber crushes. Both a local cracking and a local crushing certainly happened. The analysis proceeds considering first the crushing of the concrete: the type of crushing, local or global, can be determined through an N-M domain verification. If the solicitation point lays inside the domain, the column is able to withstand external actions and therefore the crushing is local. If the point is out of the domain, it means that the member fails under such actions, thus it fails because of a global crushing.

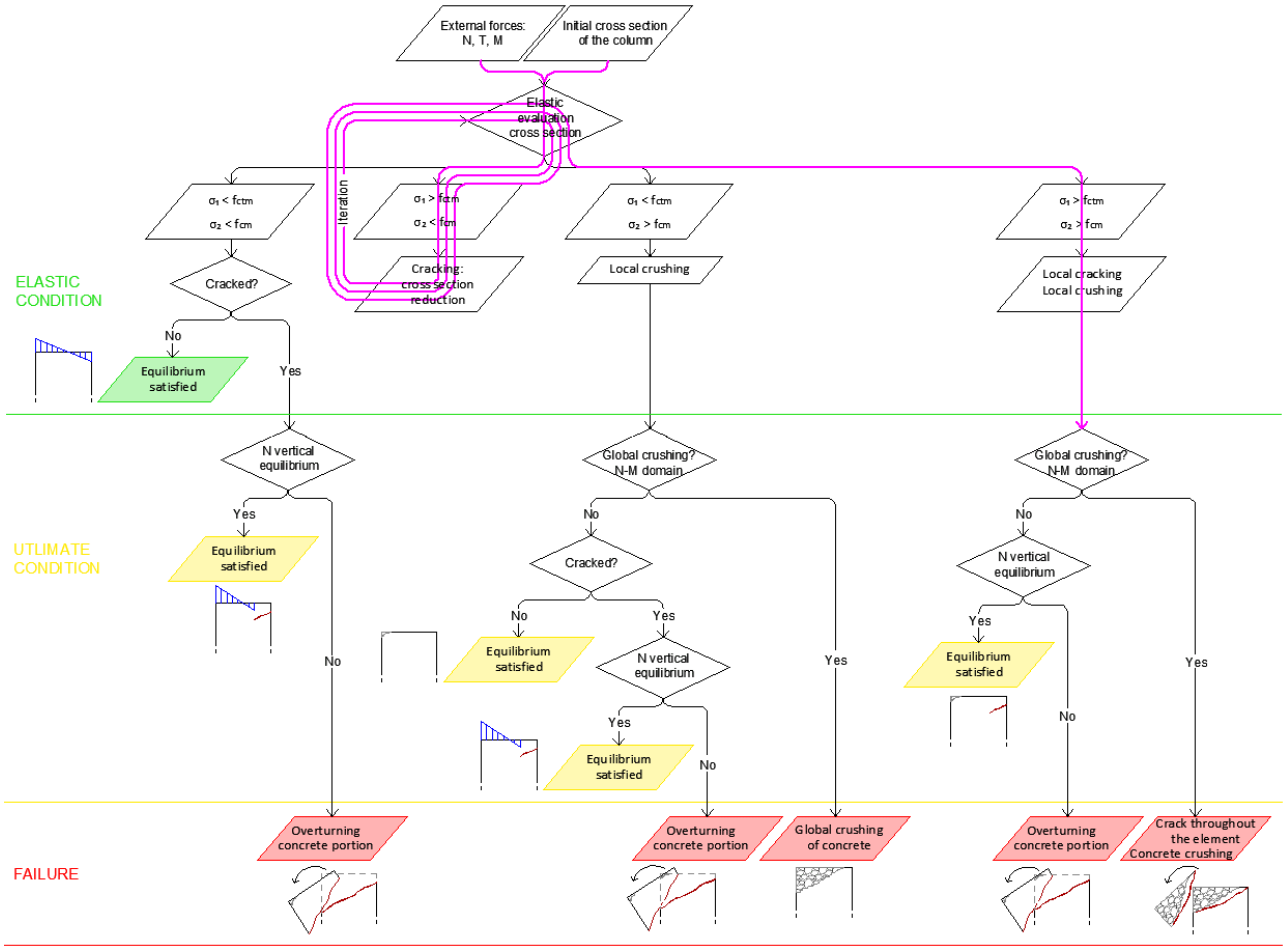

Figure 6.4.3.4.3 – Procedure on the flow diagram: global crushing verification

The script goes on with the N-M domain verification.

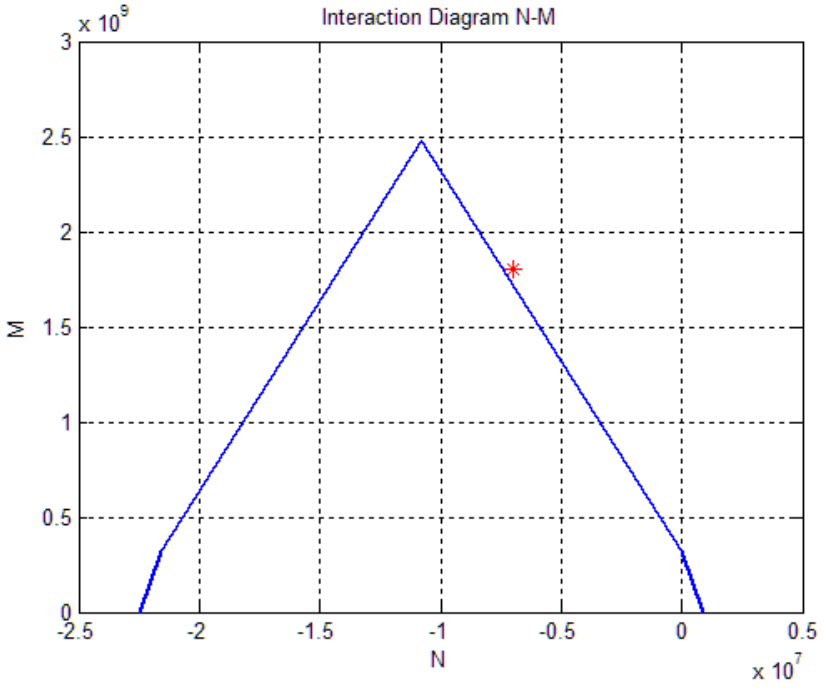

Figure 6.4.3.4.4 – N-M interaction domain

As shown in the figure, the point is outside the interaction diagram; the script returns “The verification of the N-M domain is not satisfied, global crushing of the element”. The whole element crushes; the path on the flow chart follow the *“Yes”* alternative. Since the column has already failed because of the crushing, the verification of the crack is worthless.

The procedure ends with the failure of the column. The script returns “The crack develops throughout the cross section and global crushing of the column”.

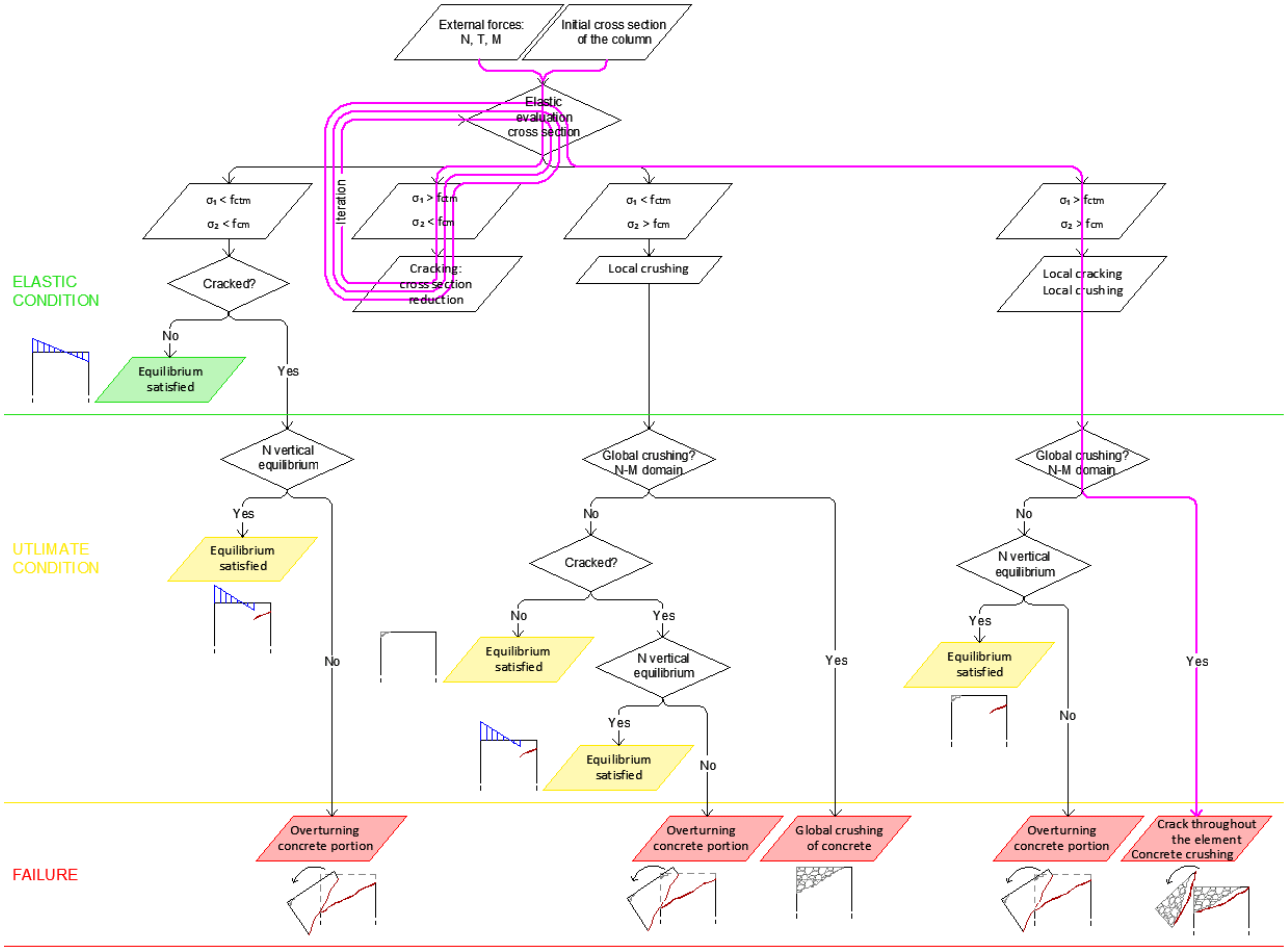

Figure 6.4.3.4.5 – Procedure on the flow diagram: end of the procedure

7. Design of the Laboratory Test

Theoretical considerations are not enough to validate the procedure suggested. This approach requires a practical, experimental analysis in order to verify the reliability of the aforementioned method.

In this chapter, the design of a laboratory test, necessary to understand if the procedure captures the actual behaviour of columns under specific external forces.

The reason why this study has undertaken relates to the collapse of three real columns: they all showed same types of damages, which could attribute to the interaction of axial force, shear and bending moment.

This laboratory test could be used to both validate the procedure and, at the same time, deeply investigate the failures of those elements. Therefore, the experimental tests should be realised on three elements, characterised by same features of the real collapsed members.

For what concerns geometrical properties, the three elements are

- $300 \times 300\ mm^2$;
- $500 \times 500\ mm^2$;
- $600 \times 800\ mm^2$.

The cover of steel reinforcement could be the same for all the elements, equal to $40\ mm$.

Longitudinal reinforcements, placed at the four corners of the cross section, are respectively:

- $4\ \Phi\ 10$;
- $4\ \Phi\ 24$;
- $4\ \Phi\ 22$.

Transversal reinforcements define as follows:

- $\Phi\ 6/100$;
- $\Phi\ 6/200$;
- $\Phi\ 8/100$.

Concerning material properties, assuming that the tensile strength of the concrete is always one tenth of the compressive one, the strength of the steel and the compressive strength of the concrete are:

- $f_{yd} = 450\ MPa,\ f_{cd} = 10\ MPa$;
- $f_{yd} = 600\ MPa,\ f_{cd} = 60\ MPa$;
- $f_{yd} = 580\ MPa,\ f_{cd} = 45\ MPa$.

Once specified the geometrical and material properties, it has to define the loading technique. The article about the experimental study conducted at the University of Toronto, *"Evaluation of Shear Design Procedures for RC Members under Axial Compression", Pawan R. Gupta and Michael P. Collins, ACI Structural Journal, 2001*, was used as a guideline to decide what kind of loading procedure employ.

As for the experimental test in Toronto, where the specimens had almost the same dimensions of the three column considered in this research, the elements should be loaded using four sets of six jacks spread throughout the top and the bottom faces of the members; high-strength bolts employed to apply the load.

In this case, the procedure accounts for columns fixed at the bottom extremity and partially restrained at the other edge, subjected to a bending moment acting at the top of the columns always in the same direction; therefore, in the laboratory test, the bending moment applies only at the top extremity, maintaining the same direction throughout the loading.

In each experiment, the axial force, the shear and the bending moment increased proportionally up to failure.

Both tangential and normal deformations should be measured by means of linear variable displacement transducer, to define the deformation of the element during the test.

This design of the laboratory test tries to achieve the best compromise between costs and a satisfying evaluation of the procedure. Having no limits on the costs of the laboratory test, the analysis could extended. The specimens could be more than three, in that case all the characteristics, geometrical and material properties, of the columns could vary; this could enable the study of the effects of such features on the type of damages. The effects of the dimensions of the cross section, the amount of longitudinal and transversal reinforcement, the strength of both the concrete both the steel.
Several loading methods could have tested: a proportional increase of the axial force, the shear and the bending up to failure, but also an instantaneous application of the final, failure loads experienced by each column. This could be useful to understand if the failure conditions, e.g. the external forces that generated the collapse of the elements, appeared on the member after a gradually increase or they sudden acted on the column. Understanding how failure conditions established on the columns could be used to improve the suggested procedure.

8. Conclusions

The analysis of the interaction between the axial force, the shear and the bending moment in reinforced concrete elements, underlined several important aspects.

The literature review clearly showed that the problem has still not considered in a precise, detailed and complete way. Many researches tried to approach analytically the topic but many hypotheses and approximations were required.
Experimental articles, describing experimental programs, demonstrated that a large compression on reinforced concrete elements, results in no significant cracking until just before failure, then, suddenly, strongly inclined cracks both at the top and at the bottom of the element, appear. This probably corresponds to the conditions of the real columns collapsed, reason why this research begun.

First, the interaction between only two components of solicitations, the axial force and the shear, has considered. The analysis led to the construction of an elastic domain of the two components, then compared with the one coming from the *Modified Compression Field Theory*. The domains almost coincide, especially for traction states of stress, but also for compression axial forces, the difference is negligible.

The study proceeded considering the interaction between all three solicitations. The result was a tridimensional elastic domain whose surface corresponds to the combination of axial force, shear and bending producing the crushing or the cracking of the concrete. Unfortunately, no tridimensional domains found in literature to compare results. Further analyses should develop to verify the truthfulness of the domain and to construct the one corresponding to ultimate conditions of the element.

The analysis continued focusing on the development of a procedure aimed at analyzing the behavior of the cross section subjected to axial force, shear and bending. This has approached considering the actual distribution of stresses along the cross section, not the column as a whole. According to principal stresses on the most solicited fibers, the iterative process goes on or stops. It consists in a non-linear analysis as a sequence of linear ones. According to stresses distributions, the procedure makes different verifications and returns the final condition of the element, which could be an elastic or ultimate equilibrium condition, or failure due to global crushing or cracking.

The process as applied to several real cases of columns collapsed in order to verify the reliability of the procedure. In all cases, the analysis ends with the failure of the element because both the global crushing and the development of the crack throughout the cross section. According to what can be established from the pictures of those collapsed columns, they experienced both these types of failures. Therefore, for what concerns those elements, the procedure accurately predict their behaviors.

A laboratory test should perform in order to verify carefully the reliability of the procedure. It could be also useful to examine in depth the ways of collapse of real columns mentioned.

Bibliography

Frank J. Vecchio, Michael P. Collins [1986] *"The Modified Compression Field Theory for Reinforced Concrete Elements Subjected to Shear," ACI Structural Journals*, Vol. 83, pp. 219-231.

Michael P. Collins, Denis Mitchell, Perry Adebar, Frank J. Vecchio [1996] *"A General Shear Design Method," ACI Structural Journals*, Vol. 93, pp. 36-45.

M. J. Nigel Priestley, Ravindra Verma, Yan Xiao, [1999] *"Seismic Shear Strength of Reinforced Concrete Columns," Journal of Engineering Mechanics*, Vol. 120.

Evan C. Bentz, Frank J. Vecchio, Michael P. Collins [2006] *"Simplified Modified Compression Field Theory for Calculating Shear Strength of Reinforced Concrete Element," ACI Structural Journals*, Vol. 104, pp. 614-624.

Hossein Mostafei, Toshimi Kabeyasawa [2007] *"Axial-Shear-Flexure Interaction Approach for Reinforced Concrete Columns," ACI Structural Journals*, Vol. 104, pp. 218-226.

Hossein Mostafei, Frank J. Vecchio [2007] *"Axial-Shear-Flexure Interaction Approach for Reinforced Concrete Columns," Journal of Structural Engineering,* Vol. 134, pp. 1538-1547.

Marco Petrangeli, Paolo Emilio Pinto, Vincenzo Ciampi [1999] *"Fiber Element for Cyclic Bending and Shear of Reinforced Concrete Structures. I: Theory," Journal of Engineering Mechanics,* Vol. 125, pp. 994-1001.

Marco Petrangeli [1999] *"Fiber Element for Cyclic Bending and Shear of Reinforced Concrete Structures. II: Verification," Journal of Engineering Mechanics,* Vol. 125, pp. 1002-1009.

Pier Paolo Diotallevi, Luca Landi, Filippo Cardinetti [2008] *"A Fiber Beam Column Element for modelling the Flexure-Shear Interaction in the Non-Linear Analysis of RC Structures," Proceedings of 14th World Conference on Earthquake Engineering,* Beijing, China.

Luca Martinelli [2008] *"Modelling Shear-Flexure Interaction in Reinforced Concrete Elements Subjected to Cyclic Lateral Loading," ACI Structural Journals*, Vol. 105, pp. 675-684.

Pawan R. Gupta, Michael P. Collins [2001] *"Evaluation of Shear Design Procedure for Reinforced Concrete Members under Axial Compression," ACI Structural Journals*, Vol. 98, pp. 537-547.

Liping Xie, Evan C. Bentz, Michael P. Collins [2011] *"Influence of Axial Stress on Shear Response of Reinforced Concrete Elements," ACI Structural Journals*, Vol. 108, pp. 745-754.

Matthew T. Smith, Daniel A. Howell, Mary Ann T. Triska, and Christopher Higgins [2014] *"Effects of Axial Tension on Shear-Moment Capacity of Full-Scale Reinforced Concrete Girders," ACI Structural Journals*, Vol. 111, pp. 211-222.

Tarutal Ghosh Mondal, Dr. S. Suriya Prakash [2014] *"Nonlinear Finite Element Analysis for RC Bridge Columns under Torsion with or without Axial Compression," Journal of Bridge Engineering.*

Ibrahim M. Metwally [2012] *"Evaluate the capability and accuracy of response 2000 program in prediction of the shear capacities of reinforced and prestressed concrete members," Housing and Building National Research Centre,* Vol. 8, pp. 99-106.

Halil Sezen, Jack P. Moehle [2006] *"Seismic Tests on Reinforced Concrete Columns with Light Transverse Reinforcements," ACI Structural Journal,* Vol. 103, pp. 842-849.

Valeria Fort [2014] *"Retrofit Solutions for Gravity-Load-Designed RC Frame Structures Employing Self-Centring Energy-Dissipative (SCED) Braces,"* University of Naples, Naples, Italy.

Paolo Ricci [2010] *"Seismic Vulnerability of Existing RC Buildings,"* IUSS, Pavia, Italy.

Cosenza E., Manfredi G., Pecce M. [2008] *"Strutture in cemento armato. Basi della progettazione,"* Hoepli, Milano, Italy.

Aurelio Ghersi [2012] *"Il cemento armato,"* Dario Flaccovio Editore.

Erasmo Viola [2012] *"Lezioni di Scienza delle Costruzioni,"* Pitagora Editrice, Bologna, Italy.

Mario Salvadori, Robert A. Heller [1963] *"Structure in Architecture,"* Prentice-Hall Editor.

Luigi Santarella [1998] *"Il cemento armato. La tecnica e la statica,"* Hoepli, Milano, Italy.

Decreto Ministeriale 14 gennaio 2008 (NTC08) [2008] *"Norme Tecniche per la Costruzione,"* Gazzetta Ufficiale 4 febbraio 2008 n. 29.

CEN [2005] *"European Standard EN-1998: 2005 Eurocode8: Design of Structures for Earthquake Resistance,"* European Committee for Standardization, Brussels, Belgium.

CEN [2004] *"European Standard EN-1992: 2004 Eurocode8: Design of Concrete Structures,"* European Committee for Standardization, Brussels, Belgium.